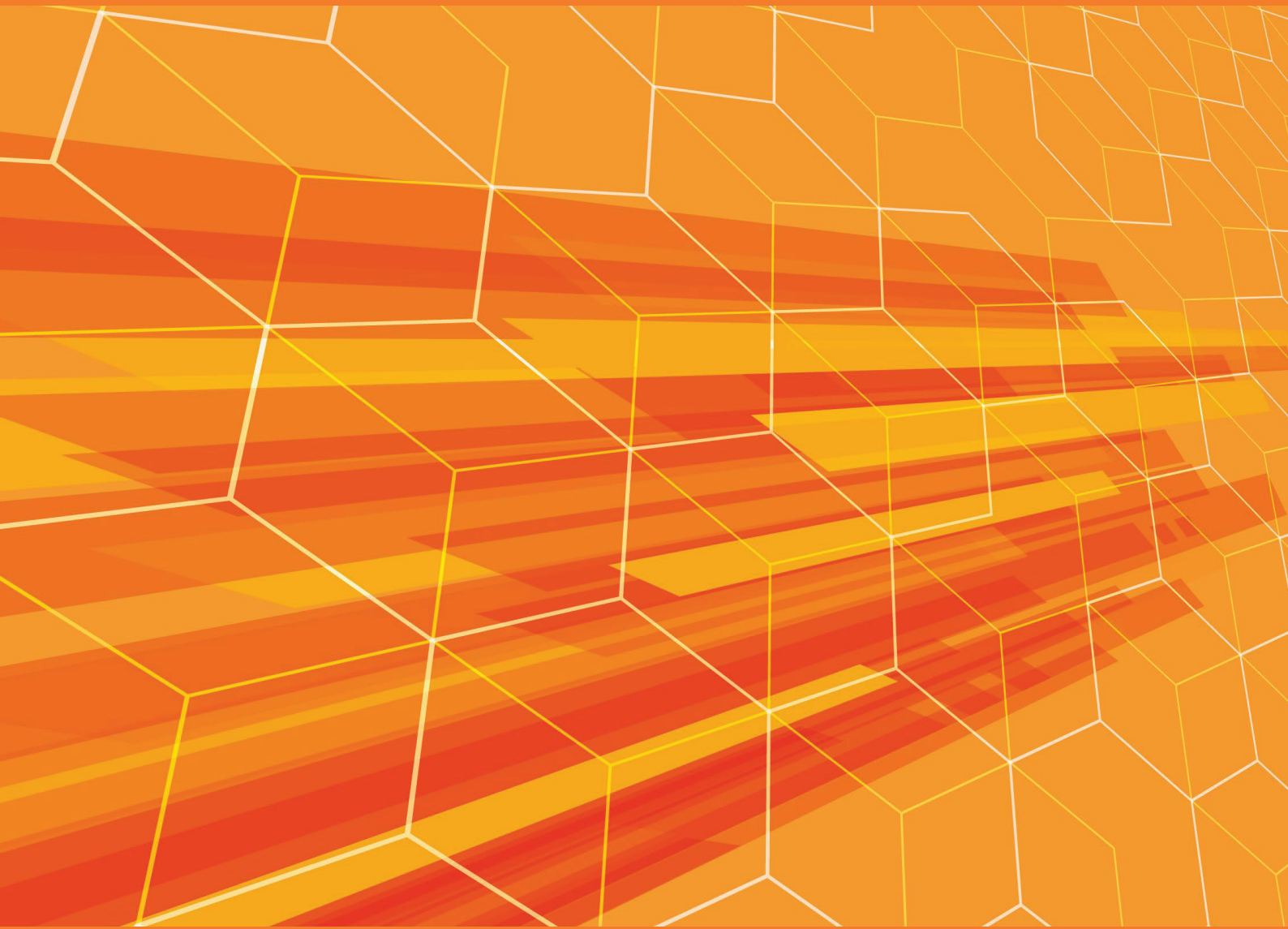


Volume 18 | Number 1 | January-December 2024

# DTI

# Drug Target Insights



ABOUTSCIENCE

**Aims and Scope**

**Drug Target Insights** covers current developments in all areas of the field of clinical therapeutics and focusing on molecular drug targets which include disease-specific proteins, receptors, enzymes, and genes. The journal seeks to elucidate the impact of new therapeutic agents on patient acceptability, preference, satisfaction and quality of life.

**Abstracting and Indexing**

CNKI Scholar  
CrossRef  
DOAJ  
Ebsco Discovery Service  
Embase  
Emerging Sources Citation Index (ESCI)  
Google Scholar  
J-Gate  
OCLC WorldCat  
Opac-ACNP (Catalogo Italiano dei Periodici)  
Opac-SBN (Catalogo del servizio bibliotecario nazionale)  
PubMed Central  
ROAD (Directory of Open Access Scholarly Resources)  
Scilit  
Scimago  
Scopus  
Sherpa Romeo  
Transpose  
Web of Science

**Publication process**

Peer review  
Papers submitted to DTI are subject to a rigorous peer review process, to ensure that the research published is valuable for its readership. DTI applies a single-blind review process and does not disclose the identity of its reviewers.

**Lead times**

Submission to final decision: 6-8 weeks  
Acceptance to publication: 2 weeks

**Publication fees**

All manuscripts are submitted under Open Access terms. Article processing fees cover any other costs, that is no fee will be applied for supplementary material or for colour illustrations. Where applicable, article processing fees are subject to VAT.

**Open access and copyright**

All articles are published and licensed under Creative Commons Attribution-NonCommercial 4.0 International license (CC BY-NC 4.0).

**Author information and manuscript submission**

For full author guidelines and online submission visit [www.aboutscience.eu](http://www.aboutscience.eu)

**EDITORIAL BOARD***Ad interim Editor in Chief***Giulio Zuanetti**

*Milan, Italy*

**Section Editors****Antimicrobial Resistance (AMR)**

Vijay Kothari  
*Nirma University, Ahmedabad - India*

**Natural Products & Phytotherapeutics**

Marcello Iriti  
*Milan State University, Milan - Italy*

**Assistant Editor**

Barbara Bartolini  
*AboutPharma, Milan - Italy*

**Editorial Board**

**Marianna K. Baum PhD** - *Miami, USA*  
**Xiuping Chen PhD** - *Macau, China*  
**Karine Cohen-Solal PhD** - *New Brunswick, USA*  
**Giovanna Lucia Maria Damia PhD** - *Milan, Italy*  
**Neha Jain** - *Kanwar, India*  
**Chad Johnson** - *Baltimore, USA*  
**Chinmayi Joshi** - *Visnagar, India*  
**Anna Koumariou MD PhD** - *Athens, Greece*  
**Salvatore D. Lepore PhD** - *Boca Raton, USA*  
**Andrea Mazzanti** - *Pavia, Italy*  
**Dale G. Nagle PhD** - *Mississippi, USA*  
**Marko Radic PhD** - *Memphis, USA*  
**Emanuele Rezoagli MD** - *Monza (MB), Italy*  
**Raja Solomon Viswas PhD** - *Nagoya, Japan*

**ABOUTSCIENCE**

Aboutscience Srl  
Piazza Duca d'Aosta, 12 - 20124 Milano (Italy)

**Disclaimer**

The statements, opinions and data contained in this publication are solely those of the individual authors and contributors and do not reflect the opinion of the Editors or the Publisher. The Editors and the Publisher disclaim responsibility for any injury to persons or property resulting from any ideas or products referred to in the articles or advertisements. The use of registered names and trademarks in this publication does not imply, even in the absence of a specific statement, that such names are exempt from the relevant protective laws and regulations and therefore free for general use.

**Editorial and production enquiries**  
[dti@aboutscience.eu](mailto:dti@aboutscience.eu)

**Supplements, reprints and commercial enquiries**  
Lucia Steele - email: [lucia.steele@aboutscience.eu](mailto:lucia.steele@aboutscience.eu)

**Publication data**  
eISSN: 1177-3928  
Continuous publication  
Vol. 18 is published in 2024

- 1** Evaluation of non-conformities in the drafting of bulletins for urine cytobacteriological examinations at Sikasso Hospital (Mali)  
*Luka Diarra, Moussa Mariko, Salif Traore, Safi Bazi Dicko, Aboudou Dolo, Moussa Coulibaly, Daouda Sidibé, Moumouni Daou, Hachimi Poma, Madou Traoré, Ibrahim Guindo*
  
- 4** Long-term response with the atypical reaction to nivolumab in microsatellite stability metastatic colorectal cancer: A case report  
*Nataliya Babyshkina, Nataliya Popova, Evgeny Grigoryev, Tatyana Dronova, Polina Gervas, Alexey Dobrodeev, Dmitry Kostromitskiy, Victor Goldberg, Sergei Afanasiev, Nadejda Cherdyntseva*
  
- 8** The dark side of drug repurposing. From clinical trial challenges to antimicrobial resistance: analysis based on three major fields  
*Iyad Y. Natsheh, Majd M. Alsaleh, Ahmad K. Alkhawaldeh, Duaa K. Albadawi, Maisa' M. Darwish, Mohammed Jamal A. Shammout*
  
- 20** RBD mutations at the residues K417, E484, N501 reduced immunoreactivity with antisera from vaccinated and COVID-19 recovered patients  
*Dablu Lal Gupta, Jhasketan Meher, Anjan Kumar Giri, Arvind Kumar Shukla, Eli Mohapatra, Manisha M Ruikar, DN Rao*
  
- 27** Tuberculosis research: Quo vadis  
*Nerges Mistry*
  
- 30** Molecular targets and therapeutic potential of baicalein: a review  
*Kavita Munjal, Yash Goel, Vinod Kumar Gauttam, Hitesh Chopra, Madhav Singla, Smriti, Saurabh Gupta, Rohit Sharma*
  
- 47** In vivo analgesic, anti-inflammatory, sedative, muscle relaxant activities, and docking studies of 3',4',7,8-tetrahydroxy-3-methoxyflavone isolated from *Pistacia chinensis*  
*Abdur Rauf, Umer Rashid, Najla Al Masoud, Zuneera Akram, Anees Saeed, Naveed Muhammad, Taghrid S. Alomar, Saima Naz, Marcello Iriti*
  
- 54** Deciphering the molecular mechanisms underlying anti-pathogenic potential of a polyherbal formulation Enteropan® against multidrug-resistant *Pseudomonas aeruginosa*  
*Sweety Parmar, Gemini Gajera, Nidhi Thakkar, Hanmanthrao S. Palep, Vijay Kothari*
  
- 70** Enhancement of apoptosis in Caco-2, Hep-G2, and HT29 cancer cell lines following exposure to *Toxoplasma gondii* peptides  
*Firooz Shahriyar, Javid Sadraei, Majid Pirestani, Ehsan Ahmadpour*
  
- 78** Levofloxacin induces erythrocyte contraction leading to red cell death  
*Hafiz Muhammad Aslam, Azka Sohail, Ammara Shahid, Maham Abdul Bari Khan, Muhammad Umar Sharif, Razia Kausar, Samia Nawab, Waqas Farooq, Kashif Jilani, Majeeda Rasheed*
  
- 84** Cytotoxic activity, selectivity, and clonogenicity of fruits and resins of Saudi medicinal plants against human liver adenocarcinoma  
*Ali Hendi Alghamdi, Aimun A. E. Ahmed, Mahadi Bashir, Hiadar Abdalgadir, Asaad Khalid, Mohamed E. Abdallah, Riyadh Almainani, Bassem Refaat, Ashraf N. Abdalla*
  
- 94** Investigating the combinatory effect of *Sclerocarya birrea* with doxorubicin against selected colorectal cancer cell lines  
*Thembehle Nxasana, Innocensia Mangoato, Patricia Masiu, Abhay Mishra, Motlalepula Matsabisa*
  
- 105** Faricimab versus the standard of care for neovascular age-related macular degeneration in Italy: an indirect treatment comparison  
*Carlotta Galeone, Federica Turati, Massimo Nicolò, Mariacristina Parravano, Stela Vujosevic, Laura Bianchino, Emilia Sicari, Paolo Lanzetta*



# Evaluation of non-conformities in the drafting of bulletins for urine cytobacteriological examinations at Sikasso Hospital (Mali)

Luka Diarra<sup>1</sup>, Moussa Mariko<sup>1,2</sup>, Salif Traore<sup>3</sup>, Safi Bazi Dicko<sup>4</sup>, Aboudou Dolo<sup>5</sup>, Moussa Coulibaly<sup>6</sup>, Daouda Sidibé<sup>7</sup>, Moumouni Daou<sup>7</sup>, Hachimi Poma<sup>8</sup>, Madou Traore<sup>4</sup>, Ibrahim Guindo<sup>9,10</sup>

<sup>1</sup>Medical Biology Laboratory, Sikasso Hospital, Bamako - Mali

<sup>2</sup>Sikasso Hospital Pharmacy, Sikasso Hospital, Bamako - Mali

<sup>3</sup>Urology Department, Sikasso Hospital, Bamako - Mali

<sup>4</sup>Infectious and Tropical Diseases Department, Sikasso Hospital, Bamako - Mali

<sup>5</sup>Nephrology Department, Sikasso Hospital, Bamako - Mali

<sup>6</sup>Obstetrics and Gynaecology Department, Sikasso Hospital, Bamako - Mali

<sup>7</sup>General Management, Sikasso Hospital, Bamako - Mali

<sup>8</sup>Paediatrics Department, Sikasso Hospital, Bamako - Mali

<sup>9</sup>National Institute of Public Health, Bamako - Mali

<sup>10</sup>Faculty of Technical Sciences and Technology, Bamako - Mali

## ABSTRACT

**Background:** Non-compliance in the drafting of examination bulletins makes it difficult to perform them and interpret the results. With the aim of continuously improving laboratory services and guaranteeing the quality of urine cytobacteriological examination (ECBU) results, we initiated this study to evaluate non-compliance in the drafting of ECBU reports.

**Materials and methods:** This was a retrospective descriptive cross-sectional study which focused on non-compliance in the drafting of ECBU reports analysed in the laboratory from January to December 2022.

**Results:** During the study period, we collected 383 non-compliant ECBU reports out of 672, with a frequency of 56.99%. Non-compliances were related to age (2.68%), profession (24.40%), clinical information (6.70%) and residence (52.08%). The majority of non-compliant reports came from the medicine (35.51%) and urology (25.85%) departments.

**Conclusion:** The high frequency of non-compliance is a cause for concern and is of concern to all prescribers in this hospital.

**Keywords:** Bulletins, ECBU, Mali, Non-compliance, Sikasso

## Introduction

A biological test report is a medical prescription for diagnostic purposes, specifying the parameter to be measured, in relation to the diagnostic hypothesis envisaged, and all the information needed for the laboratory to carry out the test correctly (1). Non-compliance in the prescription of medical

biology tests makes it difficult to carry them out and interpret the results (2). A number of researchers have concluded that non-compliance has a number of possible consequences for patients, such as misdiagnosis, mismanagement and treatment, as well as therapeutic abstention (3). In Burkina Faso, 59.4% of non-compliances concerning clinical information were reported in a study in 2021 (2). In Niger, Djobo et al recorded 53.99% of non-compliances concerning failure to notify the name of the service on biological examination forms (4). In Mali, 41% of non-compliances concerning clinical information were found (5). With a view to continuous quality improvement and guaranteeing the quality of urine cytobacteriological examination (ECBU) results, we initiated this study with the aim of evaluating non-compliance in the drafting of ECBU reports analysed at the Sikasso Hospital laboratory.

**Received:** September 25, 2023

**Accepted:** November 30, 2023

**Published online:** January 16, 2024

**Corresponding author:**

Luka Diarra

lukadiarra@yahoo.fr



**Materials and methods**

**Study design and population**

This was a retrospective descriptive cross-sectional study of non-compliance in the completion of ECBU reports at Sikasso Hospital from January to December 2022. The study population consisted of reports containing the ECBU analysed in the laboratory during the study period. Data were collected from examination request forms and the laboratory register.

**Inclusion criteria**

All bulletins with ECBU analysed at the hospital laboratory were included in this study.

**Non-inclusion criteria**

All reports of ECBU analysed in other laboratories, as well as reports of biological examinations other than ECBU were not included.

**Study variables**

The study variables were age, sex, occupation, clinical information and place of residence.

**Statistical analysis**

Excel 2013 and Epi Info 7.2.1.0 were used for statistical analysis of the data.

**Ethical considerations**

Anonymity was preserved before each inclusion.

**Results**

During the study period, we identified 383 non-compliant reports out of 672, with a frequency of 56.99%. The non-compliances identified were related to age, profession, clinical information and residence (Tab. I).

**TABLE I** - Frequency of non-compliance by age, profession, clinical information and residence

Variables	Number	Frequency (%)
<b>Non-compliance by age</b>		
Yes	18	2.68
No	654	97.32
<b>Non-compliance by profession</b>		
Yes	164	24.40
No	508	75.60
<b>Non-compliance by clinical information</b>		
Yes	45	6.70
No	627	93.30
<b>Non-compliance by residence</b>		
Yes	350	52.08
No	322	47.92

The majority of non-compliance bulletins came from the medicine (35.51%) and urology (25.85%) departments (Fig. 1).

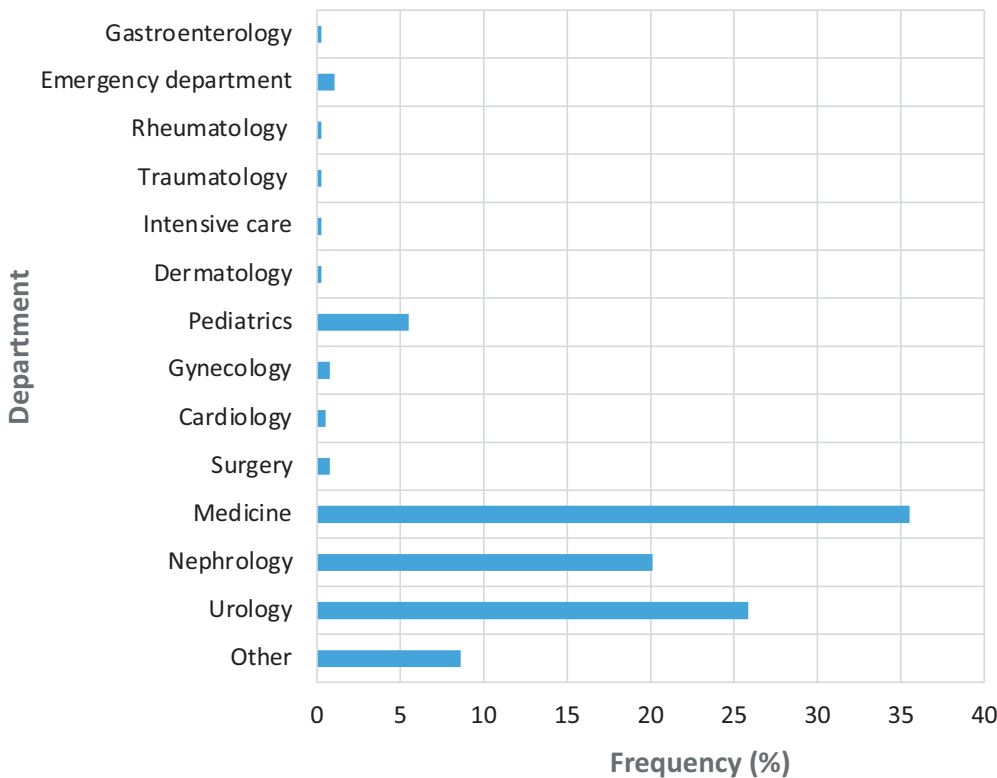


**Fig. 1** - Breakdown of non-compliant forms by department.



The non-compliances concerning age were 35.29% for the medicine department and 29.41% for the urology department. The lack of information on prescriptions in the urology department was 41.98%, and 21.60% in the nephrology department. The absence of clinical information was frequent on the urology department forms (44.19%). Non-compliances concerning residence accounted for 39.08% for medicine and 22.70% for urology.

### Study limitations

The non-conformities concerned only ECBU bulletins, which justifies their high frequency during the course of this work.

### Discussion

Prescription is the result of careful consideration, taking into account the epidemiological and clinical context on the one hand, and precise knowledge of what can be expected from the examination on the other (6). ECBU reports received during the course of this study were 56.99% non-compliant. Yacouba et al in Burkina Faso reported a non-compliant rate of 5.2% (2). Our result could be explained by the size of our sample, which was not large enough, and by the fact that the study was limited to ECBU reports. The majority of non-compliant reports came from medicine (35.51%) and urology (25.85%) departments. Djobo et al found 3.64% and 1.33%, respectively, for the medicine and urology departments (4). This could be explained by automatic prescribing, which is often based on personal habits rather than established protocols (6). In our study, non-compliance relating to clinical information accounted for 6.70%. This proportion is lower than that reported by Djobo et al, who found the rate to be 46.63%. This situation could be explained by the lack of awareness of the importance of this parameter in the interpretation of ECBU by several of our prescribers (4). Including clinical and therapeutic information can help the biologist in choosing the technique to be used, or lead him/her to advise against a costly investigation and suggest a more appropriate one (2). Age was missing from 2.68% of the forms in our study. This low rate confirms our prescribers' mastery of the impact of this parameter in interpreting the results (2). Those with no occupation or residence accounted for 24.40% and 52.08%, respectively. These socio-demographic parameters are one of the factors that will add value to our knowledge of the factors that contribute to urinary tract infections. Reporting them on ECBU reports will be of epidemiological interest.

### Conclusion

This study has provided information on the completeness of ECBU reports. The high frequency of non-compliance is a

cause for concern and is of concern to all prescribers in the hospital. Close collaboration between prescribers and biologists would help to control non-compliance in the drafting of examination reports.

### Conflicts of interest

The authors declare that they have no competing interests.

### Authors' contributions

Luka Diarra collected the data and wrote the article. Moussa Mariko contributed to the data analysis. All other authors reviewed and approved the final manuscript.

### Funding

The authors received no funding for this work.

### Acknowledgements

The authors sincerely thank all the staff of Sikasso Hospital for their contributions. Special thanks to the general management of the hospital for their support throughout the process.

---

### References

1. Adeoti MF, Silue A, Sawadogo D, Dosso M, Sess ED. Reflection on good practice in writing the medical analysis bulletin. *Immunol Anal Biol Spec.* 2004;19(6):370-373. [Online CrossRef](#)
2. Yacouba A, Kiello K, Kiba-Koumare TCRA, Kabre E, Sakande J. Writing quality of the laboratory request forms at Yalgado Ouédraogo teaching hospital, Burkina Faso. *Int J Biol Chem Sci.* 2019;13(6):2683-2690. [Online CrossRef](#)
3. Jnah A, Yagoubi M, Seffar M, El Hamzaoui S, Hamamouchi J, Zouhdi M. Control of non-conformities in the pre-analytical phase at the Bacteriology Laboratory of the Ibn Sina University Hospital in Rabat (Morocco). *Tunis Med.* 2022;100(3):247-254. [Online PubMed](#)
4. Djobo K, Yacouba A, Alhousseini D, et al. Multicentre analysis of the editorial quality of biological analysis bulletins in Niger. *Pan Afr Med J.* 2022;43(59). [Online](#)
5. Bahachimi A. Pre-analytical non-conformities in the biomedical laboratory of the Mali hospital 2020. [Online](#)
6. Gérôme P, Dusseau JY, Masseron T, Bercion R. The pre-analytical phase in bacteriology. *Revue Française des Laboratoires.* 2001;2001(335):23-30. [Online CrossRef](#)



# Long-term response with the atypical reaction to nivolumab in microsatellite stability metastatic colorectal cancer: a case report

Nataliya Babyshkina<sup>1,2</sup>, Nataliya Popova<sup>3</sup>, Evgeny Grigoryev<sup>4</sup>, Tatyana Dronova<sup>1</sup>, Polina Gervas<sup>1</sup>, Alexey Dobrodeev<sup>5</sup>, Dmitry Kostromitskiy<sup>5</sup>, Victor Goldberg<sup>3</sup>, Sergey Afanasiev<sup>5</sup>, Nadejda Cherdyntseva<sup>1</sup>

<sup>1</sup>Department of Molecular Oncology and Immunology, Cancer Research Institute, Tomsk National Research Medical Center, Russian Academy of Sciences, Tomsk - Russian Federation

<sup>2</sup>Siberian State Medical University, Tomsk - Russian Federation

<sup>3</sup>Department of Chemotherapy, Cancer Research Institute, Tomsk National Research Medical Center, Russian Academy of Sciences, Tomsk - Russian Federation

<sup>4</sup>Department of Diagnostic Imaging, Cancer Research Institute, Tomsk National Research Medical Center, Russian Academy of Sciences, Tomsk - Russian Federation

<sup>5</sup>Department of Abdominal Oncology, Cancer Research Institute, Tomsk National Research Medical Center, Russian Academy of Sciences, Tomsk - Russian Federation

## ABSTRACT

Immunotherapy has become an integral part of a comprehensive treatment approach to metastatic colorectal cancer (mCRC). Nivolumab (Opdivo) is a human immunoglobulin G4 monoclonal antibody that blocks the interaction between the programmed cell death 1 (PD-1) receptor and its ligands 1/2 (PD-L1/PD-L2), leading to inhibition of T-cell proliferation, cytokine secretion, and enhanced immune response. The US Food and Drug Administration (FDA) has approved this drug for use in high microsatellite instability (MSI-high)/deficiencies in mismatch repair (dMMR) advanced CRC patients. However, its efficacy is extremely limited in microsatellite stability (MSS)/mismatch repair proficient (pMMR) patients. We report a case of a 42-year-old man diagnosed with MSS/pMMR mCRC who has achieved a durable response to nivolumab after a progression under chemotherapy with antiangiogenic treatment. We observed for the first time an atypical response after 8 months of nivolumab treatment, with the regression of previous primary pulmonary lesions and the presence of new para-aortic lymph node lesions. This report demonstrates that a subset of pretreated mCRC patients with the MSS/pMMR phenotype may benefit from nivolumab and these patients need more attention.

**Keywords:** Dissociated response, iRECIST, Metastatic colorectal cancer, Microsatellite stability, Nivolumab

## Background

Immunotherapy has become an integral part of a comprehensive treatment approach to metastatic colorectal cancer (mCRC). Nivolumab, one of the first immune checkpoint inhibitors, was approved by the US Food and Drug Administration (FDA) in 2017 for use in patients whose tumors harbor deficient mismatch repair (dMMR), or high microsatellite

instability (MSI-high) and have progressed after conventional chemotherapy. The nivolumab action is directed at the programmed cell death 1 (PD-1) receptor, a member of the CD28 superfamily, which is expressed on the surface of activated T and B lymphocytes. Activation of PD-1/programmed cell death ligands 1/2 (PD-L1/PD-L2) on the tumor and the tumor microenvironment leads to enhanced immunosuppressive effects (1). Nivolumab binds to the PD-1 receptor and blocks its interaction with PD-L1 and PD-L2, inhibiting the PD-1-mediated immune response.

Nivolumab approval was based on data from CheckMate 142 multicenter phase 2 study investigating its efficacy and safety in the cohort of MSI-high/dMMR mCRC patients who had progressed during or after prior treatment with a fluoropyrimidine-, oxaliplatin-, or irinotecan-based chemotherapy. In this study, 68.9% of patients responded to treatment, with 31.1% achieving an objective response rate (2).

**Received:** July 19, 2023

**Accepted:** January 8, 2024

**Published online:** January 23, 2024

## Corresponding author:

Nataliya Babyshkina  
nbabyshkina@mail.ru



Further studies have confirmed that nivolumab provides a long-term overall survival in MSI-high/dMMR mCRC (3). Recent clinical trials data suggest that the combination of nivolumab with multikinase or histone deacetylase inhibitors demonstrates promising synergistic activity in patients with microsatellite stability (MSS)/mismatch repair proficient (pMMR) mCRC, which is detected in approximately 95% of all mCRC cases (4,5). However, the molecular features of MSS/pMMR that lead to enhanced tumor immunogenicity and sensitivity to immune checkpoint inhibitors are to be discussed.

The use of immune checkpoint inhibitors, including nivolumab, has introduced new atypical response patterns, such as dissociated response. The most common definition of a dissociated response is the coexistence of both responding and non-responding lesions within the same patient (6). However, there is no established terminology as well as standard criteria of definition for dissociated response; different terms such as mixed or heterogeneous response are used. Although various types of dissociated response to nivolumab have been described in many solid tumors (7-9), there are no data regarding such response in mCRC patients with MSS/pMMR phenotype.

Here we report a case diagnosed with MSS/pMMR mCRC who has achieved a durable response to nivolumab with atypical reaction after progression following first- and second-line chemotherapy with antiangiogenic therapy.

**Case report**

**Patient information**

A 42-year-old man, never smoker, with abdominal pain accompanied by nausea was taken by ambulance to the local hospital in August 2017, where intestinal obstruction was verified. His medical history included chronic cholecystitis, chronic pancreatitis, and mixed etiology of hepatitis. The patient underwent abdominal stoma surgery. Biopsy revealed a highly differentiated adenocarcinoma. The patient independently visited Tomsk Cancer Research Institute for further

examination, where he underwent left hemicolectomy and colostomy suturing. Pathologic verification of resection specimens confirmed moderately differentiated adenocarcinoma with mucinous features and foci of severe fibrosis, as well as comedo necrosis and with an accompanying lymphocytic infiltrate and invasion into the serous membrane. The patient was diagnosed with splenic flexure colon cancer, T4N3M0, stage IIIC. However, a month later, during an additional examination in October 2017, supraclavicular lymph node metastases on both sides were detected. Due to definitive evidence of disseminated disease, the patient was upstaged to stage IV. Molecular testing of the tumor revealed the KRASp.G12D mutation.

**MSS/pMMR phenotype**

Immunohistochemistry analysis of MMR protein expression (MLH1, MSH2, MSH6, and PMS2) demonstrated a homogeneous pattern of their proficiency in colon tumor tissue (Fig. 1A). Polymerase chain reaction (PCR) assay confirmed the MSS phenotype for three different colon tumor specimens (Fig. 1B). With respect to PD-L1 status, a weak expression (TPS-1% and CPS-6.0) in several colon tumor specimens was independently detected by two researchers.

**Chemotherapeutic intervention**

Patient was started on a first-line FOLFOX plus bevacizumab regimen, which consisted of bevacizumab 5 mg/kg on day 1, oxaliplatin 85 mg/m<sup>2</sup> on day 1, leucovorin 400 mg/m<sup>2</sup> on day 1, and 5-fluorouracil 400 mg/m<sup>2</sup> bolus injection followed by 46-hour continuous infusion of 5-fluorouracil 2,400 mg/m<sup>2</sup> on day 1. After four cycles of treatment, the partial response per RECIST 1.1 was recorded. In June 2018, the patient completed 14 cycles of chemotherapy and following the chest computed tomography (CT) images showed the appearance of randomly located focal nodules of up to 7 mm in size consistent with lung metastases. The levels of tumor markers such as CEA, CA19-9, and CA242 did not exceed the

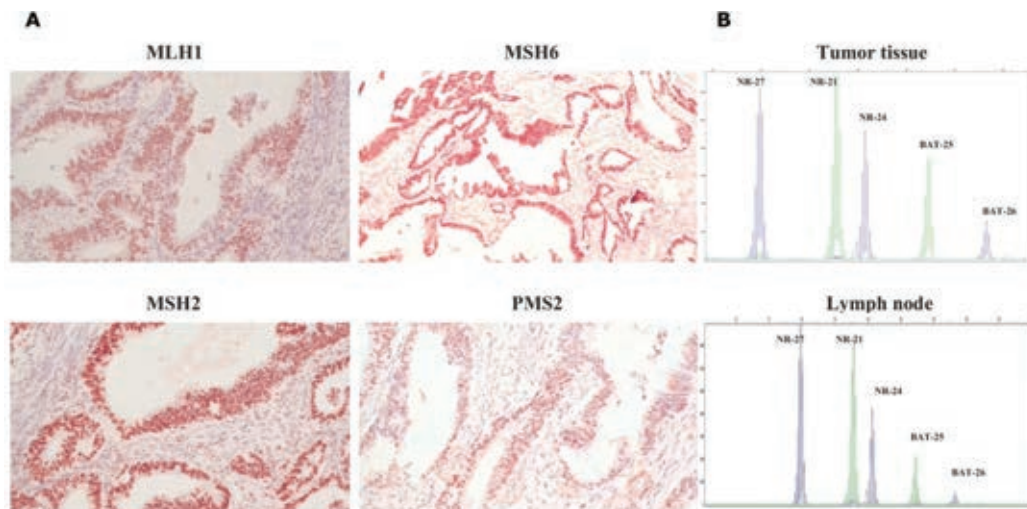


**Fig. 1** - Immunohistochemical staining of MMR proteins. Positive expression of MLH1, MSH2, MSH6, and PMS2 in the colon tumor tissue (magnification ×200) (A); MSI test electropherograms with NR-27, NR-21, NR-24, BAT25, and BAT26 markers in the colon tumor and lymph node specimens (B). MMR = mismatch repair; MSI = microsatellite instability.



normal values, being 0-3.40 ng/mL for CEA, 0-34 U/mL for CA19-9, and 0-20.0 U/mL for CA242.

Second-line treatment with FOLFIRI and aflibercept (aflibercept 4 mg/kg on day 1, irinotecan 180 mg/m<sup>2</sup> on day 1, leucovorin 400 mg/m<sup>2</sup> on day 1, 5-fluorouracil 400 mg/m<sup>2</sup> bolus injection followed by 46-hour continuous infusion of 5-fluorouracil 2,400 mg/m<sup>2</sup>) was initiated. Repeat CT images after three cycles showed no growth of focal nodules in the lung. This treatment was associated with adverse events such as of grade 2 hypertension, nausea, and thrombocytopenia. CT assessment after seven cycles of treatment confirmed a stable response. Due to an acute exacerbation of mixed etiology hepatitis (chronic hepatitis B with serum hepatitis B virus DNA titer >10<sup>5</sup> copies/mL and toxic hepatitis) and an abnormal alanine aminotransferase exceeding nine times the upper limit of normal at baseline, subsequent treatment was interrupted. The patient received hepatoprotective and detoxification treatment. Approximately 2 months later, CT scans showed an increase of nodule size in the lung (Fig. 2A).

### Nivolumab administration

Given the fast progression and PD-L1 status, treatment with nivolumab at a dose 240 mg was started in December 2018. Three months later, most of the previously identified focal nodules in the lung were not clearly visualized by CT, the remaining lesions decreased in size up to 1-2 mm. In May 2019, chest CT scans confirmed the reduction of lung nodules (Fig. 2B). However, a para-aortic lymph node (PALN) on the left up to 15×12 mm was found (Fig. 2C). Using the iRECIST as a modified immune RECIST criterion (10), the response was classified as a dissociated response. MSS phenotype in lymph node was further verified by PCR (Fig. 1B).

Further administration of nivolumab allowed achieving positive dynamics in terms of the disappearance of lesions in the lung (Fig. 2D) and the absence of the growth of PALN metastases in August 2019 (Fig. 2E). An immune stable disease (iSD) per iRECIST was recorded until September 2021, when we had to discontinue treatment due to the patient being infected with COVID-19. The administration of nivolumab was resumed;

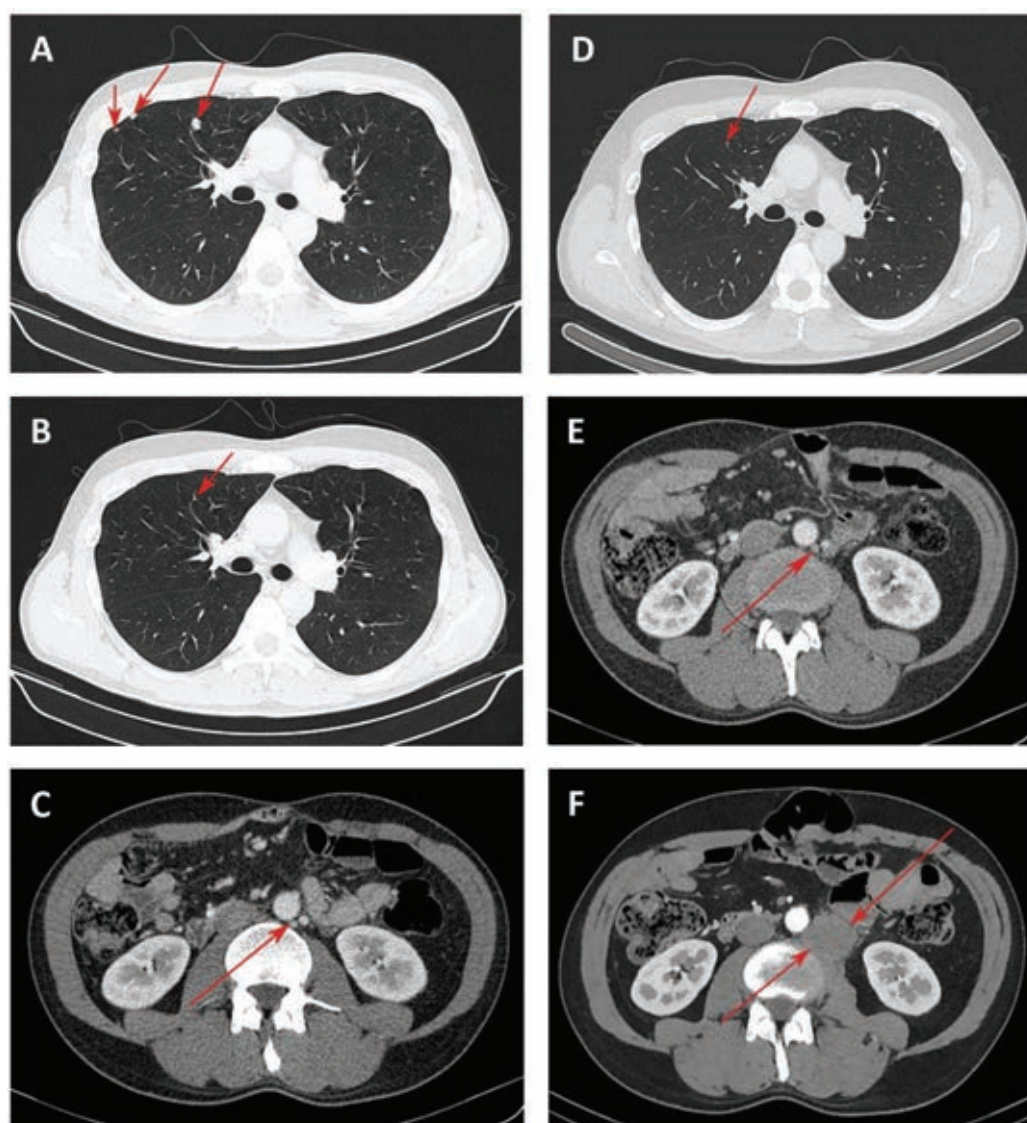


**Fig. 2** - Chest computed tomography (CT) of the lung lesions and para-aortic lymph node lesion. Focal nodules in the lung at start of nivolumab treatment (A); 5 months after nivolumab treatment, reduction of lung nodules (B) and para-aortic lymph node lesion up to 12 mm (C); 8 months after nivolumab treatment, disappearance of lung lesions (D) and lack of growth of para-aortic lymph node lesion (E); increase of para-aortic lymph node lesion 40 months after nivolumab treatment (F).

however, in April 2022, CT scans revealed an increase in the size of PALN by 7 mm compared with the baseline (Fig. 2F). The decision to initiate FOLFOX plus bevacizumab therapy (bevacizumab 5 mg/kg on day 1, oxaliplatin 85 mg/m<sup>2</sup> on day 1, leucovorin 400 mg/m<sup>2</sup> on day 1, and 5-fluorouracil 400 mg/m<sup>2</sup> bolus injection followed by 48 hours continuous infusion of 5-fluorouracil 2,400 mg/m<sup>2</sup> on day 1) was taken by a multidisciplinary staff. Due to the experience of hypersensitivity reaction to oxaliplatin after three cycles, the patient was switched to the bevacizumab in combination with capecitabine regimen (bevacizumab 5 mg/kg and capecitabine 2,500 mg/day, days 1 and 14). Currently, the patient has completed 10 cycles of this therapy with good tolerance.

## Conclusion

We have reported a patient with MSS/pMMR mCRC who has achieved a complete response to nivolumab after a progression on chemotherapy and antiangiogenic treatment, with a response duration of 32 months. Based on the presence of PD-L1 weak expression, the potential immunogenic features of the tumor leading to benefit from PD-1/PD-L1 targeting therapy could be suggested. Present case report demonstrates that a subset of pretreated mCRC patients with MSS/pMMR phenotype may benefit from nivolumab. We will undertake a high-throughput transcriptome sequencing of both colon tumor and lymph node specimens to establish possible molecular background for a dissociated response.

## Disclosures

Conflict of interest: The authors have no conflicts of interest to declare that are relevant to the content of this article.

Ethical approval: This study was performed in line with the principles of the Helsinki Declaration. Approval was granted by the Ethics Committee of the Cancer Research Institute, Tomsk National Research Medical Center (Date: 01/19/22).

Informed consent: Written informed consent was obtained from the patient.

Financial support: The study was supported by the Russian Science Foundation, grant #22-15-00212; [Online](#).

## Author contributions

All authors contributed to the study conception and design. Material preparation, data collection, and analysis were performed by Evgeny Grigoryev, Tatyana Dronova, Polina Gervas, Alexey Dobrodeev, Dmitry Kostromitskiy, Victor Goldberg, and Sergey Afanasiev. The first draft of the

manuscript was written by Nataliya Babyskhina and Nataliya Popova, and all authors commented on previous versions of the manuscript. All authors read and approved the final manuscript.

## References

1. Xiao Y, Freeman GJ. The microsatellite instable subset of colorectal cancer is a particularly good candidate for checkpoint blockade immunotherapy. *Cancer Discov.* 2015;5(1):16-18. [CrossRef](#) [PubMed](#)
2. Overman MJ, McDermott R, Leach JL, et al. Nivolumab in patients with metastatic DNA mismatch repair-deficient or microsatellite instability-high colorectal cancer (CheckMate 142): an open-label, multicentre, phase 2 study. *Lancet Oncol.* 2017;18(9):1182-1191. [CrossRef](#) [PubMed](#)
3. Overman MJ, Bergamo F, McDermott RS, et al. Nivolumab in patients with DNA mismatch repair-deficient/microsatellite instability-high (dMMR/MSI-H) metastatic colorectal cancer (mCRC): Long-term survival according to prior line of treatment from CheckMate-142. *J Clin Oncol.* 2018;36(4\_suppl):554-554. [CrossRef](#)
4. Fakhri M, Raghav KPS, Chang DZ, et al. Regorafenib plus nivolumab in patients with mismatch repair-proficient/microsatellite stable metastatic colorectal cancer: a single-arm, open-label, multicentre phase 2 study. *EClinicalMedicine.* 2023;58:101917. [CrossRef](#) [PubMed](#)
5. Saunders MP, Graham J, Cunningham D, et al. CXD101 and nivolumab in patients with metastatic microsatellite-stable colorectal cancer (CAROSELL): a multicentre, open-label, single-arm, phase II trial. *ESMO Open.* 2022;7(6):100594. [CrossRef](#) [PubMed](#)
6. Humbert O, Chardin D. Dissociated response in metastatic cancer: an atypical pattern brought into the spotlight with immunotherapy. *Front Oncol.* 2020;10:566297. [CrossRef](#) [PubMed](#)
7. Wong A, Vellayappan B, Cheng L, et al. Atypical response patterns in renal cell carcinoma treated with immune checkpoint inhibitors-navigating the radiologic potpourri. *Cancers (Basel).* 2021;13(7):1689. [CrossRef](#) [PubMed](#)
8. Tazdait M, Mezquita L, Lahmar J, et al. Patterns of responses in metastatic NSCLC during PD-1 or PDL-1 inhibitor therapy: comparison of RECIST 1.1, irRECIST and iRECIST criteria. *Eur J Cancer.* 2018;88:38-47. [CrossRef](#) [PubMed](#)
9. Sato Y, Morimoto T, Hara S, et al. Dissociated response and clinical benefit in patients treated with nivolumab monotherapy. *Invest New Drugs.* 2021;39(4):1170-1178. [CrossRef](#) [PubMed](#)
10. Seymour L, Bogaerts J, Perrone A, et al; RECIST working group. iRECIST: guidelines for response criteria for use in trials testing immunotherapeutics. *Lancet Oncol.* 2017;18(3):e143-e152. [CrossRef](#) [PubMed](#)



# The dark side of drug repurposing. From clinical trial challenges to antimicrobial resistance: analysis based on three major fields

Iyad Y. Natsheh<sup>1</sup>, Majd M. Alsaleh<sup>1,2</sup>, Ahmad K. Alkhalaf<sup>1</sup>, Duaa K. Albadawi<sup>1</sup>, Maisa' M. Darwish<sup>2,3</sup>, Mohammed Jamal A. Shammout<sup>4</sup>

<sup>1</sup>Department of Medical Applied Sciences, Zarqa University College, Al-Balqa Applied University, Salt - Jordan

<sup>2</sup>Department of Biology, School of Science, University of Jordan, Amman - Jordan

<sup>3</sup>National Agricultural Research Center, Amman - Jordan

<sup>4</sup>Chemistry Department, Faculty of Science, Applied Science Private University, Amman - Jordan

## ABSTRACT

Drug repurposing is a strategic endeavor that entails the identification of novel therapeutic applications for pharmaceuticals that are already available in the market. Despite the advantageous nature of implementing this particular strategy owing to its cost-effectiveness and efficiency in reducing the time required for the drug discovery process, it is essential to bear in mind that there are various factors that must be meticulously considered and taken into account. Up to this point, there has been a noticeable absence of comprehensive analyses that shed light on the limitations of repurposing drugs. The primary aim of this review is to conduct a thorough illustration of the various challenges that arise when contemplating drug repurposing from a clinical perspective in three major fields—cardiovascular, cancer, and diabetes—and to further underscore the potential risks associated with the emergence of antimicrobial resistance (AMR) when employing repurposed antibiotics for the treatment of noninfectious and infectious diseases. The process of developing repurposed medications necessitates the application of creativity and innovation in designing the development program, as the body of evidence may differ for each specific case. In order to effectively repurpose drugs, it is crucial to consider the clinical implications and potential drawbacks that may arise during this process. By comprehensively analyzing these challenges, we can attain a deeper comprehension of the intricacies involved in drug repurposing, which will ultimately lead to the development of more efficacious and safe therapeutic approaches.

**Keywords:** Thalidomide, Levofloxacin, Minocycline, Doxycycline, Azithromycin, Hydroxychloroquine

## Introduction

Drug repurposing, otherwise referred to as drug repositioning, is a tactical attempt encompassing the identification of novel therapeutic applications for already existing pharmaceuticals. It presents itself as a highly advantageous strategy due to its cost-effective nature and ability to save time in the drug discovery process, all while mitigating the risks of failure as opposed to customary approaches (1). Drug repurposing is an extremely advantageous technique in the field of pharmaceutical research because it capitalizes on

the unintentional off-target effects of extant medications (2). This novel approach includes the use of pharmaceuticals that have previously been approved, drugs that have been declared ineffective in clinical trials, and drugs that have been removed from the market for a variety of reasons (3). By venturing into the realm of drug repurposing, researchers can unlock a vast reservoir of therapeutic potential that has hitherto remained untapped.

However, the question posed by several readers, researchers, and patients is as follows: “Have any drugs that have been repurposed actually received approval for their new indications?” At first, one may find oneself engaged in confident mental processes, but with an impassive countenance, while seeking to recall enough examples to confirm the current reaction. Still, a memorable case, such as thalidomide, will spring to mind (4). The drug, infamously recognized in its devastating original form as a sedative and curative for morning sickness, returned to the medical world for the treatment of leprosy and, subsequently, multiple

**Received:** January 2, 2024

**Accepted:** April 18, 2024

**Published online:** May 10, 2024

**Corresponding author:**

Majd M. Alsaleh

email: [majd.alsaleh@bau.edu.jo](mailto:majd.alsaleh@bau.edu.jo)



myeloma (5). It is worth noting that the discovery of thalidomide's efficacy in treating leprosy, specifically erythema nodosum leprosum, was a serendipitous occurrence (6). The story behind this accidental discovery is recounted in the book *Dark Remedy*. In this tale, a physician administered the only sedative available in the hospital's pharmacy, which had not been previously attempted, to a suffering leprosy patient. Astonishingly, the drug had a dramatic and unexpected effect on the patient's condition (7). This is a perfect example of repurposing a medicine that was authorized and then abandoned (and the method in which it was abandoned) to treat a completely other ailment (8). Another example of drug repurposing that is widely recognized is sildenafil, which is also commonly known as Viagra. Initially, this medication was prescribed for the treatment of arterial narrowness, hypertension, and heart disease in both humans and animals. However, it was fortuitously discovered that sildenafil has beneficial effects on erectile tissue dysfunction in male genital organs (9). Following its approval by the US Food and Drug Administration (FDA) in 1998, sildenafil has brought about a significant transformation in the management of erectile dysfunction (ED) and has contributed to a deeper comprehension of the underlying scientific principles behind ED and its impact on men's overall well-being (10). In addition to its application in treating ED, sildenafil has also demonstrated efficacy in addressing pulmonary arterial hypertension (PAH) (11). Early investigations and clinical trials have explored the potential favorable impacts of sildenafil on various organs, including the heart, liver, kidney, brain, and intestines (12). Nevertheless, further research is necessary in order to fully comprehend the effects of sildenafil on different diseases and organs (13). Despite the numerous obstacles and unsuccessful attempts that we have elaborated on in the preceding sections, there have been instances of drug repurposing that have achieved success. Notable examples include the utilization of zidovudine (azidothymidine, AZT) as a therapeutic agent against human immunodeficiency virus (HIV) (14) and the repurposing of tocilizumab for the treatment of COVID-19 (15). The practice of repurposing drugs has demonstrated its effectiveness in the development of therapeutic strategies for various diseases and holds promise in addressing rare and difficult conditions (3). This approach entails a combination of experimental and computational methods, leveraging existing safety data and redirecting the application of drugs based on validated target molecules (16). The utilization of Application Programming Interfaces (APIs) in drug repurposing is increasingly being acknowledged as a promising technique for expediting the process of drug discovery and development (17). Integrative approaches that extract data from multiple sources through APIs offer the advantages of adaptability, reusability, and transparency (18). One particular study outlined a strategy for ligand-based in silico drug repurposing utilizing the analytical platform KNIME, which entailed targeted data retrieval, data curation, and substructure searches in DrugBank and other databases (19). Another study developed a fully automated and parameter-free virtual screening server called DrugRep, which conducted molecular structure construction, docking, similarity comparison, and binding affinity screening in a completely

autonomous manner (20). These computational tools furnish researchers with user-friendly interfaces and interactive predictions, thereby enhancing the accessibility and efficiency of drug repurposing (21). Through the optimization of the therapeutic potential of already existing drugs, drug repurposing enhances the likelihood of attaining successful outcomes and offers a means to promptly identify effective treatments (22). Thinking deeply, we can conclude that the development of repurposed medications necessitates the application of creativity and innovation in designing the development program, as the body of evidence differs for each individual case not depending on the chance (23).

Several research studies have focused their attention on investigating and understanding the potential advantages and positive outcomes associated with the practice of drug repurposing. However, it is worth noting that, up until now, there has been a lack of comprehensive reviews that shed light on the potential drawbacks and negative aspects of drug repurposing. Therefore, the main aim of this particular review is to provide an in-depth analysis and exploration of the various challenges that arise when considering drug repurposing from a clinical perspective in the fields of cardiovascular disease, cancer, and diabetes. Additionally, the primary objective of this analysis is to underscore the heightened risk associated with the development of AMR that arises from the utilization of antibiotics for purposes other than their original intended use, whether it be for treating various infectious diseases or noninfectious conditions that deviate from their initial approved indications.

### Drug repurposing challenges in clinical view

The process of drug repurposing has a number of drawbacks. One key barrier is the pharmaceutical industry's restricted focus on diseases that provide more financial rewards, lowering the amount of repurposing chances for orphan diseases and neglected tropical disorders (24). Furthermore, there are legal concerns surrounding repurposed medications, including restricted patent coverage and obstacles encountered during the execution of clinical trials, both of which decrease the likelihood of success (25). It is imperative to address additional challenges that require attention, such as the generation of false-positive signals during data mining and the vulnerability of hypothesis validation to bias and confounding (26). Moreover, the absence of clear regulatory guidance poses yet another hindrance in the field of drug repurposing (27). Despite the inherent advantages of this technique, such as cheaper costs and faster time frames, it is crucial to recognize substantial failures found during clinical trials, when the repurposed medicine may fail to exhibit a good balance of benefits and risks (28). Consequently, a comprehensive analysis of these challenges and limitations must precede the pursuit of drug repurposing strategies.

### Challenges in cardiovascular endeavor

The clinical perspective on drug repurposing has faced numerous challenges and trials that have not been successful. Despite the potential benefits of repurposing current



drugs for unique applications, there are specific limitations that hinder success in this endeavor. These limitations encompass a lack of resources, difficulties with accessing data, and concerns regarding personnel, all of which can impede the process of drug profiling (29). Within the realm of cardiovascular disease, repurposing anti-inflammatory medicines has proven to be challenging due to unforeseen consequences and the necessity for prolonged therapy (30). In a study conducted by Ridker et al (31), it was found that the repurposing of the therapeutic agent canakinumab possesses the capacity to induce unfavorable outcomes, which encompasses the occurrence of neutropenia as well as an elevated susceptibility to mortality specifically attributed to infection or sepsis, as illustrated in Figure 1.

Another instance exemplified in Figure 1 arises when etanercept is employed as a repurposed therapeutic agent for the management of cardiovascular ailments. The clinical trials were terminated prematurely due to the conspicuous absence of any discernible benefit (32). In the same domain, another agent, colchicine, which had been repurposed, was subjected to different clinical trials as illustrated in Figure 2. These trials brought to light a noteworthy escalation in adverse gastrointestinal symptoms and an increased vulnerability to pneumonia (33,34). Moreover, it is important to note

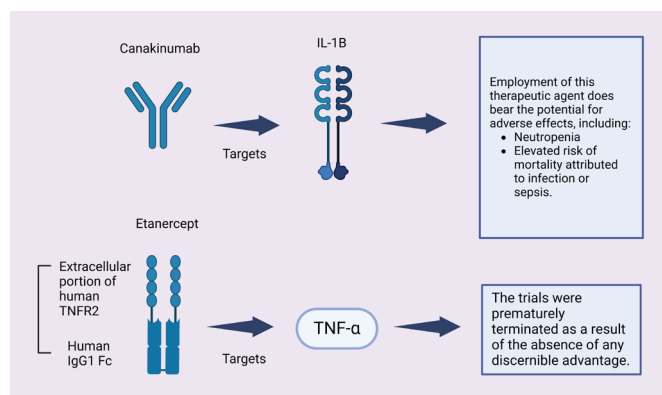


**FIGURE 1** - Examples on drug repurposed in cardiovascular endeavor. Canakinumab (ACZ885, Ilaris), a monoclonal antibody targeting human anti-interleukin-1 $\beta$ , has been developed by Novartis (37). In June 2009, the US Food and Drug Administration granted approval for its use in the treatment of familial cold autoinflammatory syndrome and Muckle-wells syndrome, both of which pertain to cryopyrin-associated periodic syndromes, a group of inflammatory diseases. However, the attempt by Novartis to repurpose this drug, which has been approved for rare inflammatory diseases, for a cohort of heart attack survivors has been rejected by the US Food and Drug Administration, as announced by the Swiss pharmaceutical company (38). It is worth noting that although the scientific community highly praised the results obtained from Novartis' Cantos study, some cardiovascular experts were less enthusiastic. These experts concluded that the benefits of this medication were not significant enough to warrant expanding its approved use to include routine treatment of cardiac patients. A noteworthy example supporting the viewpoint of these cardiovascular experts is the study conducted by Ridker et al (31), which demonstrated that the repurposing of this therapeutic agent yielded various adverse effects, as depicted in this figure.

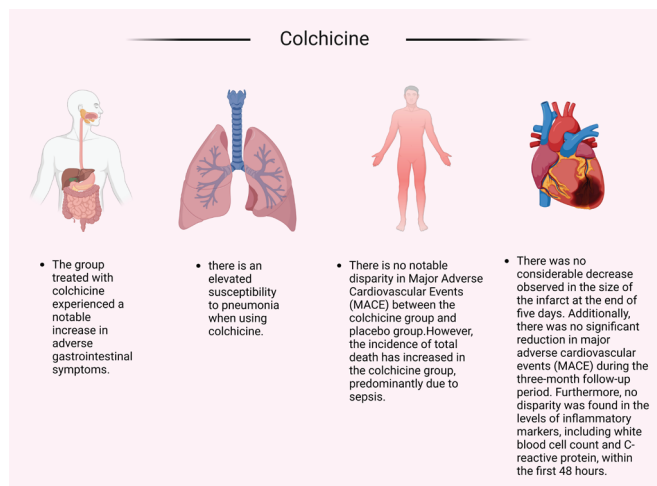


**FIGURE 2** - Challenges in clinical trials using colchicine. In the year 2009, the US FDA granted approval for the use of colchicine in the treatment of familial Mediterranean fever (FMF) and the prevention and management of gout attacks (41). Detailed investigations into the mechanisms of action have revealed that colchicine exhibits its effects by binding to microtubules, thereby exerting an influence on numerous cellular processes (42). Additionally, colchicine has been found to impede the expression of various inflammatory cytokines (43). The concept that chronic inflammation contributes to the development of cardiovascular diseases, such as coronary artery disease (CAD), is currently gaining considerable scientific attention (44). The distinctive anti-inflammatory mechanism of colchicine has consequently prompted further investigations in the domain of cardiovascular medicine (45). At present, the utilization of colchicine in cardiovascular therapy remains quite limited (46,47). This constraint may be attributed to the adverse effects observed in clinical trials focused on cardiovascular conditions. These adverse effects, as depicted in the figure, encompass gastrointestinal disorders (33), pneumonia (34), and sepsis, which may ultimately lead to an increased incidence of overall mortality (35). Furthermore, individuals treated with this medication did not exhibit any notable differences in terms of infarct size or levels of inflammatory markers, including white blood cell count and C-reactive protein, within the initial 48-hour period. Moreover, a significant decrease in the occurrence of MACE was not observed during the 3-month follow-up period (36).

that there was no significant discrepancy observed in major adverse cardiovascular events (MACEs) between the group administered with colchicine and the group administered with a placebo (35). However, it is worth mentioning that the incidence of total mortality exhibited an augmentation in the colchicine group, primarily due to sepsis (35). Additionally, in a study conducted by Mewton et al (36), it was observed that there was no substantial reduction in the size of the infarct at the conclusion of a 5-day period (36). Within the same clinical trial, there was no significant decrease in MACE during the 3-month follow-up period. Furthermore, no disparity was discovered in the levels of inflammatory markers, including white blood cell count and C-reactive protein (CRP), within the initial 48 hours.

On the other hand, etanercept is a pharmaceutical agent employed for the purpose of managing and addressing autoimmune disorders, such as plaque psoriasis, rheumatoid

arthritis, psoriatic arthritis, juvenile idiopathic arthritis, and ankylosing spondylitis. It belongs to the class of biologic fusion proteins categorized as tumor necrosis factor (TNF) blockers (39). Although the approval of systemic etanercept for adults occurred in 2004, the FDA declined to approve its use in children with psoriasis in 2018 (40). However, the FDA later revised their risk-benefit assessment in light of a better understanding of the disease burden, the unmet medical needs, and the impact of off-label use in children with psoriasis. Consequently, in 2016, this led to the approval of etanercept as the first systemic biologic product for the treatment of moderate to severe psoriasis in children aged 4-17. Despite these findings, some researchers have attempted to repurpose this drug for the treatment of cardiovascular diseases. An example of such an attempt is seen in a clinical trial, depicted in the accompanying figure, which was terminated due to the absence of any significant advantages (32).

Another drug repurposed for cardiovascular diseases that faces challenges during clinical trials is methotrexate. As indicated by the study conducted by Moreira et al (48), methotrexate demonstrates no disparity in the duration of a 6-minute walk before and after treatment. It also exhibits no impact on the levels of CRP, nor does it affect the incidence of MACE when compared to a placebo. Moreover, the same author's additional study (49) reveals that methotrexate has no effect on the release of creatine kinase during the initial 72 hours, no discrepancy in CRP levels, a significantly poorer left ventricular ejection fraction (LVEF) in the methotrexate group at 3 months, and no impact on the incidence of MACE. Conversely, in Ridker et al's (50) study, the trial was terminated prematurely due to the absence of any benefits. No difference was observed in the incidence of MACE or in the levels of inflammatory markers (white blood cell count, CRP, interleukin-1 $\beta$ , interleukin-6) at 8 months. However, an increased occurrence of leukopenia and non-basal cell skin cancer was noted.

The final example in the realm of cardiovascular medicine is the drug known as cyclosporine. Since its introduction into clinical practice in the late 1970s (51), the discovery and utilization of cyclosporine has had a significant impact on the advancement of transplant medicine (52,53). While it has shown improvements in the rates of acute rejection and early graft survival, the evidence regarding long-term survival of renal allografts is less convincing (54). The identification of acute reversible nephrotoxicity and nephrotoxicity in nonrenal transplants has subsequently led to the widely accepted notion that there is also a chronic and more irreversible component to this drug (55). Consequently, there has been a strong interest in developing protocols that aim to minimize or even eliminate the use of calcineurin inhibitors altogether (56). Despite these considerations, cyclosporine has been repurposed for various other diseases, including cardiovascular diseases (57,58). In two separate trials involving patients with ST-segment elevation myocardial infarction (STEMI), cyclosporine failed to demonstrate any beneficial effects on ST-segment resolution, left ventricular remodeling, or the incidence of cardiovascular events during the respective trial periods of 6 months and 1 year (57,58). Moreover, the use of cyclosporine in cardiovascular medicine has been

associated with certain side effects such as hypertension, hyperlipidemia, and diabetes mellitus (59). These side effects may contribute to the high cardiovascular morbidity in renal transplant patients and the development of chronic transplant nephropathy (60). In conclusion, while cyclosporine has revolutionized transplant medicine, its use in cardiovascular medicine comes with potential side effects that must be carefully monitored and managed to ensure patient safety and optimal outcomes (61).

### Challenges in cancer endeavor

In the field of hematological malignancies, despite the introduction of drug repurposing, which presents new possibilities for innovative treatments, achieving complete remission remains an arduous task (62). Clinical trials that explore the repurposing of drugs in oncology have exhibited varying levels of success, with certain limitations such as limited sample sizes and participant heterogeneity (63). An illustration of repurposing challenges in multiple clinical trials has come to light. One such instance involves the repurposing of bortezomib to target hematological malignancies. However, this drug proved to be ineffective as a stand-alone treatment for other malignancies, including acute myelogenous leukemia (AML) (62). Another example that showcases the act of appropriating preexisting resources for alternative purposes pertains to the potential drawbacks that arise when repurposing the chemical compound valproic acid (VPA) for various medical applications. These disadvantages, such as its lack of improvement in clinical outcomes for patients with myelodysplastic syndrome (MDS) or elderly patients with AML in a randomized phase II study of low-dose decitabine with VPA, have been observed (64). Additionally, another study found that VPA did not have an impact on the objective response rate or overall survival (65). Furthermore, a randomized phase III study examining the safety and efficacy of combining VPA and all-trans retinoic acid (ATRA) with induction therapy (idarubicin and cytarabine) for the treatment of elderly AML patients was terminated prematurely due to the absence of clinical improvement in the VPA group compared to standard treatment (66). This lack of improvement was further compounded by hematologic toxicity and higher mortality rates associated with VPA (67). All of these clinical studies shed light on the limitations and challenges inherent in using VPA in contexts other than its original intention. However, there is promising potential for computational drug repurposing to forecast the effectiveness of repurposed medications in phase III clinical trials, thereby streamlining the process (68).

### Challenges in diabetes endeavor

Drug repurposing trials in the field of diabetes have encountered numerous hurdles and instances of failure. A particular study examined the inability of prominent pharmaceutical companies to develop novel treatments for type 2 diabetes (T2D) despite significant investments in traditional drug development pipelines (69). Another scholarly article highlighted the challenges faced by potentially effective



medications during the advanced stages of clinical trials for diabetes management (70). Researchers in the same field are presently attempting to repurpose antidiabetic medications with the aim of addressing dementia, characterized by the prevalence of insulin sensitizers and insulin substrates. Despite the initial appearance of promise and the potential for success, none of the clinical trials conducted thus far have achieved the desired outcome of mitigating the cognitive deterioration associated with late-onset dementia (71).

In recent years, there has been a significant focus on the repurposing of antidiabetic drugs for the purpose of weight control, alongside the use of other medications. The use of antidiabetic drugs, such as metformin, glyburide, and SGLT-2 inhibitors, has shown promising results in terms of promoting weight loss, which has garnered considerable attention (72). Additionally, disulfiram, a medication commonly prescribed for chronic alcoholism, has demonstrated a significant capability to counteract obesity in rats (73). Although the specific mechanisms by which these drugs facilitate weight loss are still being investigated, their potential as treatments for obesity should not be underestimated. It is important to note that despite the positive effects of these repurposed drugs for obesity, there is also a focus on the repurposing of antidiabetic drugs such as semaglutide and tirzepatide, which were initially developed to address the challenges associated with T2D (74). These drugs can be traced back to a peptide that was discovered in the venom of the Gila monster and have the ability to mimic the actions of a naturally occurring hormone that is released after food consumption. As a result, they have shown promising results in terms of inducing weight loss. However, it is essential to acknowledge that

these drugs do come with their fair share of adverse effects, particularly in the gastrointestinal realm. Potential side effects such as nausea, vomiting, diarrhea, and constipation have been reported with their use. Therefore, it is crucial to strike a careful balance between the beneficial effects and the potential adverse effects when considering the use of these drugs for the treatment of obesity.

### Potential risk of repurposed antibiotics

One of the foremost concerns that need careful study is the repurposing of antibiotics for noninfectious disorders, some antibiotics of which are listed in Table 1. In this context, it is crucial to assess both the efficacy of these repurposed drugs and their potential to exacerbate the problem of multi-drug resistance (75). In a study conducted by Wang et al (76), it was shown that some non-antibiotic medications, when present at levels that are both clinically and ecologically relevant, had a notable impact on the dissemination of antibiotic resistance. This effect was shown through the absorption of exogenous antibiotic resistance genes (ARGs) (77,78), due to the fact that the administration of non-antibiotic substances has the potential to increase the likelihood of the development of multidrug resistance at the clinical level (79). It is plausible to suggest that the utilization of repurposed drugs could exacerbate this issue even further. Therefore, the present work strives to clarify this threat in the subsequent section. The phenomenon of antibiotic resistance has been steadily increasing over the past few decades, with no new categories of antibiotics or viable alternatives receiving clinical approval within the last three decades (75,80).

**TABLE 1** - Some repurposed antibiotics and microbes that developed resistance to these antibiotics

	Antibiotic	Repurposed for	Microbes resistant to this antibiotic
1	Levofloxacin	- Lung cancer - Alzheimer's disease - Anti-amyloidogenic	- <i>Cutibacterium avidum</i> (82) - <i>Stenotrophomonas maltophilia</i> (83,84) - <i>Haemophilus</i> , <i>Streptococcus</i> , <i>Corynebacterium</i> , <i>Staphylococcus</i> , and <i>Bordetella</i> (85) - <i>Helicobacter pylori</i> (86) - <i>Acinetobacter baumannii</i> (87) - <i>Acinetobacter</i> spp. and <i>Escherichia coli</i> (88)
2	Benzylpenicillin	Alzheimer's disease	- All of the strains of nonfermenting gram-negative bacteria (NGNB) exhibited resistance to benzylpenicillin. <i>Pseudomonas cepacia</i> and <i>P. stutzeri</i> were identified as the species displaying the highest levels of resistance (89). - <i>Pseudomonas aeruginosa</i> (90) - Indole-positive <i>Proteus</i> strains are uniformly resistant to benzylpenicillin (91).
3	Doxycycline	Treatment of malaria	- A range of anaerobic bacteria, such as <i>Bac teroides fragilis</i> , exhibit resistance to attainable blood levels of doxycycline (92). - In the oral cavity, the prevailing type of antibiotic-resistant bacteria discovered were gram-positive cocci (93). - All isolated gram-negative strains, such as <i>E. coli</i> , <i>E. fergusonii</i> , and <i>Proteus mirabilis</i> , exhibited resistance to doxycycline (94).
4	Azithromycin	- COVID-19 pandemic - Treatment of malaria	25 different strains of <i>Legionella pneumophila</i> exhibited resistance to the antimicrobial drug azithromycin.



There is an ongoing endeavor to discover novel drugs or alternative approaches to combat bacterial infections, but unfortunately, the rate at which bacterial resistance develops surpasses the pace of these endeavors (81).

While the notion of repurposing drugs may appear rational and a scientific approach to addressing previously incurable ailments such as Alzheimer's, cancer, and Parkinson's, the repurposing of antibiotic medications has generated concerns regarding their use in treating such diseases, particularly in light of the widespread prevalence of AMR that has wreaked havoc in our contemporary era. AMR is well-known for its devastating impact, with over 700,000 deaths occurring globally as a result, and projections indicating that this number could escalate to approximately 10 million people worldwide by the year 2050 (95). A number of research studies have delved into the utilization of antibiotics for the treatment of conditions other than bacterial infections, attempting to repurpose these medications (96-98). However, these studies have failed to adequately acknowledge the grave peril associated with employing antibiotics for repurposing, namely the progression of AMR (as depicted in Fig. 1).

The antibiotic levofloxacin has recently been proposed as a potential repurposed medication for Alzheimer's disease (AD) (98). However, several other studies examining the effects of this antibiotic on Alzheimer's patients have been disregarded. One of these studies involves a case report that observed an increase in seizures in an AD patient who was administered a dose of 500 mg/day of levofloxacin (99). Additionally, research on the gut microbiome of Alzheimer's patients has indicated that *Helicobacter pylori* infection may serve as a trigger for the release of inflammatory mediators in AD patients (104). It is worth noting that *H. pylori* is known for its resistance to levofloxacin (Tab. 1) (105). The primary concern with repurposed antibiotics lies in their dosage, duration of use, and their impact on AMR. Antibiotics are typically administered at doses significantly higher than non-antibiotic drugs (27). In fact, a concentration of 400 mg of minocycline was found to be ineffective in delaying the progression of cognitive or functional impairment in patients with mild AD over a 2-year period (106). Despite their potential as candidates in laboratory settings, the efficacy of these antibiotics in vivo is not guaranteed. Moreover, long-term exposure to antibiotics, whether at clinical or sub-stoichiometric doses, can lead to the development of drug resistance among gut microbes. Chronic administration of these antibiotics is necessary for the treatment or management of AD. Consequently, the chronic use of antibiotics at clinical doses may result in antibiotic resistance, making it challenging to treat common infections. Furthermore, prolonged antibiotic use may increase a patient's susceptibility to infections. If any antibiotics demonstrate potential as anti-Alzheimer's agents in either laboratory or clinical studies, it is imperative to assess their long-term consequences.

There has been a lack of comprehensive research aimed at comprehending the prolonged implications of utilizing repurposed antibiotics to enhance AMR. However, existing data have demonstrated a direct correlation between the consumption of antibiotics and the emergence of AMR (107). Consequently, an escalation of multidrug resistance may occur as the consumption of these repurposed antibiotics increases. For example,

doxycycline is an antibiotic that has been repurposed for the treatment of malaria (Tab. 1). While there is no documented evidence of increased AMR due to the use of doxycycline for malaria prophylaxis, reports have indicated the development of doxycycline resistance and coresistance to other antibiotics when used to treat other diseases. A study revealed that doxycycline-induced stress led to the emergence of coresistance to colistin, which is considered a last-resort antibiotic for extensively drug-resistant bacteria (108). This study shed light on a potential mechanism of doxycycline-selected resistance and coresistance in *Vibrio cholerae*, emphasizing the need for stringent regulations regarding the indiscriminate use of antibiotics. Another aspect to consider is the unrestricted sale of these antibiotics without prescription, particularly in developing countries such as India, which is one of the largest consumers of antibiotics (109). Consequently, the controlled usage of these repurposed antibiotics may be compromised. Prolonged use of repurposed antibiotics could exert selective pressure, resulting in the survival of multidrug-resistant and extremely drug-resistant bacteria. In the absence of a competitive environment, these drug-resistant strains may thrive more successfully, leading to the elimination of phenotypically sensitive strains, as illustrated in Figure 3 (110).

During the COVID-19 pandemic, health professionals turned to the administration of azithromycin alone or in combination with drugs like hydroxychloroquine. This repurposing of an antibiotic without any evidence of its antiviral

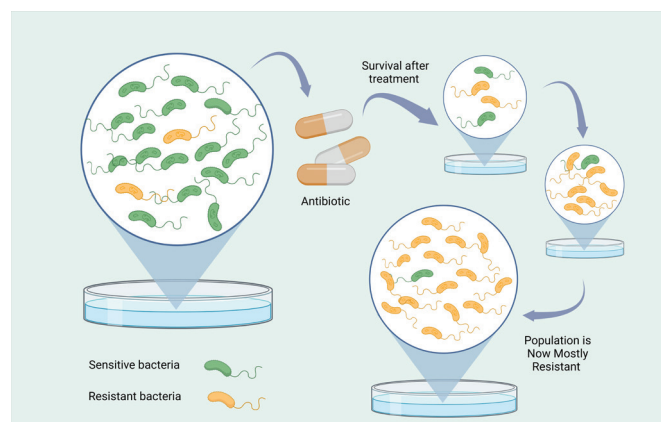


**FIGURE 3** - Progression of antimicrobial resistance. Antimicrobial resistance may arise as a consequence of the improper utilization of antibiotics or their employment for indications other than the treatment of bacterial infections (100). This resistance can manifest through the transmission of genes associated with antimicrobial resistance when bacteria are subjected to prolonged exposure to low levels of antibiotics (101). Such a situation can result in the emergence of bacteria that are resistant to multiple drugs, thereby impeding the effective management of bacterial infections and presenting a significant public health challenge (102). To effectively address antimicrobial resistance, it is imperative to advocate for the responsible and prudent utilization of antibiotics, ensuring their administration solely when warranted and in accordance with appropriate dosages and durations (103). This diagram elucidates the manner in which the inappropriate employment of antibiotics, whether in terms of sublethal dosages or durations, leads to the dissemination of resistance genes within bacterial populations, consequently giving rise to an entirely resistant population.

properties became a highly controversial practice. However, its utilization continued to increase with the successive waves of COVID-19. The future implications of such unregulated and unscientific use of antibiotics remain uncertain. The consequences of this practice on AMR will further exacerbate the situation (111). In addition to the repurposing of azithromycin in the context of the COVID-19 pandemic, numerous studies have revealed its antimalarial properties. The eradication of *Plasmodium falciparum* parasites is accomplished through two distinct mechanisms: delayed death by means of inhibiting the apicoplast ribosomes and rapid elimination throughout the blood stage development (112). A trial carried out in Burkina Faso discovered that a solitary oral dose of azithromycin did not result in a reduction in malaria positivity; however, it did alleviate caregiver-reported fever as an adverse event (113). Furthermore, an additional study determined that the supplementation of azithromycin to seasonal malaria chemoprevention did not yield improved nutritional outcomes among children (114). Furthermore, novel derivatives of azithromycin that exhibit swift action have been developed, manifesting exceptional antimalarial activity in both in vitro and in vivo settings, while employing a distinct mode of action compared to the more gradual acting azithromycin (115). Although azithromycin has indeed exhibited potential as an antimalarial agent, further investigation is necessary to optimize its efficacy and comprehend its mechanisms of action. Considering the positive correlation between extensive antibiotic usage and the worsening of the antibiotic resistance crisis in the present era, it is imperative to enhance AMR stewardship at an international level in order to mitigate the impact of antibiotic use on the menace of antibiotic resistance. Particular emphasis should be placed on comprehending the ramifications of antibiotic repurposing.

There is a profound necessity to explore alternatives to antibiotics in the context of repurposing, especially those that have already demonstrated resistance. The successful repurposing of non-antibiotic drugs for cancer treatment has been documented (116,117) and a similar approach can be adopted for other diseases as well. While the repurposed antibiotics may circumvent clinical trials, the absence of substantial studies addressing the grave issue of AMR may prove to be catastrophic for the already advancing AMR against most antibiotics. The role of AMR in exacerbating challenges in the management of nosocomial infections and the resulting mortality due to multidrug resistance should not be underestimated, particularly in an era where the efficacy of most antibiotics is waning and treatment regimens rely on last-resort antibiotics (118). It is imperative to find a solution that does not further burden the existing load of AMR. Therefore, we propose that clinicians and researchers raise awareness about the rampant problem of AMR and its consequences, while discouraging the use of antibiotics in drug repurposing.

After considering the knowledge mentioned above, one could potentially inquire whether the practice of repurposing antibiotics to address noninfectious ailments could potentially elevate the likelihood of AMR. Furthermore, one may also wonder about the implications of reusing antibiotics that

were originally approved for the treatment of one specific infection in the context of treating a different infection.

In previous times, newer antibiotics were consistently being surpassed by more recent ones, which were devised to circumvent the most recent resistance mechanism discovered in clinical isolates. Nevertheless, numerous companies have abandoned initiatives aimed at developing novel anti-infectives due to the time and expense associated with clinical trials. The insufficient availability of new drugs has provided a compelling impetus to repurpose older antibiotics for treating multidrug-resistant strains or to combine them with agents capable of targeting multiple distinct pathways within the pathogen or activating the resistance pathways of host cells. This approach is anticipated to result in heightened effectiveness and reduce the likelihood of resistance emergence (119).

Reverting to previous antibiotics can, under certain circumstances, overcome antibiotic resistance. For instance, strains of tuberculosis that are resistant to the drug combinations currently in use can be found in all regions of the world. One effective tuberculosis medication, known as isoniazid, hinders the enzyme *InhA*, thereby obstructing the synthesis of the mycolic acids that constitute the cell wall of the mycobacterium. The resistance to isoniazid, which is a prodrug, largely arises from mutations in the bacterial enzymes that are necessary for its activation. Recently, it has been discovered that an older antibiotic derived from natural sources, called pyridomycin and first identified in the 1950s, directly inhibits *InhA*. Consequently, it can be employed to treat infections caused by drug-resistant strains of tuberculosis that survive due to their inability to activate isoniazid (120). The comprehension of this mechanism of action may also promote the utilization of pyridomycin in conjunction with other medications (121). However, there are several difficulties in repurposing drugs for infectious diseases, and the subsequent sections will outline some of the primary challenges that arise in this domain.

### **The complexity of microorganisms and the limited understanding of the complicated interactions between pathogens and their hosts**

Identifying appropriate therapeutic targets for anti-infective medications is a challenging endeavor due to the complex nature of infection processes and the intricate interplay between hosts and pathogens (122). Pathogens, encompassing viruses, bacteria, protozoa, and nematodes, acquire significant genetic diversity through mutation and recombination, resulting in the emergence of drug-resistant mutants (123). Consequently, the development of drugs that can effectively target all viral variations becomes arduous. Hence, it is imperative to consistently exert efforts to stay ahead of evolving resistance mechanisms (124). Furthermore, certain infections, including *Neisseria* spp. or *Plasmodium* spp., possess the capability to undergo antigenic variation, wherein they modify the surface proteins on their cells to evade detection and attack by the host organism's immune system. This ongoing process of adaptation poses challenges in identifying consistent therapeutic targets and potential



candidates for vaccination (125). Additionally, several pathogens like *Trypanosoma cruzi*, *Mycobacterium tuberculosis*, and herpes viruses can establish latent or chronic infections, wherein they remain inactive within host cells and successfully evade immune detection (126,127). Effectively managing such infections requires medications that can specifically target the pathogen during both its active and latent stages. Moreover, certain bacteria such as *Pseudomonas aeruginosa*, *Acinetobacter baumannii*, and *Staphylococcus aureus* can form biofilms, which augment their resistance to drugs and impede drug accessibility, thereby making the eradication of infections more formidable (75,128).

### Lack of efficient animal models

Developing animal models that accurately replicate human infections is essential for preclinical testing. However, creating suitable models for specific infectious diseases can pose challenges due to the intricate interactions between hosts and pathogens that are difficult to accurately simulate (129). The absence of appropriate predictive models can hinder the progress of drug development, as it becomes arduous to comprehend the disease mechanisms and evaluate the effectiveness of potential medications (130). An example is the complexity involved in modeling diseases like COVID-19 that necessitates the consideration of various factors such as stochasticity, evolving transmission dynamics, and spatial configurations (131).

A significant advancement in the field of antimalarial drug research and development was the establishment of a NOD-SCID mouse model for *P. falciparum* infection, which proved valuable for testing drug efficacy (132). Moreover, the utilization of organoid cultures derived from stem cells holds significant promise in providing valuable insights into infectious diseases by effectively mimicking in vivo disease characteristics and enhancing the comprehension of host-microbe interactions (133,134). In addition, the integration of sophisticated mathematical models such as the SEIR model, incorporating multiple variables, can greatly assist in forecasting disease dissemination, particularly for infections characterized by prolonged incubation periods and asymptomatic carriers (135). The optimization of the modeling process through the formulation of well-defined research questions, implementation of quality assurance measures, and meticulous reporting practices can substantially elevate the relevance and comprehensibility of findings, thereby playing a pivotal role in improving decision-making processes related to disease management (136).

On the other hand, epidemiological models, such as agent-based simulation models and compartmental models, play a crucial role in understanding disease spread dynamics and evaluating intervention strategies (137-139). These models often involve making assumptions that may limit their scope, such as focusing on single-strain and single-vector scenarios, simplistic human behavior modeling, and ignoring data quality evaluation (140). To improve the reliability of these models, it is essential to consider factors like information quality, human behavior, multi-vector, and multi-strain scenarios, as they significantly impact the model outcomes

without significantly increasing computational costs (141). Collaborative efforts between researchers and modelers are crucial to enhancing the accuracy of predictions and optimizing models for effective public health decision-making and for repurposing antibiotics.

### Elevated likelihood of clinical failure

Clinical trials for anti-infective medications frequently encounter significant attrition rates as a result of inadequate effectiveness, apprehensions regarding safety, or difficulties in the recruitment of patients (142). Additionally, the execution of clinical trials and the subsequent monitoring in resource-constrained environments, along with the absence of suitable surrogate endpoints for infectious diseases, collectively contribute to the elevated levels of unsuccessful outcomes (143).

In conclusion, while there is potential in repurposing drugs to overcome antibiotic resistance in infectious diseases, several difficulties arise in this domain. The complexity of microorganisms and the intricate interactions between pathogens and their hosts pose challenges in identifying suitable therapeutic targets. Pathogens' ability to evolve, undergo antigenic variation, establish latent or chronic infections, and form biofilms further complicate the development of effective medications. Addressing these challenges will require continued research and collaboration to develop novel strategies and therapies to combat drug-resistant infections.

### Conclusion

Drug repurposing is a strategic initiative that involves the exploration and identification of fresh therapeutic applications for pharmaceuticals that already exist in the market. This approach has proven to be beneficial due to its cost-effectiveness and ability to save time in the drug discovery process. However, it is important to consider various factors before fully embracing this strategy. One such factor is the fact that numerous repurposed drugs have failed to achieve their intended targets during clinical trials, leading to concerns about the effectiveness of this approach. Additionally, there is a growing apprehension about the potential increase in the risk of multidrug resistance, which further emphasizes the need for caution when repurposing drugs.

The development of repurposed medications requires a high level of creativity and innovation in designing the development program. This is because each case presents a unique set of circumstances and evidence that must be thoroughly evaluated. Therefore, it is crucial to approach each drug repurposing project with a comprehensive understanding of the ethical and pharmaceutical considerations involved. Furthermore, it is imperative that repurposed drugs undergo rigorous clinical trials before they can be approved for use. This ensures that the safety and efficacy of these drugs are thoroughly evaluated, and any potential risks and side effects are identified and mitigated. In conclusion, the process of selecting a repurposed drug should be guided by a range of ethical and pharmaceutical considerations. It is important to acknowledge the limitations and challenges associated



with drug repurposing, such as the potential failure to reach therapeutic targets and the risk of multidrug resistance. By prioritizing the application of creativity and innovation in the development program, as well as ensuring the completion of rigorous clinical trials, we can maximize the potential benefits of repurposed drugs while minimizing the associated risks.

## Disclosures

**Conflicts of interest:** The authors declare no conflict of interest.

**Funding:** This research received no external funding.

**Data availability statement:** The data presented in this study are available on request from the corresponding author.

**Author contributions:** Conceptualization, I.Y.N. and M.M.A.; software, D.K.A. and M.M.D.; validation, I.Y.N. and A.K.A.; formal analysis, D.K.A. and M.M.A.; investigation, A.K.A. and M.M.D.; resources, I.Y.N., M.M.D., M.J.A.S., and A.K.A.; data curation, D.K.A. and M.M.A.; writing—original draft preparation, M.M.A. and I.Y.N.; writing—review and editing, M.M.A., M.J.A.S., and D.K.A.; visualization, I.Y.N., M.J.A.S., and A.K.A.; supervision, M.M.A. and I.Y.N.; project administration, I.Y.N. All authors have read and agreed to the published version of the manuscript.

## References

1. Agnihotri Jaya, R Sunanda, Patil et al. "Drug repurposing: A futuristic approach in drug discovery". *Journal of pharmaceutical and biological sciences*, vol. 11, no. 1, 66-69, 2023.
2. Hyeong-Min L, Yuna K. Drug repurposing is a new opportunity for developing drugs against neuropsychiatric disorders. *Schizophr Res Treatment*. 2016;2016:6378137.
3. Meera M, Sekar S, Mahatao R. A novel approach for drug discovery-drug repurposing. *Natl J Physiol Pharm Pharmacol*. 2022;12(5):546-551.
4. Iacopetta D. Special issue on "anticancer drugs activity and underlying mechanisms". *Appl Sci (Basel)*. 2021;11(17):8169. [CrossRef](#)
5. Pardo-Yules B, Gallego-Durán R, Eslam M, et al. Thalidomide with peginterferon alfa-2b and ribavirin in the treatment of non-responders genotype 1 chronic hepatitis C patients: proof of concept. *Rev Esp Enferm Dig*. 2011;103(12):619-625. [CrossRef PubMed](#)
6. Jesus SM, Santana RS, Leite SN. The organization, weaknesses, and challenges of the control of thalidomide in Brazil: a review. *PLoS Negl Trop Dis*. 2020;14(8):e0008329. [CrossRef PubMed](#)
7. Duarte D, Vale N. Antidepressant drug sertraline against human cancer cells. *Biomolecules*. 2022;12(10):1513. [CrossRef PubMed](#)
8. Rehan M, Ahmed F, Howlader SM, et al. A computational approach identified andrographolide as a potential drug for suppressing Covid-19-induced cytokine storm. *Front Immunol*. 2021;12:648250.
9. Talib Jawad Kadhim, Omer Abd Alkareem Khalf. A review search of sildenafil uses in human and in the veterinary medicine. *AIP Conf Proc*. 2023;2475:100010.
10. Al Ibrahim AH, Ghallab KQ, Alhumaid FI, et al. A systematic review of sildenafil mortality through the years. *Cureus*. 2022;14(12):e32179.
11. Hussein MA, Salah El-Din MM, Saleh EM, et al. Sildenafil (VIAGRATM): a promising anticancer drug against certain human cancer cell lines. *Asian J Chem*. 2021;33(6):1420-1424. [CrossRef](#)
12. Goldstein I, Burnett AL, Rosen RC, et al. The serendipitous story of sildenafil: an unexpected oral therapy for erectile dysfunction. *Sex Med Rev*. 2019;7(1):115-128. [CrossRef PubMed](#)
13. Ala M, Jafari RM, Dehpour AR. Sildenafil beyond erectile dysfunction and pulmonary arterial hypertension: thinking about new indications. *Fundam Clin Pharmacol*. 2021;35(2):235-259.
14. Mpoeo, A Baa, Ky. Hooe peaaee capx eapc (oop). *apaa pecpa eapcex cpec*, 2023;12(1):182-190. [CrossRef](#)
15. Krishnamurthy N, Grimshaw AA, Axson SA, Choe SH, Miller JE. Drug repurposing: a systematic review on root causes, barriers and facilitators. *BMC Health Serv Res*. 2022;22(1):1-17. [CrossRef PubMed](#)
16. Trivedi J, Mohan M, Byrareddy SN. Drug repurposing approaches to combating viral infections. *J Clin Med*. 2020;9(11):3777. [CrossRef PubMed](#)
17. Ekeomodi CC, Obetta KI, Okolocha ML, et al. Computational approaches in drug repurposing. In Rudrapal M, editor, *Drug repurposing – advances, scopes and opportunities in drug discovery*. IntechOpen; 2023.
18. Tuerkova A, Zdrzil B. A ligand-based computational drug repurposing pipeline using KNIME and Programmatic Data Access: case studies for rare diseases and COVID-19. *J Cheminform*. 2020;12(1):71. [CrossRef PubMed](#)
19. Jian Hong Gan, Ji Xiang Liu, Yang Liu, et al. DrugRep: an automatic virtual screening server for drug repurposing. *Acta Pharmacol Sinica*. 2023;44(4):888-896.
20. Sadegh S, Skelton J, Anastasi E, et al. NeDREx – an integrative and interactive network medicine platform for drug repurposing. In REXPO22, The 1st International Conference on Drug Repurposing, Maastricht; 2022. [CrossRef](#)
21. Parmar G, Chudasama JM, Shah A, Patel A. In silico pharmacology and drug repurposing approaches. In Rudrapal M, Khan J, eds, *CADD and informatics in drug discovery*. Springer; 2023: 253-281. [CrossRef](#)
22. Khan S, Agnihotri J, Patil S, Khan N. Drug repurposing: a futuristic approach in drug discovery. *J Pharm Biol Sci*. 2023;11(1):66-69. [CrossRef](#)
23. Geest R, Nijholt D, Hollander W. Clinical Development in Drug Repurposing. In REXPO22, The 1st International Conference on Drug Repurposing, Maastricht; ScienceOpen, August 2022.
24. Tan GSQ, Sloan EK, Lambert P, Kirkpatrick CMJ, Ilomäki J. Drug repurposing using real-world data. *Drug Discov Today*. 2023;28(1):103422. [CrossRef PubMed](#)
25. Juárez-López D, Schcolnik-Cabrera A. Drug repurposing: considerations to surpass while re-directing old compounds for new treatments. *Arch Med Res*. 2021;52(3):243-251. [CrossRef PubMed](#)
26. Selvaraj N, Swaroop AK, Nidamanuri BSS, Kumar RR, Natarajan J, Selvaraj J. Network-based drug repurposing: a critical review. *Curr Drug Res Rev*. 2022;14(2):116-131. [CrossRef PubMed](#)
27. Farha MA, Brown ED. Drug repurposing for antimicrobial discovery. *Nat Microbiol*. 2019;4(4):565-577. [CrossRef PubMed](#)
28. Fetro C, Scherman D. Drug repurposing in rare diseases: myths and reality. *Therapie*. 2020;75(2):157-160. [CrossRef PubMed](#)
29. Aggarwal NN, Sindhoor SM, Naveen NR, Gowthami B, Biju P. Drug reprofiling: a prospective approach to battle chronic ailments. *J Health Allied Sci* 2023;14:38-46.
30. Annabell C, David R, Greaves R. Drug repurposing in cardiovascular inflammation: successes, failures, and future opportunities. *Front Pharmacol*. 2022;13:1046406.
31. Ridker PM, Everett BM, Thuren T, et al. Antiinflammatory therapy with canakinumab for atherosclerotic disease. *N Engl J Med*. 2017;377(12):1119-1131.
32. Dhimolea E. Canakinumab. *MAbs*. 2010;2(1):3-13. [CrossRef PubMed](#)
33. Miller J. FDA snubs Novartis bid to repurpose inflammation drug for heart attacks, October 2018. [Online](#).



34. Davis JC Jr, Heijde D, Braun J, et al. Recombinant human tumor necrosis factor receptor (etanercept) for treating ankylosing spondylitis: a randomized, controlled trial. *Arthritis Rheumatol*. 2003;48(11):3230-3236.
35. Gatti J, Lindstrom JA, Beitz J. Reconsideration of 2008 decision: Food and Drug Administration approval of etanercept for systemic treatment of moderate to severe pediatric psoriasis. *Pediatr Dermatol*. 2018;35(5):688-689. [CrossRef PubMed](#)
36. Nathan Mewton, François Roubille, Didier Bresson et al. "Effect of colchicine on myocardial injury in acute myocardial infarction". *Circulation*, vol. 144, no. 11, 859–869, 2021.
37. Shah B, Pillinger M, Zhong H, et al. Effects of acute colchicine administration prior to percutaneous coronary intervention: COLCHICINE-PCI randomized trial. *Circ Cardiovasc Interv*. 2020;13(4):e008717. [CrossRef PubMed](#)
38. Tardif J-C, Kouz S, Waters DD, et al. Efficacy and safety of low-dose colchicine after myocardial infarction. *N Engl J Med*. 2019;381(26):2497-2505.
39. Tong DC, Quinn S, Nasis A, et al. Colchicine in patients with acute coronary syndrome: the Australian COPS randomized clinical trial. *Circulation*. 2020;142(20):1890-1900.
40. Mewton N, Roubille F, Bresson D, et al. Effect of colchicine on myocardial injury in acute myocardial infarction. *Circulation*. 2021;144(11):859-869. [CrossRef PubMed](#)
41. Spada A, Emami J, Sanaee F, et al. Design and evaluation of albumin nanoparticles for the delivery of a novel  $\beta$ -tubulin polymerization inhibitor. *J Pharm Pharm Sci*. 2021;24:344-362. [CrossRef PubMed](#)
42. Kaddoura M, Allbrahim M, Hijazi G, et al. Covid-19 therapeutic options under investigation. Vol 11. In Uckun FMM. *Frontiers in pharmacology*; 2020.
43. Ge P, Fu Y, Qi S, et al. Colchicine for prevention of post-operative atrial fibrillation: meta-analysis of randomized controlled trials. Vol 9. *Front Cardiovasc Med*. 2022;9:1032116.
44. Akrami M, Izadpanah P, Bazrafshan M, et al. Effects of colchicine on major adverse cardiac events in next 6-month period after acute coronary syndrome occurrence; a randomized placebo-control trial. *BMC Cardiovasc Disord*. 2021;21(1):583. [CrossRef PubMed](#)
45. Meyer-Lindemann U, Mauersberger C, Schmidt A, et al. Colchicine impacts leukocyte trafficking in atherosclerosis and reduces vascular inflammation. *Front Immunol*. 2022;13:898690.
46. Huang W, Wang Y, Tian W, et al. Biosynthesis investigations of terpenoid, alkaloid, and flavonoid antimicrobial agents derived from medicinal plants. *Antibiotics (Basel)*. 2022;11(10):1380. [CrossRef PubMed](#)
47. Zhang F-S, He Q-Z, Qin CH, Little PJ, Weng JP, Xu SW. Therapeutic potential of colchicine in cardiovascular medicine: a pharmacological review. *Acta Pharmacol Sin*. 2022;43(9):2173-2190. [CrossRef PubMed](#)
48. Moreira DM, Vieira JL, Gottschall CA. The effects of METHotrexate therapy on the physical capacity of patients with ISchemic heart failure: a randomized double-blind, placebo-controlled trial (METIS trial). *J Card Fail*. 2009;15(10):828-834. [CrossRef PubMed](#)
49. Moreira DM, Lueneberg ME, da Silva RL, Fattah T, Gottschall CAM. Methotrexate Therapy in ST-segment elevation myocardial infarction: a randomized double-blind, placebo-controlled trial (TETHYS Trial). *J Cardiovasc Pharmacol Ther*. 2017;22(6):538-545. [CrossRef PubMed](#)
50. Ridker PM, Everett BM, Pradhan A, et al; CIRT Investigators. Low-dose methotrexate for the prevention of atherosclerotic events. *N Engl J Med*. 2019;380(8):752-762. [CrossRef PubMed](#)
51. Borel JF. Comparative study of in vitro and in vivo drug effects on cell-mediated cytotoxicity. *Immunology*. 1976;31(4):631-641. [PubMed](#)
52. Tedesco D, Haragsim L. Cyclosporine: a review. *J Transplant*. 2012;2012:230386.
53. Lim SW, Doh KC, Jin L, et al. Oral administration of ginseng ameliorates cyclosporine-induced pancreatic injury in an experimental mouse model. *PLoS One*. 2013;8(8):e72685. [CrossRef PubMed](#)
54. Kern G, Mair SM, Noppert SJ, et al. Tacrolimus increases Nox4 expression in human renal fibroblasts and induces fibrosis-related genes by aberrant TGF-beta receptor signalling. *PLoS One*. 2014;9(5):e96377. [CrossRef PubMed](#)
55. Thorat A, Chou H-S, Lee C-F, et al. Effects of converting tacrolimus formulation from twice-daily to once-daily in liver transplantation recipients. *BioMed Res Int*. 2014;2014:265658.
56. Abdelkader M, Hilal M, Torky AR, Elsayed H, Allam W. Experimental study of renal toxicity of cyclosporine and the ameliorative effect of N-acetylcysteine in albino rat. *Ain Shams J Forensic Med Clin Toxicol*. 2021;37(2):8-15. [CrossRef](#)
57. Cung T-T, Morel O, Cayla G, et al. Cyclosporine before PCI in patients with acute myocardial infarction. *N Engl J Med*. 2015;373(11):1021-1031. [CrossRef PubMed](#)
58. Ottani F, Latini R, Staszewsky L, et al; CYCLE Investigators. Cyclosporine A in reperfused myocardial infarction: the multicenter, controlled, open-label CYCLE trial. *J Am Coll Cardiol*. 2016;67(4):365-374. [CrossRef PubMed](#)
59. Elgendy A, Alshawadfy E, Altaweel A, Elsaidi A. Cardiovascular and metabolic comorbidities of psoriasis. *Dermatol Case Rep*. 2016;1(1):1-9. [CrossRef](#)
60. Sakamoto H, Kurabayashi M. Cardiovascular effects of an immunosuppressive agent cyclosporin A. *Int J Immunopathol Pharmacol*. 2000;15(2):75-79. [CrossRef PubMed](#)
61. Grupper A, Shashar M, Bahry D, et al. Cyclosporine attenuates arginine transport, in human endothelial cells, through modulation of cationic amino acid transporter-1. *Am J Nephrol*. 2013;37(6):613-619. [CrossRef PubMed](#)
62. Michael AA, Balakrishnan P, Velusamy T. Drug repurposing for hematological malignancies. In Sobti RC, Lal SK, Goyal RK, eds. *Drug repurposing for emerging infectious diseases and cancer*, Singapore, Springer; 2023:217-252. [CrossRef](#)
63. Ioakeim-Skoufa I, Tobajas-Ramos N, Menditto E, et al. Drug repurposing in oncology: a systematic review of randomized controlled clinical trials. *Cancers (Basel)*. 2023;15(11):2972. [CrossRef PubMed](#)
64. Issa J-P, Garcia-Manero G, Huang X, et al. Results of phase 2 randomized study of low-dose decitabine with or without valproic acid in patients with myelodysplastic syndrome and acute myelogenous leukemia. *Cancer*. 2015;121(4):556-561. [CrossRef PubMed](#)
65. Lübbert M, Grishina O, Schmoor C, et al. Results of the randomized phase II study decider (AMLSG 14-09) comparing decitabine (DAC) with or without valproic acid (VPA) and with or without all-trans retinoic acid (ATRA) add-on in newly diagnosed elderly non-fit AML patients. *Blood*. 2016;128(22):589. [CrossRef](#)
66. Tassarà M, Döhner K, Brossart P, et al. Valproic acid in combination with all-trans retinoic acid and intensive therapy for acute myeloid leukemia in older patients. *Blood*. 2014;123(26):4027-4036. [CrossRef PubMed](#)
67. Wojcicki AV, Kadapakkam M, Frymoyer A, Lacayo N, Chae HD, Sakamoto KM. Repurposing drugs for acute myeloid leukemia: a worthy cause or a futile pursuit? *Cancers (Basel)*. 2020;12(2):441. [CrossRef PubMed](#)
68. Zong N, Chowdhury S, Zhou S, et al. Artificial intelligence-based efficacy prediction of phase 3 clinical trial for repurposing heart failure therapies. *medRxiv*, 2023:2023.05.25.23290531.



69. Turner N, Zeng X-Y, Osborne B, Rogers S, Ye J-M. Repurposing drugs to target the diabetes epidemic. *Trends Pharmacol Sci*. 2016;37(5):379-389. [CrossRef PubMed](#)
70. Mandrup-Poulsen T. Perspective: testing failures. *Nature*. 2012;485(7398):S17. [CrossRef PubMed](#)
71. Mantik KEK, Kim S, Gu B, et al. Repositioning of anti-diabetic drugs against dementia: insight from molecular perspectives to clinical trials. *Int J Mol Sci*. 2023;24(14):11450. [CrossRef PubMed](#)
72. Pathak K, Pathak MP, Saikia R, et al. Therapeutic repurposing of antidiabetic drugs in diabetes-associated comorbidities. *Curr Drug Ther*. 2024;19(2):178-194.
73. Haddad F, Dokmak G, Bader M, Karaman R. A comprehensive review on weight loss associated with anti-diabetic medications. *Life (Basel)*. 2023;13(4):1012. [CrossRef PubMed](#)
74. Gussow L. More questions than answers about injectable weight loss drugs. *Emerg Med News*. 2023;45(7):10. [CrossRef](#)
75. Natsheh IY, Elkhader MT, Al-Bakheit AA, et al. Inhibition of *Acinetobacter baumannii* biofilm formation using different treatments of silica nanoparticles. *Antibiotics (Basel)*. 2023;12(9):1365. [CrossRef PubMed](#)
76. Wang Y, Lu J, Engelstädter J, et al. Non-antibiotic pharmaceuticals enhance the transmission of exogenous antibiotic resistance genes through bacterial transformation. *ISME J*. 2020;14(8):2179-2196. [CrossRef PubMed](#)
77. Stevenson C, Hall JP, Harrison E, Wood A, Brockhurst MA. Gene mobility promotes the spread of resistance in bacterial populations. *ISME J*. 2017;11(8):1930-1932. [CrossRef PubMed](#)
78. Gillings MR, Gaze WH, Pruden A, et al. Using the class 1 integron-integrase gene as a proxy for anthropogenic pollution. *ISME J*. 2015;9(6):1269-1279.
79. Chawla M, Verma J, Gupta R, Das B. Antibiotic potentiators against multidrug-resistant bacteria: discovery, development, and clinical relevance. *Front Microbiol*. 2022;13(887251):887251. [CrossRef PubMed](#)
80. Cunningham SA, Rodriguez C, Woerther P-L, et al. In vivo emergence of dual resistance to rifampin and levofloxacin in osteoarticular *Cutibacterium avidum*. *Microbiol Spectr*. 2023;11(4):e0368722.
81. Dulyayangkul P, Calvopiña K, Heesom KJ, Avison MB. Novel mechanisms of efflux-mediated levofloxacin resistance and reduced amikacin susceptibility in *Stenotrophomonas maltophilia*. *Antimicrob Agents Chemother*. 2020;65(1):e01284-20. [CrossRef PubMed](#)
82. Zajac OM, Tyski S, Laudy AE. The contribution of efflux systems to levofloxacin resistance in *Stenotrophomonas maltophilia* clinical strains isolated in Warsaw, Poland. *Biology (Basel)*. 2022;11(7):1044. [CrossRef PubMed](#)
83. Ramdhani D, Azizah SN, Kusuma SAF, Sediana D. Antibiotic resistance: evaluation of levofloxacin treatment in acute respiratory tract infections cases at the Tasikmalaya City Health Center, Indonesia. *J Adv Pharm Technol Res*. 2020;11(3):113-116. [CrossRef PubMed](#)
84. Trespacios-Rangél AA, Otero W, Arévalo-Galvis A, Poutou-Piñales RA, Rimbara E, Graham DY. Surveillance of levofloxacin resistance in *Helicobacter pylori* isolates in Bogotá-Colombia (2009-2014). *PLoS One*. 2016;11(7):e0160007. [CrossRef PubMed](#)
85. Abdelaal AM, Mahmood SS. The role of efflux pump *adeI* gene in levofloxacin resistance among *A. baumannii*. *Syst Rev Pharm*. 2020;11(10):1105-1110.
86. Asaduzzaman M, Hasan MZ, Khatun M, et al. Resistance pattern of levofloxacin against uropathogens causing urinary tract infection in selected areas of Dhaka city. *Bangladesh J Biol Agric Healthc*. 2018;8(4):74-81.
87. Iskhakova Khl. Antibiotic sensitivity of nonfermenting gram-negative bacteria. *Antibiotiki i Khimioterapiia*. 1988;33(11):823-827.
88. Rolinson GN. Bacterial resistance to penicillins and cephalosporins. *Proc R Soc Lond, B*. 1971;179(1057):403-410. [CrossRef PubMed](#)
89. Lachmajer-Lutoslawska M, Bobrowski M. Resistance to beta-lactam antibiotics Proteus strains. *Acta Microbiol Pol A*. 1975;8(3):141-149. [PubMed](#)
90. Chow AW, Patten V, Guze LB. Comparative susceptibility of anaerobic bacteria to minocycline, doxycycline, and tetracycline. *Antimicrob Agents Chemother*. 1975;7(1):46-49. [CrossRef PubMed](#)
91. Larsen T. Occurrence of doxycycline resistant bacteria in the oral cavity after local administration of doxycycline in patients with periodontal disease. *Scand J Infect Dis*. 1991;23(1):89-95. [CrossRef PubMed](#)
92. Eliopulos N, Alsina L, Diana L, Brandl S. Multiple antimicrobial resistance in Enterobacteriaceae isolated from a Sea Lion (*Otaria flavescens*) specimen from Isla de Lobos, Uruguay: a case report. *Brazilian J Animal Environ Res*. 2022;5(4):3477-3486. [CrossRef](#)
93. Belousoff MJ, Venugopal H, Wright A, et al. cryoEM-guided development of antibiotics for drug-resistant bacteria. *ChemMedChem*. 2019;14(5):527-531. [CrossRef PubMed](#)
94. Richardson LL. Alternating antibiotics render resistant bacteria beatable. *PLoS Biol*. 2015;13(4):e1002105.
95. O'neill J. Antimicrobial resistance: tackling a crisis for the health and wealth of nations. In *Review on Antimicrobial Resistance*. London: Wellcome Trust; 2014.
96. Song M, Wu H, Wu S, et al. Antibiotic drug levofloxacin inhibits proliferation and induces apoptosis of lung cancer cells through inducing mitochondrial dysfunction and oxidative damage. *Biomed Pharmacother*. 2016;84:1137-1143. [CrossRef PubMed](#)
97. Alsalahat I, Al-Majdoub ZM, Taha MO, et al. Inhibition of aggregation of amyloid- $\beta$  through covalent modification with benzylpenicillin; potential relevance to Alzheimer's disease. *Biochem Biophys Rep*. 2021;26:100943. [CrossRef PubMed](#)
98. Khan AN, Qureshi IA, Khan UK, Uversky VN, Khan RH. Inhibition and disruption of amyloid formation by the antibiotic levofloxacin: a new direction for antibiotics in an era of multi-drug resistance. *Arch Biochem Biophys*. 2021;714:109077. [CrossRef PubMed](#)
99. Lanckohr C, Bracht H. Antimicrobial stewardship. *Curr Opin Crit Care*. 2022;28(5):551-556. [CrossRef PubMed](#)
100. Rangapriya M, Lorange A, Varghese AM, Hanif A, Aruna S. Awareness and perception on antibiotics and antimicrobial resistance: a questionnaire based study. *Int J Pharm Sci Rev Res*. 2020;65(1):27-32. [CrossRef](#)
101. Xiang L, Akakuru OU, Xu C, Wu A. Harnessing the intriguing properties of magnetic nanoparticles to detect and treat bacterial infections. *Magnetochemistry*. 2021;7(8):112. [CrossRef](#)
102. Zhu D, Li Q, Shen Y, Zhang Q. Risk factors for quinolone-resistant *Escherichia coli* infection: a systematic review and meta-analysis. *Antimicrob Resist Infect Control*. 2020;9:11.
103. Bird SB, Orr PG, Mazzola JL, Brush DE, Boyer EW. Levofloxacin-related seizure activity in a patient with Alzheimer's disease: assessment of potential risk factors. *J Clin Psychopharmacol*. 2005;25(3):287-288. [CrossRef PubMed](#)
104. Doulberis M, Kotronis G, Gialamprinou D, et al. Alzheimer's disease and gastrointestinal microbiota; impact of *Helicobacter pylori* infection involvement. *Int J Neurosci*. 2021;131(3):289-301. [CrossRef PubMed](#)
105. Mehrotra T, Devi TB, Kumar S, et al. Antimicrobial resistance and virulence in *Helicobacter pylori*: genomic insights. *Genomics*. 2021;113(6):3951-3966. [CrossRef PubMed](#)



106. Howard R, Zubko O, Bradley R, et al; Minocycline in Alzheimer Disease Efficacy (MADE) Trialist Group. Minocycline at 2 different dosages vs placebo for patients with mild Alzheimer disease: a randomized clinical trial. *JAMA Neurol.* 2020;77(2):164-174. [CrossRef PubMed](#)
107. Gandra S, Mojica N, Klein EY, et al. Trends in antibiotic resistance among major bacterial pathogens isolated from blood cultures tested at a large private laboratory network in India, 2008-2014. *Int J Infect Dis.* 2016;50(50):75-82. [CrossRef PubMed](#)
108. Narendrakumar L, Chandrika SK, Thomas S. Adaptive laboratory evolution of *Vibrio cholerae* to doxycycline associated with spontaneous mutation. *Int J Antimicrob Agents.* 2020;56(3):106097. [CrossRef PubMed](#)
109. Kotwani A, Joshi J, Lamkang AS. Over-the-counter sale of antibiotics in India: a qualitative study of providers' perspectives across two states. *Antibiotics (Basel).* 2021;10(9):1123. [CrossRef PubMed](#)
110. Fair RJ, Tor Y. Antibiotics and Bacterial Resistance in the 21st century. *Perspect. Medicin Chem;* 2014;6:25-64.
111. Yacouba A, Olowo-Okere A, Yunusa I. Repurposing of antibiotics for clinical management of COVID-19: a narrative review. *Ann Clin Microbiol Antimicrob.* 2021;20(1):37-38. [CrossRef PubMed](#)
112. Burns AL, Sleebs BE, Gancheva M, et al. Targeting malaria parasites with novel derivatives of azithromycin. *Front Cell Infect Microbiol.* 2022;12:1063407. [CrossRef PubMed](#)
113. Burns AL, Sleebs BE, Siddiqui G, et al. Retargeting azithromycin analogues to have dual-modality antimalarial activity. *BMC Biol.* 2020;18:1-23.
114. Gore-Langton GR, Cairns M, Compaoré YD, et al. Effect of adding azithromycin to the antimalarials used for seasonal malaria chemoprevention on the nutritional status of African children. *Trop Med Int Health.* 2020;25(6):740-750.
115. Peric M, Pešić D, Alihodžić S, et al. A novel class of fast-acting antimalarial agents: substituted 15-membered azalides. *Br J Pharmacol.* 2021;178(2):363-377. [CrossRef PubMed](#)
116. Advani D, Kumar P. Therapeutic targeting of repurposed anticancer drugs in Alzheimer's disease: using the multiomics approach. *ACS Omega.* 2021;6(21):13870-13887. [CrossRef PubMed](#)
117. Tímár J, Ladányi A, Forster-Horváth C, et al. Neoadjuvant immunotherapy of oral squamous cell carcinoma modulates intratumoral CD4/CD8 ratio and tumor microenvironment: a multicenter phase II clinical trial. *J Clin Oncol.* 2005;23(15):3421-3432. [CrossRef PubMed](#)
118. Avershina E, Shapovalova V, Shipulin G. Fighting antibiotic resistance in hospital-acquired infections: current state and emerging technologies in disease prevention, diagnostics and therapy. *Front Microbiol.* 2021;12:2044.
119. Tyers M, Wright GD. Drug combinations: a strategy to extend the life of antibiotics in the 21st century. *Nat Rev Microbiol.* 2019;17(3):141-155. [CrossRef PubMed](#)
120. Hartkoorn RC, Sala C, Neres J, et al. Towards a new tuberculosis drug: pyridomycin-nature's isoniazid. *EMBO Mol Med.* 2012;4(10):1032-1042.
121. Diacon AH, Dawson R, Groote-Bidlingmaier F, et al. Bactericidal activity of pyrazinamide and clofazimine alone and in combinations with pretomanid and bedaquiline. *Am J Respir Crit Care Med.* 2015;191(8):943-953.
122. Weng H-B, Chen H-X, Wang M-W. Innovation in neglected tropical disease drug discovery and development. *Infect Dis Poverty.* 2018;7(1):67. [CrossRef PubMed](#)
123. Lauring AS, Andino R. Quasispecies theory and the behavior of RNA viruses. *PLoS Pathog.* 2010;6(7):e1001005. [CrossRef PubMed](#)
124. Ventola CL. The antibiotic resistance crisis: part 1: causes and threats. *P&T.* 2015;40(4):277-283. [PubMed](#)
125. Scherf A, Lopez-Rubio JJ, Riviere L. Antigenic variation in *Plasmodium falciparum*. *Annu Rev Microbiol.* 2008;62:445-470.
126. Gomez JE, McKinney JD. *M. tuberculosis* persistence, latency, and drug tolerance. *Tuberculosis (Edinb).* 2004;84(1-2):29-44. [CrossRef PubMed](#)
127. Barrett MP, Kyle DE, Sibley LD, Radke JB, Tarleton RL. Protozoan persister-like cells and drug treatment failure. *Nat Rev Microbiol.* 2019;17(10):607-620. [CrossRef PubMed](#)
128. Donlan RM. Biofilms and device-associated infections. *Emerg Infect Dis.* 2001;7(2):277-281. [CrossRef PubMed](#)
129. Hay M, Thomas DW, Craighead JL, Economides C, Rosenthal J. Clinical development success rates for investigational drugs. *Nat Biotechnol.* 2014;32(1):40-51. [CrossRef PubMed](#)
130. Ginsberg AM, Spigelman M. Challenges in tuberculosis drug research and development. *Nat Med.* 2007;13(3):290-294. [CrossRef PubMed](#)
131. Takuadina AI, Pazykhan NP, Iskakov KT. Mathematical modeling of infectious diseases on the example of Astana city. *Sci Educ.* 2023;71.
132. Jiménez-Díaz MB, Mulet T, Viera S, et al. Improved murine model of malaria using *Plasmodium falciparum* competent strains and non-myelodepleted NOD-SCID IL2R $\gamma$ manull mice engrafted with human erythrocytes. *Antimicrob Agents Chemother.* 2009;53(10):4533-4536. [CrossRef PubMed](#)
133. Aguilar C, Alves da Silva M, Saraiva M, et al. Organoids as host models for infection biology – a review of methods. *Exp Mol Med.* 2021;53(10):1471-1482. [PubMed](#)
134. Mihaljevic JR, Borkovec S, Ratnavale S, et al. SPARSEMODr: rapidly simulate spatially explicit and stochastic models of COVID-19 and other infectious diseases. *Biol Methods Protocols.* 2022;7(1):bpac022.
135. Blutt SE, Estes MK. Organoid models for infectious disease. *Annu Rev Med.* 2022;73(1):167-182. [CrossRef PubMed](#)
136. Smith GC, Kao RR, Walker M. Infectious disease modelling to inform policy. *Rev Sci Tech.* 2023;42:173-179. [CrossRef PubMed](#)
137. Anna PGS, Henrique dos Santos M, Banerjee A. A statistical examination of distinct characteristics influencing the performance of vector-borne epidemiological agent-based simulation models. *Modelling.* 2021;2(2):166-196. [CrossRef](#)
138. Raja D. The power of epidemiological modelling in understanding and managing infectious diseases. *Chettinad Health City Med J (E-2278-2044 & P-2277-8845),* 2023;12(1):1-2.
139. Rong N, Liu J. Development of animal models for emerging infectious diseases by breaking the barrier of species susceptibility to human pathogens. *Emerg Microbes Infections.* 2023;12(1):2178242.
140. Fitzpatrick MC, Bauch CT, Townsend JP, Galvani AP. Modelling microbial infection to address global health challenges. *Nat Microbiol.* 2019;4(10):1612-1619. [CrossRef PubMed](#)
141. Cartelle Gestal M, Dedloff MR, Torres-Sangiao E. Computational health engineering applied to model infectious diseases and antimicrobial resistance spread. *Appl Sci (Basel).* 2019;9(12):2486. [CrossRef](#)
142. Legrand N, Ploss A, Balling R, et al. Humanized mice for modeling human infectious disease: challenges, progress, and outlook. *Cell Host Microbe* 2009;6(1):5-9.
143. Swearingen JR. Choosing the right animal model for infectious disease research. *Animal Model Exp Med.* 2018;1(2):100-108. [CrossRef PubMed](#)



# RBD mutations at the residues K417, E484, N501 reduced immunoreactivity with antisera from vaccinated and COVID-19 recovered patients

Dablu Lal Gupta<sup>1</sup>, Jhasketan Meher<sup>2</sup>, Anjan Kumar Giri<sup>3</sup>, Arvind K Shukla<sup>4</sup>, Eli Mohapatra<sup>1</sup>, Manisha M Ruikar<sup>4</sup>, DN Rao<sup>5</sup>

<sup>1</sup>Department of Biochemistry, All India Institute of Medical Sciences (AIIMS), Raipur, Chhattisgarh - India

<sup>2</sup>Department of General Medicine, All India Institute of Medical Sciences (AIIMS), Raipur, Chhattisgarh - India

<sup>3</sup>Department of Community and Family Medicine, All India Institute of Medical Sciences (AIIMS), Raipur, Chhattisgarh - India

<sup>4</sup>Department of Community Medicine, All India Institute of Medical Sciences (AIIMS), Raipur, Chhattisgarh - India

<sup>5</sup>Department of Biochemistry, All India Institute of Medical Sciences (AIIMS), New Delhi - India

## ABSTRACT

**Introduction:** It is unclear whether induced spike protein-specific antibodies due to infections with SARS-CoV-2 or to the prototypic Wuhan isolate-based vaccination can immune-react with the emerging variants of SARS-CoV-2.

**Aim/objectives:** The main objective of the study was to measure the immunoreactivity of induced antibodies postvaccination with Covishield™ (ChAdOx1 nCoV-19 coronavirus vaccines) or infections with SARS-CoV-2 by using selected peptides of the spike protein of wild type and variants of SARS-CoV-2.

**Methodology:** Thirty patients who had recovered from SARS-CoV-2 infections and 30 individuals vaccinated with both doses of Covishield™ were recruited for the study. Venous blood samples (5 mL) were collected at a single time point from patients within 3-4 weeks of recovery from SARS-CoV-2 infections or receiving both doses of Covishield™ vaccines. The serum levels of total immunoglobulin were measured in both study groups. A total of 12 peptides of 10 to 24 amino acids length spanning to the receptor-binding domain (RBD) of wild type of SARS-CoV-2 and their variants were synthesized. The serum levels of immune-reactive antibodies were measured using these peptides.

**Results:** The serum levels of total antibodies were found to be significantly ( $p < 0.001$ ) higher in the vaccinated individuals as compared to COVID-19 recovered patients. Our study reported that the mutations in the RBD at the residues K417, E484, and N501 have been associated with reduced immunoreactivity with anti-sera of vaccinated people and COVID-19 recovered patients.

**Conclusion:** The amino acid substitutions at the RBD of SARS-CoV-2 have been associated with a higher potential to escape the humoral immune response.

**Keywords:** Antibodies, COVID-19, Immune escape, Immunoreactivity, Mutation, SARS-CoV-2

## Introduction

The coronavirus disease 2019 (COVID-19) pandemic caused significant global impact and continues to be a threat despite the introduction of vaccines (1,2). The vaccines have been highly effective in preventing COVID-19 around the

world (3). Globally, the COVID-19 pandemic is still producing a significant amount of illness and mortality (4). According to current knowledge, mildly symptomatic people represent around 80% of all instances of COVID-19, which can range in severity from asymptomatic to deadly pneumonitis (5). The virus can cause a range of symptoms, from mild to severe, and can be transmitted through the respiratory tract (6). It has significant impacts on at-risk patients and the health-care system, including high costs, loss of human resources, and psychological problems (7). COVID-19, caused by severe acute respiratory syndrome coronavirus 2 (SARS-CoV-2), enters human cells by binding the receptor-binding domain (RBD) of its spike (S) protein to the angiotensin-converting enzyme 2 (ACE2) receptor (8,9). Antibodies directed against the S-protein have the potential to neutralize the virus efficiently (10). Since the first case of SARS-CoV-2 in Wuhan,

Received: March 1, 2024

Accepted: May 7, 2024

Published online: May 31, 2024

This article includes supplementary material

Corresponding author:

Dablu Lal Gupta

email: [dr.dlgupta@aiimsraipur.edu.in](mailto:dr.dlgupta@aiimsraipur.edu.in)



China, over 774 million infections have been documented, leading to the emergence of seven major lineages with various variants (11,12). Coronaviruses have a large RNA genome and mutations can arise naturally during replication, leading to evolutionary advantages such as increased infectivity or improved receptor binding (13). The Omicron variant of SARS-CoV-2 has 30 non-synonymous amino acid mutations in the spike protein, which have been reported to enable immune evasion and reduce vaccine effectiveness (14). Variants of concern (VOCs), such as B.1.1.7, B.1.1.298, B.1.429, P.2, P.1, and B.1.351, have mutations that can increase transmissibility, virulence, or evade immune responses (15,16). These variants mainly have mutations in the spike protein, particularly in the S1 and RBD regions, which are the main targets of neutralizing antibodies.

Twelve vaccines have been approved for use in humans since the first reported case of SARS-CoV-2 in December 2019, with high efficacy in preventing COVID-19 (17). However, the emergence of new variants has raised concerns about the effectiveness of these vaccines, with some trials showing reduced efficacy against variant strains in certain countries (18). The emergence of VOCs with mutations in the S-protein raises concerns about immune evasion. Some VOCs, such as B.1.1.7 and B.1.351, have shown reduced susceptibility to neutralizing antibodies, but the immunoreactivity of induced antibodies after vaccination with individual's mutations occurred in the RBD in VOCs is not well understood (15,19). The study focuses on understanding the humoral immune responses to SARS-CoV-2 in COVID-19 convalescent donors and vaccine recipients. This study investigated the levels of SARS-CoV-2 spike protein-specific total antibodies in a cohort of individuals who have received both doses of Covishield™ vaccine (vaccinated group) and patients who have recovered from SARS-CoV-2 infections (recovered group). The aim of the study was to compare the immunoreactivity of peptides of wild-type SARS-CoV-2 and peptides of mutated SARS-CoV-2 with antisera of vaccinated people and COVID-19 recovered patients to understand the effectiveness of vaccination and potential immune evasion strategies.

## Materials and methods

### Sample size and study groups

A total of 60 individuals of age  $\geq 18$  years (30 patients recovered from COVID-19 infections, 30 received both doses of Covishield™ vaccine) were recruited in the present study. COVID-19 recovered patients of both sexes who had not received any COVID-19 vaccines were recruited for the COVID-19 recovered group, while age-matched individuals without previous history of SARS-CoV-2 infections who have received both doses of Covishield™ were recruited for the vaccinated group. Patients on immunotherapy or having any kind of organ transplantations or immunocompromised patients (patients with human immunodeficiency virus [HIV] infection, autoimmunity, chronic kidney disease [CKD], and any other immunodeficiency diseases) were excluded from the study. This study was approved by the Institute Ethics

Committee (IEC), All India Institute of Medical Sciences, Raipur, Chhattisgarh, India (1936/IEC-AIIMSRRP/2021). The completely filled up and signed written consent form was obtained from each participant before taking the blood sample for the study.

### Disease severity

Patients who tested positive for SARS-CoV-2 infection by reverse transcriptase-polymerase chain reaction (RT-PCR) and got admitted to the Institute from October 2021 to December 2022 were included in the study. COVID-19 recovered patients were divided into severe and mild groups: severe cases were defined as those requiring invasive mechanical ventilation or high-flow nasal oxygen, and mild cases as neither requiring oxygen nor in-patient hospital care.

### Sample collection

A total of 5 mL whole blood sample was collected in a plain vial by venipuncture within 3 to 4 weeks of recovery from COVID-19 infections, while the same amount of blood sample was collected within 3 to 4 weeks postvaccination with both doses of Covishield™. The serum was collected to measure the levels of total antibodies and immunoreactivity of antibodies with selected peptides of spike protein of wild type and variants of SARS-CoV-2.

### Serum isolation

The blood samples collected in the plain vial were kept for 30 minutes for clotting. After that, it was centrifuged at 1,500 rpm for 10 minutes at 4°C. The resulting supernatant called serum was separated into fresh Eppendorf tubes and stored at -80°C till further use.

### Determination of serum levels of total antibodies

The serum levels of total antibodies (immunoglobulin, Ig) were measured in the collected serum samples of the vaccinated individuals and COVID-19 recovered patients. Human SARS-CoV-2 spike (trimer) Ig total enzyme-linked immunosorbent assay (ELISA) kit (Invitrogen, ThermoFisher Scientific) was used for the estimation of total immunoglobulins as per recommended standard protocol. Ten healthy serum samples collected before 2019 were used as controls to investigate the specificity and sensitivity of ELISA kit.

### Peptide synthesis and purification

A total of 12 peptides (six for the wild-type Wuhan isolates and six for the SARS-CoV-2 variants) of RBD of the spike protein were selected based on the available sequence of SARS-CoV-2 through UniPort software. These peptides were commercially synthesized and obtained to test the antibody responses. The peptides P1, P3, P5, P7, P9, and P11 matched with wild-type SARS-CoV-2 sequence, while peptides P2, P4, P6, P8, P10, and P12 matched with variants of SARS-CoV-2 (Tab. 1). The peptides P1 and P2



**TABLE 1** - List of the peptides of the RBD from wild type and SARS-CoV-2 variants

S. No	Peptides	Sequences of amino acids in the RBD of SARS-CoV-2	Sequence number	Mutating sites	VOC/wild type
1	P1	APGQTG <b>K</b> IADYNYK	411-424	K417	Wild
2	P2	APGQTG <b>N</b> IADYNYK	411-424	417N	Common site of mutation for Delta and Omicron
3	P3	TEIYQAG <b>S</b> TPCNGV	470-483	S477, T478	Wild
4	P4	TEIYQAG <b>N</b> KPCNGV	470-483	477N, 478K	Common site of mutation for Delta and Omicron
5	P5	PCNGV <b>E</b> GFNCYFPL	479-492	E484	Wild
6	P6	PCNGV <b>A</b> GFNCYFPL	479-492	484A	Common site of mutation for Delta and Omicron
7	P7	PLQSYGFQPT <b>N</b> GVG	491-504	N501	Wild
8	P8	PLQSYGFQPT <b>Y</b> GVG	491-504	501Y	Common site of mutation for Delta and Omicron
9	P9	WNSN <b>N</b> LDSK <b>V</b> SGNYN	436-450	N440, G446	Wild
10	P10	WNSN <b>K</b> LDSK <b>V</b> SGNYN	436-450	440K, 446S	Omicron
11	P11	YFPL <b>Q</b> SYG <b>F</b> QPT <b>N</b> GVG <b>Y</b> QPYR	489-509	Q493, G496, Q498, N501, Y505	Wild
12	P12	YFPL <b>R</b> SY <b>S</b> FRPT <b>Y</b> GVG <b>H</b> QPYR	489-509	493R, 496S, 498R, 501Y, 505H	Omicron

RBD = receptor-binding domain; VOC = variants of concern.

The sites of amino acid variations in the peptide sequences are highlighted in bold.

represent wild-type and mutated SARS-CoV-2, respectively. Both peptides P1 and P2 have same number of amino acids and same sequences of amino acids (411-424), but differ from each other at single amino acid residue at position 417. Likewise, peptides P3 and P4 have same amino acid sequence and length (470-483), but differ from each other at two residues at positions 477 and 478 in wild-type and mutated SARS-CoV-2, respectively. The peptides P5 and P6 show wild-type and mutated SARS-CoV-2, respectively, at residue 484. Both peptides have a single amino acid difference at residue 484. Similarly, peptides P7, P9, P11 of wild-type SARS-CoV-2 and peptides P8, P10, and P12 of SARS-CoV-2 variants have same length and sequence of amino acids, but differ from one another by one or more than one amino acid (Tab. 1).

#### Direct binding assay

To check the immunoreactivity of peptides with SARS-CoV-2 anti-sera and vaccine anti-sera, direct binding assay was performed using standard ELISA protocol. The ELISA plate was coated with individual peptides (200 ng/well) of spike protein. After blocking and washing SARS-CoV-2 anti-sera and vaccine anti-sera were added at a dilution of 1:200 onto the ELISA plate and incubated at 37°C for 2 hours. After washing, anti-human IgG antibody conjugated with horse radish peroxidase (HRP; 1:200 dilutions) was added and incubated for 1 hour at 37°C. Washing step was repeated after incubation and 100 µL/well substrate solution (TMB) was added. The color was developed within 10-15 minutes. The color reaction was stopped by adding 50 µL/well of 2N H<sub>2</sub>SO<sub>4</sub>. The plate was read at 450 nm in the ELISA reader.

#### Statistical analysis

Data visualization was performed via GraphPad Prism version 8.0 (GraphPad software, San Diego, CA, USA) and STATA 12 (STATA software, Chicago, USA) for Windows 10.0. Result was expressed as mean and standard deviation (SD) for normal distribution, or median and interquartile range for skewed distribution. For two-group analysis, we used the Mann-Whitney U-test for continuous variables. The level of significance (p-value) in the mean antibody titer was compared and analyzed with the Student's t-test.

#### Results

##### Clinical and demographic details

The study analyzed 30 COVID-19 recovered subjects and 30 individuals vaccinated with both doses of Covishield™. The clinical and demographic details are shown in Table 2. The median age of the COVID-19 recovered patients was 48.5 years, with a range of 23 to 76 years, while the median age of vaccinated group was 45 years, with a range of 18 to 74 years. The distributions of patients based on their age <65 years and >65 years in both groups are shown in Table 2. Out of the participants, 33.33% and 40% females were found in COVID-19 recovered group and vaccinated group, respectively. Based on disease severity, COVID-19 recovered patients were divided into severe and mild groups. Out of the COVID-19 recovered patients 43.33% were severe and required intensive care unit (ICU) support in the hospital. The most prevalent comorbidities among the COVID-19 recovered patients were obesity (26.67%), diabetes (23.33%), and hypertension (6.67%), and some of the patients required intensive care and intubation



**TABLE 2** - Clinical and demographic details of COVID-19 recovered patients and individuals who have received both doses of Covishield™

Characteristics	COVID-19 Recovered patients (n = 30)	Individuals vaccinated with both doses of Covishield™ (n = 30)
Age		
Median (IQR)	48.5 (23-76)	45(18-74)
<65 years (%)	21(70)	18 (60)
65+ years (%)	9(30)	12 (40)
Female (%)	10(33.33)	12 (40)
Severity		
Severe (%)	13(43.33)	NA
Mild (%)	17(66.67)	NA
Hospitalized, no ICU (%)	17 (66.67)	NA
Hospitalized, required ICU (%)	13(43.33)	NA
Died due to COVID-19 (%)	0(0)	NA
Preexisting conditions		
No underlying disease	11(36.67)	24 (80)
Hypertension	2(6.67)	2 (6.67)
Diabetes	7(23.33)	1 (3.33)
Obesity	8(26.67)	2 (6.67)
Hypothyroidism	2(6.67)	0

ICU = intensive care unit; IQR, interquartile range.

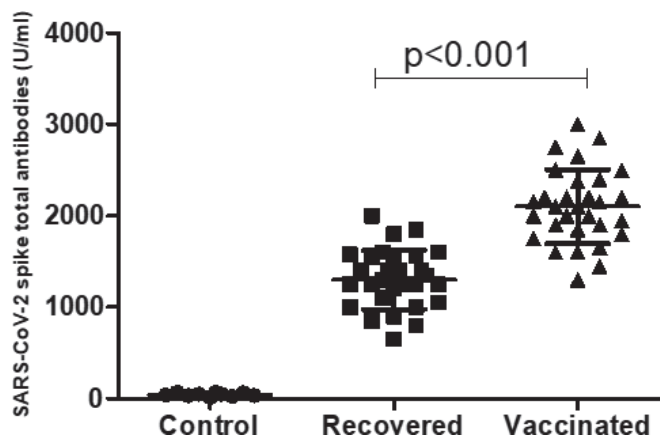
due to the severity of their condition. Obesity, hypertension, and diabetes were the most common comorbidities observed in the patients who required ICU support.

### Serum levels of total antibodies in COVID-19 recovered patients and vaccinated individuals

The sensitivity and specificity of human SARS-CoV-2 spike (trimer) Ig total ELISA kit (*Invitrogen*; ThermoFisher Scientific) were tested by the serum sample collected before 2019 as a control. SARS-CoV-2 spike protein-specific total antibodies were measured 3-4 weeks after the recovery from SARS-CoV-2 infections and after receiving the second dose of Covishield™ vaccine. The median (IQR) serum levels of SARS-CoV-2 spike-specific total antibodies were found to be 1275 U/mL (650-2000 U/mL) and 2100 U/mL (1300-3000 U/mL) in COVID-19 recovered patients and vaccinated individuals, respectively. The serum levels of total antibodies were found to be significantly ( $p < 0.001$ ) higher in the vaccinated individuals as compared to COVID-19 recovered patients (Fig. 1).

### Immunoreactivity of peptides with anti-sera of vaccinated and COVID-19 recovered patients

The individual peptides (P1, P3, P5, P7, P9, and P11) of wild-type SARS-CoV-2 and peptides (P2, P4, P6, P8, P10, and

**FIGURE 1** - Serum levels of SARS-CoV-2 spike protein-specific total immunoglobulins (Ig) within 3-4 weeks of recovery from SARS-CoV-2 infections from the hospital (n = 30) and 3-4 weeks after receiving the second dose of Covishield™ vaccine.

P12) were coated in the high-binding microtiter plate to assess the immunoreactivity with anti-sera obtained from vaccinated people and COVID-19 recovered patients. The immunoreactivity of peptides with antibodies was observed by taking the optical density (OD) at 592 nm. The difference in the OD value with corresponding peptides of wild types and mutated peptides was reported. The significant ( $p < 0.05$ ) difference in the immunoreactivity of peptides of wild type (P1, P5, P7) with peptides (P2, P6, P8) of mutated SARS-CoV-2 is reported in Figure 2. As compared to wild-type peptide sequence (P1), the mutated peptide sequence (P2) has single amino acid mutation in the RBD at position 417, which significantly reduced the immunoreactivity with anti-sera of vaccinated people and COVID-19 recovered patients (Fig. 2A). Likewise, the peptide sequence (P6) has a single amino acid mutation at residue 484 in the RBD of SARS-CoV-2, which significantly ( $p < 0.05$ ) reduced the immunoreactivity with anti-sera of vaccinated people and COVID-19 recovered patients (Fig. 2B). Similar to the mutated peptide sequences P2 and P6 of SARS-CoV-2 variants, the peptide sequence (P8) has single amino acid mutation in the RBD at the residue 501. This mutation also reduced the immunoreactivity with anti-sera of the vaccinated people and COVID-19 recovered patients (Fig. 2C). Finally, we have tested the immunoreactivity of peptide pools (P1, P5, and P7) of wild-type SARS-CoV-2 and peptide pools (P2, P6, and P8) of SARS-CoV-2 variants with the anti-sera of vaccinated people and COVID-19 recovered patients. Our finding showed a significant ( $p < 0.05$ ) reduction in immunoreactivity of anti-sera of vaccinated and COVID-19 recovered patients with peptide pools of SARS-CoV-2 variants (Fig. 2D). The amino acid mutations in the RBD of SARS-CoV-2 variants at residues 477, 478 for peptide sequence P4 and at residues 400, 446 for peptide sequence P10 did not reduce the immunoreactivity with anti-sera of vaccinated people and COVID-19 recovered patients (Supplementary figure 1, a and b). However, the mutated peptide sequence (P12) of SARS-CoV-2 variants has five amino acid mutations at residues 493, 496, 498, 501, and 505, which reduced the

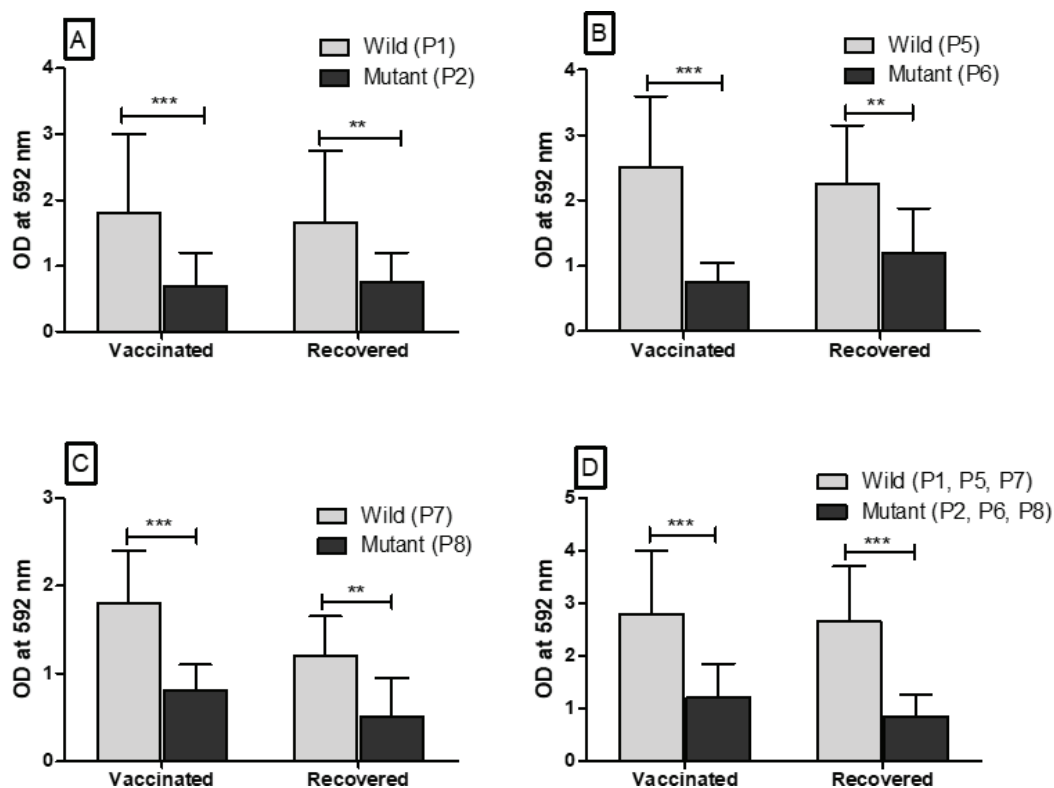


**FIGURE 2** - Immunoreactivity of peptides (P1, P5, P7) of wild-type SARS-CoV-2 and peptides (P2, P6, P8) of mutated SARS-CoV-2 variants with anti-sera obtained from healthy individuals vaccinated with both doses of Covishield™ (n = 30) and COVID-19 recovered patients from the hospital (n = 30). **A, B, and C.** The immunoreactivity of anti-sera with each peptide (P1, P5, P7) of wild-type SARS-CoV-2 and each peptide (P2, P6, P8) of mutated SARS-CoV-2 having single amino acid mutation at residues 417, 484, and 501, respectively. **D.** The immunoreactivity of anti-sera with peptide pools (P1, P5, P7) of wild-type SARS-CoV-2 and peptide pools (P2, P6, P8) of mutated SARS-CoV-2 having mutations at all three residues 417, 484, and 501.

immunoreactivity with anti-sera of vaccinated people and COVID-19 recovered patients. But, it was found to be comparable ( $p > 0.05$ ) (Supplementary figure 1c).

Finally, our study reported that the mutations in the RBD at the residues K417, E484, and N501 in SARS-CoV-2 variants have been associated with reduced immunoreactivity with anti-sera of vaccinated people and COVID-19 recovered patients (Fig. 2). The amino acid substitutions at K417, E484, and N501 residues significantly reduced antibody binding with polyclonal serum antibodies obtained from people who have recovered from COVID-19 and also vaccinated with ChAdOx1 nCoV-19 vaccines. The findings indicate that vaccination may result in a decreased long-term antibody response to Beta and Omicron RBDs, highlighting the challenges in neutralizing these variants with the existing antibody response induced by vaccination.

## Discussion

We analyzed the antibody response against SARS-CoV-2 spike protein using blood samples collected at least 3-4 weeks after recovery from nonvaccinated individuals who had recovered from COVID-19. The serum levels of total antibody were compared with individuals who had received both doses of Covishield™. The findings of the present study showed the significant rise in the levels of total antibody after 3-4 weeks of recovery from SARS-CoV-2 infections and after receiving both doses of Covishield™ (ChAdOx1 nCoV-19 coronavirus vaccines). The raised level of total antibody titer was found to be significantly higher in vaccinated people

compared to nonvaccinated people who have recovered from SARS-CoV-2 infections. Several studies have reported a significant rise in serum levels of total antibodies postvaccination with Covishield™ in healthy individuals (20,21). Few studies reported a significant difference in antibody titer with disease severity among COVID-19 recovered patients (22,23). Interestingly, among the recovered patients, those who had severe COVID-19 had higher levels of anti-spike total antibody compared to those with mild disease (24). Our study also reported significantly higher levels of SARS-CoV-2 spike protein-specific total antibody in severe COVID-19 recovered patients.

Vaccination with ChAdOx1 nCoV-19 coronavirus vaccines led to a significant increase in anti-spike antibody titers, indicating a robust humoral immune response. However, the raised antibody after vaccination could not immune-react with SARS-CoV-2 variant peptides. The polyclonal antibody response postvaccination showed limitations in binding the mutant peptides of RBDs of the Delta and Omicron variants, suggesting a potential challenge in achieving full protection against these variants (25). Findings of this study suggest that vaccination elicits a lower titer of immune-reactive antibodies against the Delta and Omicron RBDs, indicating potential challenges in neutralizing these variants. Overall, the results highlight the need for ongoing monitoring and adaptation of vaccines to address the evolving SARS-CoV-2 variants and their impact on antibody binding. The findings of our study are supported by the study of Geers et al 2021 (26). The study revealed structural analysis that the Delta and Omicron variants share a common immune escape strategy

involving specific residues (K417-E484-N501), allowing them to evade neutralization by anti-RBD antibodies (8,26). The study suggests that through mutations of this triad, SARS-CoV-2 has evolved to evade neutralization by the class I/II anti-RBD antibody fraction of hybrid immunity plasma. The findings indicate that vaccination may result in a decreased long-term antibody response to Delta and Omicron RBDs, highlighting the challenges in neutralizing these variants with the existing antibody response induced by vaccination. The study also found that the interval between vaccination and blood draw did not significantly impact antibody levels, indicating the stability of the antibody response over time. These findings highlight the need for continued monitoring and adaptation of vaccines to address the evolving SARS-CoV-2 variants and their immune evasion strategies.

Findings of our study reported reduced immunoreactivity of anti-sera of vaccinated people and COVID-19 recovered patients with a peptide having E484K mutation in the RBD of SARS-CoV-2 variants. Our finding is supported by the study done in Brazilian/Japanese variants (P.2 and P.1) with the E484K mutation, which had significantly decreased neutralization, suggesting evasion of antibody responses (27). The neutralization of the South African B.1.351 strain, which has three mutations in the RBD and has been found in reinfection cases, was significantly reduced for two-dose vaccines, similar to other distantly related coronaviruses, indicating that a small number of mutations can lead to potent humoral immune response escape (28,29). A considerable percentage of recipients did not have detectable neutralization of the B.1.351 variant after receiving two doses of either vaccine (22). Individuals with prior COVID-19 infection or significant exposure had higher neutralization titers and cross-neutralization against various variants, suggesting a combination of prior infection and vaccination may result in broader neutralizing antibody responses (30). The B.1.351 variant of SARS-CoV-2, also known as the South African variant, exhibits resistance to neutralization primarily because of mutations in the RBD of the spike protein. The RBD mutations in B.1.351, including K417N, E484K, and N501Y, contribute to the observed escape from vaccine-induced neutralization (31,32). Variants like P.2 and P.1 with specific RBD mutations reduce neutralization potency and may explain reinfection cases (33).

## Conclusion

The study concludes that multiple variants of SARS-CoV-2, including the Delta and Omicron variants, reduced immunoreactivity with polyclonal sera by vaccine-induced humoral immunity. The Delta variant's neutralization is primarily attributed to mutations in the RBD of the spike protein. The RBD mutations, such as K417N, E484K, and N501Y, play a significant role in the escape from vaccine-induced neutralization. The study highlights the need for reformulating existing vaccines to include diverse spike sequences and the development of new vaccines capable of eliciting broadly neutralizing antibodies to effectively combat the infection with variants of SARS-CoV-2 and possible future pandemic. It also emphasizes the importance of assessing other antibody-mediated functions and cellular immune responses mediated by T cells

and natural killer (NK) cells in understanding the overall protection provided by vaccines.

## Acknowledgments

We would like to acknowledge the All India Institute of Medical Science, Raipur, for providing the financial support for the study via intramural grant (No.22/41/2019/Admin/1346).

## Disclosures

**Conflict of interest:** All the authors of the manuscript do not have any conflict.

**Financial support:** The study was supported by intramural research grant sanctioned by All India Institute of Medical Sciences, Raipur, Chhattisgarh, India.

## References

1. To KKW, Sridhar S, Chiu KHY, et al. Lessons learned 1 year after SARS-CoV-2 emergence leading to COVID-19 pandemic. *Emerg Microbes Infect.* 2021;10(1):507-535. [CrossRef PubMed](#)
2. Khan M, Adil SF, Alkathlan HZ, et al. COVID-19: a global challenge with old history, epidemiology and progress so far. *Molecules.* 2020;26(1):39. [CrossRef PubMed](#)
3. Tregoning JS, Flight KE, Higham SL, Wang Z, Pierce BF. Progress of the COVID-19 vaccine effort: viruses, vaccines and variants versus efficacy, effectiveness and escape. *Nat Rev Immunol.* 2021; 21(10):626-636. [CrossRef PubMed](#)
4. Tsurkalenko O, Bulaev D, O'Sullivan MP, et al; CON-VINCE consortium and the ORCHESTRA working group. Creation of a pandemic memory by tracing COVID-19 infections and immunity in Luxembourg (CON-VINCE). *BMC Infect Dis.* 2024;24(1):179. [CrossRef PubMed](#)
5. Akhlaghi A, Darabi A, Mahmoodi M, et al. The frequency and clinical assessment of COVID-19 in patients with chronic rhinosinusitis. *Ear Nose Throat J.* 2024;103(2):NP98-NP103. [CrossRef PubMed](#)
6. Su S, Zhao Y, Zeng N, et al. Epidemiology, clinical presentation, pathophysiology, and management of long COVID: an update. *Mol Psychiatry.* 2023;28(10):4056-4069. [CrossRef PubMed](#)
7. Zaidi AK, Singh RB. Epidemiology of COVID-19. *Prog Mol Biol Transl Sci.* 2024;202:25-38. [PubMed](#)
8. Montezano AC, Camargo LL, Mary S, et al. SARS-CoV-2 spike protein induces endothelial inflammation via ACE2 independently of viral replication. *Sci Rep.* 2023;13(1):14086. [CrossRef PubMed](#)
9. Kibria MG, Lavine CL, Tang W, et al. Antibody-mediated SARS-CoV-2 entry in cultured cells. *EMBO Rep.* 2023;24(12):e57724. [CrossRef PubMed](#)
10. Li CJ, Chang SC. SARS-CoV-2 spike S2-specific neutralizing antibodies. *Emerg Microbes Infect.* 2023;12(2):2220582. [CrossRef PubMed](#)
11. Akaishi T, Fujiwara K. Insertion and deletion mutations preserved in SARS-CoV-2 variants. *Arch Microbiol.* 2023;205(4): 154. [CrossRef PubMed](#)
12. Ma KC, Shirk P, Lambrou AS, et al. Genomic surveillance for SARS-CoV-2 variants: circulation of omicron lineages – United States, January 2022-May 2023. *MMWR Morb Mortal Wkly Rep.* 2023;72(24):651-656. [CrossRef PubMed](#)
13. Aleem A, Akbar Samad AB, Vaqar S. Emerging variants of SARS-CoV-2 and novel therapeutics against coronavirus (COVID-19). In: *StatPearls*. [Internet] StatPearls Publishing; 2024, Available from [Online](#). Accessed March 1, 2024.



14. Roemer C, Sheward DJ, Hisner R, et al. SARS-CoV-2 evolution in the Omicron era. *Nat Microbiol.* 2023;8(11):1952-1959. [CrossRef PubMed](#)
15. Carabelli AM, Peacock TP, Thorne LG, et al; COVID-19 Genomics UK Consortium. SARS-CoV-2 variant biology: immune escape, transmission and fitness. *Nat Rev Microbiol.* 2023;21(3):162-177. [CrossRef PubMed](#)
16. Pather S, Madhi SA, Cowling BJ, et al. SARS-CoV-2 Omicron variants: burden of disease, impact on vaccine effectiveness and need for variant-adapted vaccines. *Front Immunol.* 2023;14:1130539. [CrossRef PubMed](#)
17. Yadav T, Kumar S, Mishra G, Saxena SK. Tracking the COVID-19 vaccines: the global landscape. *Hum Vaccin Immunother.* 2023;19(1):2191577. [CrossRef PubMed](#)
18. Wahid M, Jawed A, Mandal RK, et al. Role of available COVID-19 vaccines in reducing deaths and perspective for next generation vaccines and therapies to counter emerging viral variants: an update. *Minerva Med.* 2023;114(5):683-697. [CrossRef PubMed](#)
19. Bostanghadiri N, Ziaeefer P, Mofrad MG, Yousefzadeh P, Hashemi A, Darban-Sarokhalil D. COVID-19: An overview of SARS-CoV-2 variants – the current vaccines and drug development. *BioMed Res Int.* 2023;2023:1879554. [CrossRef PubMed](#)
20. Nanda R, Gupta P, Giri AK, Patel S, Shah S, Mohapatra E. Serological evaluation of antibody titers after vaccination against COVID-19 in 18-44-year-old individuals at a tertiary care center. *Cureus.* 2023;15(6):e40543. [CrossRef PubMed](#)
21. Dimitroff SJ, Würfel L, Meier M, et al. Estimation of antibody levels after COVID-19 vaccinations: preliminary evidence for immune interoception. *Biol Psychol.* 2023;182:108636. [CrossRef PubMed](#)
22. Huang C, Huang L, Wang Y, et al. 6-Month consequences of COVID-19 in patients discharged from hospital: a cohort study. *Lancet.* 2023;401(10393):e21-e33. [CrossRef PubMed](#)
23. Amrutha S, Kaur K, Aggarwal D, Sodhi MK, Jaswal S, Saini V. Serial evaluation of antibody titres in patients recovered from COVID-19 and their correlation with disease severity. *Monaldi Arch Chest Dis* 2023 Nov 3. [CrossRef](#)
24. de Oliveira MI, Aciole MR, Neves PAF, et al. A stronger antibody response in increased disease severity of SARS-CoV-2. *BMC Infect Dis.* 2024;24(1):17. [CrossRef PubMed](#)
25. Lavezzo E, Pacenti M, Manuto L, et al. Neutralising reactivity against SARS-CoV-2 delta and omicron variants by vaccination and infection history. *Genome Med.* 2022;14(1):61. [CrossRef PubMed](#)
26. Geers D, Shamier MC, Bogers S, et al. SARS-CoV-2 variants of concern partially escape humoral but not T-cell responses in COVID-19 convalescent donors and vaccinees. *Sci Immunol.* 2021 May 25;6(59):eabj1750. [CrossRef](#)
27. Ma QL, Huang FM, Guo W, Feng KY, Huang T, Cai YD. Machine learning classification of time since BNT162b2 COVID-19 vaccination based on array-measured antibody activity. *Life (Basel).* 2023;13(6):1304. [CrossRef PubMed](#)
28. Edara VV, Norwood C, Floyd K, et al. Reduced binding and neutralization of infection- and vaccine-induced antibodies to the B.1.351 (South African) SARS-CoV-2 variant. *bioRxiv [Preprint].* 2021 Feb 22. [CrossRef PubMed](#)
29. Ryu DK, Song R, Kim M, et al. Therapeutic effect of CT-P59 against SARS-CoV-2 South African variant. *Biochem Biophys Res Commun.* 2021;566:135-140. [CrossRef PubMed](#)
30. Sette A, Crotty S. Immunological memory to SARS-CoV-2 infection and COVID-19 vaccines. *Immunol Rev.* 2022;310(1):27-46. [CrossRef PubMed](#)
31. Viana R, Moyo S, Amoako DG, et al. Rapid epidemic expansion of the SARS-CoV-2 Omicron variant in southern Africa. *Nature.* 2022 Mar;603(7902):679-686. [CrossRef](#)
32. Wibmer CK, Ayres F, Hermanus T, et al. SARS-CoV-2 501Y.V2 escapes neutralization by South African COVID-19 donor plasma. *Nat Med.* 2021 Mar 1;27:622-625.
33. Wahid M, Jawed A, Mandal RK, et al. Variants of SARS-CoV-2, their effects on infection, transmission and neutralization by vaccine-induced antibodies. *Eur Rev Med Pharmacol Sci.* 2021;25(18):5857-5864. [PubMed](#)



# Tuberculosis research: Quo vadis

Nerges F. Mistry

The Foundation for Medical Research, Dr. Kantilal J. Sheth Memorial Building, Mumbai - India

Despite 142 years of ongoing research, since Robert Koch discovered the tuberculosis (TB) bacillus, TB continues to flourish in the most vulnerable parts of the globe in Asia, Africa and South America (1). Indeed, progressive socio-economic measures (nutrition, housing and environment) have shown to be more effective than research in disease elimination in affluent areas of the globe (2). Undoubtedly, however, areas undertaken in recent research studies underscore new knowledge that may yield far-reaching impact on disease control, if not elimination. This editorial aims to highlight such specific studies and their impact.

## Non-medical determinants

Little attention was paid to research on socio-economic measures. In this regard, two studies, viz., Bhargava et al. (3) and Shin et al. (4), stand out. Additionally, McKeown's famous graph (5) showed a dramatic decrease in TB even in the absence of drugs with good housing and a balanced diet. With the recent RATIONS (Reducing Activation of Tuberculosis by Improvement of Nutritional Status) trial in rural Jharkhand, the problem of undernutrition as a primary cause of TB was brought into the limelight though with nutrition supplementation only 54% of patients reached the desirable weight gain at 2 months of treatment (6). This poses several puzzling questions which need to be answered to establish nutrition as an effective control/prevention tool. Environmental pollution studies and its effect on TB incidence are also gaining ground with emphasis on particulate matter 2.5 and even smaller particles (7). However, the concept of healthy housing with optimal access to light and ventilation has been overlooked in India though it is prevalent in some countries of South-East Asia (8). In a study in the slums in Mumbai air exchange of 1-2 every 13 hours was seen to be the norm as opposed to the desired 6-7 per hour (FMR unpublished study). Transmission of all respiratory diseases is inevitable and will be continuous with such a large ventilation deficit and will continue to take place with compromised ventilation.

## Drugs and mutations

The most singular outcome of biomedical research in TB has been to identify new and repurposed drugs for use

against the TB bacillus. From rifampicin in the early 1970s to bedaquiline (BDQ) and delamanid in 2012 and 2013, the trickle of new drugs is envisaged as a powerful means of disease control but one that has a window of time before drug resistance sets in for a single drug/drug combination. One of the most singular findings in recent years is the theme that resistance to any drug can occur even before the drug is put to use by the disease programme. Extensive drug-resistant TB was detected in KwaZulu Natal even before the same drugs were deployed, through natural selection (9). Similarly in a cohort in India, mutations bestowing high minimum inhibitory concentrations (MICs) to BDQ such as Rv0678: c.141\_142dupTC, p.Glu55Asp, p.Leu117Arg, p.Gly162Glu; atpE: p.Glu61Asp, p.Thr51Ile, p.Ser37Ala; pepQ: p.Pro69Leu, p.Arg7Gln; mmpL5: Ile948Val, Thr794Ile, Asp767Asn (FMR unpublished data) were seen in patients not exposed to BDQ. Does the presence of such natural mutations signify a natural tendency for resistance amplification? This is a powerful phenomenon to study the evolution of drug resistance in the coming years.

Another paradigm has been the linkage of gut microbiome to the phenomenon of drug resistance in an individual (10). Modulating the microbiome towards greater diversity and speciation offers a novel way to combat the emergence of drug resistance that needs to be explored with incisive studies, especially since a disturbed gut microbiome continues to exist for over 1.2 years post-anti-TB treatment (11). The use of complex compounds in phytomedicine indicates another approach to minimizing drug resistance. These complex structures in plant products may retard the development of drug resistance to conventional anti-TB drugs by stabilizing the gut microbiome or may have anti-bacterial action directly vs drug-resistant bacteria. This would provide a relatively cost-effective approach to the treatment of drug-resistant TB. Though no scattered studies provide positive indications (12-14), rigorous in-depth research is required.

## Diagnosis

TB is well recognized as a respiratory disease spread through the air through microdroplets, especially in vulnerable communities. The ability to capture and detect such infectious droplets through masks (15,16) or through capture chambers (17) has given a profound scenario of disease biology. Increasing evidence has been generated in very recent years in even non-symptomatic individuals where disease in the preclinical stages shows the capture of such infectious droplets (18). This leads to a paradigm change in understanding the transmission of TB through non-symptomatic individuals, say, within a household in vulnerable communities and

---

Received: March 26, 2024  
Accepted: May 14, 2024  
Published online: May 31, 2024

### Corresponding author:

Nerges F. Mistry  
email: [fmr@fmrindia.org/fmrmm@gmail.com](mailto:fmr@fmrindia.org/fmrmm@gmail.com)



which can also be utilized effectively during active prevalence surveys.

The pipeline of novel TB diagnostics has never been richer. Several large consortia funded by the United States Agency for International Development, National Institutes of Health and Unitaid are currently undertaking validation study of these diagnostics for ensuring that the best are put to use. The future will stress self-sampling and self-testing technologies, which are likely to have wider acceptability.

## Surveillance

The epidemiological research in TB is likely to be transformed in the coming years through increasing use of surveillance methods be it for antimicrobial resistance (AMR), mutations, clinical profiles or drug responses. The ability of countries to sustain continued data collection and rapid analysis would allow the use of key data that can be used for disease control.

Genomic surveillance and questions on how the environment fashions *Mycobacterium tuberculosis* (M.tb) response could not have occurred without the explosion in the field of bioinformatic tools and their application. For instance, Fastlin facilitates ultra-fast and accurate mycobacterium complex lineage typing, whereas Mykrobe can predict AMR in minutes (19,20). MTBseq is a comprehensive pipeline developed for whole-genome sequencing of M.tb complex isolates (21). These have been invaluable in ascertaining strain differences and in detecting transmission of TB in hyperendemic areas or examining tissue tropism of strain in extrapulmonary TB. We anticipate the generation of crucial knowledge in the coming years through deciphering the language of the cells.

## Operations research

In operations research, the engagement of the private sector has become a key theme in recent times taken up on a global basis through the formation of public-private learning networks led by McGill University in Toronto. The Public Private Interface Agency (PPIA) introduced by the Gates Foundation in India around 2015 showed some early gains for patients accessing a PPIA-engaged physician at the first point of call (22). Whether this has translated to its successor, the Private Provider Support Agency (PPSA) overseen by the Government of India, remains to be evaluated.

The PPSA as of now is run on bureaucratic rather than functional lines, the emphasis being on orienting non-governmental organizations (the middle link between the National Tuberculosis Elimination Programme and the community) rather than sensitization and education of private sector physicians. The PPSA needs evaluation to fine-tune a potentially effective solution to early diagnosis, correct treatment and follow-up of TB patients buoyed by support mechanisms of direct cash benefit transfer for nutrition to patients.

The pioneering differentiated care model introduced by the Indian state of Tamil Nadu in 2022-2023 (23) is an innovative step today open for wider dissemination nationally and globally. It takes into account severe undernutrition, impaired lung function and overall functionality. This

model if researched well will provide crucial learnings on approaches to reducing mortality and enhancing patient care infrastructure.

An excessively strict adherence to national guidelines for disease control paradoxically retards innovative insights in clinical and microbiological research and also adversely affects patient outcomes. Structures must be instituted to examine result discrepancies so that new paradigms of knowledge can be created.

## Encouraging a comprehensive and open approach

With an eye on equitable access to knowledge and treatment, research should increasingly focus on to what extent and circumstances users stay out of the service technology net. The upfront GeneXpert (24) initiative and the SMaRT-PCR initiative (25 and [Online](#)) in diagnostic technology validation is a step in the right direction where technical performance is supplemented with an inquiry into community-level acceptability and feasibility. Two areas of applicability of such an approach are paediatric TB and post-treatment rehabilitation, an area almost completely ignored today in India. The next couple of years will give a comprehensive view of how novel technologies need to be translated for field conditions.

With the advent of big data technology globally, there comes the responsibility of open data sharing that can ward off common global threats. The trend of overt protection of country data needs to be eschewed if the common good is to be realized by the use of big data. Such global cooperation is a desirable but still yet distant goal.

## Abbreviations

TB, tuberculosis; BDQ, bedaquiline; M.tb, *Mycobacterium tuberculosis*; PPIA, Public Private Interface Agency; PPSA, Private Provider Support Agency

## Acknowledgements

Grateful thanks to Dr. Ambreen Shaikh and Ms. Poonam Daswani at The Foundation for Medical Research for their assistance in referencing for this editorial.

## Disclosures

**Conflict of Interest:** The author has no conflict of interest to declare.

**Funding:** The research received no specific grant from any funding agency in the public, commercial, or not-for-profit sectors.

## References

1. World Health Organization (WHO). Global tuberculosis report, 2023. [Online](#). Accessed 21 February 2024.
2. McKeown T, Record RG. Reasons for the decline of mortality in England and Wales during the nineteenth century. *Population Studies*. 1962;16(2):94-122. [CrossRef](#)
3. Bhargava A, Pai M, Bhargava M, Marais BJ, Menzies D. Can social interventions prevent tuberculosis?: The Papworth experiment (1918-1943) revisited. *Am J Respir Crit Care Med*. 2012;186(5):442-449. [CrossRef PubMed](#)



4. Shin S, Furin J, Bayona J, Mate K, Kim JY, Farmer P. Community-based treatment of multidrug-resistant tuberculosis in Lima, Peru: 7 years of experience. *Soc Sci Med*. 2004;59(7):1529-1539. [CrossRef PubMed](#)
5. McKeown T. The modern rise of population. Edward Arnold; 1976.
6. Bhargava A, Bhargava M, Meher A, et al. Nutritional support for adult patients with microbiologically confirmed pulmonary tuberculosis: outcomes in a programmatic cohort nested within the RATONS trial in Jharkhand, India. *Lancet Glob Health*. 2023;11(9):e1402-e1411. [CrossRef PubMed](#)
7. Dimala CA, Kadia BM. A systematic review and meta-analysis on the association between ambient air pollution and pulmonary tuberculosis. *Sci Rep*. 2022;12(1):11282. [CrossRef PubMed](#)
8. Aditama W, Sitepu FY, Saputra R. Relationship between physical condition of house environment and the incidence of pulmonary tuberculosis, Aceh, Indonesia. *Int J Sci Health Res*. 2019;4(1):227-231.
9. Gandhi NR, Moll A, Sturm AW, et al. Extensively drug-resistant tuberculosis as a cause of death in patients co-infected with tuberculosis and HIV in a rural area of South Africa. *Lancet*. 2006;368(9547):1575-1580. [CrossRef PubMed](#)
10. Matzaras R, Nikopoulou A, Protonotariou E, Christaki E. Gut microbiota modulation and prevention of dysbiosis as an alternative approach to antimicrobial resistance: a narrative review. *Yale J Biol Med*. 2022;95(4):479-494. [PubMed](#)
11. Wiperman MF, Fitzgerald DW, Juste MAJ, et al. Antibiotic treatment for tuberculosis induces a profound dysbiosis of the microbiome that persists long after therapy is completed. *Sci Rep*. 2017;7(1):10767. [CrossRef PubMed](#)
12. Mangwani N, Singh PK, Kumar V. Medicinal plants: adjunct treatment to tuberculosis chemotherapy to prevent hepatic damage. *J Ayurveda Integr Med*. 2020;11(4):522-528. [CrossRef PubMed](#)
13. Rana HK, Singh AK, Kumar R, Pandey AK. Antitubercular drugs: possible role of natural products acting as antituberculosis medication in overcoming drug resistance and drug-induced hepatotoxicity. *Naunyn Schmiedebergs Arch Pharmacol*. 2024;397(3):1251-1273. [CrossRef PubMed](#)
14. Gautam S, Qureshi KA, Jameel Pasha SB, et al. Medicinal plants as therapeutic alternatives to combat *Mycobacterium tuberculosis*: a comprehensive review. *Antibiotics (Basel)*. 2023;12(3):541. [CrossRef PubMed](#)
15. Williams CML, Cheah ESG, Malkin J, et al. Face mask sampling for the detection of *Mycobacterium tuberculosis* in expelled aerosols. *PLoS One*. 2014;9(8):e104921. [CrossRef PubMed](#)
16. Shaikh A, Sriraman K, Vaswani S, Oswal V, Mistry N. Detection of *Mycobacterium tuberculosis* RNA in bioaerosols from pulmonary tuberculosis patients. *Int J Infect Dis*. 2019;86:5-11. [CrossRef PubMed](#)
17. Wood R, Morrow C, Barry CE III, et al. Real-time investigation of tuberculosis transmission: developing the respiratory aerosol sampling chamber (RASC). *PLoS One*. 2016;11(1):e0146658. [CrossRef PubMed](#)
18. Williams CM, Abdulwhhab M, Birring SS, et al. Exhaled *Mycobacterium tuberculosis* output and detection of subclinical disease by face-mask sampling: prospective observational studies. *Lancet Infect Dis*. 2020;20(5):607-617. [CrossRef PubMed](#)
19. Derelle R, Lees J, Phelan J, Lalvani A, Arinaminpathy N, Chin-delevitch L. fastlin: an ultra-fast program for *Mycobacterium tuberculosis* complex lineage typing. *Bioinformatics*. 2023;39(11):btad648. [CrossRef PubMed](#)
20. Hunt M, Bradley P, Lapierre SG, et al. Antibiotic resistance prediction for *Mycobacterium tuberculosis* from genome sequence data with Mykrobe. *Wellcome Open Res*. 2019;4:191. [CrossRef PubMed](#)
21. Kohl TA, Utpatel C, Schleusener V, et al. MTBseq: a comprehensive pipeline for whole genome sequence analysis of *Mycobacterium tuberculosis* complex isolates. *PeerJ*. 2018;6:e5895. [CrossRef PubMed](#)
22. Shah S, Shah S, Rangan S, et al. Effect of public-private interface agency in Patna and Mumbai, India: does it alter durations and delays in care seeking for drug-sensitive pulmonary tuberculosis? *Gates Open Res*. 2020;4:32.
23. Shewade HD, Frederick A, Kiruthika G, et al. The first differentiated TB care model from India: delays and predictors of losses in the care cascade. *Glob Health Sci Pract*. 2023;11(2):e2200505. [CrossRef PubMed](#)
24. Sarin S, Huddart S, Raizada N, et al. Cost and operational impact of promoting upfront GeneXpert MTB/RIF test referrals for presumptive pediatric tuberculosis patients in India. *PLoS One*. 2019;14(4):e0214675. [CrossRef PubMed](#)
25. Shaikh A, Sriraman K, Vaswani S, et al. SMART-PCR: sampling using masks and RT-PCR, a non-invasive diagnostic tool for paediatric pulmonary TB. *Int J Tuberc Lung Dis*. 2024;28(4):189-194. [CrossRef PubMed](#)

# Molecular targets and therapeutic potential of baicalein: a review

Kavita Munjal<sup>1</sup>, Yash Goel<sup>2</sup>, Vinod Kumar Gauttam<sup>3</sup>, Hitesh Chopra<sup>4</sup>, Madhav Singla<sup>5</sup>, Smriti<sup>6</sup>, Saurabh Gupta<sup>5</sup>, Rohit Sharma<sup>7</sup>

<sup>1</sup>Department of Pharmacognosy, Amity Institute of Pharmacy, Amity University, Noida, Uttar Pradesh - India

<sup>2</sup>Department of Pharmacy, M.M. College of Pharmacy, M.M. (Deemed to be University), Mullana, Ambala, Haryana - India

<sup>3</sup>Department of Pharmacognosy, Shiva Institute of Pharmacy, Bilaspur, Himachal Pradesh - India

<sup>4</sup>Department of Biosciences, Saveetha School of Engineering, Saveetha Institute of Medical and Technical Sciences, Chennai, Tamil Nadu - India

<sup>5</sup>Department of Pharmacy, Chitkara College of Pharmacy, Chitkara University, Rajpura, Punjab - India

<sup>6</sup>Department of Pharmacology, Chameli Devi Institute of Pharmacy, Indore, Madhya Pradesh - India

<sup>7</sup>Department of Rasa Shastra and Bhaishajya Kalpana, Faculty of Ayurveda, Institute of Medical Sciences, Banaras Hindu University, Varanasi, Uttar Pradesh - India

## ABSTRACT

**Aim:** Researchers using herbs and natural products to find new drugs often prefer flavonoids because of their potential as antioxidants and anti-inflammatories. The planned review addressed baicalein research findings in detail. This manuscript provides a complete review of baicalein's potential pharmacological effects along with several molecular targets for better understanding of its therapeutic activities.

**Materials and methods:** We targeted the review on in vitro and in vivo studies reported on baicalein. For this, the literature is gathered from the database available on search engines like PubMed, ScienceDirect, Scopus, and Google Scholar up to 21 December 2023. The keywords "*Scutellaria baicalensis*", "*Oroxylum indicum*", "*Neuroprotective*", "*Cardioprotective*", "*Toxicity studies*", and "*Baicalein*" were used to fetch the content.

**Results:** Baicalein's molecular receptor binding approach has shown anticancer, antidiabetic, antimicrobial, anti-aging, neuroprotective, cardioprotective, respiratory protective, gastroprotective, hepatic protective, and renal protective effects. The synergistic effects of this drug with other selective herbs are also contributed towards significant therapeutic potential.

**Conclusion:** This systematic review article from a contemporary and scientific perspective offers fresh insight into *S. baicalensis*, *O. indicum*, and its bioactive component baicalein as a potential complementary medicine. Baicalein may be transformed into more efficacious and acceptable evidence-based medicine. However, we recommend more clinical and mechanistic approaches to confirm safety and efficacy of baicalein.

**Keywords:** Alzheimer's, Baicalein, Cancer, Epilepsy, Heart failure, Hypertension, Parkinson, Stroke

## Introduction

Baicalein, a flavone compound, is widely recognized in Chinese traditional medicine as Huang-qin or Chinese skullcap (1). Recent research has revealed the therapeutic significance and pharmacological findings of roots of *Scutellaria*

*baicalensis* and *Oroxylum indicum*. *S. baicalensis* Georgi, a member of the Lamiaceae family, stands as one of the pharmacologically significant species of flowering plant. The herbaceous perennial under investigation exhibits distinct characteristics that contribute to its overall appeal. Its papery leaves, thick roots, and branching stems provide a sturdy foundation for its growth and development. Additionally, the vibrant purple-red to blue blooms add a touch of elegance and beauty to its appearance. The presence of black-brown ovoid nutlets further enhance its appearance. Traditional Chinese medicine has a rich history of utilization and continues to be widely practiced. The cultivation of this particular plant species has been observed in various regions, including eastern Russia, Japan, China, Siberia, Mongolia, and Korea. In addition to the well-known Chinese medicinal ingredients, various *Scutellaria* species including *S. viscidula*, *S. rehderiana*, *S. amoena*, *S. likiangensis*, and *S. hypericifolia* have also

**Received:** November 6, 2023

**Accepted:** January 11, 2024

**Published online:** June 6, 2024

### Corresponding author:

Rohit Sharma  
email: rohitsharma@bhu.ac.in

Hitesh Chopra  
email: chopraontheride@gmail.com



been utilized as Huang-qin in different regions (2). There are several ways available for extracting baicalein, as shown in Table 1. The auxiliary extraction methodology achieved the maximum yield while extracting from the roots of *Scutellaria*.

*O. indicum*, commonly referred to as the Indian trumpet flower, has received significant attention in the field of research. The plant in issue belongs to the Bignoniaceae family, which is well-known for its therapeutic qualities. The subject of investigation is a compact to moderate-sized deciduous tree, characterized by presence of light grayish brown bark adorned with cory lenticels. The vibrant reddish-purple blooms grow on its outer surface, while its inner core exhibited the presence of pinkish yellow flowers. Additionally, the tree bears distinctive woody, winged, large, and flat fruits, which add to its visual allure. Furthermore, this remarkable tree exhibits presence of pinnately compound evergreen leaves, enhancing its overall appeal. The geographical distribution of this particular phenomenon primarily encompasses the countries of India, China, Thailand, Sri Lanka, Cambodia, Bangladesh, and other nations within the South Asian region.

Baicalin, also known as baicalein-7-O- $\beta$ -D-glucuronic acid, undergoes hydroxylation to yield a biologically active aglycone called baicalein (CID 64982), which is chemically known as 5,6,7-trihydroxyflavone (3). Baicalein, a naturally occurring flavonoid, exhibits a chemical structure derived from the fundamental framework of 2-phenyl chromen-4-one (also known as 2-phenyl-1-benzopyran-4-one). One intriguing aspect of bodily metabolism is the ability for certain substances to undergo a transformative process, allowing them to transition into different forms. Baicalin, a naturally occurring compound, exhibits a unique molecular structure, which contributes to the diverse biological activities and potential therapeutic applications. Understanding the structural features of baicalin is crucial for elucidating its mechanisms of action and exploring its potential in various fields of research (1,4).

This molecule demonstrates a wide range of biological actions, including significant domains such as reducing the risk of cancer, virus suppression, diabetic control, and mitigation of age-related deterioration. Additionally, it

demonstrates notable protective effects on the neurological, cardiovascular, gastrointestinal (GI), hepatic, respiratory, and renal systems (5). This comprehensive review aims to consolidate a wealth of information on the diverse pharmacological effects associated with various diseases, encompassing multiple pathways, mechanisms of action, and in vitro studies (5). This review further highlight the attractive opportunities for baicalein-associated drug discovery and research across a range of therapeutic areas.

## Chemistry of baicalein

Flavonoids, a class of polyphenolic compounds, have garnered significant attention in the realm of natural products due to their extensive research and exploration (11). One of the key structural components of this compound was produced using the acetate route, leading to the development of the phenolic ring chromophore (ring A) within its 15-carbon skeletal framework (11). One of the best examples of the most fundamental flavone molecule is chrysin, which has the unique property of retaining the necessary meta-substituted hydroxyl groups on the A-ring. The OH substitution at chrysin's C-6 position causes it to change into the trihydroxy derivative baicalein (12) having chemical formula  $C_{15}H_{10}O_5$ . More specifically, it is recognized as 5,6,7-trihydroxy-2-phenyl-4H-chromen-4-one, as Figure 1 illustrates. Using a multistep synthetic strategy, researchers have effectively recreated the biosynthetic transition of chrysin to baicalein in recent laboratory tests; 1-(2,4,6-trihydroxyphenyl)ethanone and 1-ethyl-3-phenyl-1,3-propanedione are combined in the first synthesis technique. Chen et al completed a pioneering investigation that revealed an amazing and novel method for extracting baicalein from 3,4,5-trimethoxyphenol. This approach, which consists of a brief fourstep procedure, showed promise for a more streamlined and effective manufacture of baicalein (13,14). One of the key structural characteristics that distinguishes baicalin and baicalein is the notable existence of a di-ortho OH on ring A. The remarkable characteristic exhibited by polyphenolic compounds lies in their ability to serve as efficient markers for metal chelation,

**TABLE 1** - Several methods for extraction of baicalein

S. no.	Species	Part of the plant	Extraction method	Analytical technique	Yield	Reference
1.	<i>Oroxylum indicum</i>	Stem barks	Solvent (ethanol) extraction (Reflux method)	HPTLC	26.498 mg/g	(6)
			Solvent (acetone) extraction (Reflux method)	HPTLC	8.631 mg/g	
			DMSO extract (Reflux method)	HPTLC	13.883 mg/g	
			DMF extract (Reflux method)	HPTLC	20.529 mg/g	
		Seeds	Solvent (95% ethanol) extraction (maceration method)	HPLC	0.72% $\pm$ 0.00% w/w	(7)
2.	<i>Scutellaria baicalensis</i> Georgi	Roots	Solvent (methanol) extraction (maceration method)	HPLC	0.5 mg/mL	(8)
			Auxiliary extraction method	HPLC	116.8 mg/g	(9)
			Supercritical fluid extraction	HPLC-UV	2.5-80 $\mu$ g/mL	(10)

DMF = dimethylformamide; DMSO = dimethyl sulfoxide; HPLC-UV = high-performance liquid chromatography ultraviolet; HPTLC = high-performance thin layer chromatography.



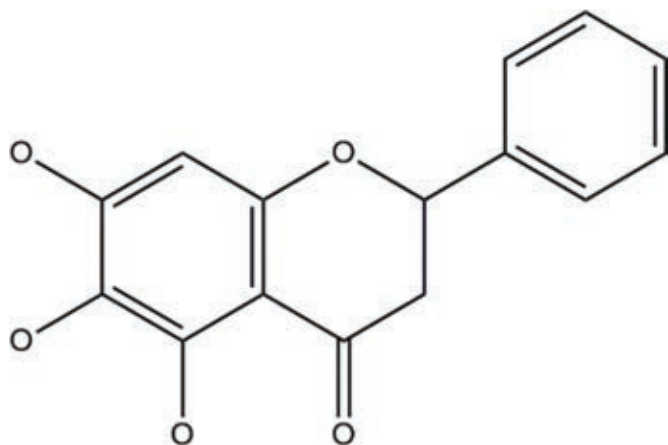


**FIGURE 1** - Structure of baicalein.

free radical scavenging properties, and enzyme inhibition. The structural features of baicalein are believed to be responsible for its reported antioxidant effects and its ability to chelate divalent metal ions (14).

### Anticancer effects of baicalein

Cancer, uncontrolled cell proliferation, can show up phenotypically in a number of ways, from benign to fatal. There are numerous factors that can lead to the development of cancer, including deoxyribonucleic acid (DNA) damage, mutations in the DNA or any by-products of that DNA, and dysfunction of the regulatory and repressor mechanisms during the cell cycle. The four phases of the cell cycle in actively dividing eukaryotes occur in the sequence starting from gap 1, synthesis, gap 2 followed by mitosis. While entering the next phase of the cell cycle, there are a number of checkpoints available en route to ensure that the actions at each phase have been appropriately completed. Phosphorylated retinoblastoma protein (pRB), cyclin subunits, cyclin-dependent kinases (CDKs), and cyclin-dependent kinase inhibitors (CDKIs) are the components of these checkpoints (15). Cell cycle arrest occurs when cells are unable to pass cell cycle checkpoints. Cell death and growth inhibition may result from G1 arrest. G2/M arrest is linked to increased apoptosis and may increase the cytotoxicity of chemotherapy (16).

It is estimated that in 2024, around 2,001,140 new cancer cases and 611,720 cancer deaths are projected to occur in the United States. With around 350 cases of lung cancer fatalities every day, lung cancer is the most common cause of cancer-related mortality (17). Baicalein induces G1/S arrest in lung squamous carcinoma (CH27) cells by downregulating CDK4 and cyclin D1, as well as upregulating cyclin E expression, a crucial regulator of the G1/S checkpoint of the cell cycle (18).

Global breast cancer rates are rising, with 364,000 United States cases anticipated by 2040 (19). Baicalein inhibited 17-estradiol-induced transactivation of the estrogen receptor in MCF-7 human breast cancer cells in the S and G2/M stages (20).

Eastern Asia currently accounts for more than 60% of cases of gastric cancer. Currently, a major problem in Eastern Asia is how to manage gastric cancer in the older population. It is anticipated that the total number of gastric cancer cases and fatalities would reach its peak soon (21). The gastric cancer cell line SGC-7901 underwent a significant S-phase arrest as a result of baicalein. It resulted in SGC-7901 cells going into apoptosis. Analysis of protein expression levels in SGC-7901 cells showed that when baicalein was administered, Bcl-2 was downregulated and Bax was increased (22).

The third most common reason for cancer-related death worldwide is primary hepatic cancer. Most patients receive a bad prognosis at an advanced stage. In an *in vitro* investigation using hepatoma carcinoma cells (Hep G2 and J2), baicalein therapy resulted in S-phase arrest. Some of the underlying mechanisms include early-stage DNA damage, the inhibition of growth-stimulating substances, and the activation of cyclin-CDKs (23).

The seventh most common cause of cancer-related fatalities worldwide is pancreatic cancer. However, many developed nations suffer from it more severely. Globally, there were 458,918 new cases of pancreatic cancer recorded in 2018, and 355,317 additional instances are expected to be reported before 2040 (24). Baicalein upregulates Bax while downregulating Bcl-2 and Mcl-1 to encourage apoptosis in pancreatic cancer cells (25). In PANC-1 cells, baicalein induced arrest of G0/G1 phase when studied *in vitro* (26).

Rising death rates from colorectal cancer (CRC) are a burden shared by developing Asian nations. Patients with CRC may be at danger if they are underweight or overweight (27). In HCT-116 CRC cells, baicalein causes a significant arrest of S phase and promotes apoptosis by activating caspase 3 and caspase 9 (28).

The most common form of male cancer in developed nations is prostate cancer (PC). In PC cells, baicalein caused G0/G1 arrest by lower down cyclins (D1 and D3) and pRB (29).

Bladder cancer (BC) ranks in the top 10 most common cancers globally. Baicalein caused G2/M arrest in TSGH8301 and BFTC905 BC cells by altering two essential proteins (cyclin B1 and phospho-Cdc2) required to initiate the final stage of cell cycle (30,31).

Ovarian cancer is the seventh most prevalent malignant tumor in women, gravely endangering the reproductive health of women. It has a poor prognosis, unknown pathophysiology, missed diagnoses, and a high recurrence rate (38). It only affects women and has a fatality rate of 46.2% after 5 years, making it unique to the female population (38). Baicalein inhibits the synthesis of vascular endothelial growth factor (VEGF), HIF-1, c-Myc, and nuclear factor kappa B (NF- $\kappa$ B) in the G1 and S phases of ovarian cancer cell lines (OVCAR-3 and CP-70). It inhibited the growth of ovarian cancer cells by lowering the expression of matrix metalloproteinase (MMP)-2 (32-35).

Osteosarcoma (OS) is the most prevalent primary bone cancer in children and adolescents. In its advanced stages, it has a low survival rate (36,37). Baicalein produced intracellular reactive oxygen species (ROS) and activated BNIP3 to slow down the development and hasten the apoptosis of MG-63, OS cells (38).

By reducing the levels of cyclin D1 and CDK4, which inhibits the advancement of the G1 phase, it slowed the growth of OS cells. By decreasing the levels of cyclin D1 and CDK4, it inhibited the growth of OS cells by inhibiting cell cycle progression at the G1 phase of division (Tab. 2) (39).

### Baicalin for neuroprotection and cognitive enhancement

Alzheimer's disease is responsible for the more than 25 million cases of dementia that exist today. Both in industrialized and developing nations, Alzheimer's disease has a substantial impact on those who are affected, the caregivers, and society (40). One of the cellular disorders hypothesized to be responsible for the loss of neurons in Alzheimer's disease is aggregation of A $\beta$  (41). Baicalein exhibits neuroprotective qualities against amyloid (AN) functions by preventing AN from aggregating in PC12 neuronal cells to cause A $\beta$ -induced cytotoxicity (42). By activating GABA receptors, baicalein encourages non-amyloidogenic processing of APP, which lowers the generation of A $\beta$  and enhances cognitive function (43). Baicalein demonstrated a potent inhibitory effect on A $\beta$ -induced cell death (43,44).

The prevalence of Parkinson's disease looks to be rising with age, and it is a global concern. Males are affected by the disease 1.5-2 times more frequently than females worldwide.

The prevalence of Parkinson's disease appears to be higher in Western nations than in Asian nations (45). Amyloid-specific proteins aggregate to cause Parkinson's disease. In  $\beta$ -sheet fibrillar aggregate, formed by several proteins including  $\alpha$ -syn amyloid proteins are especially prevalent. The main constituent of Lewy bodies is abnormally folded aggregates of  $\alpha$ -syn, which manifest as intracellular inclusions in nigral dopaminergic neurons in the brains of Parkinson's disease patients (46). As a result,  $\alpha$ -syn represents a viable therapeutic target for Parkinson's disease treatment to stop the disease growth and spread (47). Baicalein functions by impeding the aggregation of disease-specific  $\alpha$ -syn protein. Both baicalein and its oxidized counterpart prevent the production of  $\alpha$ -syn fibrils at lower micromolar levels. Moreover, baicalein demonstrated the capacity to disintegrate the preexisting  $\alpha$ -syn fibrils (48). Additionally, by eliminating iNOS protein, mRNA, and promoter activity in endotoxin/cytokine-induced microglia, baicalein effectively reduced NO generation and iNOS gene expression (49).

Stroke ranks second globally in terms of mortality and third globally in terms of disability, with ischemic heart disease coming in first in both categories (50). According to the Indian Global Burden of Disease Study, which was conducted between 1990 and 2019, stroke was India's leading cause of both fatalities from neurological illnesses and disability-adjusted life years (DALYs) (51). In ischemic stroke,

**TABLE 2** - In vitro studies of baicalin/baicalein against various types of cancer

Plant compound	Name of cancers	Cell lines	Cell cycle phase arrest	Mechanism	References
 <p>Scutellaria baicalensis Georgi</p> <p>↓</p> <p>Baicalein</p> <p>↑</p>  <p>Oroxylum indicum</p>	Lung cancer	CH27	G1/S	↑sed cyclin E and ↓sed levels of CDK4 and cyclin D1	(18)
	Breast cancer	MCF-7	G2/S	Blocked 17-estradiol-induced transactivation of the estrogen receptor	(20)
	Gastric cancer	SGC-7901	S	↓sed Bcl-2 and ↑sed Bax	(22)
	Hepatic cancer	Hep G2 and Hep J2	S	Activation of CDK inhibitors like p21 or p27	(23)
	Pancreatic cancer	PANC-1	G0/G1	↑sed Bax and ↓sed Bcl-2 and Mcl-1	(26)
	Colorectal cancer	HCT-116	S	Activation of Caspase 3 and 9	(28)
	Prostate cancer	LNCaP	G1/S	↓sed cyclin D1, cyclin D3, and pRB protein	(29)
	Bladder cancer	TSGH831 and BFTC905	G2/M	Altering cyclin B1 and phospho-Cdc2	(31)
	Ovarian cancer	OVCAR-3 and CP-70	G1/S	↓sed VEGF, HIF-1, c-Myc, NF-kB, and MMP-2	(34)
	Osteosarcoma	MG-63	G1	Activating BNIP3 and ↓sed cyclin D1 and CDK4	(39)

neuroprotection is achieved by inhibiting iNOS activity or by iNOS gene deletion. Neuroexcitotoxic and ischemic traumas cause the production of COX-2. Specific COX-2 inhibitors reduce brain damage brought on by localized ischemia. The optimal method for treating cerebral ischemia-reperfusion (I/R) injury involves targeting the NF- $\kappa$ B pathway, according to numerous experts. Baicalein therapy significantly decreased the expression of COX-2 and iNOS, as well as PGE2 and NF- $\kappa$ B, indicating a protective effect against cerebral I/R injury. Because baicalein blocks inflammatory mediators including LOX-1, COX-2, PGE2, and NF- $\kappa$ B, it may have anti-inflammatory and antioxidant effects that contribute to its capacity to prevent cerebral I/R (52). Baicalein therapy markedly elevated nuclear Nrf2 expression and AMPK phosphorylation in the ischemic cerebral cortex (53). Cell damage and a rise in oxidative stress are caused by an excess of ROS or by the malfunctioning of antioxidant enzymes. Basic leucine zipper transcription factor Nrf2 controls the expression of the gene that detoxifies ROS as well as the antioxidant gene (54,55).

Epilepsy is a chronic, noncommunicable brain illness that affects people of all ages. One of the most prevalent neurological conditions, epilepsy affects about 50 million people worldwide. More than 80% of people in low- and middle-income countries have epilepsy. FeCl<sub>3</sub>-induced post-traumatic epileptic seizures are a significant type of acquired epileptic seizures (56). Baicalein suppressed ferroptosis associated with 12/15-LOX, hence lessening the severity of post-traumatic epileptic episodes generated by FeCl<sub>3</sub> (57). HT22 cells were damaged by ferroptosis, which is mitigated by baicalein may be due to its lipid peroxidation inhibitor (Fig. 2) (58).

### Respiratory protective action of baicalein

Chronic respiratory conditions are among the world's leading causes of morbidity and mortality. They affect the lung's airways and other structural components. Asthma is the most prevalent chronic respiratory illnesses. There are already approximately 300 million asthmatics worldwide, and by 2025, that figure may rise by an additional 100 million. Asthma is a long-term inflammatory illness of the airways characterized by thickening of the airway wall, hyper-responsiveness and remodeling of the airways, poor relaxation, and persistent blockage of airflow by the smooth muscle of the airways (59-61). Hypersecretion of airway mucus is one of the key features of asthma pathophysiology. Baicalein therapy showed dramatic decrease in MUC5AC and MUC5B mRNA expression levels in the submucosal glands and the epithelium, respectively, which were significantly greater in asthma. Baicalein also exhibits anti-asthmatic properties by inhibiting tumor necrosis factor (TNF)- $\alpha$ -induced NF- $\kappa$ B activation in normal bronchial epithelial (BEAS-2B) cells (62), which was mostly expressed by downstream iNOS production, I $\kappa$ B $\alpha$  phosphorylation and degradation, and nuclear translocation of p65 (63).

Another structural change associated with asthma has been described as increased extracellular matrix (ECM) deposition. The primary ECM producers in the lung are myofibroblasts and fibroblasts. During allergic airway inflammation, myofibroblasts deposit collagen types I and III. ECM's constituents, especially collagens, are broken down and controlled by MMPs, which are secreted by fibroblasts. In allergic asthma, MMP-9, the main airway MMP, is upregulated, which

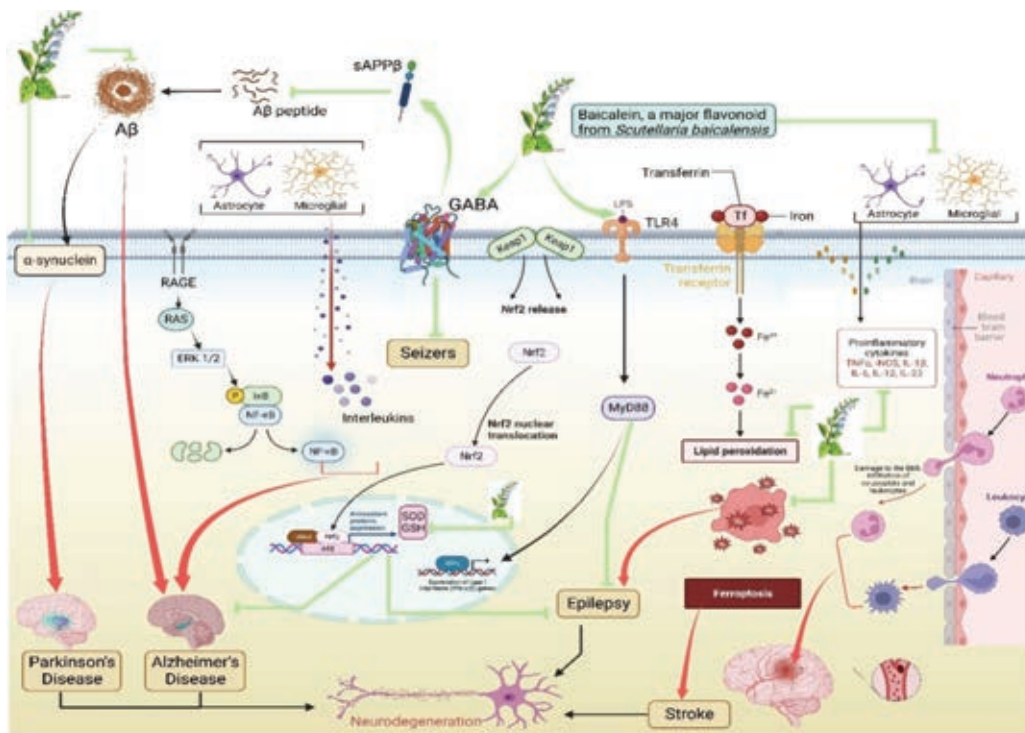


**FIGURE 2** - Baicalein regulating a wide range of signaling pathways linked to the etiology of multiple degenerative conditions.



results in airway remodeling (64). According to recent studies, baicalein administration reduces the ovalbumin (OVA)-induced expression of collagen I and MMP-9 (65).

### Cardioprotective action of baicalein

Globally, cardiovascular disease (CVD) is one of the major causes of morbidity and mortality. In past few decades, changes in lifestyle and socioeconomic conditions that have an impact on the progression of CVDs have been observed. Hypertension is a significant contributor to CVD and fatalities globally, particularly in low- and middle-income nations. As per the 2017 guidelines from the American College of Cardiology and American Heart Association, hypertension is defined as a systolic blood pressure over 130 mm Hg or a diastolic blood pressure above 80 mm Hg (66-70). Baicalin assisted in lowering high-sensitivity C-reactive protein (CRP), interleukin (IL)-6, and IL-1 levels in the serum, which served to forcibly lower blood pressure (71). Baicalin altered the expression of miR-145 and increased TNF- $\alpha$  levels in human aortic endothelial cells (HAECs), thereby reducing the inflammatory effects of TNF- $\alpha$  (72).

Angiotensin II (Ang II) may activate apoptosis-related proteins, encourage the production of ROS, and inhibit the synthesis of NO, which results in endothelial dysfunction that may lead to hypertension. Therefore, lowering cell apoptosis, suppressing oxidative stress, and preventing Ang II-induced endothelial dysfunction are effective ways to treat hypertension. Baicalin has been shown in a study utilizing the human umbilical vein endothelial cell (HUVEC) model of Ang II injury to significantly reduce oxidative stress and endothelial dysfunction caused by Ang II. The primary strategies employed to produce these beneficial effects include modulating the expression of Bax, Bcl-2, and cleaved caspase-3, activating the ACE2/Ang-(1-7)/mas axis, and upregulating the PI3K/AKT/eNOS pathway. They also found that baicalin raised NO level and total antioxidant capacity, and decreased markers of oxidative stress such as malondialdehyde (MDA) and ROS (73,74). It was also shown that the combination of baicalin and berberine relaxed blood arteries by acting on the voltage-dependent Ca<sup>2+</sup> channel (VDCC) (75). By boosting endogenous NO synthesis, which is produced by the enzyme endothelial nitric oxide synthase (eNOS), baicalin may also lower blood pressure (76).

Heart failure is a complicated clinical condition that arises when the heart is unable to pump enough blood to meet the body's needs. It arises from any ailment that impacts the ventricles' ability to fill or the blood's ability to be ejected into the systemic circulation (77). Baicalin seems to be very useful in treatment of CHF as it has an anti-fibrosis property. Baicalin may be able to treat myocardial fibrosis by inhibiting the expression of the fibrosis genes (type I and III collagen) and connective tissue growth factor (CTGF). Baicalin can efficiently induce endothelial cell migration and greatly boost the expression of VEGF when the concentration is between 10 and 50 g/mL, which aids in promoting angiogenesis. This outcome can be achieved by over-activating the ERR/PGC-1 $\alpha$  pathway (78). Baicalin also decreased caspase-3 and the Bax/Bcl-2 ratio, which lowered apoptosis. This suggests that

apoptosis inhibition could lessen adverse remodeling and the eventual development of heart failure (79).

### Gastroprotective activity of baicalein

Peptic ulcer disease (PUD), as determined by hospitalization statistics and diagnosed by physicians, had an incidence rate of 0.03%-0.17% and 0.10%-0.19% per year, respectively. Although most research indicated that PUD incidence or prevalence had decreased over time, still it is a serious and life-threatening disease (80). Acetylsalicylic acid (ASA), *Helicobacter pylori* infection, and non-steroidal anti-inflammatory drugs (NSAIDs) are the major causes of PUD. While there has been a significant improvement in *H. pylori* infection therapy recently, ASA and NSAID prescriptions have grown within the same time frame (81). According to reports, inhibiting gastric acid output and exhibiting a reduction in gastric mucosal damage are both effects of activating  $\alpha$ 2-adrenergic receptors (82). The gastroprotective properties of baicalein may be mediated through these receptors. In contrast to the formation of free radicals, glutathione (GSH) protects the stomach mucosa from damage (82). Baicalein was found to exert protective effects via raising the tissue's GSH concentration, signaling to an antioxidant mechanism (83). Baicalein exhibited cytoprotective effects by inducing the secretion of more gastric mucus, acting as an anti-secretory by suppressing hydrogen-potassium-ATPase activity, and acting as an antioxidant by raising GSH levels (83). By raising the SH compound, which naturally regulates mucus production, and the NO level, which is involved in maintenance of the integrity of the gastric mucosa, and regulates the secretions like acid, alkaline, mucus, and blood flow in gastric mucosa, baicalein demonstrated a gastroprotective effect against lesions (83). The stomach mucosa showed significant reductions in MDA, IL-8, and TNF- $\alpha$  contents, as well as increases in superoxide dismutase (SOD) activity and glutathione peroxidase (GPx) level due to inhibition of inflammation and ROS scavenging actions of the baicalein-Zn complex (84).

### Hepatoprotective activity of baicalein

Worldwide, the prevalence and incidence of nonalcoholic fatty liver disease (NAFLD), the main cause of liver-related morbidity and mortality, have increased as a result of the obesity epidemic (85). Men and aging both increase the risk of NAFLD and fibrosis. Despite the fact that obesity is a major risk factor for NAFLD, current studies have revealed that slim individuals can also develop the condition (86). NAFLD is defined as the condition in which 5% or more hepatic cells develop macro-vesicular steatosis, when there is no secondary etiology like alcohol or drugs (86). An excessive buildup of lipids in the liver results from the increased hepatic lipogenesis and serum non-esterified fatty acids, which causes fatty liver, decreased liver function, and ultimately liver failure (87). Baicalein has several effects against FLD, suggesting that it may be used therapeutically. In order to improve lipid metabolism and reduce hepatic de novo lipogenesis, baicalein inhibits the Ca<sup>2+</sup>/CaM-dependent protein kinase/AMP-activated protein kinase/acetyl-CoA carboxylase (CaMKK/AMPK/ACC)



pathway (88). Baicalein also has the capacity to reduce liver fibrosis, oxidative stress, and systemic inflammation in FLD. In order to reverse fibrosis, baicalein consequently inhibits the synthesis of collagen (type I and  $\alpha$ -1) chain and transforming growth factor (TGF)- $\beta$ 1 (88,89). Additionally, it inhibits the TGF-1/Smad3 pathway in vitro to reverse the epithelial-mesenchymal transition and stop the progression of liver fibrosis (90). Baicalein also has an indirect antioxidant effect by decreasing MDA levels while increasing hepatic GSH and SOD (91). By inhibiting the TGF- $\beta$ /Smad pathway, baicalein slowed down the epithelial-mesenchymal transition. Additionally, it decreased high levels of inflammatory factors such TNF- $\alpha$ , IL-1 and -6, inhibited the apoptotic proteins caspase-3 and -9, and B-cell lymphoma-2, and hindered the I $\kappa$ B kinase/I $\kappa$ B/NF- $\kappa$ B pathway. These all helped to lessen liver disorders (92). Because of its inhibitory influence on the production of p-p38, MAPK, p-CREB, FoxO1, PGC-1, PEPCK, and G6Pase, baicalein considerably reduces insulin concentrations brought on by a high-fat meal. Thus, because of its numerous pharmacological actions, baicalein may prevent FLD (93).

### Baicalein action as a renal protective agent

Chronic kidney disease (CKD) prevalence is acknowledged as a major public health concern on a global scale. It is estimated that 13.4% (11.7%-15.1%) of the global population has KD and that 4.902-7.083 million have end-stage kidney disease (ESKD), requiring renal replacement therapy (94).

The incapacity of the kidneys to perform their excretory duties, which results in the retention of nitrogenous waste products in the blood, is known as renal failure. Kidney failure comes in two flavors: acute and chronic (95). One of the main causes of renal failure is diabetes mellitus (DM), which is why many diabetic individuals continue to struggle with diabetic nephropathy (DN), which is a serious condition (96). Patients with DN typically have elevated urine microalbumin, urine  $\beta$ 2-MG, and Urinary albumin excretion rate in Diabetic neuropathy. Among these, an increase in urine microalbumin and

urinary 2-MB indicates renal tubular injury, while an increase in UAER indicates glomerular injury (97). It was discovered that baicalin significantly reduced the patient's urine 2-MG, UAER, and microalbumin levels. Additionally, it was discovered to considerably enhance the patient's quality of life, reduce the rate at which DN progresses, and enhance kidney function (98-100).

Acute renal injury is a serious adverse effect of the anti-cancer drug cisplatin. Increased ROS generation from cisplatin damages endogenous intracellular targets like proteins, lipids, and DNA, resulting in cellular malfunction and death (101). Additionally, the toxic effects of cisplatin are made worse by the activation of various signaling pathways, such as MAPKs, NF- $\kappa$ B, and p53, by cisplatin-induced ROS (114). A key factor in the pathophysiology of cisplatin-induced kidney injury is the production of iNOS and strong cytotoxic peroxy-nitrite through the interaction of superoxide radical and NO (102). Baicalein has been demonstrated to have a significant antioxidant impact. Baicalein has been shown to adequately remove peroxy-nitrite anion radicals and inhibit peroxy-nitrite-induced cell death in LLC-PK1 cells. Pretreatment with baicalein significantly decreased these changes. Therefore, baicalein's capacity to lessen cisplatin-induced nephrotoxicity is probably due, at least in part, to the attenuation of renal oxidative and/or nitrative stress (Fig. 3) (102).

### Baicalein as an antimicrobial agent

Across the world, infectious diseases are a leading source of morbidity and mortality (103). The emergence of drug-resistant forms of bacteria has diminished the impact of antibiotics on germs and resulted in ongoing difficulties, despite notable advancements in the treatment of microbial infections (104). Combination therapy was developed in response to this problem, and as a result of the expanding prevalence of antibiotic resistance, it has improved treatment efficacy and partially reduced drug resistance. Furthermore, the bacterial resistance to antibiotics has motivated the creation of innovative antibacterial drugs for the treatment of infectious

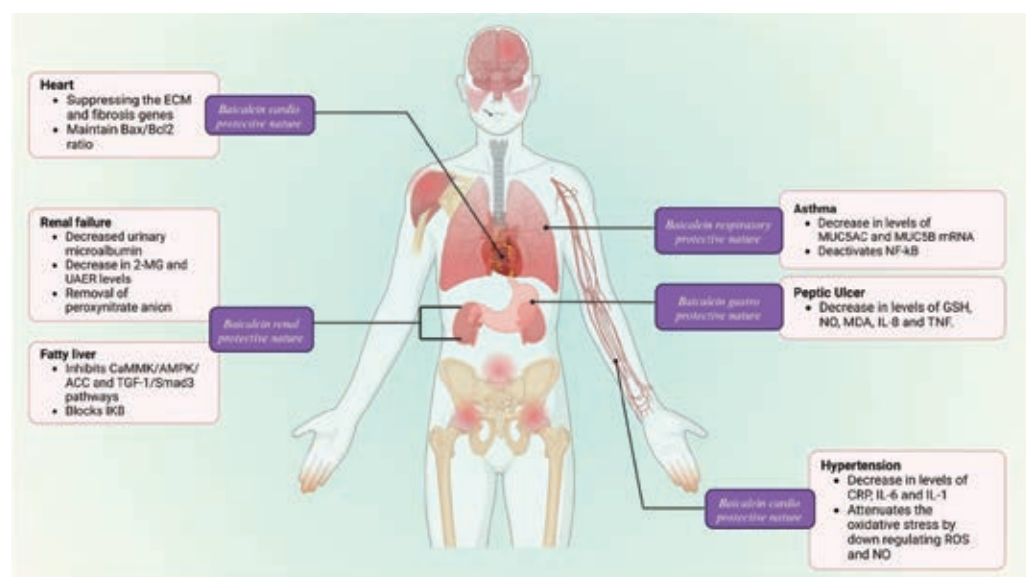


**FIGURE 3** - The healing potential of baicalein by modulating several signaling pathways mitigating the symptoms of certain illnesses such as cardiac, renal, respiratory, and gastric.

disorders. People from many cultures have used a variety of herbal remedies for many generations, and some of these natural medicines are crucial for the treatment and prevention of infectious diseases (105,106). Baicalein's function as an antibacterial agent is crucial. Baicalin inhibits pro-inflammatory cytokine release, MAPK activation, NF- $\kappa$ B pathway activation, and NLRP3 to diminish inflammation in periodontal cells. By promoting the expression of interferon regulatory factor (IRF)4 and inhibiting the expression of IRF5, baicalin also lessens inflammation by regulating the transition of M1 to M2 macrophages. Baicalin inhibited NF- $\kappa$ B and p38 phosphorylation as well as mRNA expression, which decreases pro-inflammatory cytokines TNF- $\alpha$ , IL- $\beta$ , and IL-6 levels (107).

Bacterial growth occurs naturally as biofilms, which are abundant in the environment (108). Biofilm production leads to an increase in resistance to antibiotics and antimicrobial agents. Quorum sensing (QS), a mechanism responsible for the intercellular exchanges of information, is essential to the production of biofilms (109). Baicalin suppresses the QS system, which inhibits inflammatory responses. Baicalein has been shown to have antimicrobial properties against *Meningococcus*, *Staphylococcus aureus*, *Corynebacterium diphtheriae*, *Pseudomonas aeruginosa*, and dysentery bacillus. Through a number of mechanisms, such as enhancing the host immune system, preventing the formation of biofilms, lowering antimicrobial medicine resistance, suppressing bacterial secretions, and upsetting microbial morphology, baicalin acts as a herbal antimicrobial agent against several microbial infections (110).

Baicalin has also been shown to suppress apoptosis, decrease FAS protein expression, block the caspase-8 pathway, and decrease Bax protein production. These actions are all thought to contribute to its antiviral efficacy (111). Baicalin lowers the raised levels of hepatic markers alanine transaminase (ALT), aspartate aminotransferase (AST), and total bilirubin along with hepatitis B virus (HBV)-DNA in patients with chronic hepatitis B. It can also be used in conjunction with other medications to treat viral infections in patients with an H1N1 influenza infection. Baicalin regulates the numbers of T-lymphocyte subsets and upregulates CD3+, CD4+/CD8+, and other positive lymphocyte subsets (112).

Invasive fungal infections increase morbidity and death of patients who have impaired immune systems (113). Currently, polyenes, echinocandins, and azoles are the three primary classes of frontline clinical antifungal agents used to treat such infections (114). However, each of these groups has drawbacks that may restrict their clinical use for the management of invasive fungal infections, and it is urgently necessary to identify new antifungal medicines that target novel targets. Baicalein has demonstrated potential antifungal activity. It significantly inhibits the growth of *Aspergillus fumigatus*, *Cryptococcus neoformans*, and *Candida* species. Because it targets Eno1, BE (baicalein) has anti-*C. albicans* action via preventing glycolysis. BE (baicalein) has a substantial inhibitory effect on CaEno1's enolase activity (115). Baicalein inhibits TSLP/TSLPR pathway activity, which suppresses inflammatory response and protects against *A. fumigatus* keratitis by preventing fungal growth, biofilm formation, and adhesion (Tab. 3) (116,117).

## Antidiabetic property of baicalein

DM is the most prevalent endocrine disorder in the 21st century, and is spreading all over the world. Diabetes increases blood sugar levels. Neglecting to manage it consistently and carefully increases the risk of significant adverse effects, including stroke and heart failure. Type 1, type 2, and gestational diabetes are the three most prevalent forms of the disease. By preventing islet cell death, baicalein reduces hyperglycemia, improves glucose intolerance, and encourages insulin production (118). Baicalein is used to treat diabetes, which lowers total cholesterol, plasma triglyceride plasma levels along with sugar lowering effect (119).

Baicalein additionally showed antihyperglycemic effects in both in vivo and in vitro models via blocking the  $\alpha$ -glucosidase action in 3T3-L1 adipocyte cell line. The main function of the enzyme  $\alpha$ -glucosidase is to catalyze the breakdown of starches and carbs in food to produce glucose that may be absorbed through the digestive tract (120). As a result, delaying the synthesis of glucose after meal digestion may minimize hyperglycemia. It was discovered that baicalein had  $\alpha$ -glucosidase inhibitory effects comparable to those of the commonly prescribed, clinically effective  $\alpha$ -glucosidase inhibitor, acarbose (120). The synergistic impact of baicalein and acarbose treatment is reported for showing reduced harmful hepatic side effects associated with using high dosages of the acarbose alone to treat diabetes by lowering the dosage from high (20 mg/kg) to low (4 mg/kg) levels (121).

Glycation of bovine serum albumin (BSA) is a complicated chain of events wherein reducing sugars like glucose alter the structure of the protein. Due to the excess glucose molecules in their serum, diabetics usually have greater glycation rates. This can lead to nonfunctional proteins and further activate several signaling pathways, increasing the risk of beta-cell damage, insulin resistance, and diabetes complications. Baicalein also has the potential to cure hyperglycemia by reducing BSA glycation (122).

## Baicalein action as an antiaging agent

Skin aging is a natural process that is defined by the skin's progressive physiologic and anatomical changes. The dermis experiences striking alterations including the huge deposition of irregular elastic fibers, collagen deterioration, and hyaluronic acid loss. Skin aging is caused by a variety of extrinsic (usually linked to aging) and natural (mostly genetically determined) factors, such as exposure to ultraviolet (UV) radiation, high intake of alcohol, and pollution. UV radiation is the main cause of photoaging in human skin (123).

Baicalein may find use in skin care products and as a photoprotective agent. UV radiation significantly raised the activities of MMP-1 mRNA (123), while baicalin treatment inhibited this UV radiation-induced action of MMP-1 and resulted in the formation of procollagen type 1. Rich baicalein inhibited collagen fiber loss, wrinkle formation, and skin thickness brought on by UV radiation.

UV causes high levels of ROS to be produced in the skin tissues. This can cause increase of oxidative stress to a variety of cellular macro and micro molecules, including proteins,



nucleic acids, and cell membranes. ROS have a major contribution in both the onset and development of skin aging. MDA is a result of lipid peroxidation whose quantity reveals the extent of oxidative stress on cells. The antioxidant defense of the normal cell against ROS is carried out by SOD and GSH-Px enzymes (125). The results demonstrate that UV rays cause oxidative damage and slow down the dermal tissue capacity to eliminate ROS. It was also revealed that UVA radiation considerably elevated MDA levels in fibroblasts and significantly decreased SOD and GSH-Px activities. Additionally, baicalin therapy by itself dramatically reduced MDA levels in fibroblasts and increased SOD and GSH-Px activity (125).

## Pharmacokinetics

### *Clinical and toxicological studies*

It has been shown that baicalein is a unique, potentially effective medicinal agent for treating a range of illnesses. Therefore, clinical trials are required to ensure the therapeutic role of baicalein. Several studies are designed by various research groups for the purpose. Two phase I clinical trials were conducted on healthy adults in China to evaluate the safety and efficacy using chewable baicalein pills.

Seventy-two healthy Chinese adults participated in a phase I (2014) random, double-blind investigation to examine the pharmacokinetic (PK) characteristics of baicalein using a single-dose trial (100-2800 mg) (126). Blood, urine, and feces samples were obtained at fixed schedules for up to 48 hours post drug administration. After that, baicalein was investigated by the spectrometric analysis of samples through liquid chromatography with tandem mass spectrometry (LC/MS/MS). The PK profile of baicalein was found to be multiphasic, with a median  $T_{max}$  of 0.75-3.5 hours and a  $t_{1/2}$  of 1.90-15.01 hours. The proportionality coefficient (90% CI) estimates for  $C_{max}$ ,  $AUC_{0-t}$ , and  $AUC_0$  were 0.83 (0.70-0.96), 0.91 (0.81-1.00), and 0.92 (0.82-1.02), in that order. The predefined ranges of 0.89-1.11, 0.93-1.07, and 0.93-1.07, respectively, encompass all values. It was unclear what the dose proportionality was for a baicalein dose range of 100-2800 mg. Baicalein excreted in urine makes up 1% of the total. Baicalein was eliminated as a medication in approximately 27% of the feces. Baicalein's  $C_{max}$  and  $C_{avg}$  values at 800 mg single dose and 800 mg multiple dose, respectively, were higher than the in vitro effective concentration (0.1  $\mu$ M) against SARS-CoV-2 (127). Baicalein was highly tolerable. Eleven adverse treatment-related occurrences were detected; all were considered "minor" and retreated on their own. There were no significant adverse occurrences. As a result, healthy volunteers tolerated single oral dosages of baicalein of 100-2800 mg without any adverse effects (127).

The study by Li M, Shi A, Pang H, et al. published in the Journal of Ethnopharmacology in 2014 investigated the safety, tolerability, and pharmacokinetics of a single ascending dose of baicalein chewable tablets in healthy subjects. The research found that single oral doses of 100-2800 mg of baicalein were safe and well tolerated by healthy individuals, with no serious adverse events occurring. The study concluded that baicalein chewable tablets were generally safe

and well-tolerated, supporting the further exploration of baicalein in clinical studies due to its favorable safety profile and pharmacokinetic properties (128). Baicalein suppressed the generation of mid-late mRNA, hence suppressing the H1N1 and H3N2 influenza viruses, A/FM1/1/47, and A/Beijing/32/92, respectively (163). Baicalein and its metabolites were found at higher concentrations, but not in a dose-proportionate way. In healthy Chinese volunteers, baicalein tablets within the studied dosage range were well-tolerated and safe, with no severe or potentially fatal side effects (128).

In order to assess the safety and efficacy of capecitabine (CAP) in conjunction with PHY906, a combination of four traditional Chinese herbs—*Scutellaria baicalensis* Georgi, *Glycyrrhiza uralensis* Fisch., *Ziziphus jujuba* Mill., and *Paeonia lactiflora* Pall.—in the treatment of advanced pancreatic carcinoma (APC), another study was carried out in 2006. Preclinical studies indicate that PHY906 is a potent inhibitor of NF- $\kappa$ B and that it works in concert with CAP to exhibit synergistic antitumor effects in PANC-1 cell lines. PHY906 does not alter the PK of CAP, as studies on several tumor types have shown, but it may reduce the GI toxicities associated with chemotherapy, especially diarrhea. These data have motivated the phase I/II study of the safety and tolerability of a weekly (7/7) dose-intense schedule for CAP plus PHY906. Patients with advanced solid tumors (STs) who did not respond to conventional therapy were recruited for the phase I research. On days 1-4, patients were given 800 mg of PHY906 twice a day, and for 14 days, they were given 1,500 mg/m<sup>2</sup> of CAP every day. Patients with gemcitabine-refractory APC will be recruited for the phase II research. The study's findings show that CAP and PHY906 together have tolerable toxicity in patients with ST (130).

In phase I/II clinical trials oral administration of baicalein has been shown to be safe for humans (130). However, more detailed research on baicalein's therapeutic potential in patients with various diseases is required.

### *Nano-formulations of baicalein*

Srivastava et al created baicalein-loaded mixed micelles to improve the solubility and bioavailability of baicalein oral preparation to treat breast cancer. Micelles encapsulating baicalein in pluronic F127 (F127) and D-tocopherol polyethylene glycol 1000 succinate (TPGS) were investigated for their anticancer properties. The micelles in the optimal formulation exhibited a zeta potential of 4.01 mV and a mean particle size of 25.04 nm. Baicalein was released from micelles in vitro with a sustained release profile at pH 7.4, and an 83.43% computed entrapment efficiency percentage was obtained. In vitro cell culture studies showed a significant increase in the absorption and cytotoxicity of baicalein formulation and performance evaluation of polymeric in-loaded micelles targeting MDAMB-231 cell lines. The cell cycle analysis findings demonstrated that cells were halted in the G0/G1 phase of the cell cycle and that baicalein micelles had a greater capacity to induce apoptosis than did baicalein in its free form. The results of the ROS and mitochondrial membrane potential experiment demonstrate that the novel formulation suppresses cell growth through the ROS-dependent mitochondrial-mediated apoptotic pathway (131).



Majumdar et al developed baicalein-loaded nanoliposome gel formulation, which was easy to apply to the skin's surface because it has a high degree of homogeneity, a pH that is about equivalent to that of the skin, and an appropriate thixotropic characteristic. Baicalein's release was greatly extended and concentration-independent after the development of nanoliposomal gel. In contrast to commercially available formulations, the nanoliposomes loaded with baicalein demonstrated remarkable anti-inflammatory effectiveness throughout testing. Accordingly, the engineered nanoliposomal gel filled with baicalein may be employed as an effective carrier for baicalein topical administration to suppress inflammatory reactions (132).

The efficacy of baicalein-loaded iron oxide nanoparticles (NPs) against the triple-negative breast cancer (TNBC) cell line MDA-MB-231 was examined by Kavithaa et al. Using an electron microscope to analyze a subset of cancer cells, it was revealed that the particles were absorbed by the various subcellular components of the cells. Furthermore, the assessment of mitochondrial membrane potential was conducted using flow cytometry employing JC-1 labeling. The results indicated the presence of significant aggregates in cells treated with iron oxide NPs loaded with baicalein, indicating a considerable reduction in mitochondrial membrane potential. Baicalein-loaded iron oxide NPs elevated apoptotic genes such as Bad, Bax, GADD45, and poly(ADP-ribose) polymerase (PARP) cleavage in a dose-dependent manner while downregulating anti-apoptotic genes. Comprehensive kit-based flow cytometric analysis confirms that nano conjugates may clearly induce apoptosis, DNA damage, and cell cycle arrest, as well as reduce the rate of cell proliferation in TNBC cells (133).

Li et al investigated the releasing patterns and loading efficiencies of baicalein (BE) and baicalin (BA) enclosed in mesoporous silica nanoparticles (MSNs) that were produced and modified with amines (Nano-BA and Nano-BE, respectively). Using primary human gingival epithelial cells (hGECs), the cytotoxicity of Nano-BA and Nano-BE was examined, and a transmission electron microscope was used to observe the cells' uptake of the compounds. Their anti-inflammatory effects in IL-1-treated hGECs were measured using the cytokine array and the enzyme-linked immunosorbent test. This study shows that amine-modified MSNs are capable of encapsulating BA and BE, and that this nano-encapsulation greatly increases the rate of drug delivery and prolongs the release of BA and BE for up to 216 hours. Furthermore, when exposed to a solution devoid of NPs, hGECs were able to internalize Nano-BA and Nano-BE and maintain them inside the cells for at least 24 hours. It is noteworthy that IL-1-induced expression of IL-6 and IL-8 in hGECs is effectively suppressed by pretreatment with Nano-BE. To summarize, BE encapsulated in a NP may efficiently release its contents and be taken up by cells, which has major anti-inflammatory effects (134).

Researchers created a pH-responsive drug delivery system (DDS) encapsulating baicalein zeolite imidazole framework-8 (ZIF-8). The synthesized nanocomposite exhibited a drug-loading capacity of 40.32%. The in vitro drug release kinetics from the nanocomposite showed excellent stimuli-responsive drug release capabilities in an acidic

environment. The growth of *E. coli*, *S. aureus*, *P. aeruginosa*, and *Staphylococcus epidermidis* was significantly inhibited by the nanocomposite. The synergistic effect of zinc (II) ions and baicalein molecules was demonstrated to be the antibacterial mechanism of the BA@ZIF-8 nanocomposite. According to in vitro biocompatibility tests, BA@ZIF-8 did not cause any cytotoxicity in L929 fibroblast cells. The created nanocomposite dramatically enhanced the number of proliferating and migrating cells in the wounded area, according to tests conducted on a scratch wound. According to the findings of the pH-responsive drug release mechanism, the synthesized nanocomposite exhibited greater stability at a neutral pH. The nanocomposite demonstrated rapid baicalein release (65.8%) in acidic conditions, indicating that it is a great choice for pH-responsive drug delivery (135).

This investigation of the anticancer properties of BSA-baicalein @Zn-Glu nanostructure-mediated GluRs was conducted using human glioblastoma U87 cells. The transport of baicalein active component was studied with hybrid NPs of BSA-Ba@Zn-Glu. BSA-Ba@Zn-Glu NPs were effectively synthesized in a single reduction process. The cytotoxic efficacy and apoptotic rate of the nanostructures on U87 glioblastoma cells were assessed using 3-(4,5-dimethylthiazol-a-yl)-2,5 diphenyltetrazolium bromide (MTT) assays and flow cytometry, respectively. The synthesized BSA-Ba@Zn-Glu nanostructures, with diameters ranging from 142.40 to 177.10 nm and zeta potentials between 10.57 and 35.77 mV, have the potential to extravasate into cancer cells. The drug release of BSA-Ba@Zn NPs was both pH-dependent and pH-controlled. In vitro, it was demonstrated that BSA-Ba@Zn-Glu NPs significantly reduced cell viability and increased apoptosis in U87 cancer cells. A green manufacturing approach was used to create Zn NPs, and it was shown that these particles had a deadly effect in addition to increasing the uptake of NPs by cells via Glu receptors. Glu conjugation and drug delivery of baicalein were achieved through the use of BSA NPs as a nano-platform. BSA-Ba@Zn-Glu NPs can cause dose-dependent cytotoxicity and death in human brain cancer cells (U87). Finally, future research on targeted medication delivery in vivo may make use of this nanostructure. It may also be paired with other treatments, such as x-ray irradiation (Table 3) (136).

## Patents on baicalein

The patents related to pharmacological activity of baicalein have been tabulated in Table 4.

## Conclusion

This systematic review provides a new scientific and modern perspective on the traditional Chinese medicine baicalein as a possible supplementary therapy. Baicalein contains anticancer, antimicrobial, antidiabetic, and antiaging properties in addition to protective effects on the brain, heart, lungs, stomach, hepatic, and renal systems, based on the published data reviewed. Repeatedly administering baicalein orally, at dosages ranging from 200 to 600 mg, was shown to be safe and well-tolerated by healthy individuals. There



**TABLE 3** - Studies of nano-formulated baicalein/baicalin in several disorders

S. no.	Disorder	Formulation	Combination	Application	Outcome	Reference
1.	Diabetes	NLC	No	In vitro and in vivo	B-NLCs possess favorable physical stability and enhanced capability for drug retention along with improved antidiabetic effectiveness	(137)
		Selenium NPs	Naringenin + baicalin	In vitro and in vivo	Maintain optimal blood glucose levels by enhancing insulin sensitivity, production, and mitigating the dysfunction of pancreatic $\beta$ -cells in T2DM	(138)
2.	Breast cancer	Iron oxide NPs	No	In vitro	At a very low dose, it inhibits antiapoptotic protein and increases apoptotic proteins	(139)
		Nanoemulsion	Paclitaxel + baicalein	In vitro and in vivo	Improved permeability and retention effects	(140)
3.	Human lung cancer cells	Nanoparticles (prodrug)	Paclitaxel + baicalein	In vitro and in vivo	Exhibited synergism and anticancer potential and reduction of multidrug resistance of paclitaxel occurs	(142)
4.	Cervical tumor	Nanoliposomes	No	In vivo	This formulation demonstrated significant antitumor efficacy	(142)
5.	Cerebral ischemia	SLN	OX26 antibody + baicalin	In vivo	It regulates amino acid levels, which are responsible for the therapeutic effect of treating excitotoxic neuronal damage	(143)

NLC = nanostructured lipid carriers; NP = nanoparticle; SLN = solid lipid nanoparticles; T2DM = type 2 diabetes mellitus.

**TABLE 4** - Patents related to baicalein

S. no.	Patent number	Year of publishing/grant	Details of patent
1.	CN1411815A	2003	The current innovation relates to the preparation method for baicalin eye drops. The root of the natural Chinese medicinal plant <i>Scutellaria</i> is the source of baicalin, the main active element in the product. It exhibits a robust therapeutic effect in the management of pathogen-induced ophthalmopathy without causing ocular discomfort or deleterious side effects.
2.	CN103720650A	2014	The innovation is an injection of baicalin that has anti-influenza viral properties. Baicalin, 2.16 g of disodium hydrogen phosphate, 0.6 g of sodium dihydrogen phosphate, and 100 mL of injection water make up this mixture. The injection is sterilized by applying high pressure while keeping the sodium hydroxide pH at 7.0. The medication blocks neuraminidase action, which prevents the virus from releasing its infection. It is highly bioavailable and rarely causes negative side effects.
3.	CN101642426B	2009	The innovation is a technique for making nanoscale eye drops of the baicalein adhesion type. Baicalein (w/w) = 0.001%-3%, lipid (w/w) = 0.1%-20%, surfactant (w/w) = 0.1%-10%, preservative (w/w) = 0.001%-3%, isotonic regulator (w/w) = 0.1%-10%, penetration enhancer (w/w) = 0.005%-10%. The remaining volume of deionized water is used to create the baicalin adhesion type nanoscale eye drops, with the pH being kept between 5 and 9.
4.	CN101856350A	2010	The use of baicalein in the preparation of medications for the treatment and prevention of PD is disclosed in the invention. The formulation has the ability to improve and treat PD symptoms while also lowering the trembling frequencies and amplitudes. By preventing damage to dopaminergic neurons, the formulation can effectively prevent and treat pathological changes and the development of PD. Baicalein, on the other hand, inhibits Parkinson's symptoms by acting on nervous systems and protects dopaminergic neurons through apoptosis resistance, inflammatory resistance, and antioxidation.
5.	CN101701245A	2010	The innovation offers a way to extract the major proteinase inhibitor of the SARS coronavirus from a traditional Chinese remedy. The steps in the procedure are as follows: (1) Determining the exosomatic suppressive activities of different extractives from a single traditional Chinese medicine that are main proteinase inhibitors of the SARS coronavirus; (2) choosing the extractive that has the highest exosomatic suppressive activity; and (3) sorting and choosing the extractives chosen in step (2) at least once. The substance that the procedure separated has exosomatic inhibitory actions on the major proteinase of the SARS coronavirus, making it a potentially ideal medication or a viable prodrug for commercialization.

(Continued)



TABLE 4 - (Continued)

S. no.	Patent number	Year of publishing/grant	Details of patent
6.	CN102068452A	2011	The invention relates to a pharmaceutical composition with a synergistic antiviral ratio of 20:1 to 1:10 for baicalein and ribavirin. It lessens the minimum medicine tolerance as well as the adverse effects and side effects. Moreover, the antiviral component works by inhibiting viral replication. It has great advantages and looks to have a bright future in treating and preventing influenza viruses.
7.	CN105560177A	2016	The invention discloses the veterinary mixed suspension containing amoxicillin and baicalein, as well as the manufacturing process. The suspension is made by dispersing the active components, amoxicillin and baicalein, 1:1, in a dispersion medium. The problems of amoxicillin being easily broken down in an aqueous solution and the medication being slowly released in an oily mixed suspension are both solved for time-dependent antibiotics. T>MIC is prolonged, effective acting time is prolonged, and a user only needs to take the medication three times consecutively at intervals of 12 hours.
8.	CN112007023A	2020	According to the invention, baicalein alpha, beta, or (beta 0+ beta 1) mixed crystal form can be used for preventing and/or treating obesity and its related conditions. More precisely, to the administration of a drug in the range of 0.001-2000 mg/kg/day/po as an active element in the management of obesity and its by-products, including hyperlipidemia, insulin resistance, and blood sugar.
9.	CN108653206B	2020	The innovation, which falls under the category of pharmaceutical preparations, describes how to prepare a baicalein nanosuspension. The following elements comprise the baicalein nanosuspension prescription, expressed as a percentage by mass: phospholipid (0.05%-10%), F-68 (0.1-3%), glycerol (1%-10%), and the rest water. 0.1%-2% of the phospholipid compound is called baicalein. The invention offers a low cost and energy consumption, excellent safety, enhanced stability, better medication loading rate, and a straightforward and convenient operation.
10.	CN112691102A	2021	The invention describes using baicalein to make a medication that treats and prevents PD as well as the depressive symptoms of Parkinson's syndrome. The invention finds that baicalein can clearly increase the levels of neurotransmitters like DA, NE, and 5-HT in the brain and metabolites thereof, decrease the level of neuroinflammation factors in blood plasma, and improve the symptoms of a rotenone-induced depression mood model of a PD/Parkinson syndrome mouse. Consequently, baicalein can be utilized to make medications that prevent and treat PD as well as the symptoms of depression associated with the condition.
11.	CN113244216A	2021	The innovation reveals the use of baicalein in the development of a medication to suppress a novel coronavirus and reveals that baicalein and SARS-CoV-2Mpro can be coupled, also preventing SARS-CoV-2Mpro from functioning as an enzyme in vitro. The protease activity, which impedes the new coronavirus's ability to replicate, has promising applications in the field of creating new coronavirus drugs.
12.	WO2021159570A1	2021	This invention involves using baicalein to make a drug that will either treat or prevent a disease caused by a novel coronavirus infection. The invention in question pertains specifically to the use of baicalein and a pharmaceutical composition containing baicalein in the preparation of a drug intended to prevent and/or treat diseases caused by novel coronavirus infections (SARS-CoV-2). These infections can range in severity from mild to severe, and they include novel coronavirus pneumonia.
13.	CN113925861A	2022	The invention describes the use of a <i>Scutellaria</i> flavone active ingredient and its preparation in the manufacturing of a medication intended to cure or prevent inflammatory storm. Wogonin, oroxylin A, and baicalein are the components from which the active ingredient of baicalein is chosen. Reducing the frequency of inflammatory storms, particularly in patients who are severely ill, helps to lessen organ damage and halt the disease's course. The innovation finds that wogonin, baicalein, and oroxylin A all operate to varying degrees to block the mouse cytokine storm. Lung damage and inflammatory cell infiltration brought on by an inflammatory storm can be lessened by baicalein. Thus, the medication for both preventing and treating the inflammatory storm can be made using the active ingredient of baicalein.

DA = dopamine; MIC = minimum inhibitory concentration; NE = norepinephrine; PD = Parkinson's disease; SARS-CoV = severe acute respiratory syndrome coronavirus.



was no impairment seen in liver and renal function; however, it may affect the metabolism of triglycerides. Baicalein is rapidly and extensively metabolized in the body, resulting in the production of several metabolites. Out of the seven metabolites, 7-BS and BGG exhibited a significantly larger amount in the plasma. The scientific literature has shown the antiviral activity of baicalein and baicalin (7-BG). There are direct and indirect consequences among them. It is critical to know each mode of action in order to maximize this flavonoid's efficacy in treating diseases. There are direct and indirect consequences among them. Clinical research on this natural substance's efficacy, however, did not provide enough information. Consequently, additional evidence-based clinical trials are required to verify the safety and effectiveness of baicalein as a potential therapeutic agent for a range of human illnesses and for the good of humanity.

## Acknowledgment

The images were created using Biorender software.

## Disclosures

**Conflict of interest:** The authors declare no conflict of interest.

**Financial support:** Nil

**Author contributions:** Kavita Munjal, YashGoel, Vinod Kumar Gautam: conceptualization, methodology, investigation, data collection, and writing—original manuscript. Hitesh Chopra, Madhav Singla, Smriti, Saurabh Gupta, Rohit Sharma: editing and proofreading. Hitesh Chopra, Rohit Sharma: supervision. All authors approved the submission of the final manuscript.

## References

- Liang W, Huang X, Chen W. The effects of baicalin and baicalein on cerebral ischemia: a review. *Aging Dis.* 2017;8(6):850-867. [CrossRef PubMed](#)
- Li-Weber M. New therapeutic aspects of flavones: the anticancer properties of Scutellaria and its main active constituents Wogonin, Baicalein and Baicalin. *Cancer Treat Rev.* 2009;35(1):57-68. [CrossRef PubMed](#)
- Nik Salleh NNH, Othman FA, Kamarudin NA, Tan SC. The biological activities and therapeutic potentials of baicalein extracted from *Oroxylum indicum*: a systematic review. *Molecules.* 2020;25(23):5677. [CrossRef PubMed](#)
- Rossi M, Meyer R, Constantinou P, et al. Molecular structure and activity toward DNA of baicalein, a flavone constituent of the Asian herbal medicine "Sho-saiko-to". *J Nat Prod.* 2001;64(1):26-31. [CrossRef PubMed](#)
- Gao Y, Snyder SA, Smith JN, Chen YC. Anticancer properties of baicalein: a review. *Med Chem Res.* 2016;25(8):1515-1523. [CrossRef PubMed](#)
- Adin SN, Gupta I, Ahad A, Aqil M, Mujeeb M. A developed high-performance thin-layer chromatography method for the determination of baicalin in *Oroxylum indicum* L. and its antioxidant activity. *J Planar Chromatogr Mod TLC.* 2022;35(4):383-393. [CrossRef](#)
- Rajsanga P, Bunsupa S, Sithisarn P. Flavones contents in extracts from *Oroxylum indicum* seeds and plant tissue cultures. *Molecules.* 2020;25(7):1545. [CrossRef PubMed](#)
- Yu H, Han Y, Liu C, et al. Preparation of baicalein from baicalin using a baicalin- $\beta$ -D-glucuronidase from *Aspergillus niger* b.48 strain. *Process Biochem.* 2020;97:168-175. [CrossRef](#)
- Wang H, Ma X, Cheng Q, Wang L, Zhang L. Deep eutectic solvent-based ultrahigh pressure extraction of baicalin from *Scutellaria baicalensis* Georgi. *Molecules.* 2018;23(12):3233. [CrossRef PubMed](#)
- Li HB, Jiang Y, Chen F. Separation methods used for *Scutellaria baicalensis* active components. *J Chromatogr B Analyt Technol Biomed Life Sci.* 2004;812(1-2):277-290. [CrossRef PubMed](#)
- de Oliveira MR, Nabavi SF, Habtemariam S, Erdogan Orhan I, Daglia M, Nabavi SM. The effects of baicalein and baicalin on mitochondrial function and dynamics: A review. *Pharmacol Res.* 2015;100:296-308. [CrossRef PubMed](#)
- Jelić D, Lower-Nedza AD, Brantner AH, et al. Baicalein and Baicalein Inhibit Src Tyrosine Kinase and Production of IL-6. *J Chem.* 2016;2510621. [CrossRef](#)
- Li L, Liu WY, Feng F, Wu CY, Xie N. Synthesis and in vitro cytotoxicity evaluation of baicalein amino acid derivatives. *Chin J Nat Med.* 2013;11(3):284-288. [CrossRef PubMed](#)
- Huang WH, Lee AR, Chien PY, Chou TC. Synthesis of baicalein derivatives as potential anti-aggregatory and anti-inflammatory agents. *J Pharm Pharmacol.* 2005;57(2):219-225. [CrossRef PubMed](#)
- Suski JM, Braun M, Strmiska V, Sicinski P. Targeting cell-cycle machinery in cancer. *Cancer Cell.* 2021;39(6):759-778. [CrossRef PubMed](#)
- Cheng YH, Li LA, Lin P, et al. Baicalein induces G1 arrest in oral cancer cells by enhancing the degradation of cyclin D1 and activating AhR to decrease Rb phosphorylation. *Toxicol Appl Pharmacol.* 2012;263(3):360-367. [CrossRef PubMed](#)
- Siegel RL, Giaquinto AN, Jemal A. Cancer statistics, 2024. *CA Cancer J Clin.* 2024;74(1):12-49. [CrossRef PubMed](#)
- Lee HZ, Leung HW, Lai MY, Wu CH. Baicalein induced cell cycle arrest and apoptosis in human lung squamous carcinoma CH27 cells. *Anticancer Res.* 2005;25(2A):959-964. [PubMed](#)
- Arzanova E, Mayrovitz HN. The Epidemiology of Breast Cancer. In: Mayrovitz HN, ed. *Breast Cancer [Internet Brisbane (AU): Exon Publications.* 2022 Aug 6:chap 1. [CrossRef](#)
- Wang CZ, Li XL, Wang QF, Mehendale SR, Yuan CS. Selective fraction of Scutellaria baicalensis and its chemopreventive effects on MCF-7 human breast cancer cells. *Phytomedicine.* 2010;17(1):63-68. [CrossRef PubMed](#)
- Sekiguchi M, Oda I, Matsuda T, Saito Y. Epidemiological trends and future perspectives of gastric cancer in Eastern Asia. *Digestion.* 2022;103(1):22-28. [CrossRef PubMed](#)
- Mu J, Liu T, Jiang L, et al. The Traditional Chinese Medicine Baicalein Potently Inhibits Gastric Cancer Cells. *J Cancer.* 2016;7(4):453-461. [CrossRef PubMed](#)
- Zheng, YH, Yin, LH, Grahn TH, Ye AF, Zhao YR, & Zhang QY. Anticancer effects of baicalein on hepatocellular carcinoma cells. *Phytother Res.* 2014;28(9):1342-1348. [CrossRef](#)
- Rawla P, Sunkara T, Gaduputi V. Epidemiology of pancreatic cancer: global trends, etiology and risk factors. *World J Oncol.* 2019;10(1):10-27. [CrossRef PubMed](#)
- Takahashi H, Chen MC, Pham H, et al. Baicalein, a component of *Scutellaria baicalensis*, induces apoptosis by Mcl-1 down-regulation in human pancreatic cancer cells. *Biochim Biophys Acta.* 2011;1813(8):1465-1474. [CrossRef PubMed](#)
- Tong WG, Ding XZ, Witt RC, Adrian TE. Lipoxigenase inhibitors attenuate growth of human pancreatic cancer xenografts and induce apoptosis through the mitochondrial pathway. *Mol Cancer Ther.* 2002;1(11):929-935. [PubMed](#)



27. Doleman B, Mills KT, Lim S, Zelhart MD, Gagliardi G. Body mass index and colorectal cancer prognosis: a systematic review and meta-analysis. *Tech Coloproctol.* 2016;20(8):517-535. [CrossRef PubMed](#)
28. Phan T, Nguyen VH, A'Incourt Salazar M, et al. Inhibition of Autophagy Amplifies Baicalein-Induced Apoptosis in Human Colorectal Cancer. *Mol Ther Oncolytics.* 2020;19:1-7. [CrossRef PubMed](#)
29. Pidgeon GP, Kandouz M, Meram A, Honn KV. Mechanisms controlling cell cycle arrest and induction of apoptosis after 12-lipoxygenase inhibition in prostate cancer cells. *Cancer Res.* 2002;62(9):2721-2727. [PubMed](#)
30. Dianatinasab M, Forozani E, Akbari A, et al. Dietary patterns and risk of bladder cancer: a systematic review and meta-analysis. *BMC Public Health.* 2022;22(1):73. [CrossRef PubMed](#)
31. Chao JI, Su WC, Liu HF. Baicalein induces cancer cell death and proliferation retardation by the inhibition of CDC2 kinase and survivin associated with opposite role of p38 mitogen-activated protein kinase and AKT. *Mol Cancer Ther.* 2007;6(11):3039-3048. [CrossRef PubMed](#)
32. Wu J, Zhou T, Wang Y, Jiang Y, Wang Y. Mechanisms and advances in anti-ovarian cancer with natural plants component. *Molecules.* 2021;26(19):5949. [CrossRef PubMed](#)
33. Liu H, Dong Y, Gao Y, et al. The fascinating effects of baicalein on cancer: a review. *Int J Mol Sci.* 2016;17(10):1681. [CrossRef PubMed](#)
34. Chen J, Li Z, Chen AY, et al. Inhibitory effect of baicalin and baicalein on ovarian cancer cells. *Int J Mol Sci.* 2013;14(3):6012-6025. [CrossRef PubMed](#)
35. Yan H, Xin S, Wang H, Ma J, Zhang H, Wei H. Baicalein inhibits MMP-2 expression in human ovarian cancer cells by suppressing the p38 MAPK-dependent NF- $\kappa$ B signaling pathway. *Anticancer Drugs.* 2015;26(6):649-656. [CrossRef PubMed](#)
36. Sanapour N, Malakoti F, Shanebandi D, et al. Thymoquinone augments methotrexate-induced apoptosis on osteosarcoma cells. *Drug Res (Stuttg).* 2022;72(4):220-225. [CrossRef PubMed](#)
37. Ye F, Wang H, Zhang L, Zou Y, Han H, Huang J. Baicalein induces human osteosarcoma cell line MG-63 apoptosis via ROS-induced BNIP3 expression. *Tumour Biol.* 2015;36(6):4731-4740. [CrossRef PubMed](#)
38. Verma S, Gupta S, Das R, et al. Unravelling the approaches to treat osteoarthritis: a focus on the potential of medicinal plants. *Pharmacognosy Res.* 2023;15(1):13-25. [CrossRef](#)
39. Zhang Y, Song L, Cai L, Wei R, Hu H, Jin W. Effects of baicalein on apoptosis, cell cycle arrest, migration and invasion of osteosarcoma cells. *Food Chem Toxicol.* 2013;53:325-333. [CrossRef PubMed](#)
40. Qiu C, Kivipelto M, von Strauss E. Epidemiology of Alzheimer's disease: occurrence, determinants, and strategies toward intervention. *Dialogues Clin Neurosci.* 2009;11(2):111-128. [CrossRef PubMed](#)
41. Malik J, Munjal K, Deshmukh R. Attenuating effect of standardized lyophilized *Cinnamomum zeylanicum* bark extract against streptozotocin-induced experimental dementia of Alzheimer's type. *J Basic Clin Physiol Pharmacol.* 2015;26(3):275-285. [CrossRef PubMed](#)
42. Choi RC, Zhu JT, Yung AW, et al. Synergistic action of flavonoids, baicalein, and daidzein in estrogenic and neuroprotective effects: a development of potential health products and therapeutic drugs against Alzheimer's disease. *Evid Based Complement Alternat Med.* 2013;2013:635694. [CrossRef PubMed](#)
43. Zhang S-Q, Obregon D, Ehrhart J, et al. Baicalein reduces  $\beta$ -amyloid and promotes nonamyloidogenic amyloid precursor protein processing in an Alzheimer's disease transgenic mouse model. *J Neurosci Res.* 2013;91(9):1239-1246. [CrossRef PubMed](#)
44. Zhu JT, Choi RC, Chu GK, et al. Flavonoids possess neuroprotective effects on cultured pheochromocytoma PC12 cells: a comparison of different flavonoids in activating estrogenic effect and in preventing beta-amyloid-induced cell death. *J Agric Food Chem.* 2007;55(6):2438-2445. [CrossRef PubMed](#)
45. Patil RR. Epidemiology of Parkinson's disease—current understanding of causation and risk factors. In: Arjunan SP, Kumar DK, eds. *Techniques for assessment of parkinsonism for diagnosis and rehabilitation.* Springer Singapore 2022; 31-48.
46. Spillantini MG, Schmidt ML, Lee VM, Trojanowski JQ, Jakes R, Goedert M. Alpha-synuclein in Lewy bodies. *Nature.* 1997;388(6645):839-840. [CrossRef PubMed](#)
47. Glabe CG, Kaye R. Common structure and toxic function of amyloid oligomers implies a common mechanism of pathogenesis. *Neurology.* 2006;66(2)(suppl 1):S74-S78. [CrossRef PubMed](#)
48. Zhu M, Rajamani S, Kaylor J, Han S, Zhou F, Fink AL. The flavonoid baicalein inhibits fibrillation of alpha-synuclein and disaggregates existing fibrils. *J Biol Chem.* 2004;279(26):26846-26857. [CrossRef PubMed](#)
49. Suk K, Lee H, Kang SS, Cho GJ, Choi WS. Flavonoid baicalein attenuates activation-induced cell death of brain microglia. *J Pharmacol Exp Ther.* 2003;305(2):638-645. [CrossRef PubMed](#)
50. Feigin VL, Brainin M, Norrving B, et al. World Stroke Organization (WSO): Global Stroke Fact Sheet 2022. *Int J Stroke.* 2022;17(1):18-29. [CrossRef PubMed](#)
51. Singh G, Sharma M, Kumar GA, et al; India State-Level Disease Burden Initiative Neurological Disorders Collaborators. The burden of neurological disorders across the states of India: the Global Burden of Disease Study 1990-2019. *Lancet Glob Health.* 2021;9(8):e1129-e1144. [CrossRef PubMed](#)
52. Zhou P, Iadecola C. iNOS and COX-2 in ischemic stroke. In: Lajtha A, Chan PH, eds. *Handbook of neurochemistry and molecular neurobiology: acute ischemic injury and repair in the nervous system.* New York, NY: Springer US 2007; 33-45.
53. Yuan Y, Men W, Shan X, et al. Baicalein exerts neuroprotective effect against ischaemic/reperfusion injury via alteration of NF- $\kappa$ B and LOX and AMPK/Nrf2 pathway. *Inflammopharmacology.* 2020;28(5):1327-1341. [CrossRef PubMed](#)
54. Chen W, Teng X, Ding H, et al. Nrf2 protects against cerebral ischemia-reperfusion injury by suppressing programmed necrosis and inflammatory signaling pathways. *Ann Transl Med.* 2022;10(6):285. [CrossRef PubMed](#)
55. Vaibhav K, Shrivastava P, Javed H, et al. Piperine suppresses cerebral ischemia-reperfusion-induced inflammation through the repression of COX-2, NOS-2, and NF- $\kappa$ B in middle cerebral artery occlusion rat model. *Mol Cell Biochem.* 2012;367(1-2):73-84. [CrossRef PubMed](#)
56. Pitkänen A, McIntosh TK. Animal models of post-traumatic epilepsy. *J Neurotrauma.* 2006;23(2):241-261. [CrossRef PubMed](#)
57. Li Q, Li QQ, Jia JN, et al. Baicalein exerts neuroprotective effects in FeCl<sub>3</sub>-induced posttraumatic epileptic seizures via suppressing ferroptosis. *Front Pharmacol.* 2019;10:638. [CrossRef PubMed](#)
58. Li Y, Chen Q, Ran D, et al. Changes in the levels of 12/15-lipoxygenase, apoptosis-related proteins and inflammatory factors in the cortex of diabetic rats and the neuroprotection of baicalein. *Free Radic Biol Med.* 2019;134:239-247. [CrossRef PubMed](#)
59. The Lancet. GBD 2017: a fragile world. *Lancet.* 2018;392(10159):1683. [CrossRef PubMed](#)
60. Dharmage SC, Perret JL, Custovic A. Epidemiology of asthma in children and adults. *Front Pediatr.* 2019;7:246. [CrossRef PubMed](#)
61. Quirt J, Hildebrand KJ, Mazza J, Noya F, Kim H. Asthma. *Allergy Asthma Clin Immunol.* 2018;14(S2)(suppl 2):50. [CrossRef PubMed](#)



62. Alsharairi NA. *Scutellaria baicalensis* and their natural flavone compounds as potential medicinal drugs for the treatment of nicotine-induced non-small-cell lung cancer and asthma. *Int J Environ Res Public Health*. 2021;18(10):5243. [CrossRef PubMed](#)
63. Xu T, Ge X, Lu C, et al. Baicalein attenuates OVA-induced allergic airway inflammation through the inhibition of the NF- $\kappa$ B signaling pathway. *Aging (Albany NY)*. 2019;11(21):9310-9327. [CrossRef PubMed](#)
64. Westergren-Thorsson G, Larsen K, Nihlberg K, et al. Pathological airway remodelling in inflammation. *Clin Respir J*. 2010;4(s1)(suppl 1):1-8. [CrossRef PubMed](#)
65. Sampsonas F, Kaparianos A, Lykouras D, Karkoulas K, Spiropoulos K. DNA sequence variations of metalloproteinases: their role in asthma and COPD. *Postgrad Med J*. 2007;83(978):244-250. [CrossRef PubMed](#)
66. Bakhtiyari M, Kazemian E, Kabir K, et al. Contribution of obesity and cardiometabolic risk factors in developing cardiovascular disease: a population-based cohort study. *Sci Rep*. 2022;12(1):1544. [CrossRef PubMed](#)
67. Gaziano TA, Bitton A, Anand S, Abrahams-Gessel S, Murphy A. Growing epidemic of coronary heart disease in low- and middle-income countries. *Curr Probl Cardiol*. 2010;35(2):72-115. [CrossRef PubMed](#)
68. Sharma A, et al. Combination effect of *Spirulina fusiformis* with rutin or chlorogenic acid in lipopolysaccharide-induced septic cardiac inflammation in experimental diabetic rat model. *Pharmacogn Mag*. 2021;17(6):257-267. [CrossRef](#)
69. Satyavert GS, Gupta S, Choudhury H, et al. Pharmacokinetics and tissue distribution of hydrazinocurcumin in rats. *Pharmacol Rep*. 2021;73(6):1734-1743. [CrossRef PubMed](#)
70. Al-Makki A, DiPette D, Whelton PK, et al. Hypertension pharmacological treatment in adults: A World Health Organization guideline executive summary. *Hypertension*. 2022;79(1):293-301. [CrossRef PubMed](#)
71. Wu D, Ding L, Tang X, Wang W, Chen Y, Zhang T. Baicalin protects against hypertension-associated intestinal barrier impairment in part through enhanced microbial production of short-chain fatty acids. *Front Pharmacol*. 2019;10:1271. [CrossRef PubMed](#)
72. Li M, Ren C. Exploring the protective mechanism of baicalin in treatment of atherosclerosis using endothelial cells deregulation model and network pharmacology. *BMC Complement Med Ther*. 2022 Oct 3;22(1):257. [CrossRef PubMed](#)
73. Sampaio WO, Souza dos Santos RA, Faria-Silva R, da Mata Machado LT, Schiffrin EL, Touyz RM. Angiotensin-(1-7) through receptor Mas mediates endothelial nitric oxide synthase activation via Akt-dependent pathways. *Hypertension*. 2007;49(1):185-192. [CrossRef PubMed](#)
74. Alshehri B, Vijayakumar R, Senthilkumar S, et al. Therapeutic potential of nitric oxide synthase inhibitor from natural sources for the treatment of ischemic stroke. *Saudi J Biol Sci*. 2022;29(2):984-991. [CrossRef PubMed](#)
75. Huang P, Gao JW, Shi Z, et al. A novel UPLC-MS/MS method for simultaneous quantification of rhein, emodin, berberine and baicalin in rat plasma and its application in a pharmacokinetic study. *Bioanalysis*. 2012;4(10):1205-1213. [CrossRef PubMed](#)
76. Xin L, Gao J, Lin H, Qu Y, Shang C, Wang Y, Lu Y, Cui X. Regulatory Mechanisms of Baicalin in Cardiovascular Diseases: A Review. *Frontiers in Pharmacology*. 2020; 2;11:583200. [CrossRef](#)
77. Wencker D, Chandra M, Nguyen K, et al. A mechanistic role for cardiac myocyte apoptosis in heart failure. *J Clin Invest*. 2003;111(10):1497-1504. [CrossRef PubMed](#)
78. Zhang K, Lu J, Mori T, et al. Baicalin increases VEGF expression and angiogenesis by activating the ERK $\alpha$ /PGC-1 $\alpha$  pathway. *Cardiovasc Res*. 2011;89(2):426-435. [CrossRef PubMed](#)
79. Pang H, Wu T, Peng Z, Tan Q, Peng X, Zhan Z, Song L, Wei B. Baicalin induces apoptosis and autophagy in human osteosarcoma cells by increasing ROS to inhibit PI3K/Akt/mTOR, ERK1/2 and  $\beta$ -catenin signaling pathways. *Journal of Bone Oncology*. 2022; 1;33:100415. [CrossRef PubMed](#)
80. Sung JJ, Kuipers EJ, El-Serag HB. Systematic review: the global incidence and prevalence of peptic ulcer disease. *Aliment Pharmacol Ther*. 2009;29(9):938-946. [CrossRef PubMed](#)
81. Cheng HC, Gleason EM, Nathan BA, Lachmann PJ, Woodward JK. Effects of clonidine on gastric acid secretion in the rat. *J Pharmacol Exp Ther*. 1981;217(1):121-126. [PubMed](#)
82. DiJoseph JF, Eash JR, Mir GN. Gastric antisecretory and antiulcer effects of WHR1582A, a compound exerting alpha-2 adrenoceptor agonist activity. *J Pharmacol Exp Ther*. 1987;241(1):97-102. [PubMed](#)
83. Ribeiro ARS, do Nascimento Valença JD, da Silva Santos J, et al. The effects of baicalein on gastric mucosal ulcerations in mice: protective pathways and anti-secretory mechanisms. *Chem Biol Interact*. 2016;260:33-41. [CrossRef PubMed](#)
84. Yang H, Lu Y, Zeng XF, et al. Antichronic gastric ulcer effect of zinc-baicalin complex on the acetic acid-induced chronic gastric ulcer rat model. *Gastroenterol Res Pract*. 2018;2018:1275486. [CrossRef PubMed](#)
85. Riazi K, Azhari H, Charette JH, et al. The prevalence and incidence of NAFLD worldwide: a systematic review and meta-analysis. *Lancet Gastroenterol Hepatol*. 2022;7(9):851-861. [CrossRef PubMed](#)
86. Huh Y, Cho YJ, Nam GE. Recent epidemiology and risk factors of nonalcoholic fatty liver disease. *J Obes Metab Syndr*. 2022;31(1):17-27. [CrossRef PubMed](#)
87. Maurice J, Manousou P. Non-alcoholic fatty liver disease. *Clin Med (Lond)*. 2018;18(3):245-250. [CrossRef PubMed](#)
88. Yang JY, Li M, Zhang CL, Liu D. Pharmacological properties of baicalin on liver diseases: a narrative review. *Pharmacol Rep*. 2021;73(5):1230-1239. [CrossRef PubMed](#)
89. Ma Y, Yang F, Wang Y, et al. CaMKK $\beta$  is involved in AMP-activated protein kinase activation by baicalin in LKB1 deficient cell lines. *PLoS One*. 2012;7(10):e47900. [CrossRef PubMed](#)
90. Guo HX, Liu DH, Ma Y, et al. Long-term baicalin administration ameliorates metabolic disorders and hepatic steatosis in rats given a high-fat diet. *Acta Pharmacol Sin*. 2009;30(11):1505-1512. [CrossRef PubMed](#)
91. Zhong X, Liu H. Baicalin attenuates diet induced nonalcoholic steatohepatitis by inhibiting inflammation and oxidative stress via suppressing JNK signaling pathways. *Biomed Pharmacother*. 2018;98:111-117. [CrossRef PubMed](#)
92. Wu T, Liu T, Xing L, Ji G. Baicalin and puerarin reverse epithelial-mesenchymal transition via the TGF- $\beta$ 1/Smad3 pathway *in vitro*. *Exp Ther Med*. 2018;16(3):1968-1974. [CrossRef PubMed](#)
93. Fang P, Sun Y, Gu X, et al. Baicalin ameliorates hepatic insulin resistance and gluconeogenic activity through inhibition of p38 MAPK/PGC-1 $\alpha$  pathway. *Phytomedicine*. 2019;64:153074. [CrossRef PubMed](#)
94. Lv JC, Zhang LX. Prevalence and disease burden of chronic kidney disease. *Adv Exp Med Biol*. 2019;1165:3-15. [CrossRef PubMed](#)
95. Basile DP, Anderson MD, Sutton TA. Pathophysiology of acute kidney injury. *Compr Physiol*. 2012;2(2):1303-1353. [CrossRef PubMed](#)
96. Gauttam V, Munjal K, Mujwar S, Sawale J, Rohilla M, Gupta S. Comparative study of developed formulation and market formulation for antidiabetic potential in alloxan-induced diabetic Wistar rats. *J Young Pharm*. 2022;14(4):387-393. [CrossRef](#)
97. Ahad A, Mujeeb M, Ahsan H, Siddiqui WA. Prophylactic effect of baicalein against renal dysfunction in type 2 diabetic rats. *Biochimie*. 2014;106:101-110. [CrossRef PubMed](#)



98. Yang M, Kan L, Wu L, Zhu Y, Wang Q. Effect of baicalin on renal function in patients with diabetic nephropathy and its therapeutic mechanism. *Exp Ther Med*. 2019;17(3):2071-2076. [CrossRef PubMed](#)
99. Haye A, Ansari MA, Saini A, et al. Polyherbal formulation improves glucose-lipid metabolism and prevent hepatotoxicity in streptozotocin-induced diabetic rats: plausible role of IRS-PI3K-Akt-GLUT2 signaling. *Pharmacogn Mag*. 2022;18(77):52. [CrossRef](#)
100. Hu Z, Guan Y, Hu W, Xu Z, Ishfaq M. An overview of pharmacological activities of baicalin and its aglycone baicalein: new insights into molecular mechanisms and signaling pathways. *Iran J Basic Med Sci*. 2022;25(1):14-26. [PubMed](#)
101. Piao XL, Cho EJ, Jang MH. Cytoprotective effect of baicalein against peroxynitrite-induced toxicity in LLC-PK(1) cells. *Food Chem Toxicol*. 2008;46(5):1576-1581. [CrossRef PubMed](#)
102. Sahu BD, Mahesh Kumar J, Sistla R. Baicalein, a bioflavonoid, prevents cisplatin-induced acute kidney injury by up-regulating antioxidant defenses and down-regulating the MAPKs and NF- $\kappa$ B pathways. *PLoS One*. 2015;10(7):e0134139. [CrossRef PubMed](#)
103. Kirtane AR, Verma M, Karandikar P, Furin J, Langer R, Traverso G. Nanotechnology approaches for global infectious diseases. *Nat Nanotechnol*. 2021;16(4):369-384. [CrossRef PubMed](#)
104. Fair RJ, Tor Y. Antibiotics and bacterial resistance in the 21st century. *Perspect Medicin Chem*. 2014;6:25-64. [CrossRef PubMed](#)
105. Aghazadeh M, Zahedi Bialvaei A, Aghazadeh M, et al. Survey of the antibiofilm and antimicrobial effects of zingiber officinale (in vitro study). *Jundishapur J Microbiol*. 2016;9(2):e30167. [CrossRef PubMed](#)
106. Li C, Huang P, Wong K, et al. Coptisine-induced inhibition of *Helicobacter pylori*: elucidation of specific mechanisms by probing urease active site and its maturation process. *J Enzyme Inhib Med Chem*. 2018;33(1):1362-1375. [CrossRef PubMed](#)
107. Guo M, Zhang N, Li D, et al. Baicalin plays an anti-inflammatory role through reducing nuclear factor- $\kappa$ B and p38 phosphorylation in *S. aureus*-induced mastitis. *Int Immunopharmacol*. 2013;16(2):125-130. [CrossRef PubMed](#)
108. Ozma MA, Khodadadi E, Pakdel F, et al. Baicalin, a natural antimicrobial and anti-biofilm agent. *J Herb Med*. 2021;27:100432. [CrossRef](#)
109. Luo J, Dong B, Wang K, et al. Baicalin inhibits biofilm formation, attenuates the quorum sensing-controlled virulence and enhances *Pseudomonas aeruginosa* clearance in a mouse peritoneal implant infection model. *PLoS One*. 2017;12(4):e0176883. [CrossRef PubMed](#)
110. Chen Y, Liu T, Wang K, et al. Baicalein inhibits *Staphylococcus aureus* biofilm formation and the quorum sensing system in vitro. *PLoS One*. 2016;11(4):e0153468. [CrossRef PubMed](#)
111. Li K, Liang Y, Cheng A, et al. Antiviral properties of baicalin: a concise review. *Rev Bras Farmacogn*. 2021;31(4):408-419. [CrossRef PubMed](#)
112. Su Y, Xiang Y. Clinical efficacy of baicalin combined with antivirals in the treatment of severe influenza A H1N1 influenza. *Chin Hosp Pharm J*. 2014;34:306-308.
113. Jenks JD, Cornely OA, Chen SC, Thompson GR III, Hoenigl M. Breakthrough invasive fungal infections: who is at risk? *Mycoses*. 2020;63(10):1021-1032. [CrossRef PubMed](#)
114. Campoy S, Adrio JL. Antifungals. *Biochem Pharmacol*. 2017;133:86-96. [CrossRef PubMed](#)
115. Li L, Lu H, Zhang X, et al. Baicalein acts against *Candida albicans* by targeting Eno1 and inhibiting glycolysis. *Microbiol Spectr*. 2022;10(4):e0208522. [CrossRef PubMed](#)
116. Zhu Y, Peng X, Zhang Y, Lin J, Zhao G. Baicalein protects against *Aspergillus fumigatus* keratitis by reducing fungal load and inhibiting TSLP-induced inflammatory response. *Invest Ophthalmol Vis Sci*. 2021;62(6):26. [CrossRef PubMed](#)
117. Wang T, Shi G, Shao J, et al. In vitro antifungal activity of baicalin against *Candida albicans* biofilms via apoptotic induction. *Microb Pathog*. 2015;87:21-29. [CrossRef PubMed](#)
118. Singh J, Kakkar P. Modulation of liver function, antioxidant responses, insulin resistance and glucose transport by *Oroxylum indicum* stem bark in STZ induced diabetic rats. *Food Chem Toxicol*. 2013;62:722-731. [CrossRef PubMed](#)
119. Fu Y, Luo J, Jia Z, et al. Baicalein protects against type 2 diabetes via promoting islet  $\beta$ -cell function in obese diabetic mice. *Int J Endocrinol*. 2014;2014:846742. [CrossRef PubMed](#)
120. Alqahtani AS, Hidayathulla S, Rehman MT, et al. Alpha-amylase and alpha-glucosidase enzyme inhibition and antioxidant potential of 3-oxolupenal and katechinic acid isolated from *Nuxia oppositifolia*. *Biomolecules*. 2019;10(1):61. [CrossRef PubMed](#)
121. Sun W, Sang Y, Zhang B, et al. Synergistic effects of acarbose and an *Oroxylum indicum* seed extract in streptozotocin and high-fat-diet induced prediabetic mice. *Biomed Pharmacother*. 2017;87:160-170. [CrossRef PubMed](#)
122. Vlassara H, Uribarri J. Advanced glycation end products (AGE) and diabetes: cause, effect, or both? *Curr Diab Rep*. 2014;14(1):453. [CrossRef PubMed](#)
123. Min W, Liu X, Qian Q, et al. Effects of baicalin against UVA-induced photoaging in skin fibroblasts. *Am J Chin Med*. 2014;42(3):709-727. [CrossRef PubMed](#)
124. Yun M-Y, Won E-Y, Lee J-H, Jung J-I, Choi H-J. Bioconversion from *Scutellaria baicalensis* (baicalin) fermented with *Leatiporus sulphureus* into enriched-baicalein and anti-wrinkle effects. *Pharmacogn Mag*. 2018;14(57):S453-457. [Online](#)
125. Bossi O, Gartsbein M, Leitges M, Kuroki T, Grossman S, Tennenbaum T. UV irradiation increases ROS production via PKC $\delta$  signaling in primary murine fibroblasts. *J Cell Biochem*. 2008;105(1):194-207. [CrossRef PubMed](#)
126. Dong R, Li L, Gao H, et al. Safety, tolerability, pharmacokinetics, and food effect of baicalein tablets in healthy Chinese subjects: A single-center, randomized, double-blind, placebo-controlled, single-dose phase I study. *J Ethnopharmacol*. 2021;274:114052. [CrossRef PubMed](#)
127. Song J, Zhang L, Xu Y, et al. The comprehensive study on the therapeutic effects of baicalein for the treatment of COVID-19 in vivo and in vitro. *Biochem Pharmacol*. 2021;183:114302. [CrossRef PubMed](#)
128. Li M, Shi A, Pang H, et al. Safety, tolerability, and pharmacokinetics of a single ascending dose of baicalein chewable tablets in healthy subjects. *J Ethnopharmacol*. 2014;156:210-215. [CrossRef PubMed](#)
129. Tyagi S, Raghvendra, Sing U, et al. Applications of metabolomics—a systematic study of the unique chemical fingerprints: an overview. *International Journal of Pharmaceutical Sciences Review and Research* 2010;3:83-86 [Online](#) (Accessed October 2023)
130. Hoimes CJ, Lamb L, Ruta S, et al. A phase I/II study of PHY906 plus capecitabine (CAP) in patients (pts) with advanced pancreatic cancer (APC). *J Clin Oncol*. 2008;26(15\_suppl):15538. [CrossRef](#)
131. Srivastava S, Kumar A, Yadav PK, et al. Formulation and performance evaluation of polymeric mixed micelles encapsulated with baicalein for breast cancer treatment. *Drug Dev Ind Pharm*. 2021;47(9):1512-1522. [CrossRef PubMed](#)
132. Majumdar S, Dey S, Ganguly D, Mazumder R. Enhanced topical permeability of natural flavonoid baicalein through nano



- liposomal gel: in vitro and in vivo investigation. *J Drug Deliv Sci Technol.* 2020;57:101666. [CrossRef](#)
133. Kavithaa K, Sumathi S, Padma P. Intracellular uptake of PEG-functionalized baicalein loaded iron oxide nanoparticles regulates apoptotic genes in triple negative breast cancer cells: mitochondrial pathway targeted therapy for breast cancer. *J Cluster Sci.* 2017;28(4):2057-2073. [CrossRef](#)
134. Li X, Luo W, Ng TW, et al. Nanoparticle-encapsulated baicalein markedly modulates pro-inflammatory response in gingival epithelial cells. *Nanoscale.* 2017;9(35):12897-12907. [CrossRef](#) [PubMed](#)
135. Yang J, Chen A, He X, Lu S. Fabrication of baicalein-encapsulated zeolitic imidazole framework as a novel nanocomposited wound closure material to persuade pH-responsive healing efficacy in post-caesarean section wound care. *Int Wound J.* 2023;20(6):1921-1933. [CrossRef](#) [PubMed](#)
136. Gharbavi M, Johari B, Ghorbani R, Madanchi H, Sharafi A. Green synthesis of Zn nanoparticles and in situ hybridized with BSA nanoparticles for Baicalein targeted delivery mediated with glutamate receptors to U87-MG cancer cell lines. *Appl Organomet Chem.* 2023;37(1):e6926. [CrossRef](#)
137. Shi F, Wei Z, Zhao Y, Xu X. Nanostructured lipid carriers loaded with baicalin: an efficient carrier for enhanced antidiabetic effects. *Pharmacogn Mag.* 2016;12(47):198-202. [CrossRef](#) [PubMed](#)
138. Abdel Maksoud HA, Abou Zaid OAR, Elharrif MG, Omnia MA, Alaa EA. Selenium cleome droserifolia nanoparticles (Se-CNPs) and its ameliorative effects in experimentally induced diabetes mellitus. *Clin Nutr ESPEN.* 2020 Dec;40:383-391. [CrossRef](#) [PubMed](#)
139. Kavithaa K, Paulpandi M, Padma PR, Sumathi S. Induction of intrinsic apoptotic pathway and cell cycle arrest via baicalein loaded iron oxide nanoparticles as a competent nano-mediated system for triple negative breast cancer therapy. *RSC Adv.* 2016;6(69):64531-64543. [CrossRef](#)
140. Yadav PK, Saklani R, Tiwari AK, et al. Ratiometric codelivery of Paclitaxel and Baicalein loaded nanoemulsion for enhancement of breast cancer treatment. *Int J Pharm.* 2023;643:123209. [CrossRef](#) [PubMed](#)
141. Wang W, Xi M, Duan X, Wang Y, Kong F. Delivery of baicalein and paclitaxel using self-assembled nanoparticles: synergistic antitumor effect in vitro and in vivo. *Int J Nanomedicine.* 2015;10:3737-3750. [PubMed](#)
142. Li K, Zhang H, Gao L, et al. Preparation and characterization of baicalein-loaded nanoliposomes for antitumor therapy. *J Nanomater.* 2016;2861915. [CrossRef](#)
143. Liu Z, Zhang L, He Q, et al. Effect of Baicalin-loaded PEGylated cationic solid lipid nanoparticles modified by OX26 antibody on regulating the levels of baicalin and amino acids during cerebral ischemia-reperfusion in rats. *Int J Pharm.* 2015;489(1-2):131-138. [CrossRef](#) [PubMed](#)



# In vivo analgesic, anti-inflammatory, sedative, muscle relaxant activities, and docking studies of 3',4',7,8-tetrahydroxy-3-methoxyflavone isolated from *Pistacia chinensis*

Abdur Rauf<sup>1</sup>, Umer Rashid<sup>2</sup>, Najla Al Masoud<sup>3</sup>, Zuneera Akram<sup>4</sup>, Anees Saeed<sup>2</sup>, Naveed Muhammad<sup>5</sup>, Taghrid S. Alomar<sup>3</sup>, Saima Naz<sup>6</sup>, Marcello Iriti<sup>7,8</sup>

<sup>1</sup>Department of Chemistry, University of Swabi, Anbar, Khyber Pakhtunkhwa - Pakistan

<sup>2</sup>Department of Chemistry, COMSATS University Islamabad, Abbottabad Campus, Abbottabad - Pakistan

<sup>3</sup>Department of Chemistry, College of Science, Princess Nourah bint Abdulrahman University, Riyadh - Saudi Arabia

<sup>4</sup>Department of Pharmacology, Faculty of Pharmaceutical Sciences, Baqai Medical University, Karachi - Pakistan

<sup>5</sup>Department of Pharmacy, Abdul Wali Khan University Mardan, Khyber Pakhtunkhwa - Pakistan

<sup>6</sup>Department of Biotechnology, Bacha Khan University, Khyber Pakhtunkhwa - Pakistan

<sup>7</sup>Department of Biomedical, Surgical and Dental Sciences, University of Milan, Milan - Italy

<sup>8</sup>National Interuniversity Consortium of Materials Science and Technology (INSTM), Firenze - Italy

## ABSTRACT

**Background:** *Pistacia chinensis* is extensively employed in traditional medicine. This study aimed to isolate and evaluate the therapeutic effects of 3',4',7,8-tetrahydroxy-3-methoxyflavone from *P. chinensis* crude extract.

**Materials and Methods:** The study utilized column chromatography for isolation. The plant extract and its isolated compound were assessed for in vivo analgesic (hot plate model), anti-inflammatory (carrageenan-induced paw edema), sedative (open field model), and muscle relaxing properties (inclined plane and traction test).

**Results:** In the thermal-induced analgesic model, a significant analgesic effect was observed for the extract (25, 50, and 100 mg/kg) and the isolated compound (2.5, 5, 10, and 15 mg/kg) at higher doses. The extract (100 mg/kg) significantly prolonged latency time (21.98 seconds) after 120 minutes of administration. The isolated compound elevated the latency time (20.03 seconds) after 30 minutes, remaining significant up to 120 minutes with a latency time of 24.11 seconds. The anti-inflammatory effect showed a reduction in inflammatory reactions by 50.23% (extract) and 67.09% (compound) after the fifth hour of treatment. Both samples demonstrated significant sedative effects, with the extract hindering movement by 54.11 lines crossed compared to the negative control (180.99 lines). The isolated compound reduced the number of lines crossed to 15.23±SEM compared to the negative control. Both samples were also significant muscle relaxants. Docking studies indicated that the compound's therapeutic effect is due to inhibiting COX and nociceptive pathways.

**Conclusion:** The isolated compound from *Pistacia chinensis* exhibits significant analgesic, anti-inflammatory, sedative, and muscle relaxing properties, with potential therapeutic applications by inhibiting COX and nociceptive pathways.

**Keywords:** Anacardiaceae, Analgesic, Anti-inflammatory, In vivo, Muscle relaxant, *Pistacia chinensis*, Sedative

## Introduction

Plants have been acknowledged for millennia as having direct therapeutic effects for treating common disorders (1,2). The etymology of the term *pistachio* can be traced back to its Avestan origin, precisely the word *pstk*, which translates

to *pistag*. The term *pistachio* can also be traced back to the word *pista* in many languages, such as Persian and the early classical tongues of Central Asia (3,4). The Anacardiaceae (R.Br.) Lindl. family (order Sapindales) originally comprised 82 genera and 700 species of pantropical (tropical and subtropical) trees, shrubs, and lianas that secrete gums and resins (5). Recently included are 83 genera and 860 tree species (6).

The *kakra shringi* is the Chinese *Pistacia chinensis* variety *integerrima*. Located in the Himalayas from the Indus to Kumaon, this moderate-sized deciduous tree reaches heights of 18 m (7). The leaves and petioles of plants infested by the *Pemphigus* species of bug develop hard, horn-shaped, rugose, hollow galls (8). The crushed and dried galls possess

Received: November 28, 2023

Accepted: May 6, 2024

Published online: June 18, 2024

### Corresponding authors:

Abdur Rauf and Marcello Iriti

email: mashaljc@yahoo.com and marcello.iriti@unimi.it



a distinct aroma and flavor reminiscent of terebinth. The flavor profile of these items exhibits a sharp and slightly spicy taste reminiscent of terebinthine notes. Additionally, there is a subtle balsamic aroma present (9).

*P. chinensis* is a widespread *Pistacia* species found in Asia. Traditional applications of *P. chinensis* include wood, seed oil, ornamental uses, and folk remedies for detoxification, sore pharynx, and diarrhea (10). According to De Pooter et al (11), the primary chemical components of *P. chinensis* leaf essential oils grown in Egypt were trans-8-ocimene limonene. Two 3-3'-dimeric 4-phenyl dihydro coumarin compounds with estrogen-like activity were isolated from the twig extract of *P. chinensis* (12). The galls of *P. chinensis* are used in Ayurvedic medicine to treat a wide range of ailments, including but not limited to hiccups, asthma, chronic bronchitis, fever, vomiting in infants, skin diseases, psoriasis, snake bites, scorpion stings, and increased hunger (13). The plant has considerable therapeutic potential under its pharmacological activity and active constituents. The *P. integerrima* plant has captured the interest of researchers, and a wealth of literature is already available (14). Few studies explored particular aspects of *P. chinensis*. In Pakistan, hepatitis and liver disorders are treated with *P. chinensis* galls. There have been reports of its leishmanicidal (15), depressant (16), analgesic and anti-inflammatory (17), spasmolytic (18), and hyperuricemic (10) properties. Noreen et al (19) concluded that bioactive antioxidants found in the bark of *P. chinensis* could be a suitable source for isolating potent antioxidant compounds.

In addition to its therapeutic uses, *P. chinensis* has numerous applications in ecology and energy production, among others (19). *P. chinensis* oil, mostly fatty acids with 16 to 18 carbon chain lengths, is chemically identical to fossil diesel (C15 C19) (20). *P. chinensis* biodiesel meets EU, US, and Chinese light diesel standards (21). A compound with a chemical structure of 2-(3,4-dihydroxyphenyl)-7,8-dihydroxy-3-methoxy-4H-chromen-4-one compound derived from *P. chinensis* exhibits properties that can help regulate blood sugar levels and prevent glycation (22). *P. chinensis* isolated flavonoids have been shown to exhibit ENPP1 inhibition, which is a therapeutic intervention (23).

To date, only a limited number of flavones have been successfully commercialized, despite their potential as analgesics, sedatives, muscle relaxants, and anti-inflammatory agents. Considerable evidence exists regarding the potential toxicity and adverse effects associated with nearly all commercially available flavones. Hence, the present study was designed to investigate the potential in vivo analgesic, sedative, muscle relaxant, and anti-inflammatory properties of the compound 3',4',7,8-tetrahydroxy-3-methoxyflavone derived from *P. chinensis*. The aim was to determine if these effects could be achieved with minimal adverse effects, taking into consideration the traditional use of the plant.

## Materials and methods

### Plant collection

*P. chinensis* (Bunge) seeds were acquired from the University of Peshawar's botanical garden. Dr. Muhammad Ilyas, Department of Botany, University of Swabi, KP, Pakistan,

identified the plant species delivered to the department. The specimen with the voucher number *Pistacia chinensis* was stored in the department's herbarium.

The obtained seeds were shade-dried for 20 days and washed with water to remove grit. After that, the desiccated grain was ground into a powder using a grinder. One kilogram of powdered plant material was immersed in methanol for 10 days to extract the most significant number of polar secondary metabolites. The obtained extract was concentrated at low temperature and pressure using a rotary evaporator, yielding 18.9 g of extract (2.11%).

### Extraction and isolation

The seeds of *P. chinensis* were rinsed with water to remove dust. The washed seeds (8.32 kg) were pulverized using a machine to produce the powdered plant materials. The plant material was subjected to a 20-day cold extraction with methanol (10 mL). The extract was concentrated using a rotary evaporator under reduced temperature and pressure, yielding 112 g of crude extract. To remove the less polar compounds from the crude extract, it was defatted with n-hexane. The 22.2 g defatted crude extract was subjected to column chromatography, yielding compound 1 (Figure 1). Physical and spectroscopic data were compared to previously reported data to determine the isolated compound chemical structure (20,21,24).

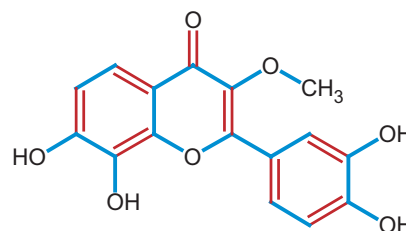


**FIGURE 1** - The chemical structure of the isolated compound 1 from *Pistacia chinensis*.

### Classification of animals

The BLAB/c mice of either sex weighing 23-27 g were obtained from the National Institute of Health Islamabad, Pakistan. The animals were classified for the in vivo experiments as negative control (treated with normal saline, 10 mL/kg), positive control (treated with standard drug), and extract/compounds were administered to the tested groups. This study was approved by the ethical committee (SOU/Pharm-23), Department of Pharmacy, University of Swabi, KP, Pakistan, on January 15, 2023.

### Analgesic screening

A hot plate analgesia meter was used to evolve the analgesic effect. Animals were classified as above. All the animals were tested on hot plates for positive responses. The animals were treated with extract or compound, and after 30 minutes of treatment, each animal was placed at the center of a

hot plate, and the time of stay on the hot plate was counted in seconds (latency time). The animal that stayed more than 25 seconds (cut-off time) was excluded from the study. The latency time was periodically observed at 30, 60, 90, and 120 minutes posttreatment (25). Tramadol was used as a standard drug.

### Anti-inflammatory activity

After correctly classifying animals into the abovementioned categories, the negative control group was administered normal saline, and the positive control group was administered diclofenac sodium. The rest of the groups were treated with extract and isolated compound 1. After 30 minutes of these treatments, carrageenan (1%, 0.05 mL) was administered subcutaneously to the right hind paw of each animal. The induced inflammation was determined in the form of paw edema. This paw volume was measured regularly, and the anti-inflammatory effect percentage was calculated using the following formula:

$$\text{Percent effect} = \frac{A - B}{A} \times 100$$

where A and B represent the paw edema of the negative and positive control groups, respectively (26).

### Sedative screening

Using our previously published paradigm, the open-field method was used to evaluate the sedative effect of the extract and the compound. The experimental room's sound-proofing consisted of a wooden cage with equal space. The animals were categorized as described earlier, and the positive control group was administered diazepam (0.5 mg/kg). After 30 minutes of treatment with normal saline (negative control), diazepam (positive control), and extract/compound (tested groups), the sedative effect of each animal in the special wooden box was evaluated. The animal was deposited

in the center of the box, and for 10 minutes, the number of lines it crossed was recorded. The greater the number of crossed lines, the less sedative the drug, and vice versa (27).

### Muscle relaxant activity

Inclined plane and traction tests were used to determine muscle coordination potential. In the inclined plane test, a plane was designed with an angle of 65° on which an animal will slide. A metallic wire coated with rubber was used in case of traction test on which the animal will hang. After correctly classifying animals into various groups as above, the groups were appropriately treated with normal saline, diazepam, and extract/compound. After 30 minutes of these treatments, the animal's muscle coordination effect was checked on an inclined plan for 5 seconds and the hanging duration for 5 seconds. The sliding of animals within 5 seconds meant animals with relaxed muscles, and the passing of animals to hang with wire for 5 seconds reflects no muscle relaxation effect.

### Docking

Interaction analysis via docking between receptors and ligands is essential for finding ligand inhibition patterns. We performed docking studies using MOE software version MOE 2016.0802 (Chemical Computing Group, Canada). Interactions of the new ligand and the superimposed co-crystallized ligand have been found.

### Results

The extract and isolated compound were significantly analgesic in thermally induced algesia, as shown in Table 1. The analgesic effect of the extract (25, 50, and 100 mg/kg) and the isolated compound (2.5, 5, 10, and 15 mg/kg) was dose dependent. The extract (100 mg/kg) exhibited a significant ( $p < 0.01$ ) prolonged latency time (16.76 seconds) as

**TABLE 1** - Analgesic effect of *Pistacia chinensis* crude extract and isolated compound

Group	Dose (mg/kg)	Time (minutes)			
		30	60	90	120
NS	10 mL	9.18 ± 0.06	9.19 ± 0.09	9.17 ± 0.10	9.20 ± 0.08
Tramadol	10	25.23 ± 0.07***	25.30 ± 0.13***	26.00 ± 0.15***	26.43 ± 0.12***
Extract	25	9.65 ± 0.90	13.98 ± 0.43	14.00 ± 0.27	13.90 ± 0.87
	50	12.43 ± 0.79	16.09 ± 0.66**	16.98 ± 0.64**	17.00 ± 0.54**
	100	14.76 ± 0.66	19.49 ± 0.65**	17.07 ± 0.43**	16.90 ± 0.23**
	250	16.76 ± 0.76**	21.65 ± 0.54***	22.24 ± 0.21***	21.98 ± 0.11***
Compound 1	2.5	11.76 ± 0.45	14.98 ± 0.54	15.00 ± 0.34	14.87 ± 0.39
	5	13.09 ± 0.66	17.34 ± 0.28**	17.98 ± 0.54**	17.32 ± 0.40**
	10	17.32 ± 0.55	20.87 ± 0.51***	20.98 ± 0.28***	20.07 ± 0.45***
	15	20.03 ± 0.45***	24.08 ± 0.55	24.65 ± 0.54***	24.11 ± 0.43***

ANOVA = analysis of variance; NS = normal saline, SEM = standard error of the mean.

\*\*\* $p < 0.001$ , \*\* $p < 0.01$ .

Data are presented as mean ± SEM. The level of statistical significance was calculated through GraphPad Prism using an ANOVA analysis test.



compared to negative control after 30 minutes of administration, and this effect remained significant ( $p < 0.001$ ) up to 120 minutes (21.98 seconds latency time) after administration. The isolated compound elevated the latency time (20.03 seconds) after 30 minutes where the effect remained significant up to 120 minutes with a latency time of 24.11 seconds.

The anti-inflammatory effect of the extract and compound is exhibited in Figure 2. The extract reduced the edema by 20.23% after 3 hours of administration and significantly by 50.23% after 5 hours of experimental duration. The isolated compound attenuated the inflammatory reactions up to 86.32% after 3 hours, and this anti-inflammatory process was improved by 67.09% after 5 hours of compound administration.

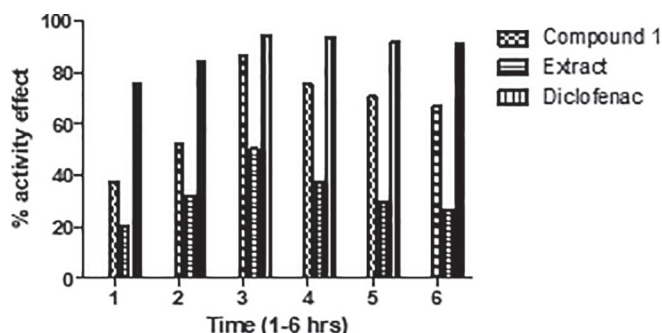


**FIGURE 2** - Percentage of the anti-inflammatory effect of crude extract and isolated compound 1 of *Pistacia chinensis* on carrageenan paw in mice.

The crude extract and isolated compound from *P. chinensis* were found to be significant sedatives in the open-field model, as shown in Table 2. No sedative effect was observed in lower doses (25 and 50 mg/kg), while the higher doses (100 and 250 mg/kg) demonstrated significant ( $p < 0.001$ ) hindrance in the movement of animals. The isolated compound resulted in a more sedative effect as compared to the extract. The movement of animals was significantly ( $p < 0.01$ )

**TABLE 2** - Sedative activity of crude extract and isolated compound from *Pistacia chinensis*

Samples	Dose (mg/kg)	Number of lines crossed
NS	5 mL	180.99 ± 3.54
Diazepam	0.5	2.32 ± 0.43***
Extract	25	85.29 ± 3.33
	50	76.76 ± 3.09
	100	67.09 ± 2.64*
	250	54.11 ± 2.65**
Compound 1	2.5	45.24 ± 2.01**
	5	36.23 ± 1.77***
	10	25.09 ± 1.50***
	15	15.23 ± 1.32***

ANOVA = analysis of variance; NS = normal saline, SEM = standard error of the mean.

\*\*\* $p < 0.001$ , \*\* $p < 0.01$ .

Data are presented as mean ± SEM. The level of statistical significance was calculated through GraphPad Prism using the ANOVA analysis test.

hindered (54.11 lines crossed as compared to the negative control – 180.99 lines crossed by animals). The isolated compound reduced the number of lines crossed up to 15.23 compared to the negative control.

The effect on muscle coordination of crude extract and isolated compound from *P. chinensis* is presented in Table 3. A significant muscle relaxant effect was noticed in both experimental models. Uniform muscle relaxation was noted dose-dependently and time-dependently. The extract (250 mg/kg) demonstrated a 42.88% and 43.56% effect in the inclined plane and traction model, respectively. The isolated compound exhibited up to 70% muscle relaxation at 15 mg/kg.

We also performed docking studies by using Molecular Operating Environment (MOE) software. Compound 3',4',7,8-tetrahydroxy-3-methoxyflavone isolated from *P. chinensis*

**TABLE 3** - Muscle relaxant effect of crude extract and isolated compound from *Pistacia chinensis*

Group	Dose (mg/kg)	Inclined plane model (%)			Traction model (%)		
		30	60	90	30	60	90
NS	10 mL/kg	–	–	–	–	–	–
Diazepam	0.5	100 ± 0.0	100 ± 0.0	100 ± 0.0	100 ± 0.0	100 ± 0.0	100 ± 0.0
Crude extract	25	14.43 ± 3.02	20.43 ± 2.76	21.98 ± 2.00	15.23 ± 2.54	21.43 ± 2.87	22.06 ± 2.41
	50	20.98 ± 2.87	26.98 ± 2.80	27.55 ± 2.04	21.64 ± 2.89	27.98 ± 2.98	28.54 ± 2.47
	100	27.43 ± 2.88	33.98 ± 2.82	34.80 ± 2.76	28.09 ± 2.54	34.09 ± 2.93	34.87 ± 2.44
	250	34.54 ± 2.90	41.09 ± 2.66	42.88 ± 2.54	35.88 ± 2.34	43.09 ± 2.65	43.56 ± 2.56
Compound 1	2.5	41.67 ± 2.20	47.54 ± 2.12	48.54 ± 2.10	42.01 ± 2.11	47.99 ± 2.04	48.39 ± 3.01
	5	48.09 ± 2.80	55.87 ± 2.00	55.32 ± 2.11	49.32 ± 1.80	56.43 ± 2.13	56.91 ± 2.98
	10	56.43 ± 2.32	63.98 ± 2.34	63.98 ± 2.65	57.13 ± 1.90	64.36 ± 2.06	65.08 ± 2.662
	15	62.09 ± 2.77	68.33 ± 2.66	69.03 ± 2.90	62.78 ± 1.66	70.02 ± 2.08	70.98 ± 2.14

ANOVA = analysis of variance; NS = normal saline, SEM = standard error of the mean.

\*\*\* $p < 0.001$ , \*\* $p < 0.01$ .

Data are presented as mean ± SEM. The level of statistical significance was calculated through GraphPad Prism using the ANOVA analysis test.



(Anacardiaceae) docked in the binding sites of pain modulating and inflammatory receptors having PDB accession codes 1EQG, 1CX2, 4EJ4, 4DJH, 4DKL for COX-1, COX-2, DOR, KOR, and MOR (28-31).

Two-dimensional interaction plots of native ligand ibuprofen and isolated flavone in the binding sites of cyclooxygenase (COX)-1 are shown in Figure 3. Ibuprofen showed hydrogen bonding interaction with the receptor COX-1 (Fig. 3A). Isolated flavone interacts with COX-1 residues (Gly526, Ser530, Tyr355) and showed good interactions for inhibiting pain and inflammation modulation that includes one conventional hydrogen bond with residue Ser530,  $\pi$ - $\pi$  interaction with residue Gly526, and amide- $\pi$  stacking with residue Tyr355 (Fig. 3B).

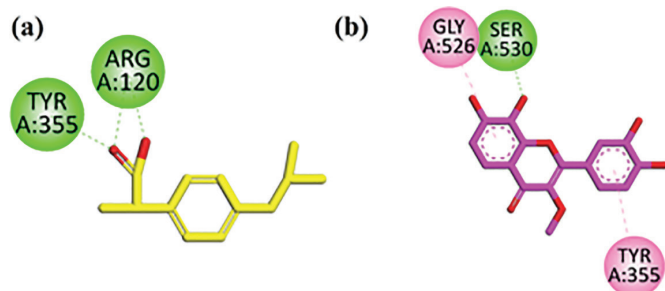


**FIGURE 3 - A)** Ibuprofen (co-crystallized native ligand) two-dimensional interaction plot in the cyclooxygenase-1 (COX-1) receptor binding site. **B)** Isolated compound 3',4',7,8-tetrahydroxy-3-methoxyflavone two-dimensional interaction plot in the COX-1 receptor.

Two-dimensional interaction plots of native ligand SC-558 and isolated compound in the binding site of COX-2 are shown in Figure 4. SC-558 inhibitor has good hydrogen bonding interaction with the receptor COX-2 (Fig. 4A). Isolated flavone interacts with the COX-2 receptor and showed five conventional hydrogen bond interactions with residues Tyr385, Leu352, His90, Arg120, and Tyr355, which enhance the ligand-inhibiting efficacy (Fig. 4B).

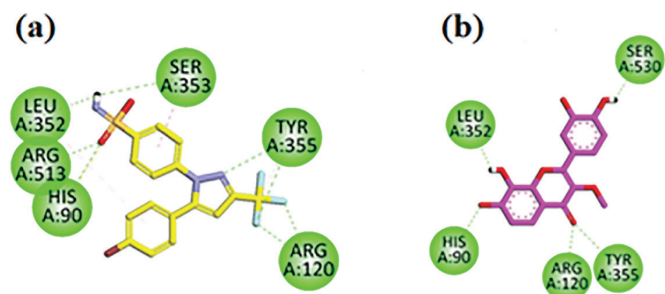


**FIGURE 4 - A)** SC-558 (co-crystallized native ligand) two-dimensional interaction plot in the cyclooxygenase-2 (COX-2) receptor binding site. **B)** Isolated flavone two-dimensional interaction plot in the COX-2 receptor binding site.

Two-dimensional interaction plots of native ligand naltrindole and isolated compound in the binding site of delta opioid receptor (DOR) are shown in Figure 5. Naltrindole has good interactions such as conventional hydrogen bonding

interaction and  $\pi$ -sulfur with the DOR (Figure 5A). Isolated compound flavone interacts with the DOR by residues Met132, His278, Asp128, Ile304 and exhibited three conventional hydrogen bonds with residues His278, Asp128, Ile304 and a  $\pi$ -sulfur interaction with residue Met132 (Figure 5B).

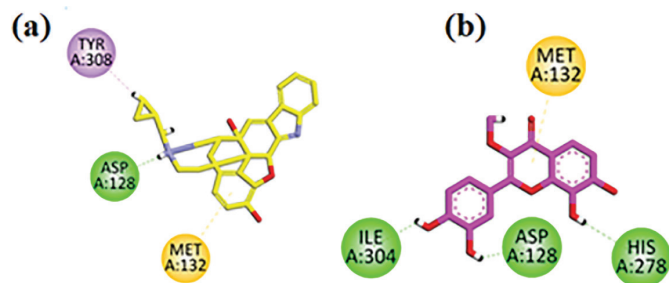


**FIGURE 5 - A)** Naltrindole (co-crystallized native ligand) two-dimensional interaction plot in the delta opioid receptor (DOR) receptor binding site. **B)** Isolated flavone two-dimensional interaction plot in the DOR binding site.

Two-dimensional interaction plots of native ligand JDtic and isolated compound in the binding site of kappa opioid receptor (KOR) are shown in Figure 6. JDtic inhibitor has good interactions such as conventional hydrogen bonding,  $\pi$ - $\pi$  stacking, and  $\pi$ -sulfur interaction with KOR (Figure 6A). Isolated flavone interacted with KOR residues (Met142, His291, Tyr312, Tyr139) and showed three conventional hydrogen bonds with residues His291, Tyr312, Tyr139 and  $\pi$ -sulfur interaction with residue Met142 (Figure 6B).

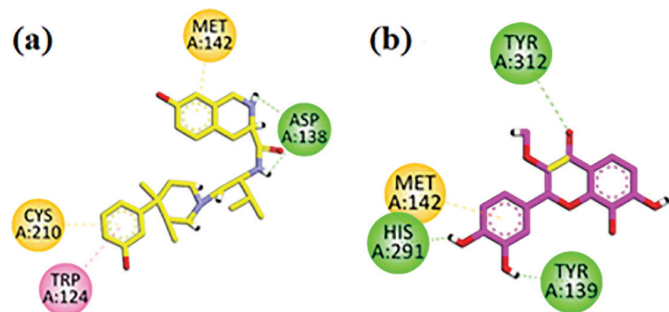


**FIGURE 6 - A)** JDtic (co-crystallized native ligand) two-dimensional interaction plot in the kappa opioid receptor (KOR) receptor binding site. **B)** Isolated flavone two-dimensional interaction plot in the KOR binding site.

Two-dimensional interaction plots of native ligand (b-FNA) and isolated compound in the binding site of mu opioid receptor (MOR) are shown in Figure 7. The co-crystallized ligand has good interactions, such as conventional hydrogen bonding and  $\pi$ -sulfur interaction with the MOR (Figure 7A). Isolated compound interacts with MOR binding site residues Val300, Asp147, Tyr326, Asn150, and His297 and showed good interactions for inhibiting pain, euphoria, sedation, and respiratory depression receptors, which included three conventional hydrogen bonds with residues Asp147, Asn150, His297,  $\pi$ - $\pi$  stacking with residue Tyr326, and  $\pi$ -sigma interaction with residue Val300 (Figure 7B).

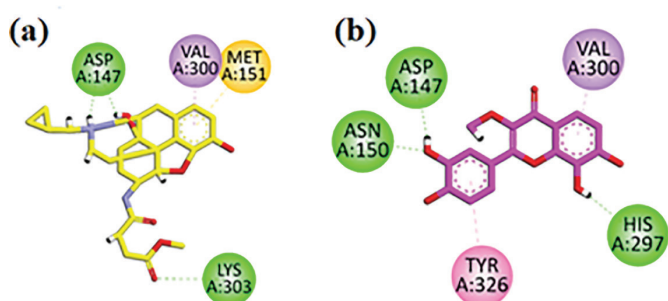


**FIGURE 7 - A)** b-FNA (co-crystallized native ligand) two-dimensional interaction plot in the mu opioid receptor (MOR) receptor binding site. **B)** Isolated compound two-dimensional interaction plot in the MOR binding site.

## Discussion

The search for new, safe and effective economical drug candidates is challenging for medicinal chemists in the modern era. The pain, inflammation, and insomnia are treated with various drug regimens, and each of these analgesic, anti-inflammatory, and sedative drugs has mild or significant side effects. Due to these side effects, patient compliance is declining, and ultimately, the patient seeks an alternative therapeutic agent. This switching of therapeutic options leads to therapy failure. Therefore, searching for a safe and effective drug molecule is essential. The present study was conducted to find a suitable drug molecule from *P. chinensis*. This medicinal plant is used locally to treat pain, inflammation (31), fever, and depression (10). To provide a scientific background to this folklore, the crude extract and isolated compound of *P. chinensis* were tested for analgesic, anti-inflammatory, and muscle coordination effects. The extract and isolated constituent demonstrated a significant analgesic effect in the thermal-induced pain model. This pain model is used to find central analgesic potential (32). The prolongation of latency time by extracting and isolating molecules reflects the central analgesic potential. The central analgesic pathway is attributed to the stimulation of opioid receptors (25). Once these inhibitor receptors link with inhibitor proteins and are stimulated with ligand, the neurotransmitters' (substance p) release is blocked, and pain sensation is diminished. The results of the hot plate indicate that the extract or compound might be agnostic for opioid receptors. The samples to be tested also attenuated the induced paw edema in the inflammatory model. This attenuation of induced paw edema by inflammatory mediators (carrageenan) indicates the COX inhibitory potential. The extract and compound also proved to be a sedative following previous studies (33). The muscle relaxation effect is also a promising adjuvant with analgesic and anti-inflammatory effects.

Docking studies were performed for the isolated compound against COX-1,2, DOR, KOR, and MOR, and their interactions were also compared with native co-crystallized ligands of each receptor. Analgesic drugs help to reduce the pain and are also called painkillers. In our current study, we performed analgesic and anti-inflammatory in vivo activity by keeping the tramadol and diclofenac as standard drugs.

Results showed that isolated compounds have good analgesic and anti-inflammatory effects. COX receptors synthesize prostaglandins, prostanoids, and thromboxane, which cause inflammation and pain. COX receptor inhibition helps to get relief from pain and inflammation. COX-1 and COX-2 are the two COX receptors. Opioid receptors belong to the seven transmembrane G protein-coupled receptors (GPCRs). Opioid receptors are known for mediating the hormones and neurotransmitters. Opioid receptors are also the primary target for anti-analgesics, anti-inflammatory drugs, antidepressants, sedatives, and muscle relaxant medications. Opioid receptors are extensively dispersed in the central and peripheral nervous systems (CNS and PNS). Opioid receptors are classified as delta, kappa, and mu opioid receptors.

In our current study, the experimental results showed that the isolated compound has a significant sedative and muscle relaxant effect. We performed docking studies on two forms of COX (COX-1, COX-2) and three opioid receptors (delta, kappa, and mu). Isolated flavone from *P. chinensis* (Anacardiaceae) showed strong interactions with COXs. In the binding site of COX-1, the compound exhibited one hydrogen bond formed with residue Ser530,  $\pi$ - $\pi$  interaction with Gly526, and amide- $\pi$  stacking with residue Tyr355. In contrast, the isolated flavone interacted with two critical residues (His90 and Leu352) in the COX-2-specific binding site. The computed crucial energy values for isolated flavone in the binding sites of COX-1 and COX-2 are  $-6.374$  and  $-7.019$  kcal/mol, respectively. These values showed that it predominantly inhibited COX-2. However, it may be classified as a non-selective COX inhibitor. Isolated flavone also exhibited strong interactions with all studied opioid receptors. The calculated binding energy values for DOR, KOR, and MOR are  $-6.2942$ ,  $-6.7136$ , and  $-6.6148$  kcal/mol, respectively. Docking studies on COX isoforms and opioid receptors showed that the compound exerts its therapeutic effect by inhibiting COX and nociceptive pathways.

*P. chinensis* extract and isolated compound exhibited potent analgesic, anti-inflammatory, sedative, and muscle relaxant properties. Consequently, our findings justify using *P. chinensis* extract and isolated compounds to treat numerous diseases. The discovery of novel pharmaceutical products will result from the detailed mechanism studies conducted for drug discovery. Docking studies on COX isoforms and opioid receptors showed that the compound exerts its therapeutic effect by inhibiting COX and nociceptive pathways.

## Acknowledgment

The authors thank Princess Nourah bint Abdulrahman University researchers supporting project number (PNURSP 2024R18), Princess Nourah bint Abdulrahman University, Riyadh, Saudi Arabia.

## Disclosures

**Financial support:** The financial contributors had no role in the design, analysis, or writing of this article.

**Data availability statement:** The datasets used and/or analyzed during the current study are available from the corresponding author upon reasonable request.



**Authors contributions:** Conceptualization, AR, UR, ZA; Methodology, AS, NM, NA, Formal analysis, TSA, SM; Writing original draft preparation, Supervision, AR, MI; Writing-Editing, MI. All authors read this article and approved it for submission.

## References

- Sharma V, Gautam DNS, Radu AF, Behl T, Bungau SG, Vesa CM. Reviewing the traditional/modern uses, phytochemistry, essential oils/extracts and pharmacology of *Embelia ribes* Burm. *Antioxidants*. 2022;11(7):1359. [CrossRef PubMed](#)
- Dai W, Long L, Wang X, Li S, Xu H. Phytochemicals targeting Toll-like receptors 4 (TLR4) in inflammatory bowel disease. *Chin Med*. 2022;17(1):53. [CrossRef PubMed](#)
- Kashaninejad M, Tabil LG. Pistachio (*Pistacia vera* L.). In Yahia EM, ed. *Postharvest biology and technology of tropical and subtropical fruits*. Cambridge, UK: Woodhead Publishing; 2011: 218-247e.
- Mir-Makhamad B, Bjørn R, Stark S, Spengler RN III. Pistachio (*Pistaciavera* L.) domestication and dispersal out of Central Asia. *Agronomy (Basel)*. 2022;12(8):1758. [CrossRef](#)
- Glimn-Lacy J, Kaufman PB. *Botany illustrated: introduction to plants, major groups, flowering plant families*. Springer; 2006.
- Christenhusz MJ, Byng JW. The number of known plants species in the world and its annual increase. *Phytotaxa*. 2016;261(3):201-217. [CrossRef](#)
- Anonymous. *The wealth of India. A dictionary of Indian raw materials and industrial products publication and information directorate*, vol 8. New Delhi: CSIR; 1998:120.
- Chopra RN, Chopra IC, Handa KL, Kapur LD. *Chopra's indigenous drugs of India*. Academic Publishers; 1994.
- Keys JD. *Chinese herbs*. Tuttle Publishing; 2011 Dec 6.
- Huang CY, Chang YY, Chang ST, Chang HT. Xanthine oxidase inhibitory activity and chemical composition of *Pistacia chinensis* leaf essential oil. *Pharmaceutics*. 2022;14(10):1982. [CrossRef PubMed](#)
- De Pooter HL, Schamp NM, Aboutabl EA, El Tohamy SF, Doss SL. Essential oils from the leaves of three *Pistacia* species grown in Egypt. *Flavour Fragrance J*. 1991;6(3):229-232. [CrossRef](#)
- Nishimuta S, Taki M, Takaishi S, Iijima Y, Akiyama T. Structures of 4-aryl-coumarin (neoflavone) dimers isolated from *Pistacia chinensis* Bunge and their estrogen-like activity. *Chem Pharm Bull (Tokyo)*. 2000;48(4):505-508. [CrossRef PubMed](#)
- Chopra RN, Badhwar RK, Ghosh S. *Poisonous plants of India*. Indian Council of Agricultural Research; 1965:270.
- Bibi Y, Zia M, Qayyum A. Review – an overview of *Pistacia integerrima* a medicinal plant species: ethnobotany, biological activities and phytochemistry. *Pak J Pharm Sci*. 2015;28(3): 1009-1013. [PubMed](#)
- Rauf A, Rashid U, Shbeer AM, et al. Flavonoids from *Pistacia chinensis* subsp. *integerrima* with leishmanicidal activity: computational and experimental evidence. *Nat Prod Res*. 2023;20:1-6. [CrossRef PubMed](#)
- Ansari SH, Ali M, Qadry JS. Essential oils of *Pistacia integerrima* Galls and their effect on the central nervous system. In *J Pharmacog* 1993; 31(2):89-95.
- Ahmad NS, Waheed A, Farman M, Qayyum A. Analgesic and anti-inflammatory effects of *Pistacia integerrima* extracts in mice. *J Ethnopharmacol*. 2010;129(2):250-253. [CrossRef PubMed](#)
- Shirole RL, Shirole NL, Saraf MN. In vitro relaxant and spasmolytic effects of essential oil of *Pistacia integerrima* Stewart ex Brandis Galls. *J Ethnopharmacol*. 2015;168:61-65. [CrossRef PubMed](#)
- Noureen F, Khan MR, Shah NA, Khan RA, Naz K, Sattar S. *Pistacia chinensis*: strong antioxidant and potent testicular toxicity amelioration agent. *Asian Pac J Trop Med*. 2017;10(4):380-389. [CrossRef PubMed](#)
- Uddin G, Ismail, Rauf A, et al. Urease inhibitory profile of extracts and chemical constituents of *Pistacia atlantica* ssp. *cabulica* Stocks. *Nat Prod Res*. 2016;30(12):1411-1416. [CrossRef PubMed](#)
- Wu J-H, Tung Y-T, Chien S-C, et al. Effect of phytochemicals from the heartwood of *Acacia confusa* on inflammatory mediator production. *J Agric Food Chem*. 2008;56(5):1567-1573. [CrossRef PubMed](#)
- Abu-Izneid T, Rauf A, Akram Z, et al. Discovery of new  $\alpha$ -glucosides, antiglycation agent, and in silico study of 2-(3,4-dihydroxyphenyl)-7,8-dihydroxy-3-methoxy-4H-chromen-4-one isolated from *Pistacia chinensis*. *Heliyon*. 2024;10(5):e27298. [CrossRef PubMed](#)
- Rauf A, Akram Z, Naveed M, et al. Studies on the inhibition of ectonucleotide pyrophosphatase/phosphodiesterase 1 (ENPP1) by 2-(3, 4-Dihydroxyphenyl)-7, 8-dihydroxy-3-methoxychromen-4-one, a flavonoid from *Pistacia chinensis*. *Chemistry (Basel)*. 2023;5(4):2094-2103. [CrossRef](#)
- Muhammad N, Saeed M, Khan H. Antipyretic, analgesic and anti-inflammatory activity of *Viola betonicifolia* whole plant. *BMC Complement Altern Med*. 2012;12(1):59. [CrossRef PubMed](#)
- Law P-Y, Loh HH. Regulation of opioid receptor activities. *J Pharmacol Exp Ther*. 1999;289(2):607-624. [PubMed](#)
- Sadiq A, Mahnashi MH, Alyami BA, Alqahtani YS, Alqarni AO, Rashid U. Tailoring the substitution pattern of pyrrolidine-2,5-dione for discovery of new structural template for dual COX/LOX inhibition. *Bioorg Chem*. 2021;112:104969. [CrossRef PubMed](#)
- Muhammad N, Saeed M, Khan H, Haq I. Evaluation of n-hexane extract of *Viola betonicifolia* for its neuropharmacological properties. *J Nat Med*. 2013;67(1):1-8. [CrossRef PubMed](#)
- Javed MA, Ashraf N, Saeed Jan M, et al. Structural modification, *in vitro*, *in vivo*, *ex vivo*, and *in silico* exploration of pyrimidine and pyrrolidine cores for targeting enzymes associated with neuroinflammation and cholinergic deficit in Alzheimer's disease. *ACS Chem Neurosci*. 2021;12(21):4123-4143. [CrossRef PubMed](#)
- Mahnashi MH, Alyami BA, Alqahtani YS, et al. Phytochemical profiling of bioactive compounds, anti-inflammatory and analgesic potentials of *Habenaria digitata* Lindl.: molecular docking based synergistic effect of the identified compounds. *J Ethnopharmacol*. 2021 Jun 12;273:113976. [CrossRef PubMed](#)
- Ullah Q, Ali Z, Rashid U, et al. Involvement of the opioidergic mechanism in the analgesic potential of a novel indazolone derivative: efficacy in the management of pain, neuropathy, and inflammation using *in vivo* and *in silico* approaches. *ACS Omega*. 2023;8(25):22809-22819. [CrossRef PubMed](#)
- Jan MS, Ahmad S, Hussain F, et al. Design, synthesis, in-vitro, in-vivo and in-silico studies of pyrrolidine-2,5-dione derivatives as multitarget anti-inflammatory agents. *Eur J Med Chem*. 2020;186:111863. [CrossRef PubMed](#)
- Sattar S, Khan MR, Shah NA, Noureen F, Naz K. Nephroprotective potential of *Pistacia chinensis* bark extract against induced toxicity in rats. *Nus Biosci*. 2016;8(2):192-200. [CrossRef](#)
- Muhammad N. In-vivo models for management of pain. *Pharmacol Pharm*. 2014;5(1):92-96. [CrossRef](#)



# Deciphering the molecular mechanisms underlying anti-pathogenic potential of a polyherbal formulation Enteropan® against multidrug-resistant *Pseudomonas aeruginosa*

Sweety Parmar<sup>1</sup>, Gemini Gajera<sup>1</sup>, Nidhi Thakkar<sup>1</sup>, Hanmanthrao S. Palep<sup>2</sup>, Vijay Kothari<sup>1</sup>

<sup>1</sup>Institute of Science, Nirma University, Ahmedabad - India

<sup>2</sup>Dr. Palep's Medical Research Foundation, Mumbai - India

Sweety Parmar, Gemini Gajera and Nidhi Thakkar contributed equally.

## ABSTRACT

**Objective:** Anti-pathogenic potential of a polyherbal formulation Enteropan® was investigated against a multidrug-resistant strain of the bacterium *Pseudomonas aeruginosa*.

**Methods:** Growth, pigment production, antibiotic susceptibility, etc., were assessed through appropriate *in vitro* assays. Virulence of the test pathogen was assessed employing the nematode worm *Caenorhabditis elegans* as a model host. Molecular mechanisms underlining the anti-pathogenic activity of the test formulation were elucidated through whole transcriptome analysis of the extract-exposed bacterial culture.

**Results:** Enteropan-pre-exposed *P. aeruginosa* displayed reduced (~70%↓) virulence towards the model host *C. elegans*. Enteropan affected various traits like biofilm formation, protein synthesis and secretion, quorum-modulated pigment production, antibiotic susceptibility, nitrogen metabolism, etc., in this pathogen. *P. aeruginosa* could not develop complete resistance to the virulence-attenuating activity of Enteropan even after repeated exposure to this polyherbal formulation. Whole transcriptome analysis showed 17% of *P. aeruginosa* genome to get differentially expressed under influence of Enteropan. Major mechanisms through which Enteropan exerted its anti-virulence activity were found to be generation of nitrosative stress, oxidative stress, envelop stress, quorum modulation, disturbance of protein homeostasis and metal homeostasis. Network analysis of the differentially expressed genes resulted in identification of 10 proteins with high network centrality as potential targets from among the downregulated genes. Differential expression of genes coding for five (*rpoA*, *tig*, *rpsB*, *rpsL*, and *rpsJ*) of these targets was validated through real-time polymerase chain reaction too, and they can further be pursued as potential targets by various drug discovery programmes.

**Keywords:** Antimicrobial resistance (AMR), Anti-virulence, *Caenorhabditis elegans*, Iron/Sulphur homeostasis, Metal homeostasis, Network analysis, Nitrosative stress, Polyherbal, Transcriptome

## Introduction

Antibiotic-resistant strains of the gram-negative bacterial pathogen *Pseudomonas aeruginosa* are responsible for considerable morbidity and mortality globally (1). As per CDC's Antibiotic Resistance Threat Report (2019),

multidrug-resistant (MDR) *P. aeruginosa* was responsible for an estimated 32,600 hospitalizations, and 2,700 deaths in 2017 (2). Healthcare costs in the United States alone attributed to these infections were estimated to be 767 million USD. Later released update to this report indicated an increase in number of infections caused by hospital-onset MDR *P. aeruginosa* in 2022 as compared to that in 2019 ([Online](#)). According to a study conducted by Wattal et al (3), India holds a leading position globally with respect to consumption of antibiotics for human use. This heavy antibiotic usage contributes significantly towards antibiotic resistance, resulting in a substantial increase in mortality among newborns who contract sepsis caused by MDR pathogens. *P. aeruginosa* displays versatility with respect to types of infections it causes, as it has been involved in

Received: April 4, 2024

Accepted: August 1, 2024

Published online: August 30, 2024

This article includes supplementary material

Corresponding author:

Vijay Kothari

email: [vijay.kothari@nirmauni.ac.in](mailto:vijay.kothari@nirmauni.ac.in)



pneumonia, urinary tract infections, bloodstream infections, and surgical site infections. Hospitalized patients on ventilators, those with catheters, surgical wounds, or burns are particularly at higher risk of contracting *P. aeruginosa* infection (4). While treating MDR *P. aeruginosa* infections, the choice of available effective antibiotics remains quite narrow (5), and hence there is an urgent need for discovery and development of novel antibacterial agents/formulations against this notorious pathogen.

Traditional medicine (TM) formulations can be a potential source of novel leads against bacterial pathogens including *P. aeruginosa*. Since TM often relies on polyherbal formulations (6,7) for treatment, and these polyherbal formulations display ‘multiplicity of targets’ (8) against susceptible pathogens, investigating the effect of such formulations in the pathogens at whole metabolome or transcriptome level can result in discovery of new molecular targets in pathogens. While dearth of novel cellular and molecular targets has been one of the major hurdles in new antibiotic discovery (9,10), elucidating the anti-pathogenic potential of polyherbal formulations at molecular level can be quite relevant. Often these polyherbal formulations exhibit anti-virulence effect (11) rather than directly inhibiting growth of the target pathogens. They may do so by affecting expression of non-essential genes (i.e. other than housekeeping genes) in the pathogens.

Present study investigated one polyherbal formulation (Enteropan) for its anti-pathogenic potential against a MDR *P. aeruginosa*. This formulation or its component plant extracts are traditionally being prescribed for treatment of irritable bowel syndrome, diarrhoea, dysentery, and other gastrointestinal problems ([Online](#)).

## Materials and methods

### Test formulation

Test formulation Enteropan® was procured from Dr. Palep’s Medical Research Foundation Pvt. Ltd, Mumbai. All the nine ingredient plants and their parts whose hydroalcoholic extracts have been mixed to prepare this formulation are listed in Table 1. We obtained the polyherbal mix from the manufacturer in dried powder form without any bulking agent, and mixed 4 g of it in 8 mL of dimethylsulfoxide (DMSO; Merck). The DMSO-soluble fraction of Enteropan was found to be  $71.17\% \pm 3.07$ . After separating the insoluble fraction through centrifugation, the remaining DMSO-dissolved fraction was stored under refrigeration.

### Test organisms

*P. aeruginosa* strain was sourced from our internal lab culture collection. Its antibiogram (Tab. S1) generated through disc diffusion assay revealed it to be resistant to three different classes of antibiotics, that is, co-trimoxazole (combination of trimethoprim and sulfamethoxazole), streptomycin (aminoglycoside), and augmentin (combination of amoxicillin and clavulanic acid). Antibiotic susceptibility of this strain to kanamycin was classified as ‘intermediate’. *Pseudomonas* broth (20 g/L peptic digest of animal tissue, 10 g/L potassium sulphate, 1.4 g/L magnesium chloride, 3% v/v glycerol, pH

**TABLE 1** - Ingredients of Enteropan formulation

Scientific name	Common English name (Indian name)	Part used	Proportion in the polyherbal mix (mg/capsule)
<i>Aegle marmelos</i>	Wood apple (Bael)	Leaves	100
<i>Myristica fragrans</i>	Nutmeg (Jaiphal)	Fruit	15
<i>Zingiber officinale</i>	Ginger (Sunthi)	Rhizome	60
<i>Aconitum heterophyllum</i>	Indian Atees (Ativisha)	Bulb	30
<i>Coriandrum sativum</i>	Coriander (Dhanyak)	Seeds	40
<i>Cyperus rotundus</i>	Nutgrass (Nagarmotha)	Rhizome	25
<i>Vetiveria zizanioides</i>	Khas Khas grass (Usheer)	Roots	50
<i>Punica granatum</i>	Pomegranate (Dadim)	Rind	50
<i>Holarrhena antidysenterica</i>	Star gooseberry (Kutaj)	Bark	27

$7.0 \pm 0.2$ ) or agar (HiMedia) was used to cultivate this bacterium. Inoculum density of this bacterium to be used in all experiments was adjusted at  $OD_{625} = 0.08-0.10$  to achieve equivalence to McFarland turbidity standard 0.5.

*Escherichia coli* OP50 procured from LabTIE B.V. the Netherlands was used as food for *Caenorhabditis elegans*, while maintaining the worm on NGM (nematode growth medium; 3 g/L NaCl, 1 M  $CaCl_2$ , 1 M  $MgSO_4$ , 2.5 g/L peptone, 5 mg/mL cholesterol, 1 M phosphate buffer of pH 6, 17 g/L agar-agar).

The nematode worm *C. elegans* (N2 Bristol, procured from IIT Gandhinagar, Gujarat, India) was used as a model host for *P. aeruginosa*. The worm was maintained on NGM agar plates. Worm synchronization was done as described in literature (12) and in our previous studies (13,14) too. Prior to all *in vivo* assays, worms were kept without food for 2 days to make them gnotobiotic.

### In vivo assays

Four different types of *in vivo* assays performed are described below. Each of them involved live-dead counting over a period of 5 days under a microscope (4x) with halogen light source. On the last day of the experiment, when plates could be opened, death was confirmed by touching them with a straight wire, wherein no movement was considered as confirmation of death. In each well, there were 10 worms in M9 buffer (3 g/L  $KH_2PO_4$ ; 6 g/L  $Na_2HPO_4$ ; 5 g/L NaCl), which were challenged with *P. aeruginosa* by adding 100  $\mu$ L ( $OD_{764} = 1.50 \pm 0.05$ ) of bacterial culture grown in *Pseudomonas* broth for  $21 \pm 1$  hours at  $35 \pm 0.5^\circ C$ .



### Anti-pathogenic assay

Ten worms of L3-L4 stage contained in 900  $\mu$ L M9 buffer were challenged with *P. aeruginosa* (100  $\mu$ L of the culture broth) in absence or presence of Enteropan (50-1,000  $\mu$ g/mL), wherein neither the bacterium nor the worms were pre-exposed to Enteropan. Incubation was done at 22°C for 5 days with live-dead microscopic count once a day.

### Anti-infective assay

*P. aeruginosa* was grown at 35°C for 20-22 hours in *Pseudomonas* broth with or without Enteropan (5-1,000  $\mu$ g/mL). Post-incubation, 100  $\mu$ L of the culture broth was mixed with 900  $\mu$ L of M9 buffer containing 10 worms (L3-L4 stage) in a 24-well plate (surface non-treated; HiMedia). This plate was incubated at 22°C for 5 days (15,16).

### Prophylactic assay

Gnotobiotic worms were incubated in M9 buffer supplemented with Enteropan (5-1,000  $\mu$ g/mL) for 96 hours. Following incubation, these worms were washed with M9 buffer twice, and then challenged with *P. aeruginosa* not pre-exposed to Enteropan (100  $\mu$ L of the culture broth) in 24-well plates (HiMedia). Worm survival was monitored over a 5-day period under microscope (17).

### Post-infection assay

Ten worms contained in M9 buffer were first challenged with pathogen, and after allowing *P. aeruginosa* (100  $\mu$ L of the culture broth) for 3 or 6 hours to establish infection, Enteropan (50-1,000  $\mu$ g/mL) was added into the well as a possible post-infection therapy. Survival of worms was observed through a live-dead count under microscope over 5 days (18).

Appropriate controls were included in all the above experiments as relevant:

**Sterility Control:** Sterile M9 buffer containing neither bacteria nor worms

**Survival Control:** M9 buffer containing 10 worms (no bacteria added)

**Toxicity Control:** 10 worms in M9 buffer supplemented with Enteropan

**Infection Control:** 10 worms in M9 buffer + 100  $\mu$ L of the *P. aeruginosa* culture broth ( $OD_{764} = 1.50 \pm 0.05$ ). These wells did not contain any plant extract.

**Vehicle Control:** 0.5% v/v DMSO was used in place of Enteropan.

**Positive Control:** Standard antibiotics employed as positive controls are detailed in the figure legends.

### In vitro assays

#### Growth and pigment quantification

The broth dilution assay was used to evaluate *P. aeruginosa*'s growth and quorum sensing (QS)-regulated pigment synthesis in the presence or absence of the test formulation.

Different concentrations (ranging from 5 to 1,000  $\mu$ g/mL) of Enteropan formulation were used to challenge the organism. The growth media employed was *Pseudomonas* broth, into which bacterial inoculum set to 0.5 McFarland turbidity standard was added at 10% v/v, followed by incubation at 35°C for 20-22 hours, with intermittent shaking. The experiment also contained an appropriate vehicle control with DMSO (0.5% v/v) and an abiotic control with extract and growth medium but no inoculum.

Bacterial growth was measured photometrically at the end of the incubation by measuring the culture density at 764 nm (Agilent Cary 60 UV-visible spectrophotometer) (19). Following this, pigment was extracted and quantified in accordance with the procedure outlined for each pigment.

One mL of culture broth was mixed in a 2:1 ratio with chloroform (Merck, Mumbai), followed by centrifugation (15,300 g) for 10 minutes. This resulted in the formation of two immiscible layers. OD of the upper aqueous layer containing the yellow-green fluorescent pigment pyoverdine was measured at 405 nm. Pyoverdine Unit was calculated as  $OD_{405}/OD_{764}$ . The lower chloroform layer containing the blue pigment pyocyanin was mixed with 0.1 N HCl (20% v/v; Merck). This caused a change of colour from blue to pink. This was followed by centrifugation (15,300 g) for 10 minutes, and OD of upper layer acidic liquid containing pyocyanin was quantified at 520 nm. Pyocyanin Unit was calculated as  $OD_{520}/OD_{764}$ .

### Biofilm assays

Biofilm formation is an important virulence trait, and hence the effect of Enteropan on biofilm forming ability of *P. aeruginosa*, as well as on pre-formed biofilm was investigated. A flow diagram depicting all four different biofilm assays is included in supplementary file (Fig. S2). Biofilm quantification was achieved through crystal violet assay (20). Biofilm viability was assessed through 3-(4,5-Dimethylthiazol-2-yl)-2,5-diphenyltetrazolium bromide (MTT) assay (21).

For the crystal violet assay, the biofilm-containing tubes (after discarding the inside liquid) were washed with phosphate-buffered saline (PBS) in order to remove all non-adherent (planktonic) bacteria, and air-dried for 15 minutes. Then, each of the washed tubes was stained with 1.5 mL of 0.4% aqueous crystal violet (Central Drug House, Delhi) solution for 30 minutes. Afterwards, each tube was washed twice with 2 mL of sterile distilled water and immediately de-stained with 1.5 mL of 95% ethanol. After 45 minutes of de-staining, 1 mL of de-staining solution was transferred into separate tubes, and read at 580 nm (Agilent Cary 60 UV-Vis).

For the MTT assay, the biofilm-containing tubes (after discarding the inside liquid) were washed with PBS in order to remove all non-adherent (planktonic) bacteria, and air-dried for 15 minutes. Then 1.8 mL of minimal media (sucrose 15 g/L,  $K_2HPO_4$  5 g/L,  $NH_4Cl$  2 g/L, NaCl 1 g/L,  $MgSO_4$  0.1 g/L, yeast extract 0.1 g/L, pH 7.4  $\pm$  0.2) was added into each tube, followed by addition of 200  $\mu$ L of 0.3% MTT [HiMedia]. Then after 2 hours of incubation at 35°C, all liquid content was discarded, and the remaining purple formazan derivatives were dissolved in 2 mL of DMSO and measured at 540 nm.



### Nitrite estimation

Quantification of nitrite in bacterial culture was achieved through a colorimetric assay using modified Griess reagent (22,23). Supernatant (250  $\mu$ L) obtained from centrifugation (13,500 g; 25°C; 10 minutes) of *P. aeruginosa* culture grown in the presence or absence of Enteropan was mixed with 250  $\mu$ L of Griess reagent (1 $\times$ ; Sigma-Aldrich), followed by 15 minutes of incubation in dark at room temperature. Absorbance of the resulting pink colour was measured at 540 nm. This absorbance was plotted on the standard curve prepared using NaNO<sub>2</sub> (0.43–65  $\mu$ M) to calculate nitrite concentration. Sodium nitroprusside (Sigma-Aldrich) was used as a positive control, as it is known to generate nitrosative stress in bacteria (24). Deionized water was used as negative control.

### Antibiotic susceptibility test

Antibiogram of *P. aeruginosa*'s overnight grown culture in *Pseudomonas* broth in the presence or absence of Enteropan was generated through disc diffusion assay in accordance with Clinical and Laboratory Standards Institute (CLSI) guidelines (25). Cells grown in *Pseudomonas* broth were separated through centrifugation (13,600 g) and washed with phosphate buffer (pH 7.0  $\pm$  0.2) followed by centrifugation. The resulting cell pellet was used to prepare inoculum for subsequent disc diffusion assay by suspending the cells in normal saline and adjusting the OD<sub>625</sub> between 0.08 and 0.10. This inoculum (100  $\mu$ L) was spread onto cation-adjusted Mueller-Hinton agar (HiMedia) plates (Borosil; 150 mm) followed by placing the antibiotic discs (Icosa G-I MINUS; HiMedia, Mumbai) on the agar surface. Incubation at 35°C was made for 18  $\pm$  1 hours, followed by observation and measurement of zone of inhibition.

### Protein estimation

Extracellular protein present in bacterial culture (grown in the presence or absence of Enteropan) supernatant, and intracellular protein in the cell lysate was quantified through Folin-Lowry method (26,27). After measuring cell density, 1 mL of *P. aeruginosa* culture was centrifuged (13,600 g), and the resulting supernatant was used for extracellular protein estimation. The remaining cell pellet was subjected to lysis (28) for release of intracellular proteins. Briefly, the cell pellet was washed with phosphate buffer (pH 7.4) and centrifuged (13,600 g). Resulting pellet was resuspended in 1 mL of chilled lysis buffer (0.876 g NaCl, 1 mL of Triton X-100, 0.5 g sodium deoxycholate, 0.1 g sodium dodecyl sulphate, and 0.60 g Tris HCl, in 99 mL of distilled water) and centrifuged (500 rpm) for 30 minutes at 4°C for agitation purpose. This was followed by further centrifugation (16,000 g at 4°C) for 20 min. Resulting cell lysate (supernatant) was used for protein estimation. Kanamycin (HiMedia; at IC<sub>50</sub>: 200  $\mu$ g/mL), an aminoglycoside antibiotic known to inhibit bacterial protein synthesis (29,30), was used as a positive control.

### Whole transcriptome analysis

To gain insight into the molecular mechanisms by which Enteropan attenuates bacterial virulence and modulates

various traits like pigment production, antibiotic susceptibility, nitrogen metabolism, protein synthesis/excretion, etc., we compared the gene expression profile of Enteropan-pre-treated *P. aeruginosa* with that of control culture at the whole transcriptome level.

### RNA extraction

Trizol (Invitrogen Bioservices; 343909) was used to extract RNA from bacterial cells (31). RNA was dissolved in nuclease-free water after precipitation with isopropanol and washing with 75% ethanol. Using the RNA HS assay kit (Thermo Fisher; Q32851) and adhering to the manufacturer's instructions, the extracted RNA was quantified using a Qubit 4.0 fluorometer (Thermo Fisher; Q33238). RNA concentration and purity were evaluated using Nanodrop 1000. Finally, RNA was checked on the TapeStation using HS RNA ScreenTape (Agilent) to yield RIN (RNA Integrity Number) values (Tab. S2).

### Library preparation

Final libraries were measured using a Qubit 4.0 fluorometer (Thermo Fisher; Q33238), a DNA HS assay kit (Thermo Fisher; Q322851), and a TapeStation 4150 (Agilent) using high-sensitivity D1000 ScreenTapes (Agilent; 5067-5582). The acquired sizes of all libraries are reported in Table S3.

### Genome annotation and functional analysis

FastQC v.0.11.9 (default parameters) was used to undertake a quality assessment of the sample's raw fastq readings (32). The reads' quality was then reevaluated using Fastq v.0.20.1 (33) after pre-processing the raw fastq reads with Fastq v.0.20.1.

The *P. aeruginosa* genome (GCA\_000006765.1\_ASM676v1) was indexed using bowtie2-build (34) v2.4.2 (default parameters). The processed reads were mapped to the *P. aeruginosa* genome using bowtie2 v2.4.2. Gene counts were determined using feature count v.0.46.1 (35) to quantify the aligned reads from the individual samples. Differential expression was estimated using the exact test (parameters: dispersion 0.1) with these gene counts as inputs in edgeR (36). The up- and downregulated sequences were extracted from the *P. aeruginosa* coding file and annotated using Blast2GO (37) to obtain the Gene Ontology (GO) keywords. These GO terms were used to create GO bar graphs with the wego tool (38).

All the raw sequence data has been submitted to the Sequence Read Archive. The relevant accession number is SRX15248092 ([Online](#)).

### Network analysis

Network analysis was carried out for Enteropan-exposed *P. aeruginosa*'s differentially expressed genes (DEG) fulfilling the dual criteria of log fold change  $\geq$  2 and false discovery rate (FDR)  $\leq$  0.001. List of DEG was fed into the database STRING (v.11.5) (39) for generating the Protein-Protein Interaction (PPI) network for the genes were arranged in decreasing order of 'node degree' (a measure of connectivity with other genes or proteins), and those above an empirically selected



threshold value (19 and 53 for up- and downregulated genes, respectively) were subjected to ranking by cytoHubba (v.3.9.1) plugin (40) of Cytoscape (41). Since cytoHubba uses 12 different ranking methods, we considered the DEG being top-ranked by  $\geq 6$  different methods (i.e. 50% of the total ranking methods) for further analysis. These top-ranked shortlisted proteins were further subjected to network cluster analysis through STRING, and those that were part of multiple clusters were considered as 'hubs' which can be taken up for further confirmation of their targetability. Here 'hub' refers to a gene or protein interacting with many other genes/proteins. Hubs thus identified were further subjected to co-occurrence analysis to see whether an anti-virulence agent targeting them is likely to satisfy the criterion of selective toxicity (i.e. targeting the pathogen without harming host). This sequence analysis allowed us to end with a limited number of proteins which satisfied various statistical and biological significance criteria simultaneously, that is, (1) log fold change  $\geq 2$ ; (2) FDR  $\leq 0.001$ ; (3) relative higher node degree; (4) top-ranking by at least six cytoHubba methods; (5) member of more than one local network cluster; (6) high probability of the target being absent from the host.

### Real-time polymerase chain reaction analysis

Polymerase chain reaction (PCR) was used to confirm the differential expression of the possible hubs discovered by network analysis of the DEG reported from whole transcriptome analysis (WTA). Primer3Plus (42) was used to design primers for the target genes (Tab. 2). These primer sequences were verified for their ability to specifically bind only to the target gene sequence throughout the whole genome file of *P. aeruginosa*. RNA extraction and purity check was executed as described in the previous section. The SuperScript™ VILO™ cDNA Synthesis Kit (Invitrogen Biosciences) was used to generate complementary DNA. Using gene-specific primers purchased from Sigma-Aldrich, the PCR experiment was carried out employing the temperature profile shown in Table S4. The gene PA3725 (*recJ*) was kept as an endogenous control. The reaction mix

used was FastStart Essential DNA Green Master mix (Roche; 06402712001). Real-time PCR (RT-PCR) assay was performed on QuantStudio 5 RT-PCR machine (Thermo Fisher Scientific, USA). Sample generation for PCR validation was done independent of that for transcriptome assay.

### Statistical analysis

All results reported are means of three or more independent experiments, each performed in triplicate. Statistical significance was assessed through t-test performed using Microsoft Excel®, and data with  $p \leq 0.05$  was considered to be significant.

## Results and discussion

### In vivo assays

#### *P. aeruginosa* displayed reduced virulence towards *C. elegans* in the presence of Enteropan

When *C. elegans* was challenged with *P. aeruginosa* in the presence of Enteropan, the bacterium could kill lesser worms than in the absence of Enteropan (Fig. 1A; Supplementary videos: A-E). The most effective concentration of Enteropan with respect to offering protection to the worm population from bacterial attack was found to be 250  $\mu\text{g}/\text{mL}$ . Since higher concentrations offered either at par or lesser protection to the worms, the dose-response relationship here can be said to be nonlinear. Irrespective of the magnitude of protection offered to worm population in the presence of Enteropan®, progeny worms were observed (third day onwards) in all experimental and positive control wells, but not in the wells pertaining to vehicle control. It might have occurred that the virulence-attenuated *P. aeruginosa* were used by the worms as food, and that allowed them to reproduce.

#### Enteropan pre-treatment reduced bacterial virulence towards *C. elegans*

Enteropan (5-1,000  $\mu\text{g}/\text{mL}$ )-pre-treated *P. aeruginosa* was found to exert lesser virulence against *C. elegans* than its not-exposed counterpart. Enteropan concentrations  $\leq 250 \mu\text{g}/\text{mL}$  could not compromise *P. aeruginosa*'s ability to kill *C. elegans*; however, concentrations  $\geq 500 \mu\text{g}/\text{mL}$  did compromise bacterial virulence significantly (Fig. 1B; Supplementary videos: F-I). Enteropan pre-treatment of the pathogen at these effective concentrations not only attenuated bacterial virulence but also supported worm fertility as evidenced by the appearance of numerous progenies in the experimental wells by the fifth day. The most effective concentration of Enteropan with respect to virulence-attenuating effect was found to be 600  $\mu\text{g}/\text{mL}$ , as the effect of higher concentrations till 1 mg/mL was statistically not different than that of 600  $\mu\text{g}/\text{mL}$ .

After confirming the anti-virulence activity of Enteropan against *P. aeruginosa*, we asked whether this pathogen can develop resistance upon repeatedly getting exposed to the test formulation. To answer this, we subcultured *P. aeruginosa* in *Pseudomonas* broth supplemented with Enteropan (600  $\mu\text{g}/\text{mL}$ ) multiple times. Enteropan-pre-exposed *P. aeruginosa* thus obtained after fifth and tenth such subculturing

TABLE 2 - Primer sequences for the target genes

Gene ID	Primers	Amplicon size (bp)
PA4238 ( <i>rpoA</i> )	FP: 5'-CGCTGAACATGAAGCTGAAG-3' RP: 5'-CAGGACCAGTTTGTCCAGGT-3'	194
PA1800 ( <i>tig</i> )	FP: 5'-ACCGAAGTCAACAAGCGTCT-3' RP: 5'-GGATTCAGCTTCTGCTCGAC-3'	208
PA3656 ( <i>rpsB</i> )	FP: 5'-GCGCAACAAGATCCATATCA-3' RP: 5'-GATCGACTGACGGATGGTCT-3'	232
PA4268 ( <i>rpsL</i> )	FP: 5'-TACATCGGTGGTGAAGGTCA-3' RP: 5'-TACTTCGAACGACCCTGCTT-3'	155
PA4264 ( <i>rpsJ</i> )	FP: 5'-GATTCGGTTGAAGGCTTTTG-3' RP: 5'-TACTGATCACGCGCATCTTT-3'	174
Control gene PA3725 ( <i>recJ</i> )	FP: 5'-CCAGTTGAGCATCCAGGAGT-3' RP: 5'-TTTCAGCACCAGCTTCAGGT-3'	157



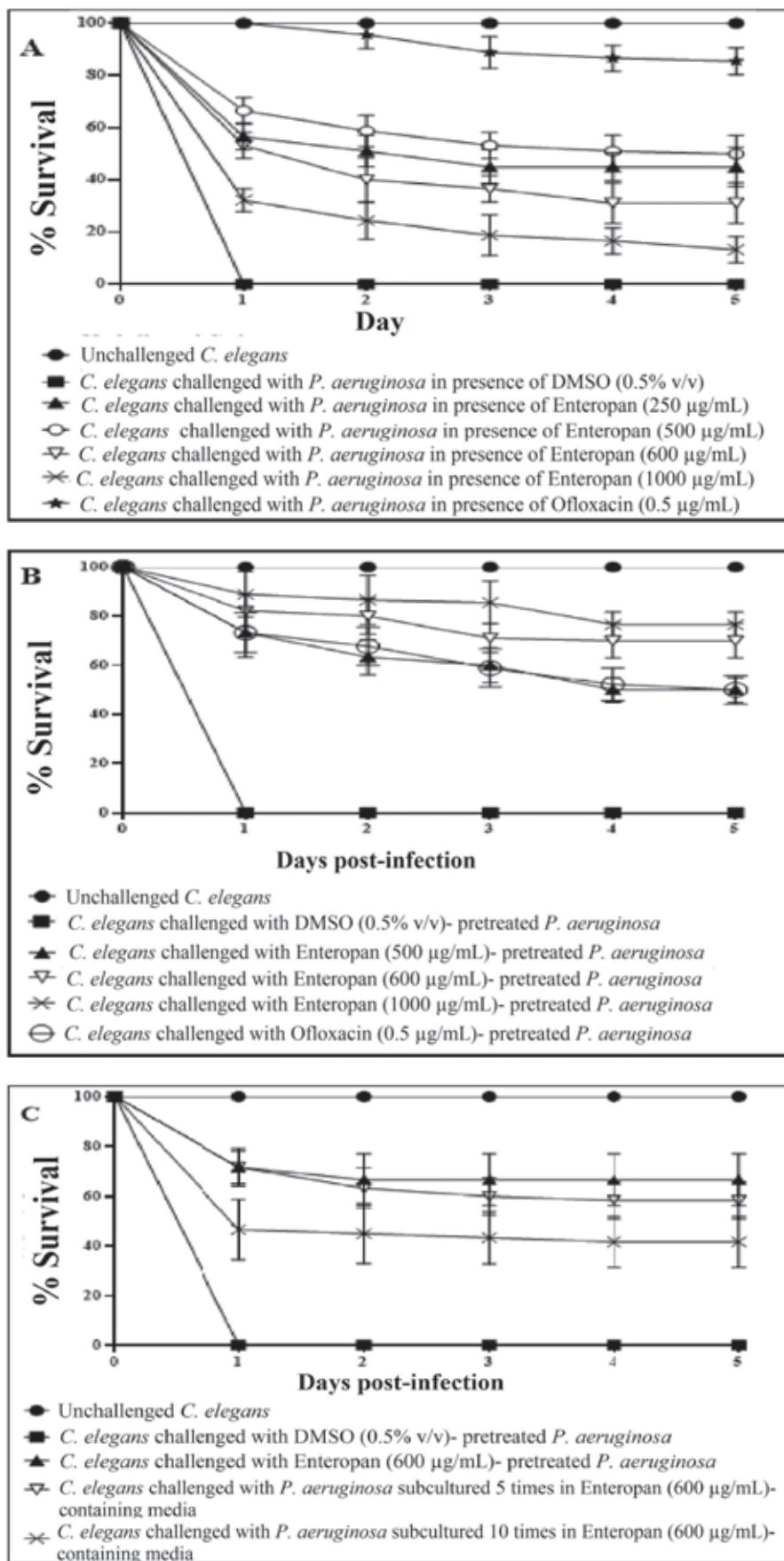


**FIGURE 1** - Enteropan attenuates *Pseudomonas aeruginosa*'s virulence towards the model host *Caenorhabditis elegans*. Dimethylsulfoxide (DMSO) present in the 'vehicle control' at 0.5% v/v did not affect bacterial virulence. Neither DMSO nor Enteropan showed any toxicity towards the worm population at tested concentrations. To avoid overcrowding in the figures (A, B), we have not shown lines corresponding to concentrations which had no effect on bacterial virulence, and also that for 750 µg/mL, as its virulence-attenuating effect was statistically a part of that of 600 µg/mL. Supplementary videos pertaining to these experiments are available at: [osf.io/fnywk](https://osf.io/fnywk). All the % values reported in this figure legend are statistically significant at  $p < 0.001$ .

**A)** *P. aeruginosa*'s virulence towards the host worm gets attenuated in the presence of Enteropan. Enteropan conferred a survival benefit on host *C. elegans* at concentrations of 250, 500, 600, 750, and 1,000 µg/mL with survival rates of  $45\% \pm 5.47$ ,  $50\% \pm 7.07$ ,  $31.11\% \pm 7.8$ ,  $35\% \pm 8.36$ , and  $13.33\% \pm 5$ , respectively. Ofloxacin (0.5 µg/mL) was employed as a positive control and conferred  $85.55\% \pm 5.27$  survival benefit on host worm. Progenies (TNTC – too numerous to count) were observed on the third day in experimental wells and positive control. See supplementary videos A-E. **B)** Enteropan pre-treatment reduced bacterial virulence towards *C. elegans*. Pre-treatment of bacteria with Enteropan at concentrations of 500, 600, 750, and 1000 µg/mL reduced its virulence towards host worm by  $50\% \pm 5$ ,  $70\% \pm 7.07$ ,  $78.88\% \pm 6$ , and  $76.66\% \pm 5$ , respectively, as per the fifth day end-point. Ofloxacin (0.5 µg/mL) pre-treatment reduced bacterial virulence towards the host worm by  $50\% \pm 5.77$ . Progenies were observed on the third day in experimental wells corresponding to  $\geq 500$  µg/mL Enteropan as well as positive control. See supplementary videos F-I. **C)** *P. aeruginosa* did not develop complete resistance even after repeated exposure to Enteropan. *P. aeruginosa* obtained after fifth and tenth subculturing in Enteropan (600 µg/mL)-containing media displayed  $58.33\% \pm 4.04$  and  $43.33\% \pm 10.3$  lesser virulence, respectively, than extract-non-exposed pathogen.



were allowed to attack *C. elegans* in M9 buffer (containing no Enteropan). No resistance seemed to have evolved in *P. aeruginosa* till fifth subculturing; however, 10 subculturings in Enteropan-supplemented media seemed to allow the pathogen to overcome this formulation's anti-virulence effect marginally (23.3%; Fig. 1C). This inability of the pathogen to develop complete resistance against Enteropan might be attributable to the polyherbal nature of the formulation. As the polyherbal formulations can have multiple bioactive compounds in them, they may exert a multiplicity of targets against the susceptible pathogen. To develop resistance in this scenario, the pathogen would be required to develop multiple simultaneous mutations, and that is a quite less probable event biologically as well statistically.

#### *Enteropan offered prophylactic protection to C. elegans*

To investigate whether Enteropan pre-feeding can offer any prophylactic benefit to worm population in the face of subsequent pathogen challenge, we allowed *P. aeruginosa* to attack worms pre-fed with Enteropan (5-1,000  $\mu\text{g/mL}$ ). Enteropan at  $\geq 50$   $\mu\text{g/mL}$  did confer prophylactic benefit on worm population. While concentrations till 500  $\mu\text{g/mL}$  supported worm survival (13%-26%) till 48 hours post-pathogen challenge (Fig. 2A), higher concentrations supported worm survival (20%-23%) till the fifth day (Fig. 2B; Supplementary videos: J-M). Considering the first-day end-point (i.e. by the time the pathogen killed 100% worms in control wells), certain Enteropan concentrations (500-750  $\mu\text{g/mL}$ ) performed at par to the positive control ofloxacin.

#### *Enteropan is effective as a post-infection therapy*

To investigate whether Enteropan is effective as a post-infection therapy, we added Enteropan (50-1,000  $\mu\text{g/mL}$ ) after 3 or 6 hours of mixing bacteria with the worms. While Enteropan addition post 6 hours of bacterial attack on worms could not rescue the host (Fig. S1), its addition post 3 hours of bacterial attack could rescue 10%-27% of the worms (Fig. 2C; Supplementary videos: N-R). As a post-infection therapy, Enteropan's performance did not improve with increase in concentration.

To have a mechanistic insight into the Enteropan-*P. aeruginosa* interaction, we checked the effect of Enteropan on various virulence traits of this pathogen *in vitro*, and also compared the gene expression profile of the Enteropan-treated *P. aeruginosa* with that of extract-non-exposed control at the whole transcriptome level.

#### ***In vitro experiments***

##### *Enteropan forced overproduction of QS-regulated pigments without affecting the bacterial growth heavily*

Enteropan till 100  $\mu\text{g/mL}$  had no effect on *P. aeruginosa* growth. Though from 250  $\mu\text{g/mL}$  onwards it had some growth inhibitory effect, the magnitude of this inhibitory effect did not increase much with increase in concentration (Fig. 3A). Except 5  $\mu\text{g/mL}$ , Enteropan at all tested concentrations enhanced production of QS-regulated pigments (pyoverdine and pyocyanin).

Hence concentrations of 25-100  $\mu\text{g/mL}$  can be said to have pure quorum-modulatory effect on *P. aeruginosa*. Though in general Enteropan's effect on pigment production seemed to be dose-dependent, bacterium's response at 600  $\mu\text{g/mL}$  seemed to deviate from this pattern in case of both the pigments.

##### *Enteropan had a moderately negative effect on pre-formed biofilm*

Though Enteropan's presence could not compromise *P. aeruginosa*'s ability to form biofilm, when Enteropan was added onto the pre-formed biofilm, it could eradicate the biofilm partly and also reduced the metabolic activity within the biofilm (Fig. 3B).

##### *Enteropan disturbed nitrogen metabolism in P. aeruginosa*

Since multiple genes associated with detoxification of reactive nitrogen species were upregulated (transcriptome data described later), we hypothesized that Enteropan-treated *P. aeruginosa*'s ability to overcome nitrosative stress is compromised. To check this hypothesis, we quantified nitrite concentration in extract-treated *P. aeruginosa* culture supernatant, wherein it was found to have 47.10% higher nitrite concentration as compared to control (Fig. 3C). This higher accumulation of nitrite can be taken as an indication of compromised denitrification efficiency, since nitrite is an important intermediate in denitrification pathway ahead of the toxic nitric oxide (43). Nitrosative stress can impact the overall bacterial fitness negatively in multiple ways (44). Reactive nitrogen species can damage biomolecules like DNA, lipids, and proteins. Resistance to nitrosative stresses is of crucial importance towards the survival of bacteria in the environment as well as inside the host. In gram-negative bacteria, several mechanisms protecting against oxidative and nitrosative stresses are present in the envelope. Excessive nitrosative stress can disturb the envelope homeostasis, and this in fact is reflected in the transcriptome of Enteropan-exposed *P. aeruginosa*, wherein 32 cell envelope (cell wall and lipopolysaccharide, LPS)-associated genes are expressed differently.

##### *Enteropan-modulated P. aeruginosa's susceptibility to imipenem and augmentin*

When Enteropan-pre-treated *P. aeruginosa* cells were subsequently challenged with different antibiotics in a disc diffusion assay, these cells exhibited marginal increase in their susceptibility to imipenem; however, their susceptibility to augmentin disappeared following Enteropan pre-treatment (Tab. S5; Fig. 3D, E). This effect of Enteropan pre-treatment on imipenem susceptibility was also confirmed in liquid culture, wherein Enteropan-pre-treated cells were observed to exhibit up to 21.43% higher susceptibility to imipenem (Fig. 3F). Imipenem belongs to the carbapenem class of beta-lactams (45), and carbapenem resistance among *P. aeruginosa* isolates are being viewed as a serious problem (46). Since this class of antibiotics are looked as a last resort for treatment of MDR *P. aeruginosa* (47), resistance modifiers capable of making this bacterium more susceptible to them can be of help in extending the lifespan of these antibiotics



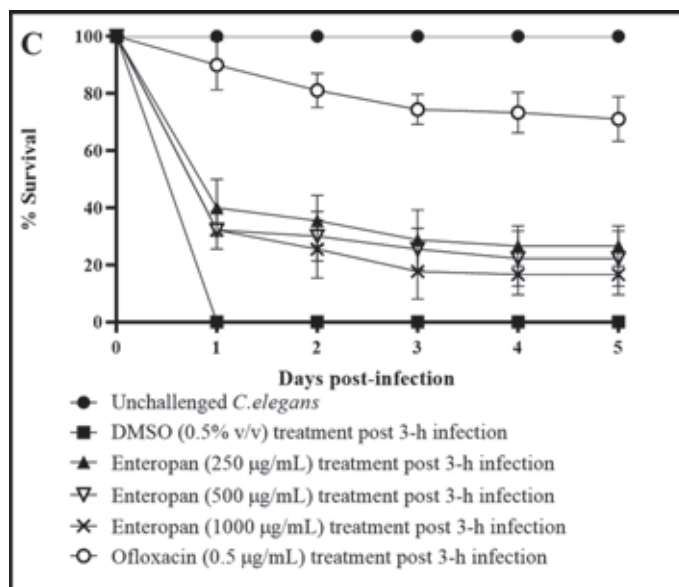
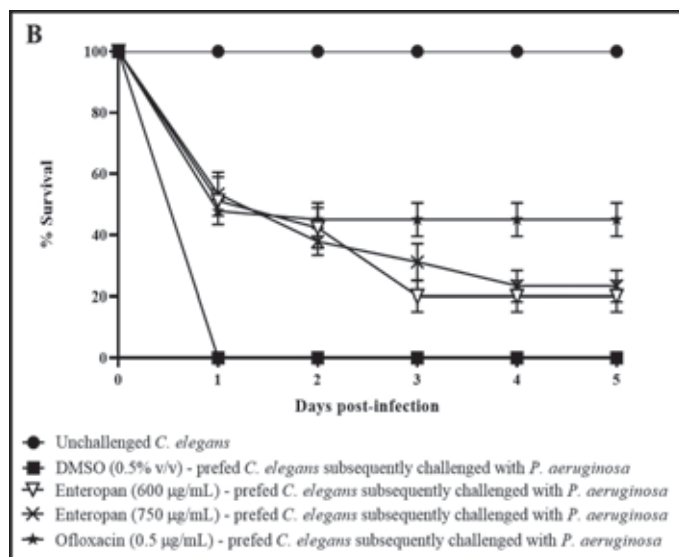
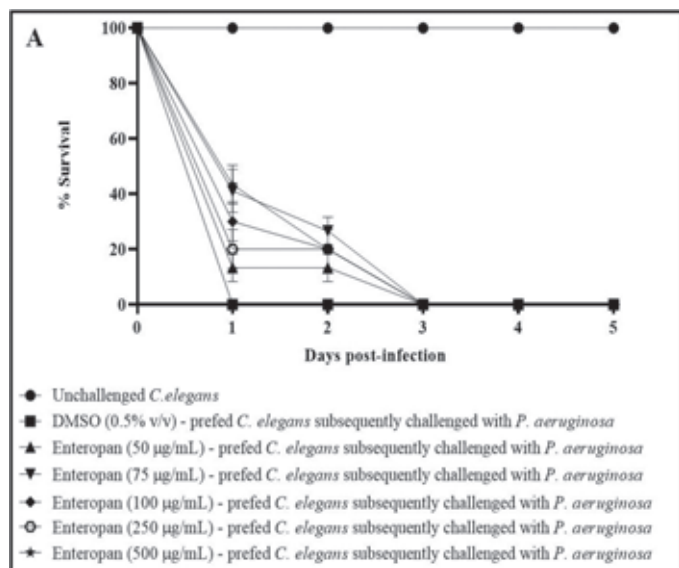


**FIGURE 2** - Prophylactic and post-infection therapeutic potential of Enteropan. All the % values reported in this figure legend are statistically significant at  $p < 0.001$ . **A-B)** Enteropan offered prophylactic protection to the worm population against subsequent bacterial challenge. Worms pre-fed with Enteropan concentrations of 50, 75, 100, 250, and 500  $\mu\text{g}/\text{mL}$  registered 13.3%  $\pm$  5, 26.6%  $\pm$  5, 20%  $\pm$  8.66, 17%  $\pm$  6.66, and 20%  $\pm$  8.66 better survival, respectively, till the second day in the face of subsequent pathogen challenge. Worms pre-fed with higher concentrations of Enteropan at 600, 750, and 1000  $\mu\text{g}/\text{mL}$  registered 51.11%  $\pm$  7.8, 53.33%  $\pm$  7.07, and 43.33%  $\pm$  8.66 survival, respectively, till the end of first day of pathogen challenge. Magnitude of the prophylactic benefit as per fifth day point was 20%  $\pm$  5, 23.33%  $\pm$  5, and 20%  $\pm$  7.07, respectively. Pre-feeding the worms with dimethylsulfoxide (DMSO, 0.5% v/v) did not alter their susceptibility to subsequent bacterial challenge. Ofloxacin (0.5  $\mu\text{g}/\text{mL}$ ) employed as a positive control conferred 44.9%  $\pm$  5.49 prophylactic benefit on the host worms. See supplementary videos J-M. **C)** Enteropan could partially rescue worm population when used as a post-infection therapy. When pre-infected worms were exposed to Enteropan at 250, 500, 600, 750, and 1000  $\mu\text{g}/\text{mL}$ , they scored 26.66%  $\pm$  7.0, 22.22%  $\pm$  9.71, 11.1%  $\pm$  3.33, 13.3%  $\pm$  6, and 16.66%  $\pm$  7.07 better survival, respectively, than control worms. Ofloxacin (0.5  $\mu\text{g}/\text{mL}$ ) employed as positive control, 3 hours post-infection, rescued 71.11%  $\pm$  7.81 worms. DMSO (0.5% v/v) did not confer any survival benefit when added post-infection. See supplementary videos N-R.



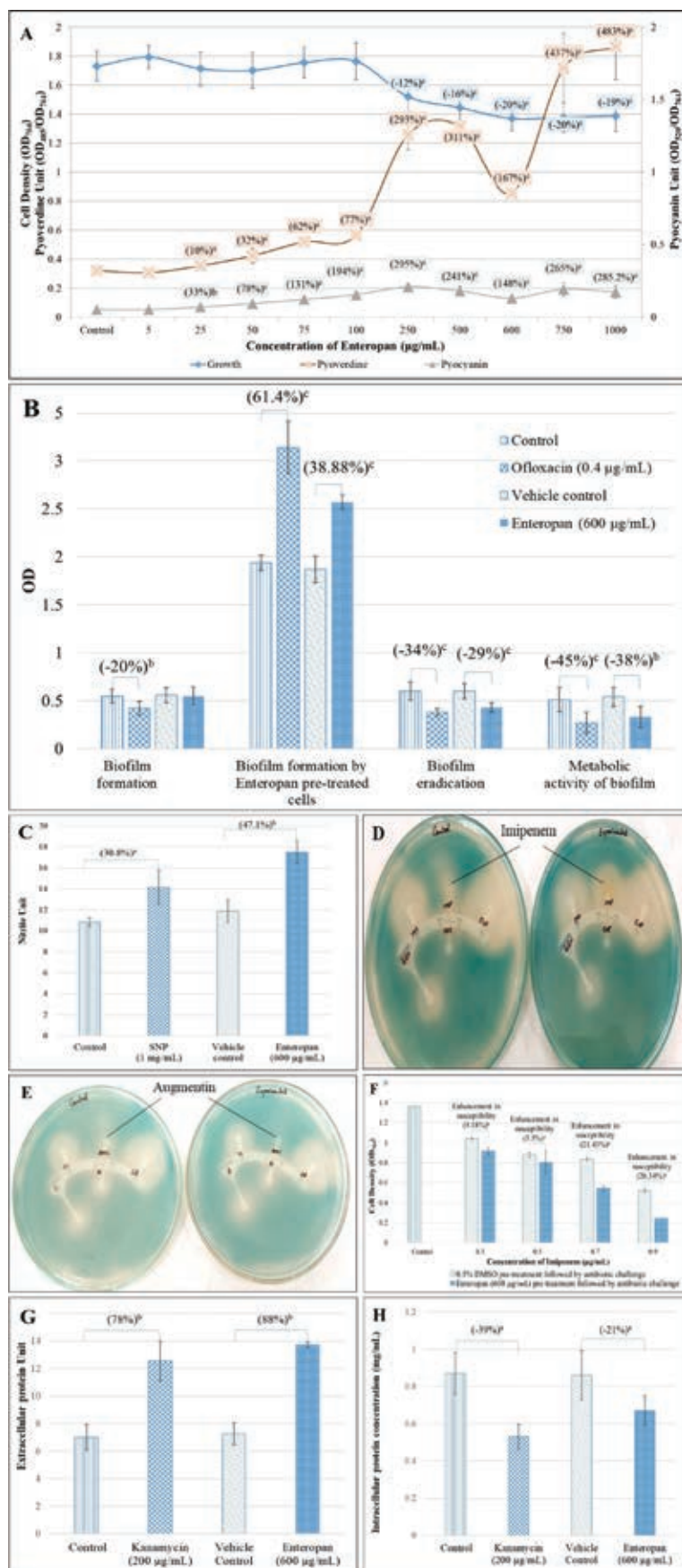


**FIGURE 3** - Enteropan's effect on various phenotypic traits of *Pseudomonas aeruginosa* revealed through different *in vitro* assays. **A)** Enteropan enhances production of quorum-regulated pigments in *P. aeruginosa*, while exhibiting a mild growth inhibitory effect. Bacterial growth was measured as OD<sub>764</sub>. Pyoverdine Unit and Pyocyanin Unit were calculated as the ratio OD<sub>405</sub>/OD<sub>764</sub> and OD<sub>520</sub>/OD<sub>764</sub> (an indication of pyoverdine and pyocyanin production per unit of growth), respectively; 'Control' shown in this figure is the vehicle control (0.5% v/v dimethylsulfoxide (DMSO)), which affected neither growth nor pigment production. Ofloxacin (0.5 µg/mL) inhibited growth by 65.6% ±5.32, while inhibiting pigment production completely. **B)** Enteropan's effect on *P. aeruginosa*'s biofilm formation capability and on pre-formed biofilm. While *P. aeruginosa*'s biofilm formation ability remained unaffected in the presence of Enteropan, Enteropan-pre-exposed cells subsequently allowed to form biofilm on glass surface accumulated higher biomass. Enteropan when added onto pre-formed biofilm could eradicate the biofilm partially, and also reduced the biofilm metabolic activity notably. DMSO (0.5% v/v) used as vehicle control did not affect biofilm of the *P. aeruginosa* in any of these four assays. **C)** *P. aeruginosa* culture accumulated higher extracellular nitrite in the presence of Enteropan. While nitrite concentration in vehicle control (*P. aeruginosa* supplemented with 0.5% v/v DMSO) was at par to that without DMSO, Enteropan caused nitrite concentration in *P. aeruginosa* culture supernatant to rise. Sodium nitroprusside used as positive control caused 30.8% higher nitrite build-up in *P. aeruginosa* culture. Nitrite Unit (i.e. Nitrite concentration:cell density ratio was calculated to nullify any effect of cell density on nitrite production). **D, E)** Enteropan-pretreated cells responded to certain antibiotics differently. Enteropan-pre-exposed *P. aeruginosa* experienced an increased or decreased susceptibility to imipenem and augmentin, respectively, as revealed in disc diffusion assay. **F)** Enteropan pre-treatment enhanced *P. aeruginosa*'s susceptibility to imipenem, as revealed in the broth dilution assay. **G)** Increased extracellular protein content in *P. aeruginosa* culture grown in the presence of Enteropan. Protein Unit was calculated as ratio of OD<sub>750</sub>/OD<sub>764</sub> (an indication of protein production per unit of growth). **H)** Reduced intracellular protein content in *P. aeruginosa* grown in the presence of Enteropan. Protein content reported in mg/mL are cell density neutralized values, wherein OD<sub>764</sub> was adjusted to 1.00 prior to cell lysis. Kanamycin employed as a positive control at its sub-minimum inhibitory concentration level also generated response similar to that of Enteropan from bacterial culture with respect to extracellular and intracellular protein content. DMSO (0.5% v/v) used as 'vehicle control' affected neither extracellular nor intracellular protein content. <sup>a</sup>p ≤ 0.05, <sup>b</sup>p ≤ 0.01, <sup>c</sup>p ≤ 0.001.

by allowing their use at lower doses. However as seen with augmentin in this study, the effect of herbals on antibiotic susceptibility of pathogen may not always be favourable.

#### *Enteropan alters protein synthesis and secretion in P. aeruginosa*

Extracellular protein concentration (after nullifying cell density) in *P. aeruginosa* culture supernatant in the presence of Enteropan was found to be 1.89-fold higher than that in the absence of Enteropan (Fig. 3G). Cell density-neutralized intracellular protein concentration of *P. aeruginosa* cells grown in the presence of Enteropan was found to be 1.40-fold lower than cells grown in the absence of Enteropan (Fig. 3H). It seems that Enteropan exerted an inhibitory effect on protein synthesis in *P. aeruginosa* and promoted protein export. This might have caused even some of the essential proteins to leave the cell. The increased export of proteins by Enteropan-treated cells may be assumed to have originated from overexpression of efflux pump/transport machinery (as suggested by the transcriptome data too described later) and a compromised cell envelope integrity suggested by differential expression of 32 genes involved in cell wall or LPS synthesis. Kanamycin, a known inhibitor of protein synthesis in bacteria, was employed as a positive control in this assay. Kanamycin belongs to the aminoglycoside group of antibiotics, which at sub-minimum inhibitory concentration (MIC) level caused *P. aeruginosa* culture supernatants to have 1.79-fold higher extracellular protein. Such increase in extracellular protein concentration in *P. aeruginosa* exposed to sub-MIC level of kanamycin was also reported by Takahashi et al (48).

#### *Enteropan treatment causes large-scale differential gene expression in P. aeruginosa*

A whole transcriptome level comparison of the gene expression profile of Enteropan (600 µg/mL)-treated *P. aeruginosa* with that of control revealed a total of 952

genes getting expressed differentially (log fold change  $\geq 2$  and FDR  $\leq 0.001$ ). This amounted to differential expression of 17% of genome, wherein 616 genes were upregulated (Tab. S6) and 336 were downregulated (Tab. S9). Corresponding volcano plot (Fig. S3) is given in supplementary file. A function-wise categorization of all the DEG is presented in Figure 4. While all DEG pertaining to cell division were downregulated (and majority of DEG pertaining to translation too), the majority of DEG associated with efflux pump/transport were upregulated. Overexpression of efflux machinery is known to compromise bacterial fitness by causing physiological dysregulation (49). Owing to the important physiological roles of efflux pumps in various functions such as intercellular communication, bacterial pathogenicity and virulence, and biofilm formation, expression of majority of them is subject to tight control by different transcriptional regulators. Any mischief with this regulation leading to overexpression of the efflux function may result in leaking of even essential items. An empirical look at the list of DEG suggested that Enteropan attenuated virulence of *P. aeruginosa* by causing dysregulation of metal homeostasis, nitrogen metabolism, transcription, amino acid and protein synthesis, carbon metabolism, motility, efflux, etc. Results of various *in vitro* assays presented in the preceding section corroborates well with the transcriptome data.

#### *Network analysis of DEG in Enteropan-exposed P. aeruginosa*

We created PPI network for up- and downregulated genes separately. PPI network for upregulated genes generated through STRING is presented in Figure 5A, which shows 610 nodes connected through 2,272 edges with an average node degree of 7.45. Since the number of edges in this PPI network is 2.06-fold higher than expected (1,101) with a PPI enrichment p-value  $< 1.0e-16$ , this network can be said to possess

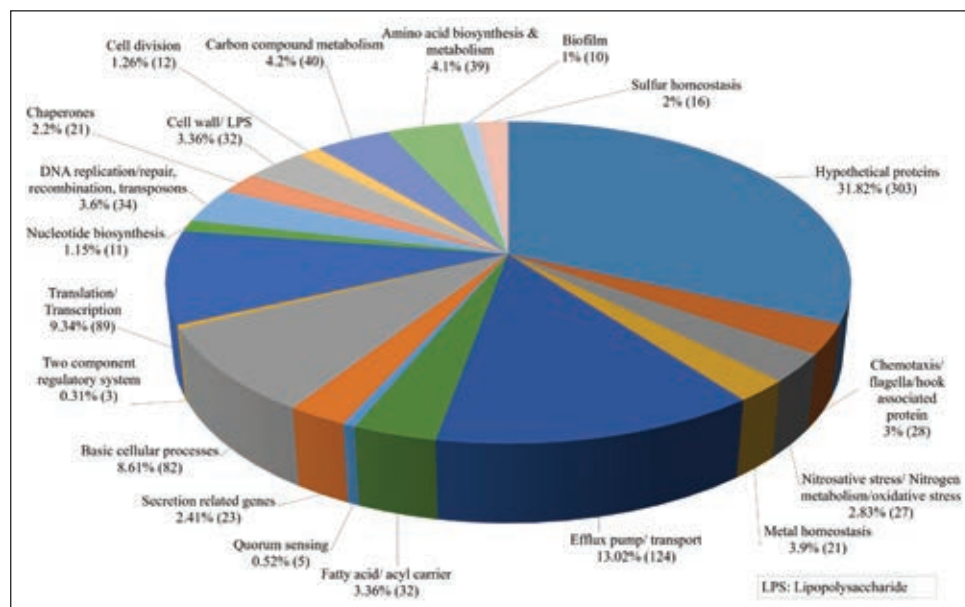


**FIGURE 4** - Function-wise categorization of the differentially expressed genes (DEG) in Enteropan-treated *Pseudomonas aeruginosa*. Percent values reported are calculated considering the total number of differently expressed genes as 100%. Values in parenthesis are number of DEG belonging to that particular category.

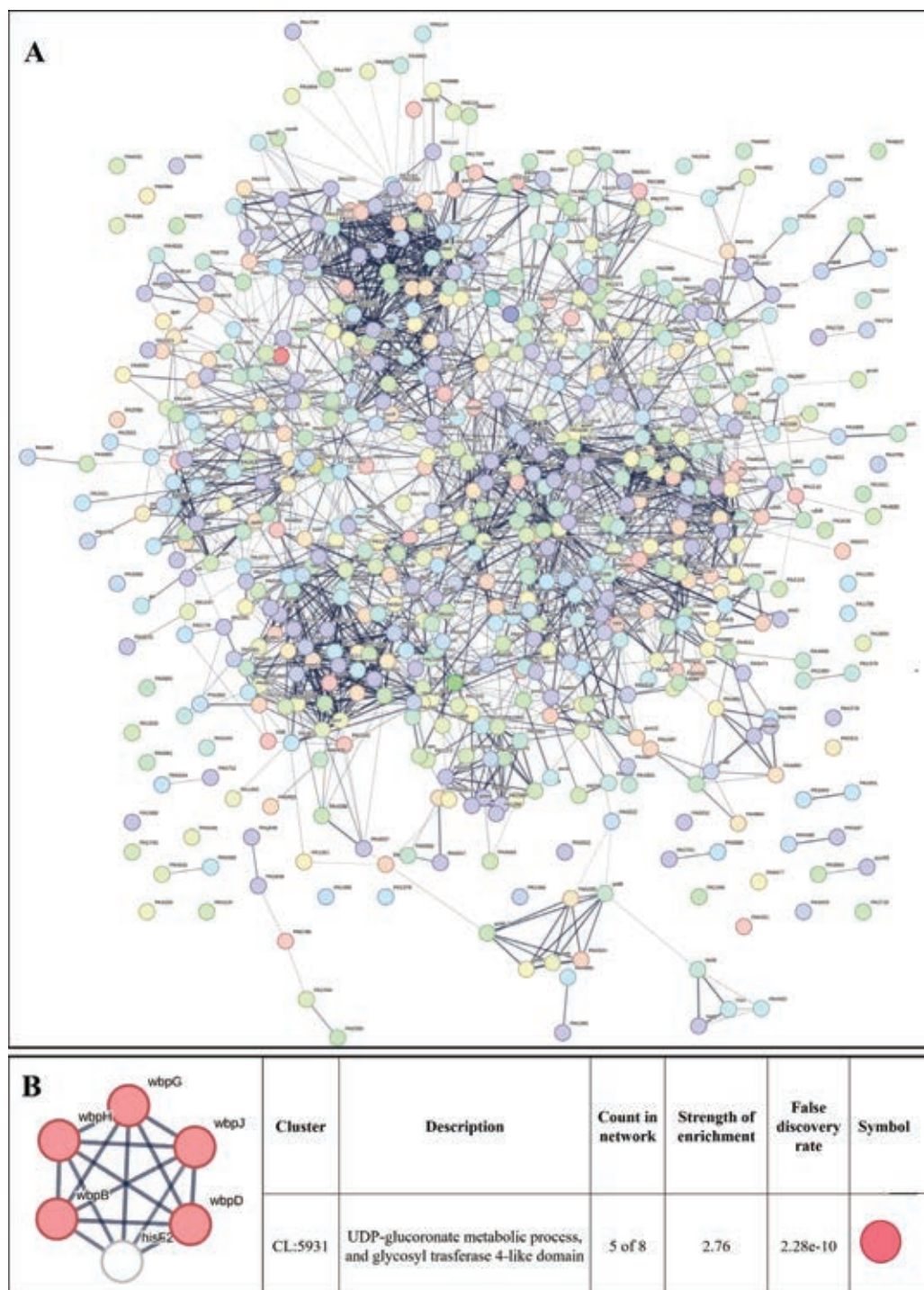


**FIGURE 5 - A)** Protein-Protein Interaction (PPI) network of upregulated genes in Enteropan-exposed *Pseudomonas aeruginosa*. Edges represent protein-protein associations that are meant to be specific and meaningful, that is, proteins jointly contribute to a shared function. This does not necessarily mean they are physically binding to each other. Network nodes represent all the proteins produced by a single, protein-coding gene locus. **B)** PPI network of top-ranked genes revealed through cytoHubba among upregulated differentially expressed genes (DEG) in Enteropan-exposed *P. aeruginosa*.

significantly more interactions among the member proteins than what can be expected for a random set of proteins of the identical sample size and degree distribution. Such enrichment can be taken as an indication of the member proteins being at least partially biologically connected. When we arranged all the upregulated DEGs in decreasing order of node degree, 572 nodes were found to have a non-zero score (Tab. S7), and we selected top 52 genes with a node

degree  $\geq 19$  for further ranking by different cytoHubba methods. Then we looked for genes which appeared among top-6 ranked candidates by  $\geq 6$  cytoHubba methods (Tab. S8), and six such genes were further checked for interactions among themselves by cluster analysis (Fig. 5B), whose overexpression can be hypothesized to disturb pathogen physiology. Interaction map of these six potential hubs showed them to be strongly networked as the average node degree score

was 5. This network possessed 15 edges as against expected (zero) for any such random set of proteins. The PPI network showed five of these six potential hubs to be part of a single local network cluster (Fig. 5B). Co-occurrence analysis showed all of these six hubs being absent from humans (Tab. 3) and

hence agonists of these hubs may be expected to target pathogen selectively without interfering with host system functioning.

PPI network for downregulated genes is presented in Figure 6A, which shows 327 nodes connected through 3,206

**TABLE 3** - Co-occurrence analysis of genes coding for potential targets in *P. aeruginosa*

Organism	Potential hubs up-regulated in <i>P. aeruginosa</i>						Potential hubs down-regulated in <i>P. aeruginosa</i>									
	hisF2	wbpG	wbpD	wbpJ	wbpH	wbpB	rpsL	rpIE	rpsD	rpsJ	rpIF	rpoA	rpsB	rpN	rpL	rpIF
<i>Pseudomonas aeruginosa</i>	■	■	■	■	■	■	■	■	■	■	■	■	■	■	■	■
<i>Homo sapiens</i>							■	■	■	■	■	■	■	■	■	■
<i>Acinetobacter baumannii</i>	■		■	■	■		■	■	■	■	■	■	■	■	■	■
<i>Enterobacteriaceae</i>	■		■	■	■	■	■	■	■	■	■	■	■	■	■	■
<i>Salmonella Serotype typhi</i>	■		■	■	■		■	■	■	■	■	■	■	■	■	■
<i>Shigella Spp.</i>	■		■	■	■		■	■	■	■	■	■	■	■	■	■
<i>Mycobacterium tuberculosis</i>	■		■	■	■		■	■	■	■	■	■	■	■	■	■

The color of the squares denotes, for each gene of interest, the degree of similarity of its best hit in a given STRING genome.

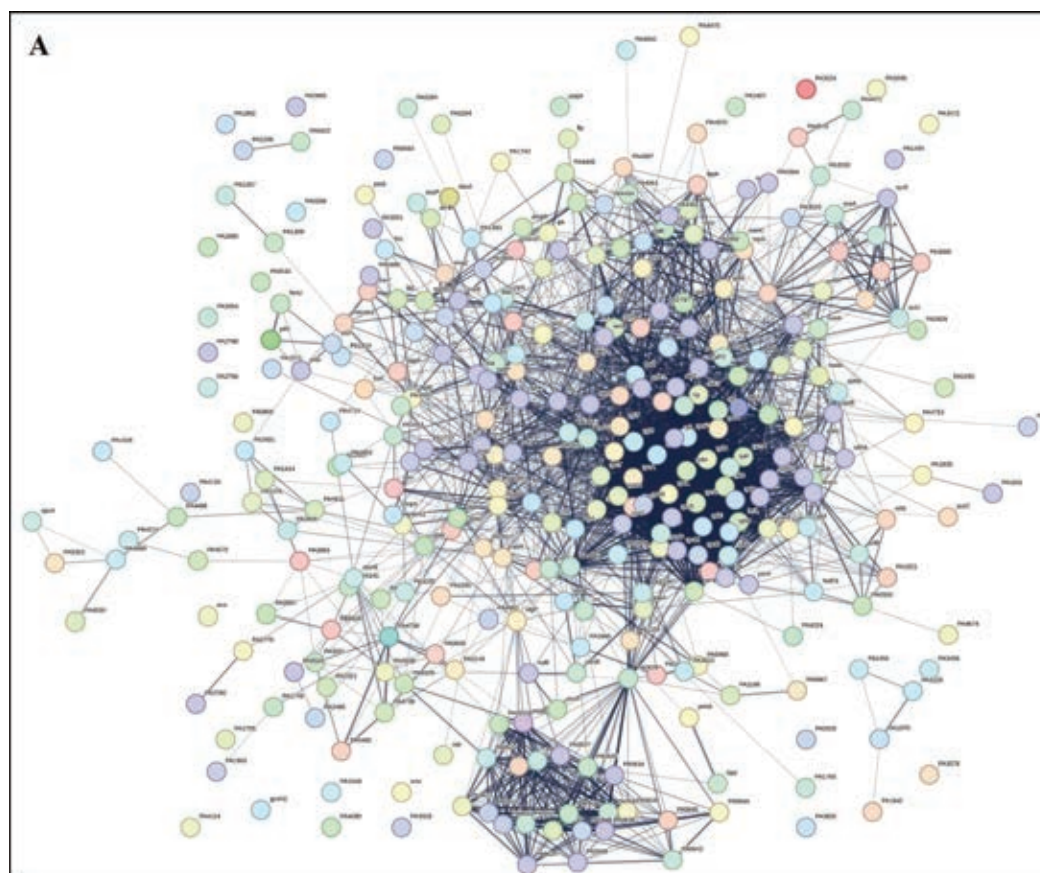


**FIGURE 6 - A)** Protein-Protein Interaction (PPI) network of downregulated genes in Enteropan-exposed *Pseudomonas aeruginosa*. **B)** PPI network of top-ranked genes revealed through cytoHubba among downregulated differentially expressed genes (DEG) in Enteropan-exposed *P. aeruginosa*.

Cluster	Description	Count in network	Strength of enrichment	False discovery rate	Symbol
CL:150	Small ribosomal subunit	2 of 7	2.2	0.0072	●
CL:96	rRNA-binding	4 of 15	2.17	1.65e-06	●
CL:93	Cytosolic large ribosomal subunit and small ribosomal subunit	6 of 25	2.13	3.22e-10	●
CL:149	Small ribosomal subunit and zinc-binding ribosomal protein	3 of 13	2.11	0.00018	●
CL:90	Ribosomal subunit	9 of 49	2.01	1.39e-15	●
CL:84	Ribosome	10 of 60	1.97	6.58e-17	●



edges with an average node degree of 19.6. Since the number of edges in this PPI network is 1.93-fold higher than expected (1,658) with a PPI enrichment p-value  $<1.0e-16$ , this network can be said to possess significantly more interactions among the member proteins that what can be expected for a random set of proteins of the identical sample size and degree distribution. Such enrichment can be taken as an indication of the member proteins being at least partially biologically connected. When we arranged all the downregulated DEGs in decreasing order of node degree, 298 nodes were found to have a non-zero score, and we selected top 50 genes with a node degree  $\geq 53$  (Tab. S10) for further ranking by different cytoHubba methods. Then we looked for genes which appear among top-10 ranked candidates by  $\geq 6$  cytoHubba methods, and 10 such genes (Tab. S11) were identified as potential hubs, whose downregulation can be hypothesized to attenuate *P. aeruginosa* virulence. Interaction map of these 10 potential hubs (Fig. 6B) showed them to be strongly networked as the average node degree score was 9. This network possessed 45 edges as against expected (15) for any such random set of proteins. The PPI network showed these 10 genes to be distributed among six different local network clusters, whose strength score ranged from 1.97 to 2.2 (Fig. 6B). Co-occurrence analysis (Tab. 3) of these 10 hub proteins indicated four (*rpsD*, *rpsJ*, *rpoA*, *rplF*) of them to be absent from humans, and hence they can be said to possess high targetability with respect to discovery of new antibiotics satisfying the criteria of selective toxicity. Since all the 10 predicted hubs are indicated by co-occurrence analysis to be present in other important bacterial pathogens too, antagonists of these proteins are likely to be useful as broad-spectrum antibiotics.

### Target validation through RT-PCR

From the 10 identified hubs among the downregulated genes, we selected five (*rpoA*, *tig*, *rpsB*, *rpsL*, *rpsJ*) for further validation through RT-PCR. From the 10 genes shown in Figure 6B, four (*rpoA*, *rpsB*, *rpsL*, *rpsJ*) passing the dual criteria of node degree  $\geq 70$  (Tab. S10) and been part of  $\geq 3$  clusters were selected for RT-PCR. Though *rpsD* (node degree 70) also passed these dual criteria, since already three *rps* genes were selected for PCR, we preferred *rpoA* (node degree 75) over it. Additionally, we included one gene (*tig*; 3.73-fold $\downarrow$ ; node degree 70) for PCR validation, though it was not among the identified hubs, because *tig* is a trigger factor involved in protein export, and we did observe a heavy increase in extracellular protein content in Enteropan-exposed *P. aeruginosa*. PCR did confirm downregulation of all the selected five genes in Enteropan-exposed *P. aeruginosa* (Fig. 7), and thus they can be considered as potential antibacterial targets worthy of attention by drug discovery programmes.

### Conclusion

The polyherbal formulation Enteropan was found to have virulence-attenuating effect against an important gram-negative bacterial pathogen *P. aeruginosa*, without affecting

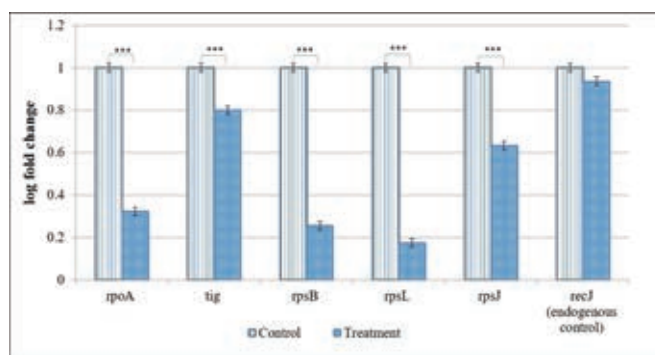


**FIGURE 7** - Confirmation of differential expression of selected genes in Enteropan-treated *Pseudomonas aeruginosa* through real-time polymerase chain reaction (RT-PCR). *recJ* selected as an endogenous control was not expressed differently (false discovery rate 1) between control and experimental bacterial cultures. \*\*\* $p \leq 0.001$ .

its growth heavily. As can be expected from any multicomponent polyherbal formulation, Enteropan also exerted multiplicity of targets against the test pathogen. A large fraction of the bacterial genome was expressed differently under influence of this anti-pathogenic formulation, which corroborated well with the altered phenotypic traits in extract-exposed bacterial culture. Major mechanisms revealed various *in vitro/in vivo* assays and transcriptome analysis through which Enteropan exerted its anti-virulence activity were found to be generating nitrosative stress, oxidative stress, quorum modulation, disturbance of protein homeostasis, and metal homeostasis. A wholistic summary depicting the mechanistic details associated with the anti-pathogenic potential of Enteropan against *P. aeruginosa* is presented in Figure 8, with particular attention on Enteropan's effect on QS machinery and virulence regulators of this notorious pathogen. Our results validate the anti-pathogenic potential of Enteropan, and also the concept of polyherbalism and its relevance in combating antimicrobial resistance.

### Acknowledgements

The authors thank Nirma Education and Research Foundation (NERF), Ahmedabad, for infrastructural support; Virupakshi Soppina (IIT-Gn) for providing worms. SP and GG acknowledge fellowship from Gujarat government under their SHODH scheme. NT acknowledges fellowship from Nirma University.

### Disclosures

**Conflict of interest:** HSP, is involved in manufacturing and marketing of the formulation Enteropan<sup>®</sup>; however, that in no way has affected the design of experiments or interpretation of results. Other authors declare no competing interest.

**Financial support:** This study did not receive any extramural financial support.

**Data availability statement:** All the relevant data has been included in the main manuscript and supplementary files.



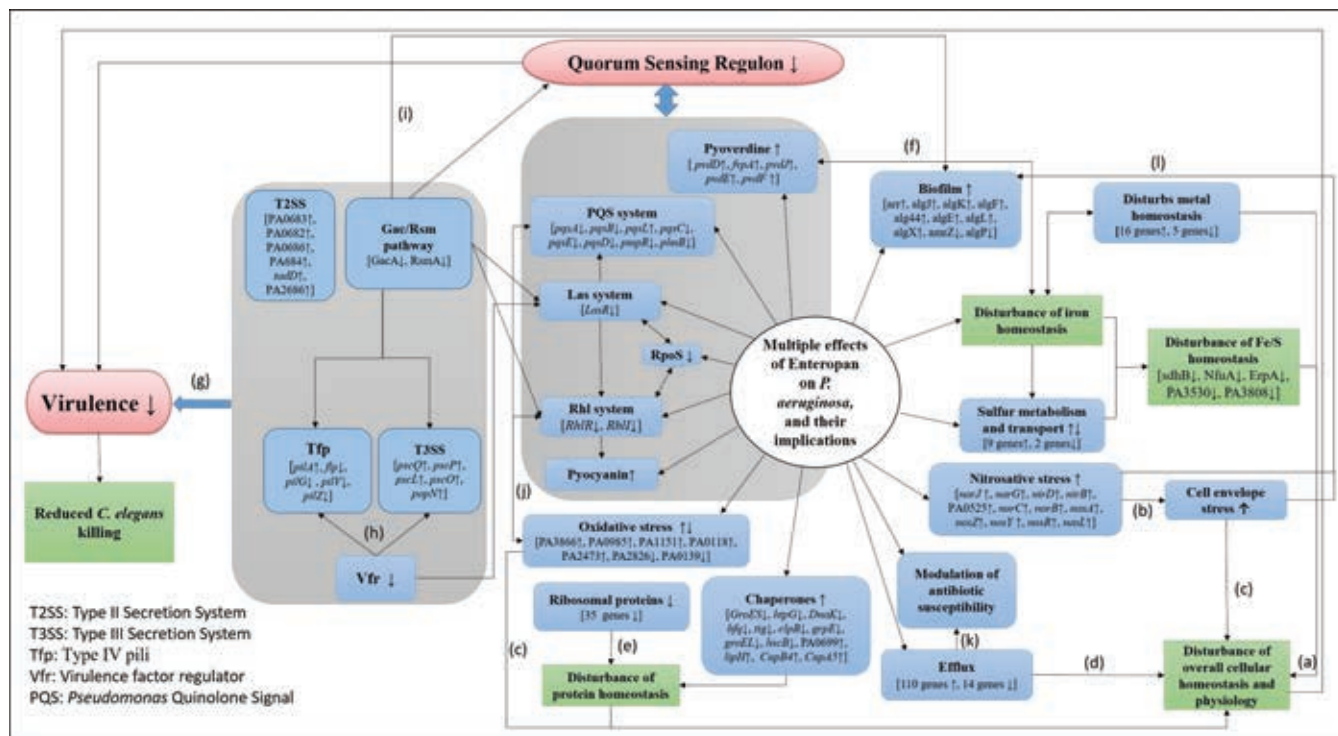


**FIGURE 8** - Large-scale disturbance of transcriptional regulation in *Pseudomonas aeruginosa* caused by Enteropan compromises its overall cellular homeostasis and virulence. This figure presents a wholistic summary of multiple effects exerted by Enteropan against *P. aeruginosa*. Various cellular, physiological, and virulence-associated traits of *P. aeruginosa* expressed differently under the influence of Enteropan are depicted. The genes shown with an up or down arrow are those getting differentially expressed with a log fold change of  $\geq 1.5$  and false discovery rate (FDR)  $\leq 0.05$ . The *Gac/Rsm pathway* inversely regulates the expression of virulence factors (*T3SS*, *Tfp*, exopolysaccharides) associated with acute and chronic disease (50). *T2SS* is responsible for secreting many secretory proteins like alkaline phosphatase, lipase, exotoxin A, phospholipase, and proteases. *T3SS* is largely involved in secretion of virulence determinants associated with acute infection. *Vfr* is a global regulator of virulence gene expression, which allows coordinated production of related virulence functions (*Tfp*, *T3SS*) necessary for adherence to an intoxication of host cells. *LasR* is a transcriptional activator of multiple virulence-associated genes in *P. aeruginosa*. It represents a central checkpoint, with the highest degree of interconnection in the network. *RpoS*, the stationary phase sigma factor, influences the expression of more than one-third of all the quorum-regulated genes. It is a central regulator of many stationary phase-inducible genes and a master stress-response regulator under a variety of stress conditions (51). *Tfp*, a major surface adhesin, mechanistically regulates virulence factors in *P. aeruginosa* (52). The *Rhl* system is a quorum sensing system acquired by *P. aeruginosa* through lateral gene transfer. *PQS* is an essential mediator of the shaping of the population structure of *P. aeruginosa* and of its response to and survival in stress conditions. <sup>a</sup>(53); <sup>b</sup>(44); <sup>c</sup>(54); <sup>d</sup>(55); <sup>e</sup>(56); <sup>f</sup>(57); <sup>g</sup>(58); <sup>h</sup>(59); <sup>i</sup>(60), <sup>j</sup>(61, 62), <sup>k</sup>(63); <sup>l</sup>(64).

**References**

1. Kunz Coyne AJ, El Ghali A, Holger D, Rebold N, Rybak MJ. Therapeutic strategies for emerging multidrug-resistant *Pseudomonas aeruginosa*. Infect Dis Ther. 2022;11(2):661-682. [CrossRef PubMed](#)
2. Craig M. CDC’s Antibiotic Resistance Threats Report 2019. Extended spectrum  $\beta$ -lactamase (ESBL)-producing Enterobacteriaceae. CDC; 2019.
3. Wattal C, Kler N, Oberoi JK, Fursule A, Kumar A, Thakur A. Neonatal sepsis: mortality and morbidity in neonatal sepsis due to multidrug-resistant (MDR) organisms: part 1. Indian J Pediatr. 2020;87(2):117-121. [CrossRef PubMed](#)
4. Sendra E, Fernández-Muñoz A, Zamorano L, et al. Impact of multidrug resistance on the virulence and fitness of *Pseudomonas aeruginosa*: a microbiological and clinical perspective. Infection. 2024 Aug;52(4):1235-1268. [CrossRef PubMed](#).
5. Diggle SP, Whiteley M. Microbe profile: *Pseudomonas aeruginosa*: opportunistic pathogen and lab rat. Microbiology (Reading). 2020;166(1):30-33. [CrossRef PubMed](#)
6. Parasuram S, Thing GS, Dhanaraj SA. Polyherbal formulation: concept of Ayurveda. Pharmacogn Rev. 2014;8(16):73-80. [CrossRef PubMed](#)
7. Benamar-Aissa B, Gourine N, Quinten M, Yousfi M. Synergistic effects of essential oils and phenolic extracts on antimicrobial activities using blends of *Artemisia campestris*, *Artemisia herba alba*, and *Citrus aurantium*. Biomol Concepts. 2024 Feb 14;15(1). [CrossRef PubMed](#)
8. Makhoba XH, Viegas C Jr, Mosa RA, Viegas FPD, Poe OJ. Potential impact of the multi-target drug approach in the treatment of some complex diseases. Drug Des Devel Ther. 2020;14:3235-3249. [CrossRef PubMed](#)
9. Kumar M, Sarma DK, Shubham S, et al. Futuristic non-antibiotic therapies to combat antibiotic resistance: a review. Front Microbiol. 2021;12:609459. [CrossRef PubMed](#)
10. Ruparel FJ, Shah SK, Patel JH, Thakkar NR, Gajera GN, Kothari VO. Network analysis for identifying potential anti-virulence targets from whole transcriptome of *Pseudomonas aeruginosa* and *Staphylococcus aureus* exposed to certain anti-pathogenic polyherbal formulations. Drug Target Insights. 2023;17(1):58-69. [CrossRef PubMed](#)



11. Allen RC, Popat R, Diggle SP, Brown SP. Targeting virulence: can we make evolution-proof drugs? *Nat Rev Microbiol.* 2014; 12(4):300-308. [CrossRef PubMed](#)
12. Corsi AK, Wightman B, Chalfie M. A transparent window into biology: a primer on *Caenorhabditis elegans*. *Genetics.* 2015;200(2):387-407. [CrossRef PubMed](#)
13. Patel H, Patel F, Jani V, et al. Anti-pathogenic potential of a classical Ayurvedic Triphala formulation. *F1000Res.* 2019 Jul 18;8:1126. [CrossRef PubMed](#)
14. Joshi C, Patel P, Palep H, Kothari V. Validation of the anti-infective potential of a polyherbal 'Panchvalkal' preparation, and elucidation of the molecular basis underlining its efficacy against *Pseudomonas aeruginosa*. *BMC Complement Altern Med.* 2019;19(1):19. [CrossRef PubMed](#)
15. Durai S, Vigneshwari L, Balamurugan K. *Caenorhabditis elegans*-based *in vivo* screening of bioactives from marine sponge-associated bacteria against *Vibrio alginolyticus*. *J Appl Microbiol.* 2013;115(6):1329-1342. [CrossRef PubMed](#)
16. Patel P, Joshi C, Palep H, Kothari V. Anti-infective potential of a quorum modulatory polyherbal extract (panchvalkal) against certain pathogenic bacteria. *J Ayurveda Integr Med.* 2020; 11(3):336-343. [CrossRef PubMed](#)
17. Patel P, Joshi C, Funde S, Palep H, Kothari V. Prophylactic potential of a Panchgavya formulation against certain pathogenic bacteria. *F1000Res.* 2018 Oct 8;7:1612. [CrossRef PubMed](#)
18. Patel P, Joshi C, Kothari V. Anti-pathogenic efficacy and molecular targets of a polyherbal wound-care formulation (Herboheal) against *Staphylococcus aureus*. *Infect Disord Drug Targets.* 2019;19(2):193-206. [CrossRef PubMed](#)
19. Joshi C, Kothari V, Patel P. Importance of selecting appropriate wavelength, while quantifying growth and production of quorum sensing regulated pigments in bacteria. *Recent Pat Biotechnol.* 2016;10(2):145-152. [CrossRef PubMed](#)
20. Hirshfield IN, Barua S, Basu P. Overview of biofilms and some key methods for their study. In: Goldman E, Green LH, eds. *Practical handbook of microbiology.* 2nd ed. CRC Press; 2008:695-708:chap 42.
21. Trafny EA, Lewandowski R, Zawistowska-Marciniak I, Stępińska M. Use of MTT assay for determination of the biofilm formation capacity of microorganisms in metalworking fluids. *World J Microbiol Biotechnol.* 2013;29(9):1635-1643. [CrossRef PubMed](#)
22. Misko TP, Schilling RJ, Salvemini D, Moore WM, Currie MG. A fluorometric assay for the measurement of nitrite in biological samples. *Anal Biochem.* 1993;214(1):11-16. [CrossRef PubMed](#)
23. Yildirim K, Atas C, Tanyel Akcit E, et al. Nitrate reductase assay for rapid determination of methicillin-resistant *Staphylococcus aureus* clinical isolates. *Lab Med.* 2024;55(2):174-178. [CrossRef PubMed](#)
24. Barnes RJ, Bandi RR, Wong WS, et al. Optimal dosing regimen of nitric oxide donor compounds for the reduction of *Pseudomonas aeruginosa* biofilm and isolates from wastewater membranes. *Biofouling.* 2013;29(2):203-212. [CrossRef PubMed](#)
25. Simner PJ, Hindler JA, Bhowmick T, et al. What's new in antibiotics? Updating CLSI M39 guidance with current trends. *J Clin Microbiol.* 2022;60(10):e0221021. [CrossRef PubMed](#)
26. Lowry OH, Rosebrough NJ, Farr AL, Randall RJ. Protein measurement with the Folin phenol reagent. *J Biol Chem.* 1951; 193(1):265-275. [CrossRef PubMed](#)
27. Dullely JR, Grieve PA. A simple technique for eliminating interference by detergents in the Lowry method of protein determination. *Anal Biochem.* 1975;64(1):136-141. [CrossRef PubMed](#)
28. Mishra M, Tiwari S, Gomes AV. Protein purification and analysis: next generation Western blotting techniques. *Expert Rev Proteomics.* 2017;14(11):1037-1053. [CrossRef PubMed](#)
29. Suzuki J, Kunimoto T, Hori M. Effects of kanamycin on protein synthesis: inhibition of elongation of peptide chains. *J Antibiot (Tokyo).* 1970;23(2):99-101. [CrossRef PubMed](#)
30. Ullah H, Ali S. Classification of anti-bacterial agents and their functions. *Antibacterial Agents.* 2017;10:1-6. [CrossRef](#)
31. Jahn CE, Charkowski AO, Willis DK. Evaluation of isolation methods and RNA integrity for bacterial RNA quantitation. *J Microbiol Methods.* 2008;75(2):318-324. [CrossRef PubMed](#)
32. Andrews S. FastQC: a quality control tool for high throughput sequence data. 2010. [Online](#)
33. Chen S, Zhou Y, Chen Y, Gu J. fastp: an ultra-fast all-in-one FASTQ preprocessor. *Bioinformatics.* 2018 Sep 1;34(17):i884-i890. [CrossRef PubMed](#)
34. Langmead B, Salzberg SL. Fast gapped-read alignment with Bowtie 2. *Nat Methods.* 2012;9(4):357-359. [CrossRef PubMed](#)
35. Liao Y, Smyth GK, Shi W. featureCounts: an efficient general purpose program for assigning sequence reads to genomic features. *Bioinformatics.* 2014;30(7):923-930. [CrossRef PubMed](#)
36. Robinson MD, McCarthy DJ, Smyth GK. edgeR: a Bioconductor package for differential expression analysis of digital gene expression data. *Bioinformatics.* 2010;26(1):139-140. [CrossRef PubMed](#)
37. Conesa A, Götz S. Blast2GO: A comprehensive suite for functional analysis in plant genomics. *Int J Plant Genomics.* 2008; 2008:619832. [CrossRef PubMed](#)
38. Ye J, Zhang Y, Cui H, et al. WEGO 2.0: a web tool for analyzing and plotting GO annotations, 2018 update. *Nucleic Acids Res.* 2018;46(W1):W71-W75. [CrossRef PubMed](#)
39. Szklarczyk D, Kirsch R, Koutrouli M, et al. The STRING database in 2023: protein-protein association networks and functional enrichment analyses for any sequenced genome of interest. *Nucleic Acids Res.* 2023;51(D1):D638-D646. [CrossRef PubMed](#)
40. Chin CH, Chen SH, Wu HH, Ho CW, Ko MT, Lin CY. cytoHubba: identifying hub objects and sub-networks from complex interactome. *BMC Syst Biol.* 2014;8(suppl 4):S11. [CrossRef PubMed](#)
41. Shannon P, Markiel A, Ozier O, et al. Cytoscape: a software environment for integrated models of biomolecular interaction networks. *Genome Res.* 2003;13(11):2498-2504. [Online CrossRef PubMed](#)
42. Untergasser A, Cutcutache I, Koressaar T, et al. Primer3 – new capabilities and interfaces. *Nucleic Acids Res.* 2012;40(15):e115. [CrossRef PubMed](#)
43. Borrero-de Acuña JM, Timmis KN, Jahn M, Jahn D. Protein complex formation during denitrification by *Pseudomonas aeruginosa*. *Microb Biotechnol.* 2017;10(6):1523-1534. [CrossRef PubMed](#)
44. Chautrand T, Depayras S, Souak D, et al. Gaseous NO<sub>2</sub> induces various envelope alterations in *Pseudomonas fluorescens* MFAF76a. *Sci Rep.* 2022;12(1):8528. [CrossRef PubMed](#)
45. Mansour H, Ouweini AEL, Chahine EB, Karaoui LR. Imipenem/cilastatin/relebactam: A new carbapenem β-lactamase inhibitor combination. *Am J Health Syst Pharm.* 2021;78(8):674-683. [CrossRef PubMed](#)
46. Souza GHA, Rossato L, Brito GT, Bet GMDS, Simionatto S. Carbapenem-resistant *Pseudomonas aeruginosa* strains: a worrying health problem in intensive care units. *Rev Inst Med Trop Sao Paulo.* 2021 Sep 27;63:e71. [CrossRef PubMed](#)
47. Pragasam AK, Raghavivedha M, Anandan S, Veeraraghavan B. Characterization of *Pseudomonas aeruginosa* with discrepant carbapenem susceptibility profile. *Ann Clin Microbiol Antimicrob.* 2016;15(1):12. [CrossRef PubMed](#)
48. Takahashi E, Lee JM, Mon H, et al. Effect of antibiotics on extracellular protein level in *Pseudomonas aeruginosa*. *Plasmid.* 2016;84-85:44-50. [CrossRef PubMed](#)



49. Sun J, Deng Z, Yan A. Bacterial multidrug efflux pumps: mechanisms, physiology and pharmacological exploitations. *Biochem Biophys Res Commun*. 2014;453(2):254-267. [CrossRef PubMed](#)
50. Sultan M, Arya R, Kim KK. Roles of two-component systems in *Pseudomonas aeruginosa* virulence. *Int J Mol Sci*. 2021;22(22):12152. [CrossRef PubMed](#)
51. Murakami K, Ono T, Viducic D, et al. Role for rpoS gene of *Pseudomonas aeruginosa* in antibiotic tolerance. *FEMS Microbiol Lett*. 2005;242(1):161-167. [CrossRef PubMed](#)
52. Persat A, Inclan YF, Engel JN, Stone HA, Gitai Z. Type IV pili mechanochemically regulate virulence factors in *Pseudomonas aeruginosa*. *Proc Natl Acad Sci USA*. 2015;112(24):7563-7568. [CrossRef PubMed](#)
53. Myriam P, Braulio P, Javiera RA, et al. Insights into systems for iron-sulfur cluster biosynthesis in acidophilic microorganisms. *J Microbiol Biotechnol*. 2022;32(9):1110-1119. [CrossRef PubMed](#)
54. Mitchell AM, Silhavy TJ. Envelope stress responses: balancing damage repair and toxicity. *Nat Rev Microbiol*. 2019;17(7):417-428. [CrossRef PubMed](#)
55. Hajiagha MN, Kafil HS. Efflux pumps and microbial biofilm formation. *Infect Genet Evol*. 2023;112:105459. [CrossRef PubMed](#)
56. Deuerling E, Gamedinger M, Kreft SG. Chaperone interactions at the ribosome. *Cold Spring Harb Perspect Biol*. 2019;11(11):a033977. [CrossRef PubMed](#)
57. Hamza EH, El-Shawadfy AM, Allam AA, Hassanein WA. Study on pyoverdine and biofilm production with detection of LasR gene in MDR *Pseudomonas aeruginosa*. *Saudi J Biol Sci*. 2023;30(1):103492. [CrossRef PubMed](#)
58. Coggan KA, Wolfgang MC. Global regulatory pathways and cross-talk control *Pseudomonas aeruginosa* environmental lifestyle and virulence phenotype. *Curr Issues Mol Biol*. 2012;14(2):47-70. [PubMed](#)
59. Marsden AE, Intile PJ, Schulmeyer KH, et al. Vfr directly activates exsA transcription to regulate expression of the *Pseudomonas aeruginosa* type III secretion system. *J Bacteriol*. 2016;198(9):1442-1450. [CrossRef PubMed](#)
60. Schuster M, Greenberg EP. Regulatory networks in pathogenic bacteria: lessons from cell-cell communication in *Pseudomonas aeruginosa*. *Virulence mechanisms of bacterial pathogens*. ASM Press; 2007:75-88. [CrossRef](#)
61. Häussler S, Becker T. The pseudomonas quinolone signal (PQS) balances life and death in *Pseudomonas aeruginosa* populations. *PLoS Pathog*. 2008;4(9):e1000166. [CrossRef PubMed](#)
62. Bradley R, Simon D, Spiga L, Xiang Y, Takats Z, Williams H. Laser desorption rapid evaporative ionization mass spectrometry (LD-REIMS) demonstrates a direct impact of hypochlorous acid stress on PQS-mediated quorum sensing in *Pseudomonas aeruginosa*. *mSystems*. 2024;9(4):e0116523. [CrossRef PubMed](#)
63. Xu Y, Zheng X, Zeng W, et al. Mechanisms of heteroresistance and resistance to imipenem in *Pseudomonas aeruginosa*. *Infect Drug Resist*. 2020;13:1419-1428. [CrossRef PubMed](#)
64. Fazeli-Nasab B, Sayyed RZ, Mojahed LS, et al. Biofilm production: a strategic mechanism for survival of microbes under stress conditions. *Biocatal Agric Biotechnol*. 2022;42:102337. [CrossRef](#)



# Enhancement of apoptosis in Caco-2, Hep-G2, and HT29 cancer cell lines following exposure to *Toxoplasma gondii* peptides

Firooz Shahrivar<sup>1</sup>, Javid Sadraei<sup>1</sup>, Majid Pirestani<sup>1</sup>, Ehsan Ahmadpour<sup>2,3</sup>

<sup>1</sup>Department of Parasitology, Faculty of Medical Sciences, Tarbiat Modares University, Tehran - Iran

<sup>2</sup>Immunology Research Center, Tabriz University of Medical Sciences, Tabriz - Iran

<sup>3</sup>Infectious and Tropical Diseases Research Center, Tabriz University of Medical Sciences, Tabriz - Iran

## ABSTRACT

**Objective:** Cancer or neoplasm is a cosmopolitan catastrophe that results in more than 20 million new cases and 10 million deaths every year. Some factors lead to carcinogenesis like infectious diseases. Parasites like *Toxoplasma gondii*, by its components, could modulate the cancer system by inducing apoptosis. The objective of this investigation is to assess the potential of peptides derived from *T. gondii* in combating cancer by examining their effects on Caco-2, Hep-G2, and HT29 cell lines.

**Materials and methods:** Candidate peptide by its similarity to anticancer compounds was predicted through the computer-based analysis/platform. The impact of the peptide on cell viability, cell proliferation, and gene expression was evaluated through the utilization of MTT assay, flow cytometry, and real-time polymerase chain reaction (PCR) methodologies.

**Results:** The cell viability rate exhibited a significant decrease ( $p < 0.001$ ) across all cell lines when exposed to a concentration of  $\leq 160$   $\mu\text{g}$ . Within the 48-hour timeframe, the half maximal inhibitory concentration ( $\text{IC}_{50}$ ) for HT29 and Hep-G2 cell lines was determined to be 107.2 and 140.6  $\mu\text{g}/\text{mL}$ , respectively. Notably, a marked decrease in the expression levels of *Bcl2* and *APAF1* genes was observed in both the Hep-G2 and HT29 cell lines.

**Conclusion:** These findings indicate that the *T. gondii* peptide affected cancer cell mortality and led to changes in the expression of genes associated with apoptosis.

**Keywords:** Anticancer, Neoplasm, Parasite, Peptides, Real-time PCR, Toxoplasmosis

## Introduction

*Toxoplasma gondii* is the most widespread protozoan parasite that gained its reputation by seropositive analysis. It has been found that more than 30%-50% of the world's population is positive for *T. gondii* (1). Felids are known to be the definitive host in which the sexual stage takes place. Terrestrial and aquatic mammals as well as birds act as intermediate hosts during the asexual stage (2).

Three developmental stages have been distinguished to infect the cell: (i) tachyzoite, which rapidly multiplies and occurs in the acute phase of the infection, (ii) bradyzoite, a form of slow multiplication that characterizes the chronic

phase, and (iii) sporozoites, which are distinctive of the sexual stage in felids and found in oocysts in feline feces (3).

Various pathways have been reported for the infection of intermediate hosts: ingestion of oocysts-contaminated fruits, vegetables, or water, consumption of raw or uncooked meat containing tissue cysts, congenital transmission, blood transfusion, and organ transplantation. Although transmission through the ingestion of non-pasteurized milk or milk products has been documented, it is not common (4). It is obvious that felines as definitive hosts can become infected through carnivorous behavior or ingestion of sporulated oocysts (5).

Cancer is referred as a composite of diseases acquired by the development of neoplastic cells (6). It contributes symptoms like eluding growth suppressors, empowering proliferative signaling, withstanding cell death, promoting the ability to replicate indefinitely, activating angiogenesis, prompting invasion and metastasis, genome vulnerability, reconstructing energy metabolism, and evading destruction by the immune system as well (7). There are more than 20 million newly diagnosed cases of cancer and almost 10 million deaths attributed to this disease every year (8). Multiple factors play a

Received: June 24, 2024

Accepted: July 11, 2024

Published online: September 30, 2024

Corresponding author:

Javid Sadraei

email: Sadraeij@modares.ac.ir



pivotal role in causing carcinogenesis like lifestyle, genes, and the microenvironment. Moreover, it is widely recognized that infectious diseases play a significant role in the development of various types of cancers. These diseases are responsible for approximately 25%-50% of all cancer cases (9). Notably, viral infections such as *papilloma virus* have been linked to cervical cancer, while bacterial infections like *Helicobacter pylori* have been associated with gastric cancer. Additionally, parasitic infections, including *Schistosoma haematobium*, have been found to be connected to urinary bladder cancer. The strong correlation between infectious diseases and cancer underscores the importance of preventive measures and early detection in reducing the burden of these malignancies. In this way, some parasites act as the inducers or promoters of the cancers and others inhibit the factors that could modulate tumorigenesis. So far, investigations show that components of parasites are able to modulate the cancer system by inducing apoptosis (10). Studies have shown that *T. gondii* is able to break tumor immune tolerance and arouse potent CD8+ T-cell immunity (11). In the current study, the effect of *T. gondii*-synthesized excretory-secretory compound in cell growth factors and inducing apoptosis was investigated.

## Materials and methods

### Synthesis of peptide

Out of the acknowledged proteomes of *T. gondii* excretory-secretory antigens, the QLEDAVSAVASVVQDE amino acid sequence belonging to part GRA1 was selected. It is noteworthy that this sequence has the most similarity to the other anticancer agents ( $\approx 91\%$ ) by the analysis done in association with the anticancer peptide database: CancerPPD site ([Online](#)). Following analysis of the nominated sequence and confirmation of its anticancer potential, ElabScience was proposed for peptide synthesis (United States, Lot No: YZIGY9RHUD) with a purity of over 97.5% and a molecular weight of 2,425.5. As per the guidelines provided by the manufacturer, by applying ultra-pure water, the synthesized peptide underwent dilution and was subsequently prepared in various concentrations to evaluate cell viability and perform molecular assays.

### Anticancer assays in vitro

#### Cell culture and treatments

The Iranian Biological Resource Center (IBRC) provided the Caco-2, Hep-G2, and HT29 cell lines, which are human gastric, colon, and liver cancer cell lines, respectively. These cell lines were cultured in Dulbecco's modified Eagle's medium (DMEM)/F12, supplemented with 10% fetal bovine serum (FBS; Gibco, Thermo Fisher Scientific) and 2 mmol/L L-glutamine (Bio Idea Co, Iran). The growth medium for all cell lines consisted of DMEM/F12 supplemented with GlutaMAX,  $\text{NaHCO}_3$ , and 15 mM HEPES. To ensure optimal conditions for cell growth, the cells were incubated at a temperature of 37°C in a humidified atmosphere consisting of 5% carbon dioxide (12).

### MTT assay for cell viability detection

After achieving a confluence of 90%, the cells were seeded into the wells using microscopic counting after being stained with trypan blue. MTT assay was administered in 96-well culture plates for cell viability. Each well was seeded with approximately  $2 \times 10^4$  cells in 200  $\mu\text{L}$  of DMEM medium. The plates were then incubated at 37°C and 5%  $\text{CO}_2$  for 24 hours to ensure proper adherence of the cells to the wells of the plate. Subsequently, Hep-G2, HT29, and Caco-2 cells were exposed to elevating concentrations of *T. gondii* peptide (40, 80, and 160  $\mu\text{g}/\text{mL}$ ) and incubated for 24 and 48 hours in the 96-well culture plates. The growth of the cells was assessed based on the activity of mitochondrial enzymes determined in the MTT assay.

Following 24- and 48-hour exposure of cell lines to the peptides, 20  $\mu\text{L}$  volume of 5  $\mu\text{g}/\text{mL}$  MTT solutions were added to the wells, and the plates were then incubated at 37°C for an additional 4 hours. Subsequently, the wells were emptied and 200  $\mu\text{L}$  of dimethyl sulfoxide (DMSO) was added to all wells; in this specific approach, living cells contain NAD(P)H-dependent oxidoreductase enzymes that facilitate the conversion of the MTT reagent into formazan crystalline product, leading to purple color. The more viable cells and metabolic activity, the more intensity of purple color (13). To measure the optical density (OD) of the wells, a microplate spectrophotometer (BioTek-ELX800, United States) was employed at 570 nm, both 24 and 48 hours after exposure. Each concentration and cell lines were subjected to triplicate experiments to ensure the accuracy and reliability of the results.

### Bcl2, APAF1 gene expression analysis

The evaluation of gene expression was conducted using the SYBR green-based quantitative real-time polymerase chain reaction (PCR) technique. In order to measure the messenger ribonucleic acid (mRNA) expression of the *Bcl2* and *APAF1* genes, the genomic content (total RNA) was extracted from all cultured cell lines. QIAzol RNA (Qiagen, United States) was utilized for this purpose, following the manufacturer's protocol. The nanodrop spectrophotometer (Thermo Scientific™ NanoDrop 2000c spectrophotometer) was used to evaluate the quantity, quality, and optimal concentration of the collected RNAs at a 260/280 nm ratio. Following this, the RNAs were transformed into complementary deoxyribonucleic acid (cDNA) by reverse transcription, utilizing RT-specific primers and glyceraldehyde 3-phosphate dehydrogenase (GAPDH) as a reference gene for data normalization (Tab. 1). A LightCycler® 96 thermal cycler (Roche, Germany) was used to conduct real-time reverse transcription (RT)-PCR. Within each reaction, a 20  $\mu\text{L}$  mixture was prepared, containing 8  $\mu\text{L}$  of SYBR Green I Master mix, 1  $\mu\text{L}$  of cDNA serving as the template, 8  $\mu\text{L}$  of nuclease-free distilled water, and 10 pmol of each primer. In the amplification program, the initial denaturation step was performed at a temperature of 95°C for a duration of 8 minutes. This was followed by 40-45 cycles of denaturation at 95°C for 10 seconds, annealing at 57-62°C for 5 seconds, and extension at 72°C for 20 seconds (14,15).



**TABLE 1** - The sequence of primer runs in real-time PCR

Gene	Seq (5'-3')	Annealing	Ref
<i>Bcl2</i>	F: TCGCCTGTGGATGACTGA	60	(14)
	R: CAGAGACAGCCAGGAGAAATCA		
<i>APAF1</i>	F: TTAGGAGCCAGGTGCGGT	58	(29)
	R: GCTTGTCTTTCTCCATTTTC		
<i>GAPDH</i>	F: ACGGATTTGGTCGATTGGG	57	(30)
	R: TGATTTTGAGGGATCTCGC		

## Apoptosis analysis

Apoptosis evaluation was conducted using the Annexin V/PI Apoptosis detection kit (cat. no. AnxF100PI, MabTag GmbH) following peptide treatments. A 6-well plate was utilized, with each well containing a volume of 2.5 mL cell suspension at a density of  $3 \times 10^5$  cells/mL. Following 24-hour cultures of all three kinds of cells in 200  $\mu$ M of the peptide, in accordance with the procedures outlined in the preceding section, the cells underwent the specified treatment. The negative control group received an equivalent amount of phosphate-buffered saline (PBS). After the incubation period, the cells were collected and underwent two rounds of washing with cold PBS at a pH of 7.4. Subsequently, the cells were suspended in annexin-binding buffer and exposed to 5  $\mu$ L of fluorescein isothiocyanate (FITC)-Annexin V and 5  $\mu$ L of propidium iodide (PI). The samples were thoroughly mixed and incubated in darkness at a temperature of 25°C for a duration of 15 minutes. The stained cells were then analyzed using a Sysmex CyFlow Space flow cytometer. The fluorescence emitted by the cells was measured at wavelengths of 495 and 519 nm following excitation at 488 nm (16).

## Statistical analysis

In the current investigation, all experiments were repeated in triplicate. Statistical analysis was conducted to compare and evaluate the treated groups in relation to both each other and the control group. The comparative Ct ( $\Delta\Delta$ Ct) method was employed to statistically analyze the data. Prior to analysis, the real-time PCR findings underwent preprocessing. Subsequently, the expression levels of selected genes (*Bcl2*, *APAF1*) among the study groups were evaluated using Kruskal-Wallis and Mann-Whitney U-tests. A p-value <0.05 was deemed to be statistically significant. All statistical analyses were assessed using GraphPad Prism v 6.1 software.

## Results

### Mortality and proliferation alter under *T. gondii* peptide impact in all cell lines

In each cell line, the effect of peptides on cell viability, mortality, and proliferation was examined at 24 and 48 hours at escalating concentrations (Fig. 1). A direct correlation

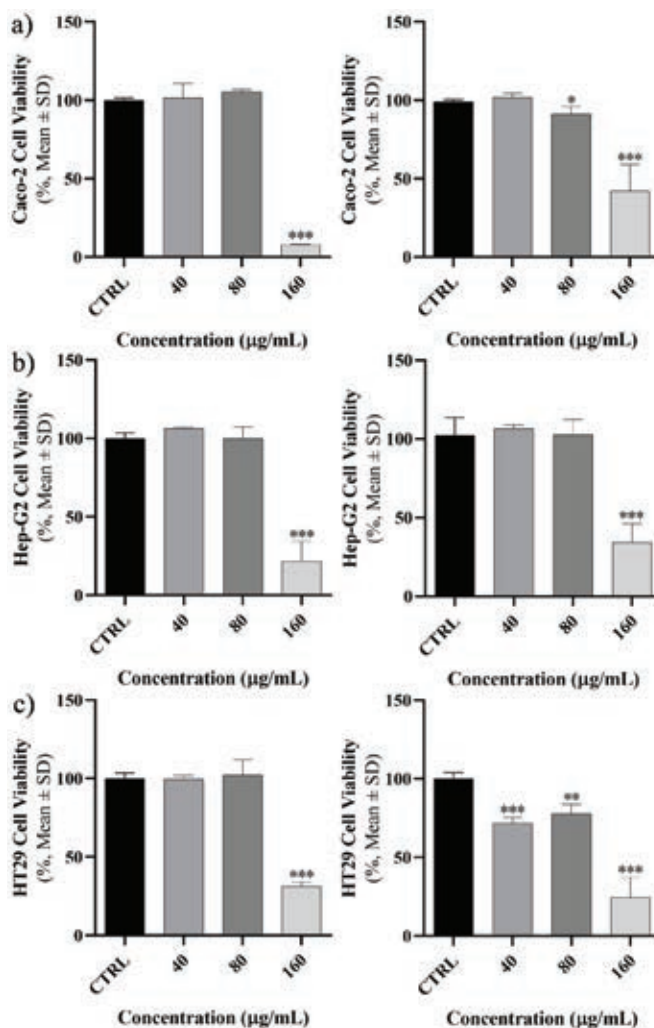


**FIGURE 1** - The cell viability of cancer cells. A) Caco-2, B) Hep-G2, and C) HT29 were assessed after 24 (left) and 48 hours (right) exposure to specific concentrations of *Toxoplasma gondii*-derived peptide (\*p <0.05; \*\*p <0.01; \*\*\*p <0.001). SD = standard deviation.

was discovered between the rise in concentration and the rise in mortality and interpreted as dose-dependent manner but wasn't time dependent. At concentrations of 40, 80, and 160  $\mu$ g, the cell viability rate exhibited a significant decrease across all cell lines. After 24 hours, the cell lines demonstrated the most significant impact when exposed to concentrations of 160  $\mu$ g (p < 0.001). Like the earlier pattern, after 48 hours of peptide exposure, cell viability declined at 40, 80, and 160  $\mu$ g concentrations in contrast to accumulative doses. In Caco-2 cells, in comparison with the control group, a significant mortality induction was experienced in the concentration of 160  $\mu$ g (p < 0.001). The same significant mortality induction was found in Hep-G2 cell line at the concentration of 160  $\mu$ g at 48 hours exposure. But in HT29 cell line this significant mortality induction started at 40  $\mu$ g concentration. Cell viability rates were assessed at

various concentrations based on the duration of each cell line. As depicted in Figure 1, it was observed that the impact of the peptide on cancer cells differed depending on the dosage administered.

The cell viability rate in each cell line was compared at the aforementioned concentrations, which have been provided in Figure 1. Briefly, a significant mortality induction in Caco-2 was started in 160 and 80  $\mu\text{g}$  at 24 and 48 hours, respectively. For Hep-G2, the significant mortality induction was in 160  $\mu\text{g}$  at 24 and 48 hours. This situation was observed in 160 and 40  $\mu\text{g}$  at 24 and 48 hours, respectively.

### The $\text{IC}_{50}$ of the excretory-secretory peptide of *T. gondii*

Based on the results obtained from the MTT assay, the  $\text{IC}_{50}$  values for each cell line were determined after exposure to the peptide at both 24 and 48 hours. At the conclusion of the 24-hour period, the Caco-2 cell line exhibited the

highest  $\text{IC}_{50}$  concentration (149.6  $\mu\text{g}/\text{mL}$ ), while the Hep-G2 cell line displayed the lowest  $\text{IC}_{50}$  concentration (126.8  $\mu\text{g}/\text{mL}$ ). Furthermore, during the 48-hour timeframe, the HT29 cell line demonstrated the lowest  $\text{IC}_{50}$  concentration (107.2  $\mu\text{g}/\text{mL}$ ), whereas the Hep-G2 cell line exhibited the highest  $\text{IC}_{50}$  concentration (140.6  $\mu\text{g}/\text{mL}$ ) (Fig. 2).

### Apoptosis-related gene expression levels

The mRNA levels of *Bcl2* and *APAF1* were evaluated in three types of cancer cells at exposed concentrations close to  $\text{IC}_{50}$  by using real-time PCR and results were reported as a fold change. Evaluated expression levels of *Bcl2* and *APAF1* genes are shown in Figure 3. In fact, the Caco-2 cell line showed an increase in gene expression level of *Bcl2* and non-elevated expression level in *APAF1* gene. A notable decline in the expression levels of *Bcl2* and *APAF1* genes was detected in Hep-G2 and HT29 cell lines (Fig. 3).

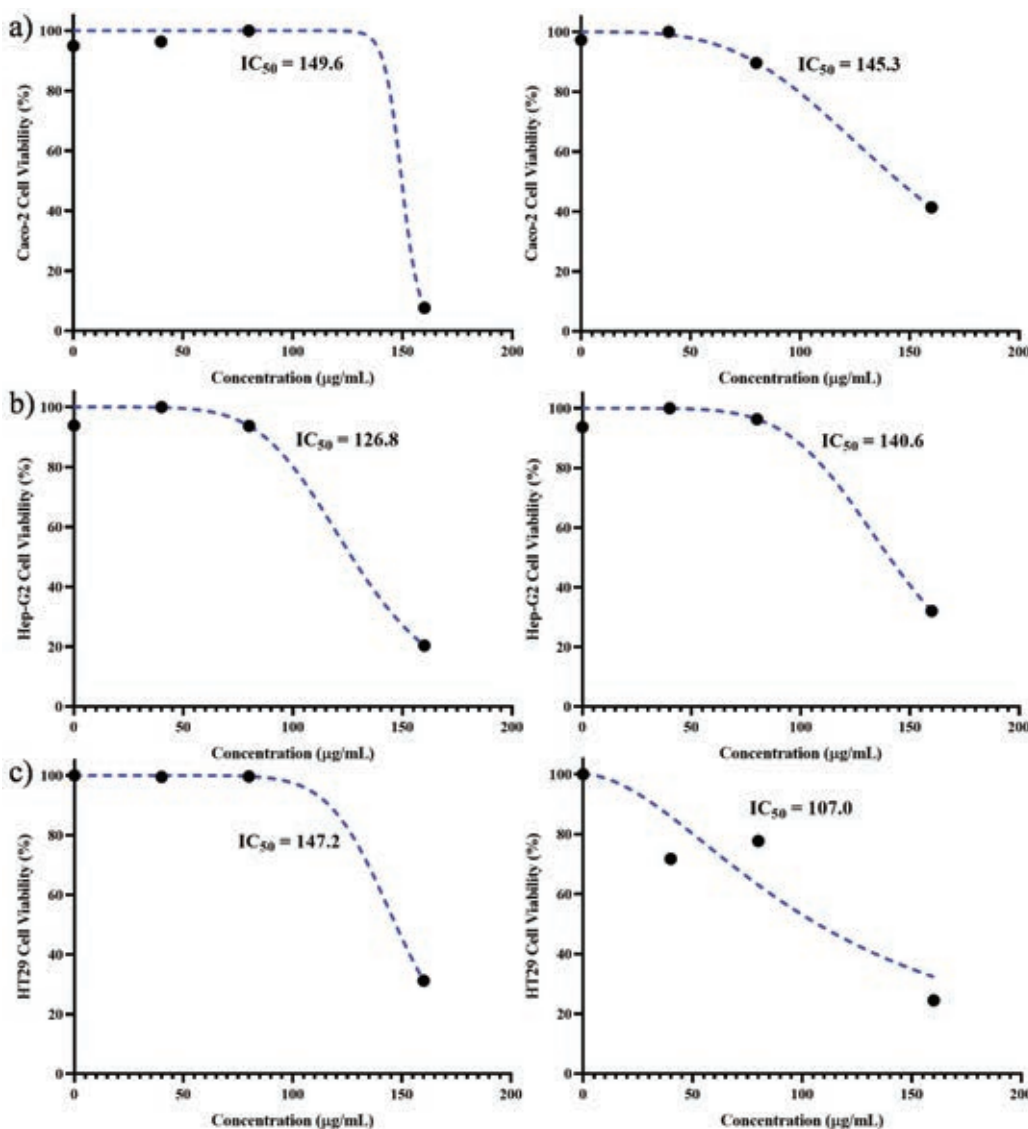


**FIGURE 2** -  $\text{IC}_{50}$  values of *Toxoplasma gondii* peptide in cell lines after 24 (left) and 48 hours (right): A) Caco-2, B) Hep-G2, and C) HT29. The highest and lowest values after 24 hours were found in Caco-2 and Hep-G2 cell lines (149.6 and 126.8  $\mu\text{g}/\text{mL}$ , respectively) and the highest and lowest values after 48 hours were 150.3 and 107  $\mu\text{g}/\text{mL}$  for Caco-2 and HT29 cell lines.

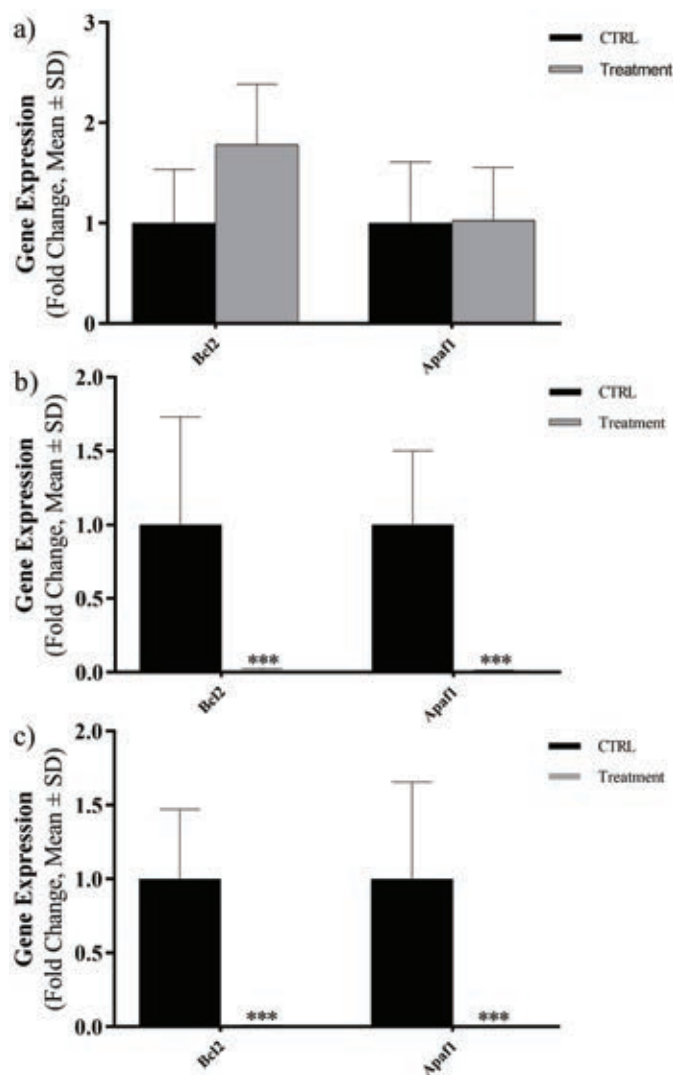


**FIGURE 3** - Expression levels of *Bcl2* and *APAF1* in three cancer cell lines exposed to *Toxoplasma gondii* peptide in terms of fold change: A) Caco-2, B) Hep-G2, C) HT29 (ns, not significant; \* $p < 0.05$ ; \*\* $p < 0.01$ ; \*\*\* $p < 0.001$ ; \*\*\*\* $p < 0.0001$ ). SD = standard deviation.

### Flow cytometry

The apoptotic effect was examined on Caco-2, Hep-G2, and HT29 cell lines following treatment with the peptide and subsequent staining with annexin V and PI (Fig. 4). After a 24-hour exposure to the peptide, a noteworthy rise in apoptosis was detected across all cell lines ( $p = 0.005$ ). Notably, the highest level of apoptosis was observed in HT29 cells, reaching a rate of 32% (Fig. 5).

### Discussion

In the current investigation, we demonstrated the anti-cancer effect of candidate *Toxoplasma* excretory-secretory antigen on three cancerous cell lines: Caco-2, Hep-G2, and

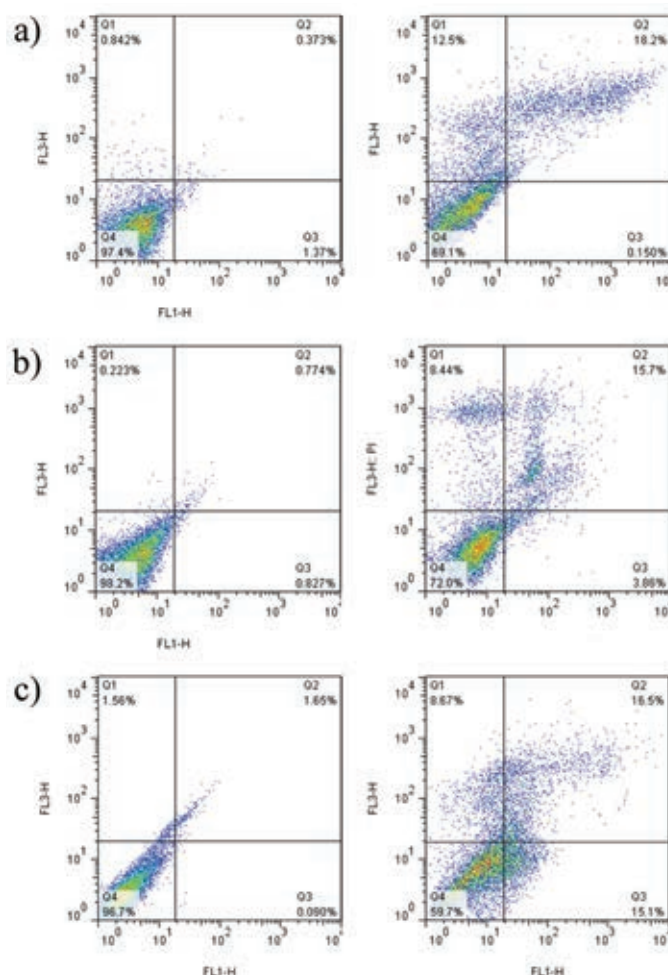


**FIGURE 4** - The distribution of apoptotic cells stained with annexin V-FITC/PI in dual parametric dot plots of PI fluorescence (Y-axis) vs. annexin V-FITC fluorescence (X-axis). Dot plots represent cancerous cell lines (A) Caco-2, B) Hep-G2, and C) HT29. The highest rate of apoptosis belongs to HT29 with 32%. FITC = fluorescein isothiocyanate; PI = propidium iodide.

HT29. Currently, researchers are still exploring different ways to treat cancer using natural substances instead of chemicals. Besides studying plant compounds, researchers are also assessing the effectiveness of different other sources in inhibiting the growth of cancer cells. Sometimes, it is troublesome to anticipate events of antagonistic impacts from chemotherapeutic drugs amid treatment (17). Cancer cells can become resistant to drugs while receiving chemotherapy. So, to get the same effect in killing tumors, more medicine is needed than what was given initially. Frequently, higher dosage administration creates a higher possibility of side effects in patients (18). Therefore, taking a blend of drugs with various mechanisms could synergistically facilitate therapeutic efficiency (19).

One of these mechanisms could be addressing live organism compounds that have a long relationship with humans and successfully adapted to the human body: parasites. Some studies were conducted by applying protozoa

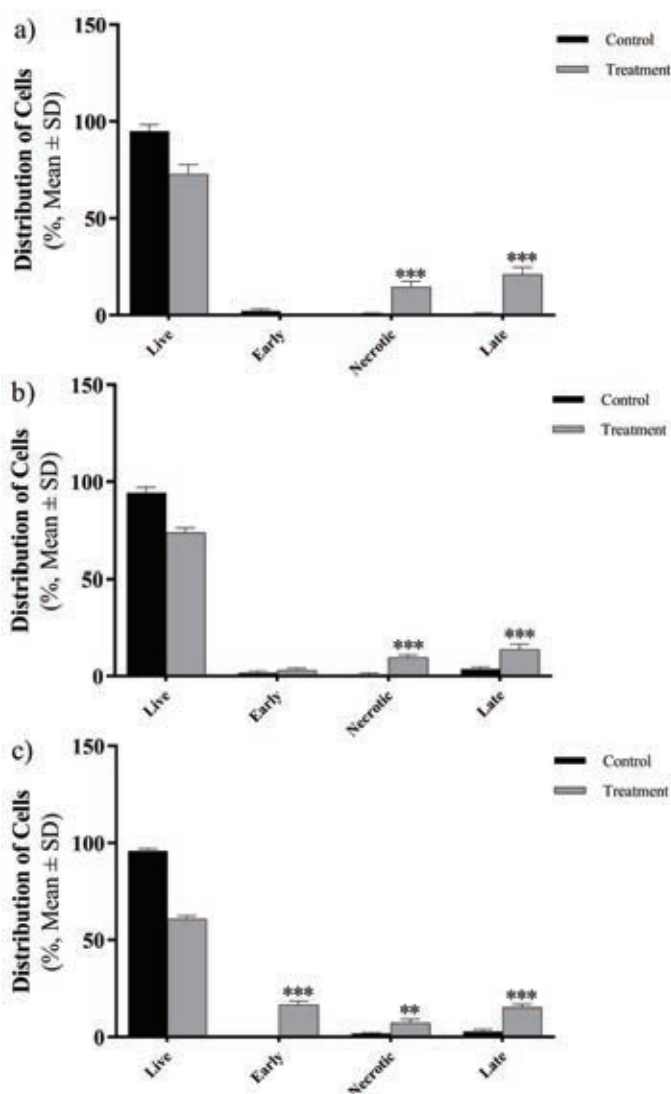


**FIGURE 5** - The effects of *Toxoplasma gondii* peptide on the viability of three cancer cell lines (A) Caco-2, B) Hep-G2, and C) HT29) show a significant increase in induction in comparison to the control. The error bars represent mean  $\pm$  SD of the triplicate measurements (\* $p < 0.05$ ; \*\* $p < 0.01$ ; \*\*\* $p < 0.001$ ; \*\*\*\* $p < 0.0001$ ). SD = standard deviation.

and helminths to improve immunotherapies concentrating against tumors aiming to empower the antitumor immune response and therefore eliminate the progressing neoplasm (7). The pioneer protozoan in uncovering antitumor effects was *Trypanosoma cruzi*, as affected patients showed no symptoms of colon cancer despite having a tumorigenic process (20). Investigations have revealed that some molecules on the surface of the parasite can induce the production of antibodies that diagnose neoplastic cells due to the antigenic similarity between them, or they could be activators of cells involved in the process of cancer cell recognition. *T. gondii* itself can trigger a cascade that starts with the induction of interleukin (IL)-12 production and continues with stimulating

natural killer (NK) cells and T cells for producing interferon gamma (IFN- $\gamma$ ) and modifying the spread of CD8 T lymphocytes and their cytotoxic capability and finally elevating antitumor immune response (21). The ability of *Toxoplasma* to modify its host immune response in several studies makes addressing this parasite as a potent inducer of antitumor responses (11).

Our investigation shows that parasite-derived peptide could induce apoptosis in cancer cell lines, which was in line with the lately done study by Bahadory et al (10). According to this study, *Toxocara canis* excretory-secretory Troponin protein peptide (ES TPP) could successfully alter the expression of apoptotic involved factors. Peptides have characteristically gained more attention in researches due to their advantages; first of all, peptides are the functional piece of natural proteins that can exhibit innumerable biological functions and offer higher selectivity and potency in comparison to ordinary small molecule drugs. Secondly, they could be simply manufactured by chemically solid-phase synthesis. Lastly, possessing amide backbone makes the peptides to be fundamentally biodegradable, which may minimize the side effects (22).

Given that the peptide was synthesized applying computer database, high concentration of peptides, regardless of online prediction, is needed to kill the cells or induce cell death. Scientists suggest that use of nanoparticles, adjuvants, and improving target cell delivery system are means for optimizing compounds with anticancer potential (23). On the basis of attained results, the applied peptide causes a significant reduction in mortality rate in cell lines, which are referred as dose dependent. Hence, in comparison to Caco-2 and Hep-G2, the least concentration to alert the mortality and viability rate was for HT29, 40  $\mu\text{g}/\text{mL}$ . It is noteworthy that the cytotoxic effect was remarkably higher on HT29 than Caco-2 and Hep-G2 with lower  $\text{IC}_{50}$  (107  $\mu\text{g}/\text{mL}$ ).

Apoptosis, a physiological mechanism of cellular demise, is prompted by intra- and extracellular signals. This process serves a crucial role in maintaining the balance and proper functioning of normal tissues during development and homeostasis. In the context of cancer progression, apoptosis acts as a barricade against the uncontrolled growth of transformed cells. Nevertheless, in tumors that have undergone significant transformation and exhibit resistance to therapeutic interventions, the occurrence of apoptosis may be reduced (6). *Bcl2* and *APAF1* are key factors in the process of cell death, which were evaluated by both MTT assay and real-time PCR; the latter is more sensitive and specific. In fact, releasing cytochrome c from mitochondria is the pivotal triggering episode associating a cell to apoptosis, resulting in the formation of apoptosome-containing caspases. *Bcl2* as an antiapoptotic protein interferes in the permeabilization of the mitochondrial outer membrane, thus barricading apoptosis (24,25). Controversy, oligomerization of *APAF1* in response to discharge of cytochrome c facilitates the formation of apoptosome, leading to downregulation of caspases and triggering apoptosis (26). In our study, there is an increase in gene expression level of *Bcl2* gene but it wasn't significant in Caco-2 cell line. A significant decrease in expression levels of *Bcl2* and *APAF1* genes was seen in both Hep-G2 and

HT29 cell lines. On the basis of update by the Nomenclature Committee on Cell Death (NCCD), regulated cell death could be classified, based on its molecular characteristics, into multiple categories in which some of them were well studied like: apoptosis, necrosis, necroptosis, and pyroptosis, while others like ferroptosis, entotic, autophagy, etc., are underestimated and less well-studied (27). For this case, we could conclude that downregulation in any of the aforementioned gene expression levels may result in consequences of any of the aforesaid cell death types. D'Arcy states that the cell in media could react in different ways when it fails to maintain homeostasis with its environment. Hence, the remains of late apoptotic cells that have lost their integrity are simply described as necrosis (28).

For future prospect, conducting experiments on animal models and assessing cell death molecular hallmarks using blotting techniques would give a better point of view for conducting upcoming researches. Challenges include being unable to synthesize the peptide in our country and the need for implementing more accurate and specific tests for applying blotting tests and to evaluate whether the peptide could enter the cells.

## Conclusion

The results demonstrated that *T. gondii* peptide exerted an influence on the mortality of cancer cells and altered the expression of apoptosis-related genes. However, further optimization and redesign of the peptide could enhance its potential as a cancer therapy. Given the potential of peptides as selective and potent therapeutic agents, enhancing them with nanoparticles and improving delivery systems could optimize their anticancer efficacy. Future research could focus on animal models and molecular analyses with blotting techniques to further evaluate and improve this promising therapeutic approach.

## Disclosures

**Authors' contributions:** All authors contributed to the study conception and design. Material preparation, data collection and analysis were performed by Javid Sadraei, Firooz Shahrivar, Majid Pirestani, and Ehsan Ahmadpour. The first draft of the manuscript was written by Firooz Shahrivar and all authors commented on previous versions of the manuscript. All authors read and approved the final manuscript.

**Data availability declaration:** The authors declare that data would be available if any formal request is sent to the corresponding author.

**Funding:** This study was funded by Tarbiat Modares University, Tehran, Iran (MED 87201).

**Conflict of interest:** The authors declare that they have no conflict of interest.

**Ethical approval:** This study was performed in line with the principles of the Declaration of Helsinki. Approval was granted by the Ethics Committee of Tarbiat Modares University (IR.MODARES.REC.1400.128).

**Consent to publish/participate:** The authors affirm that no patient/participant consent was required for publishing; meanwhile, there is no conflict or opposition for publishing the data.

## References

1. Flegr J, Prandota J, Sovičková M, Israili ZH. Toxoplasmosis – a global threat. Correlation of latent toxoplasmosis with specific disease burden in a set of 88 countries. PLoS One. 2014;9(3):e90203. [CrossRef PubMed](#)
2. Dubey JP. History of the discovery of the life cycle of *Toxoplasma gondii*. Int J Parasitol. 2009;39(8):877-882. [CrossRef PubMed](#)
3. Attias M, Teixeira DE, Benchimol M, Vommaro RC, Crepaldi PH, De Souza W. The life-cycle of *Toxoplasma gondii* reviewed using animations. Parasit Vectors. 2020;13(1):588. [CrossRef PubMed](#)
4. Stelzer S, Basso W, Benavides Silván J, et al. *Toxoplasma gondii* infection and toxoplasmosis in farm animals: risk factors and economic impact. Food Waterborne Parasitol. 2019;15:e00037. [CrossRef PubMed](#)
5. Dubey JP. The history and life cycle of *Toxoplasma gondii*. In: Weiss LM, Kim K, eds. Toxoplasma gondii. Elsevier 2020; 1-19. [CrossRef](#)
6. Hanahan D, Weinberg RA. Hallmarks of cancer: the next generation. Cell. 2011 Mar 4;144(5):646-74. [CrossRef PubMed](#)
7. Callejas BE, Martínez-Saucedo D, Terrazas LI. Parasites as negative regulators of cancer. Biosci Rep. 2018;38(5):BSR20180935. [CrossRef PubMed](#)
8. Sung H, Ferlay J, Siegel RL, et al. Global cancer statistics 2020: GLOBOCAN estimates of incidence and mortality worldwide for 36 cancers in 185 countries. CA Cancer J Clin. 2021;71(3):209-249. [CrossRef PubMed](#)
9. Knoll LJ, Hogan DA, Leong JM, Heitman J, Condit RC. Pearls collections: What we can learn about infectious disease and cancer. Public Library of Science San Francisco 2018; e1006915.
10. Bahadory S, Sadraei J, Zibaei M, Pirestani M, Dalimi A. In vitro anti-gastrointestinal cancer activity of *Toxocara canis*-derived peptide: analyzing the expression level of factors related to cell proliferation and tumor growth. Front Pharmacol. 2022;13:878724. [CrossRef PubMed](#)
11. Fox BA, Butler KL, Guevara RB, Bzik DJ. Cancer therapy in a microbial bottle: uncorking the novel biology of the protozoan *Toxoplasma gondii*. PLoS Pathog. 2017;13(9):e1006523. [CrossRef PubMed](#)
12. Soleimani M, Nadri S. A protocol for isolation and culture of mesenchymal stem cells from mouse bone marrow. Nat Protoc. 2009;4(1):102-106. [CrossRef PubMed](#)
13. Kumar P, Nagarajan A, Uchil PD. Analysis of cell viability by the MTT assay. Cold Spring Harb Protoc. 2018;2018(6):pdb.prot095505. [CrossRef PubMed](#)
14. Pan W, Yang J, Wei J, et al. Functional BCL-2 regulatory genetic variants contribute to susceptibility of esophageal squamous cell carcinoma. Sci Rep. 2015;5(1):11833. [CrossRef PubMed](#)
15. Shang J, Yang F, Wang Y, et al. MicroRNA-23a antisense enhances 5-fluorouracil chemosensitivity through APAF-1/caspase-9 apoptotic pathway in colorectal cancer cells. J Cell Biochem. 2014;115(4):772-784. [CrossRef PubMed](#)
16. McKinnon KM. Flow cytometry: an overview. Curr Protoc Immunol. 2018;120(1):5.1.1-5.1.11. [CrossRef](#)
17. Lin SR, Chang CH, Hsu CF, et al. Natural compounds as potential adjuvants to cancer therapy: preclinical evidence. Br J Pharmacol. 2020;177(6):1409-1423. [CrossRef PubMed](#)
18. Zheng H-C. The molecular mechanisms of chemoresistance in cancers. Oncotarget. 2017;8(35):59950-59964. [CrossRef PubMed](#)
19. Chen M-L, Lai C-J, Lin Y-N, Huang C-M, Lin Y-H. Multifunctional nanoparticles for targeting the tumor microenvironment to improve synergistic drug combinations and cancer treatment effects. J Mater Chem B. 2020;8(45):10416-10427. [CrossRef PubMed](#)



20. Garcia SB, Aranha AL, Garcia FRB, et al. A retrospective study of histopathological findings in 894 cases of megacolon: what is the relationship between megacolon and colonic cancer? *Rev Inst Med Trop São Paulo*. 2003;45(2):91-93. [CrossRef PubMed](#)
21. Hunter CA, Subauste CS, Van Cleave VH, Remington JS. Production of gamma interferon by natural killer cells from *Toxoplasma gondii*-infected SCID mice: regulation by interleukin-10, interleukin-12, and tumor necrosis factor alpha. *Infect Immun*. 1994;62(7):2818-2824. [CrossRef PubMed](#)
22. Fosgerau K, Hoffmann T. Peptide therapeutics: current status and future directions. *Drug Discov Today*. 2015;20(1):122-128. [CrossRef PubMed](#)
23. Lv S, Sylvestre M, Prossnitz AN, Yang LF, Pun SH. Design of polymeric carriers for intracellular peptide delivery in oncology applications. *Chem Rev*. 2021;121(18):11653-11698. [CrossRef PubMed](#)
24. Gogvadze V, Orrenius S, Zhivotovsky B. Multiple pathways of cytochrome c release from mitochondria in apoptosis. *Biochim Biophys Acta*. 2006;1757(5-6):639-647. [CrossRef PubMed](#)
25. Brunelle JK, Letai A. Control of mitochondrial apoptosis by the Bcl-2 family. *J Cell Sci*. 2009;122(Pt 4):437-441. [CrossRef PubMed](#)
26. Shakeri R, Kheirollahi A, Davoodi J. Apaf-1: regulation and function in cell death. *Biochimie*. 2017;135:111-125. [CrossRef PubMed](#)
27. Tang D, Kang R, Berghe TV, Vandenabeele P, Kroemer G. The molecular machinery of regulated cell death. *Cell Res*. 2019;29(5):347-364. [CrossRef PubMed](#)
28. D'Arcy MS. Cell death: a review of the major forms of apoptosis, necrosis and autophagy. *Cell Biol Int*. 2019;43(6):582-592. [CrossRef PubMed](#)
29. Robles AI, Bemmels NA, Foraker AB, Harris CC. APAF-1 is a transcriptional target of p53 in DNA damage-induced apoptosis. *Cancer research*. 2001 Sep 15;61(18):6660-4.
30. Liu L, Yuan G, Cheng Z, Zhang G, Liu X, Zhang H. Identification of the mRNA expression status of the dopamine D2 receptor and dopamine transporter in peripheral blood lymphocytes of schizophrenia patients. *PLoS One*. 2013;8(9):e75259. [CrossRef PubMed](#)



# Levofloxacin induces erythrocyte contraction leading to red cell death

Hafiz Muhammad Aslam<sup>1</sup>, Azka Sohail<sup>1</sup>, Ammara Shahid<sup>2</sup>, Maham Abdul Bari Khan<sup>3</sup>, Muhammad Umar Sharif<sup>3</sup>, Razia Kausar<sup>3</sup>, Samia Nawab<sup>4</sup>, Waqas Farooq<sup>5</sup>, Kashif Jilani<sup>1</sup>, Majeeda Rasheed<sup>6</sup>

<sup>1</sup>Department of Biochemistry, University of Agriculture, Faisalabad - Pakistan

<sup>2</sup>Department of Internal Medicine, Amna Anayat Medical College, Sheikhpura - Pakistan

<sup>3</sup>Department of Anatomy, Faculty of Veterinary Science, University of Agriculture, Faisalabad - Pakistan

<sup>4</sup>Department of Chemistry, Government Graduate College For Women, Township - Lahore

<sup>5</sup>Institute of Biomedical Sciences, Shanxi University, Taiyuan - China

<sup>6</sup>Department of Life Sciences, Khwaja Fareed University of Engineering and Information Technology Rahimyar Khan, Punjab - Pakistan

## ABSTRACT

**Background:** Levofloxacin, a fluoroquinolone, is an extensively used antibiotic effective against both positively and negatively staining bacteria. It works by inhibiting bacterial topoisomerase type II and topoisomerase type IV, resulting in impaired DNA synthesis and bacterial cell death. Eryptosis is another term for apoptotic cell death of erythrocyte marked by cell shrinkage, phosphatidylserine (PS) flipping, and membrane blebbing.

**Methods:** The intent of the present research was to look at the eryptotic effect of levofloxacin by exposing erythrocytes to therapeutical doses (7, 14  $\mu$ M) of levofloxacin for 48 hours. Cell size evaluation, PS subjection to outside, and calcium channel inhibition were carried out to investigate eryptosis. Oxidative stress generated by levofloxacin was measured as a putative mechanism of eryptosis using glutathione peroxidase (GPx), superoxide dismutase (SOD), and catalase activities. Similarly, hemolysis measurements demonstrated levofloxacin's cytotoxic effect.

**Results:** Our findings showed that therapeutic doses of levofloxacin can cause a considerable decline in antioxidant enzymes activities, as well as induce cell shrinkage, PS externalization, and hemolysis in erythrocytes. The role of calcium in triggering erythrocyte shrinkage was also confirmed.

**Conclusion:** In conclusion, our findings showed that the indicated levofloxacin doses caused oxidative stress, which leads to erythrocyte death via eryptosis and hemolysis. These findings emphasize the importance of using levofloxacin with caution and the need for additional research to mitigate these side effects.

**Keywords:** Eryptosis, Erythrocyte, Hemolysis, Levofloxacin, Oxidative stress

## Introduction

Levofloxacin is a third-generation antibiotic that belongs to the class of fluoroquinolones. It has more efficacy against positively staining bacteria and uncommon intracellular pathogens than prior generations of fluoroquinolones. Levofloxacin works by inhibiting bacterial type II topoisomerases, particularly the enzymes topoisomerase IV (Topo IV) and bacterial DNA gyrase. In human medicine, levofloxacin is used to treat acute rhinosinusitis, chronic bronchitis,

post-exposure inhalational anthrax, hospital-acquired infections and pneumonitis, urinary tract infections, inflammation of the prostate gland, and soft tissue or skin infection. The medicine levofloxacin is on the World Health Organization (WHO)'s list of essential medicines (1,2). In vivo and in vitro conditions levofloxacin has been demonstrated to have immunomodulatory properties by decreasing the synthesis and secretion of inflammatory cytokines (3). Nausea, vomiting, and diarrhea are among the most common side effects associated with levofloxacin. Central nervous system complications have also been reported from mild dizziness and headache to severe depression, hallucination, and seizures (4). Its widespread usage has been linked to several cases of clinically apparent liver injury. It has been proposed that reactive oxygen species (ROS) produced by the breakdown of vital mitochondrial enzymes, along with those released during RNA processing, gene transcription, and inflammatory processes, causes liver and kidneys to suffer from oxidative stress and cellular damage (5).

Received: March 1, 2024

Accepted: July 11, 2024

Published online: October 7, 2024

Corresponding author:

Majeeda Rasheed

email: [majeeda.rasheed@kfueit.edu.pk](mailto:majeeda.rasheed@kfueit.edu.pk)



The prior work using animal models demonstrated that fluoroquinolones were involved in the formation of reactive oxygen molecules, which is what causes oxidative stress (4). Oxidative stress is a shift in pro-oxidant and antioxidant balance in favor of oxidants, resulting in redox signaling/control disruption and molecular damage (6). ROS can be produced either exogenously by ultraviolet (UV) light, ionizing radiation, pollutants, and nitroaromatics or intracellularly by cytosolic enzyme systems during the course of a variety of physiological and biochemical processes (7). Moreover, levofloxacin was shown to increase lipid peroxidation, NO production, and superoxide dismutase (SOD) activity in cortex, corpus striatum, and hippocampus (8).

The normal lifespan of circulating erythrocytes is 100–120 days owing to erythrocyte aging. Prior to that, erythrocytes are rapidly removed from circulation (9). Eryptosis is the self-destruction of erythrocytes that eliminates old or superfluous erythrocytes from circulation, characterized by erythrocyte membrane perturbation, which results in the dismantling of plasma membrane symmetry and the exposure of phosphatidylserine flipping from the interior to the plasma membrane surface (10,11). Oxidative stress activates several factors that cause erythrocyte suicide, including opening of  $\text{Ca}^{+2}$  channels, caspase activation, and the formation of phospholipase A2 (PLA-2)-induced platelet-activating factor (PAF), which stimulate cellular ceramide generation through stimulating sphingomyelinase. Increased cytosolic  $\text{Ca}^{++}$  ions and ceramide levels cause phosphatidylserine exposure via membrane scrambling. Phosphatidylserine (PS)-exposed erythrocytes apparently attached to thrombospondin (TSP) are recognized by PS receptors such as PSR-1, and are removed from circulating blood. Furthermore, calcium stimulates Ca-sensitive  $\text{K}^{+}$  channel, which results in  $\text{KCl}$  loss with water that leads to cell shrinkage, and activates calpain, a protease, resulting in cytoskeleton destruction (9,12). A number of xenobiotics have been reported to induce eryptosis associated with the conditions such as anemia, diabetes, cancer, cardiovascular and liver complications, uremia, and chronic kidney disease (13,14). Levofloxacin-induced oxidative stress and anemia are rarely reported in the literature. This research was designed with the intention to look into the involvement of levofloxacin in the induction of eryptosis by oxidative stress. Isolated human red cells were given with therapeutic dosages of levofloxacin in order to evaluate its eryptotic, oxidizing, and hemolyzing or cytotoxic effects on red cells.

## Materials and methods

Noninfectious screened blood samples in heparin tubes were generously supplied by the blood bank at the Allied Hospital, Faisalabad. Leukocyte-free erythrocytes were isolated by depleting the white cells and plasma from the whole blood samples following the protocol of Fink et al. The whole blood samples were spun up at 1500 rpm for 15–20 minutes at 21°C and the leukocyte and platelet-rich afloat supernatant was discarded (15). The sorted red blood cells were put into microcentrifuge tubes, and they were incubated for 48 hours at 37°Celsius and pH 7.4 with a 0.4% hematocrit volume in Ringer solution that included

sodium chloride 125 mM, potassium chloride 5 mM, magnesium silicate 1 mM, HEPES sodium salt 32 mM, glucose 5 mM, and calcium chloride 1 mM (16). Erythrocytes were exposed to levofloxacin (Getz Pharma Pakistan) at the physiological concentrations (7, 14  $\mu\text{M}$ ). Levofloxacin was added from stock solution of 14 mM prepared by dissolving levofloxacin salt in dimethylsulfoxide (DMSO) and later diluted to get the required concentrations for the experiments.

## Oxidative stress measurement

Antioxidant enzyme assays (for glutathione peroxidase [GPx], catalase, and SOD) were conducted to assess the stress levels of erythrocytes exposed to levofloxacin.

### Superoxide dismutase

SOD activity was determined by using Naveed et al's protocol (17). The reaction mixture contained nitroblue tetrazolium (0.015 g in 17.5 mL d- $\text{H}_2\text{O}$ ), L-methionine (0.222 g in 15 mL d- $\text{H}_2\text{O}$ ), Triton-X-100 (0.0375 mL in 17.5 mL  $\text{H}_2\text{O}$ ), vitamin B2 rib (0.0132 g in 17.5 mL d- $\text{H}_2\text{O}$ ), and phosphate buffer of pH 7.4, 0.2 M. The spectrophotometer value of chromophore was taken at 525 nm.

### Glutathione peroxidase

Using the methodology described by Sattar et al (18), GPx enzyme activity was evaluated every 20 seconds at 470 nm using spectrophotometer in the reaction mixture containing guaiacol (Sigma-Aldrich; 20 mM), phosphate buffer of pH 5 (50 mM), hydrogen peroxide (40 mM), and 200  $\mu\text{L}$  enzyme extract.

### Catalase

The assessment of erythrocyte catalase activity followed the methodology outlined by Mukhtar et al (19). The reaction cocktail composed of phosphate buffer of pH 7.4 (50 mM) and 54  $\mu\text{L}$  of 5.9 nM hydrogen peroxide in 10 mL water. Equal proportions of sample and reaction solution were placed into a multiwell plate (96 wells), and the optical density measured at 240 nm using BioTek Quant.

### Cell size measurements

Variations in cell dimensions were ascertained by calculating the mean cellular volume (MCV) for both the controlled and levofloxacin-treated erythrocytes. The MCV was calculated using an HumaCount 5D hematology analyzer (Human GmbH, Wiesbaden, Germany), which provided estimated information on red blood cell volume and shape and size (20).

### Phosphatidylserine content

Concentration of externalized PS in levofloxacin-treated erythrocytes was measured using a human PS enzyme-linked immunosorbent assay (ELISA) kit (Elabscience, Beijing, People's Republic of China) according to the manufacturer's instructions. Absorbance was read at wavelength of 450 nm



on the BioTeK  $\mu$  Quant microplate reader and expressed as PS equivalents (mg/mL) (21).

### Confirmation of the role of $Ca^{++}$ ions

To validate the functional role of  $Ca^{++}$  in the initiation of eryptosis, the MCV of erythrocytes was evaluated using a hematology analyzer. Erythrocytes were treated with levofloxacin doses and 10  $\mu$ M of a calcium entry blocker (amlodipine) to ensure the involvement of calcium ions in levofloxacin-induced eryptosis (22).

### Measurement of hemolysis percentage

To validate levofloxacin's hemolytic effect on erythrocytes, controlled and levofloxacin-treated red cell samples were centrifuged at 400g for 3 minutes at 25°C to get the supernatant. The concentration of hemoglobin in supernatants was measured at 405 nm using LMSP-V310 visible spectrophotometer; 100% hemolysis was defined as the optical density of erythrocyte supernatant lysed in distilled water (23).

### Statistical analysis

The findings were presented with a mean standard error of mean ( $\pm$  SEM). Analysis of variance (ANOVA) with Tukey's test as a follow-up test was used for the statistical study where necessary (24). Statistical significance was considered as p-value <0.05.

### Results

The purpose of this study was to analyze levofloxacin's eryptotic effects by implementing the oxidative stress induction that is one of the eryptosis-stimulating mechanisms. To validate this, the antioxidant enzymatic activities, erythrocyte size, exposing of PS at the cell exterior, hemolytic activity, and substantiating the involvement of calcium in triggering the programmed cell death of erythrocytes were all evaluated. The findings of the research are showcased in graphs, featuring mean values  $\pm$ SEM with clear indications of statistical significance. The antioxidant enzyme activities in levofloxacin-treated and -nontreated cells (control group) were measured to see if levofloxacin induces oxidative stress. Figure 1 shows a notable decrease in SOD activity at 7 and 14  $\mu$ M levofloxacin compared to control cells. Figure 2 shows that 48 hours treatment with the mentioned drug concentrations resulted in a statistically substantial drop in GPx activity at 7 and 14  $\mu$ M doses compared with control groups. Similarly, Figure 3 shows that 48 hours of treatment with levofloxacin results in a relatively moderate decline at 7  $\mu$ M and highly significant decline at 14  $\mu$ M in catalase activity.

A substantial and statistically significant decrease in the MCV of red blood cells was observed after treatment with 7 and 14  $\mu$ M concentrations of levofloxacin for 48 hours (Fig. 4). Increased mean cell volume could be attributed to membrane bleb formation caused by levofloxacin-induced oxidative damage.

Results of PS exposure assay showed least absorbance in the control group, which indicates minor PS externalization,

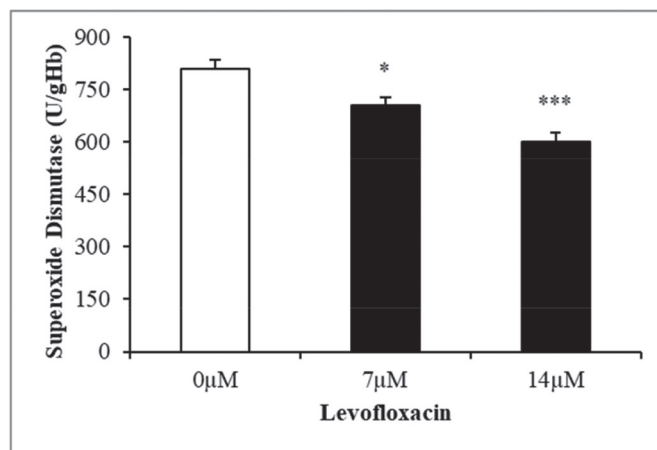


**FIGURE 1** - The effect of levofloxacin on superoxide dismutase activity in erythrocytes exposed to levofloxacin (measured in U/g Hb). Variations in erythrocyte responses (n = 15) are visible after 48 hours of incubation in Ringer's solution with varying concentrations of levofloxacin in black bars, with asterisks \* (p < 0.05) and \*\*\* (p < 0.0001) on the error bars indicating significant differences from the absence of levofloxacin in white bar (ANOVA). ANOVA = analysis of variance.

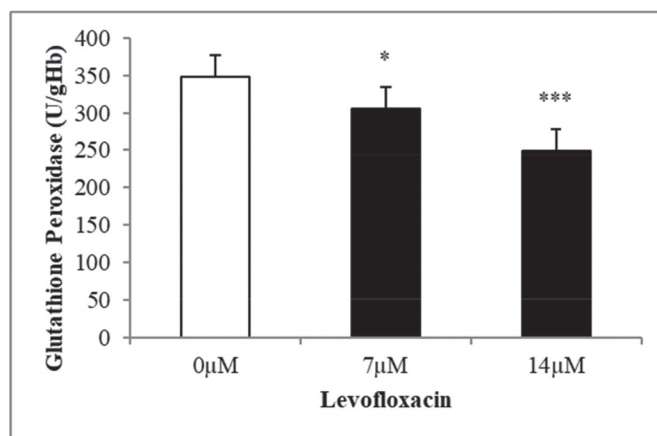


**FIGURE 2** - The effect of levofloxacin on glutathione peroxidase activity in erythrocytes exposed to levofloxacin (measured in U/g Hb). Variations in erythrocyte responses (n = 15) are visible after 48 hours of incubation in Ringer's solution with varying concentrations of levofloxacin in black bars, with asterisks \* (p < 0.05) and \*\*\* (p < 0.0001) on the error bars indicating significant distinctness from the absence of levofloxacin in white bar (ANOVA). ANOVA = analysis of variance.

while levofloxacin-exposed treatment groups showed increasing absorbance (p < 0.001) in both 7 and 14  $\mu$ M concentrations, reflecting increased PS exposure and suggesting higher levels of eryptosis. The standard curve was generated using the absorbance values of the known PS standards, which showed a linear relationship between absorbance and PS concentration (Fig. 5).

The calcium channel blocker amlodipine was employed to verify the effect of  $Ca^{++}$  in the elicitation of oxidative stress initiated by eryptosis in triggering the formation of

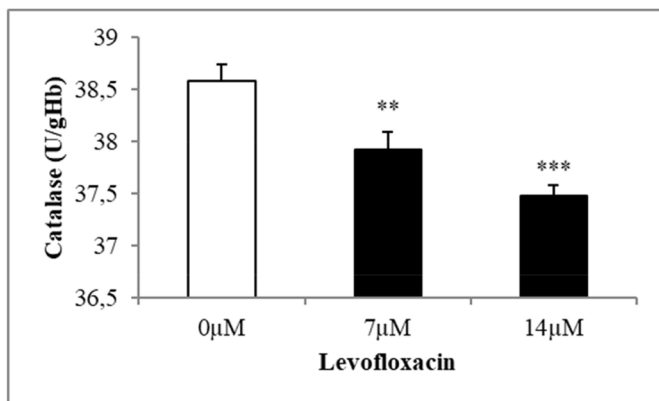


**FIGURE 3** - The effect of levofloxacin on catalase activity in erythrocytes exposed to levofloxacin (measured in U/g Hb). Variations in erythrocyte responses ( $n = 15$ ) are visible after 48 hours of incubation in Ringer's solution with varying concentrations of levofloxacin in black bars, with asterisks \*\*( $p < 0.01$ ) and \*\*\*( $p < 0.0001$ ) on the error bars indicating significant differences from the absence of levofloxacin in white bar (ANOVA). ANOVA = analysis of variance.

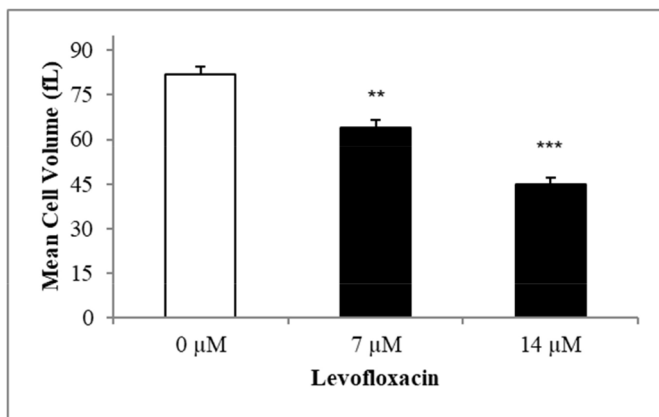


**FIGURE 4** - The effect of levofloxacin on erythrocyte mean cellular volume (fL). Mean  $\pm$  SEM ( $n = 10$ ) of erythrocytes incubated in Ringer's solution for 48 hours without levofloxacin in white bar and with levofloxacin concentrations (7, 14  $\mu$ M) in black bars. The Y-axis represents  $\pm$ SEM. \*\*( $p < 0.01$ ) and \*\*\*( $p < 0.001$ ) indicate a statistically significant distinction in groups treated with levofloxacin in comparison to the absence of levofloxacin (ANOVA). ANOVA = analysis of variance; SEM = standard error of the mean.

membrane blebs. Figure 6 showed noticeable rise in erythrocyte cell size dimensions when compared to cells that were free of amlodipine, which is most likely due to calcium entrance inhibition in the cells. This experiment revealed no shrinkage in the size of erythrocytes, due to the blockade of  $Ca^{++}$  channels confirming the significance of calcium in causing erythrocyte cell death. Figure 7 shows the findings of % hemolysis in levofloxacin-treated cells to confirm the hemolytic activity of levofloxacin. Figure 6 shows an increase in % hemolysis after 2 days of levofloxacin (14  $\mu$ M) exposure of erythrocytes.

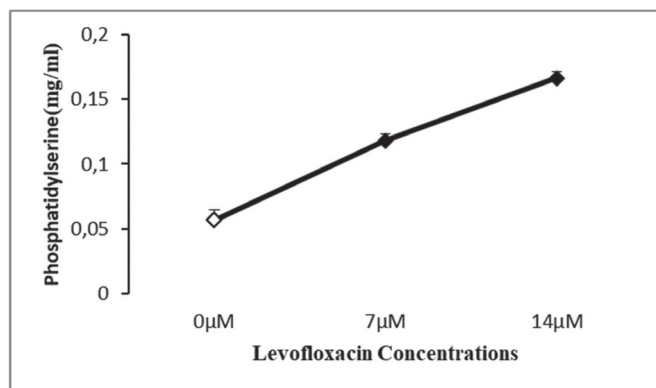


**FIGURE 5** - Effect of levofloxacin on phosphatidylserine content following incubation in Ringer's solution for 48 hours in the absence (control group) and presence of levofloxacin (7, 14  $\mu$ M).

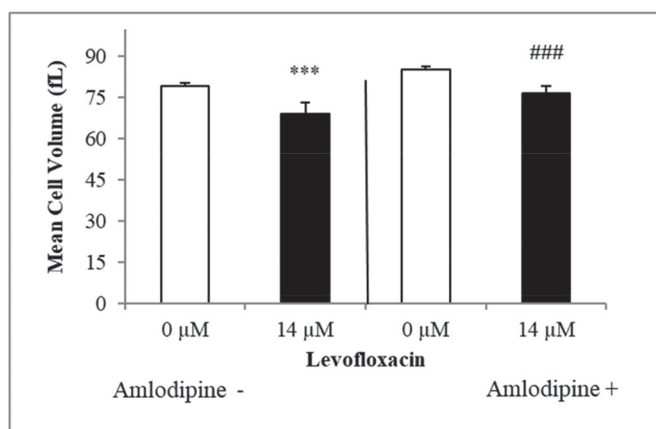


**FIGURE 6** - Measurement of erythrocyte mean cellular volume in the presence and absence of amlodipine following exposure to levofloxacin, represented by arithmetic mean  $\pm$  SEM ( $n = 10$ ) for erythrocyte incubated in Ringer's solution, with 14  $\mu$ M levofloxacin (in black bar) or without (in white bars) demonstrating a decrease in cell dimensions subsequent to amlodipine 10  $\mu$ M treatment (ANOVA) as indicated by \*\*\*( $p < 0.001$ ), ###( $p < 0.001$ ). ANOVA = analysis of variance; SEM = standard error of the mean.

In accordance with our research it was concluded that therapeutic dosages (7, 14  $\mu$ M) of levofloxacin may elevate the rate of erythrocyte elimination from the blood stream due to oxidative stress and calcium influx, leading to eryptosis and hemolyzing the red cells.

## Discussion

The intent of this study was to find the impact caused by levofloxacin on oxidative stress status and cell death of red blood cells. This objective of the study was achieved by investigating the antioxidant enzymes' status, cell dimensions, and the role of calcium in causing the programmed cell death of red cells. The levofloxacin concentrations (7, 14  $\mu$ M) employed in this investigation were the plasma concentration

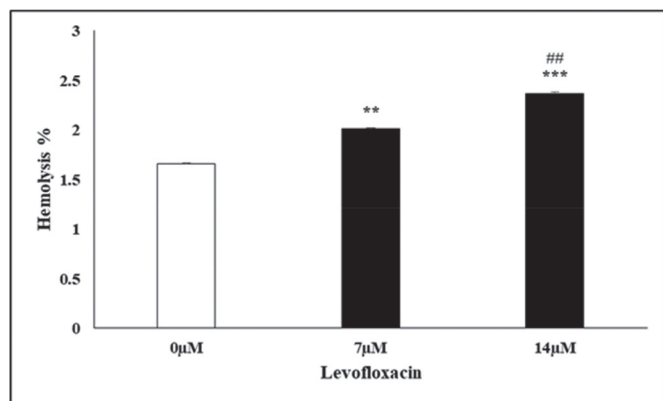


**FIGURE 7** - The % hemolysis effect of levofloxacin in red cells is shown. The arithmetic mean  $\pm$  SEM ( $n = 12$ ) for erythrocytes incubated in Ringer's solution with 7 and 14  $\mu\text{M}$  levofloxacin (in black bars) and without levofloxacin (in white bar) for 48 hours is presented, with the Y-axis indicating SEM. \*\* ( $p < 0.01$ ) and \*\*\* ( $p < 0.001$ ) served to emphasize notable differences in comparison to the absence of levofloxacin at 7 and 14  $\mu\text{M}$ , respectively (ANOVA), while ### reflects distinctions between the % hemolysis at 7 and 14  $\mu\text{M}$  levofloxacin concentration. ANOVA = analysis of variance; SEM = standard error of the mean.

reported by Fish and Chow (25). One of the primary drivers of eryptosis is oxidative stress (14), and increasing oxidative damage leads to a drop in the activities of free radical scavenger enzymes (26). The impairment in enzymatic activity of SOD could be predictive of the heightened superoxide radical concentrations, as SOD efficiently catalyzes the conversion of oxygen into  $\text{H}_2\text{O}_2$ . A decrease in SOD activity was also evaluated by repeated oral administration of levofloxacin and other fluoroquinolones in rabbits (27). Similar effect was also reported on hepatic and renal tissues of rat due to exposure of levofloxacin (28).

The experiment revealed a moderate (at 7  $\mu\text{M}$ ) and notable reduction (at 14  $\mu\text{M}$ ) in GPx activity, which might be blamed on the formation of ROS. In a related research under stress red cells, a substantial endogenous rate of  $\text{H}_2\text{O}_2$  synthesis from hemoglobin autoxidation was observed. GPx catalyzed a reaction by which glutathione is oxidized to detoxify hydrogen peroxide. Increasing oxidative stress ultimately leads to demise in GPx activity. The reduced enzyme activity is due to a decrease in glutathione concentration (29). Calderón-Salinas et al (30) reported that oxidative stress made the red cell to expose PS outside, which also decreases erythrocyte count.

Catalase activity was also seen to be declined in the present study in levofloxacin-treated erythrocytes compared with controlled groups. The decreased catalase activity might be due to peroxidative damage to lipids and injury to cellular components by levofloxacin-induced oxidative insult. Parallel results were also reported by Khan et al (27) and Farid and Hegazy (31).

Erythrocyte shrinkage and PS externalization on the erythrocyte membrane are two eryptotic markers. The high PS exposure on the outer leaflet of erythrocyte's plasma

membrane in levofloxacin-treated erythrocytes indicates that levofloxacin exposure leads to increased eryptosis. Obtained data showed significant increase in PS externalization in levofloxacin-treated erythrocytes while control group showed negligible PS exposure. Thus, increasing concentrations of levofloxacin lead to higher PS exposure, which is the main indicator of eryptosis (16). A decrease in mean cell volume confirms stimulated eryptosis (24). The activation of a calcium influx channel in red blood cells by oxidative stress results in considerable erythrocyte shrinkage (13). This action is believed to be triggered by  $\text{Ca}^{2+}$ -dependent  $\text{K}^+$  channel activation in the erythrocyte's membrane, which results in increased polarization of membrane and eventual  $\text{K}^+$  loss followed by  $\text{Cl}^-$  in the erythrocyte (32). Our results showed apparent difference in cell shrinkage in amlodipine-treated and -nontreated erythrocytes, which confirms the role of calcium ions in triggering characteristic cell shrinking of eryptotic erythrocytes.

Eryptosis has an important physiological influence on the disposal of faulty erythrocytes prior to hemolysis (33). Hemoglobin flows out from hemolyzed cells that may be contrarily filtered in the glomerulus and clog the renal tubules (34). Our results showed a high increase in % hemolysis (Fig. 6) after 48 hours of levofloxacin exposure to erythrocytes at 7 and 14  $\mu\text{M}$ . The release of erythrocyte contents, particularly hemoglobin, during hemolysis reduces NO bio-availability. This may lead to vasomotor instabilities, systemic vasoconstriction, and endothelial dysfunction, as well as crucial clinical problems such as hypertension, respiratory issues, cardiovascular disorders, impaired renal function, inflammation, coagulation, and vulnerability to infections (35).

#### Data Availability Statement

The data that support the findings of this study are available from the corresponding author upon reasonable request.

#### Acknowledgments

Acknowledge the support and guidance of the researchers and mentors at the Department of Biochemistry, University of Agriculture Faisalabad.

#### Disclosures

**Financial support:** The author(s) received no financial support for the research, authorship, and/or publication of this article.

**Conflict of interest:** The authors declare no conflict of interest.

#### References

1. Trespalacios-Rangél AA, Otero W, Arévalo-Galvis A, Poutou-Piñales RA, Rimbara E, Graham DY. Surveillance of levofloxacin resistance in *Helicobacter pylori* isolates in Bogotá-Colombia (2009-2014). PLoS One. 2016;11(7):e0160007. [CrossRef PubMed](#)
2. Sitovs A, Sartini I, Giorgi M. Levofloxacin in veterinary medicine: a literature review. Res Vet Sci. 2021;137:111-126. [CrossRef PubMed](#)
3. Zusso M, Lunardi V, Franceschini D, et al. Ciprofloxacin and levofloxacin attenuate microglia inflammatory response via

- TLR4/NF- $\kappa$ B pathway. *J Neuroinflammation*. 2019;16(1):148. [CrossRef PubMed](#)
4. Talla V, Veerareddy P. Oxidative stress induced by fluoroquinolones on treatment for complicated urinary tract infections in Indian patients. *J Young Pharm*. 2011;3(4):304-309. [CrossRef PubMed](#)
  5. Abdullah RA, Taeq FD, Thanoon IA. Effect of levofloxacin on some body tissues in mice. *Iraqi J Vet Sci*. 2021;35(1):109-111. [CrossRef](#)
  6. Sies H. The concept of oxidative stress after 30 years. In: Gelpi R, Boveris A, Poderoso J, eds. *Biochemistry of oxidative stress. Advances in biochemistry in health and disease*. vol 16. Cham: Springer; 2016. [CrossRef](#)
  7. Haider K, Haider MR, Neha K, Yar MS. Free radical scavengers: an overview on heterocyclic advances and medicinal prospects. *Eur J Med Chem*. 2020;204:112607. PubMed PMID:32721784 [CrossRef PubMed](#)
  8. Mani S, Tyagi S, Pal KV, et al. Drug-induced oxidative stress and cellular toxicity. In: Kesari KK, Jha NK, eds. *Free radical biology and environmental toxicity*. Springer; 2022: 73-113. [CrossRef](#)
  9. Lang F, Jilani K, Lang E. Therapeutic potential of manipulating suicidal erythrocyte death. *Expert Opin Ther Targets*. 2015;19(9):1219-1227. [CrossRef PubMed](#)
  10. Pyrshev KA, Klymchenko AS, Csúcs G, Demchenko AP. Apoptosis and eryptosis: striking differences on biomembrane level. *Biochim Biophys Acta Biomembr*. 2018;1860(6):1362-1371. [CrossRef PubMed](#)
  11. Dreischer P, Duszenko M, Stein J, Wieder T. Eryptosis: programmed death of nucleus-free, iron-filled blood cells. *Cells*. 2022 Feb 1;11(3):503. [CrossRef PubMed](#)
  12. Lang F, Lang KS, Lang PA, Huber SM, Wieder T. Mechanisms and significance of eryptosis. *Antioxid Redox Signal*. 2006; 8(7-8):1183-1192. [CrossRef PubMed](#)
  13. Lang F, Gulbins E, Lerche H, Huber SM, Kempe DS, Foller M. Eryptosis, a window to systemic disease. *Cell Physiol Biochem*. 2008;22(5-6):373-380. [CrossRef PubMed](#)
  14. Pretorius E, du Plooy JN, Bester J. A comprehensive review on eryptosis. *Cell Physiol Biochem*. 2016;39(5):1977-2000. [CrossRef PubMed](#)
  15. Fink M, Al Mamun Bhuyan A, Zacharopoulou N, Lang F. Stimulation of eryptosis, the suicidal erythrocyte death, by costunolide. *Cell Physiol Biochem*. 2018;50(6):2283-2295. [CrossRef PubMed](#)
  16. Bissinger R, Malik A, Jilani K, Lang F. Triggering of erythrocyte cell membrane scrambling by salinomycin. *Basic Clin Pharmacol Toxicol*. 2014;115(5):396-402. [CrossRef PubMed](#)
  17. Naveed A, Jilani K, Siddique AB, et al. Induction of erythrocyte shrinkage by omeprazole. *Dose Response*. 2020 Aug 3;18(3): 1559325820946941. [CrossRef PubMed](#)
  18. Sattar T, Jilani K, Parveen K, Mushataq Z, Nawaz H, Khan MAB. Induction of erythrocyte membrane blebbing by methotrexate-induced oxidative stress. *Dose Response*. 2022 Apr 13;20(2):15593258221093853. [CrossRef PubMed](#)
  19. Mukhtar F, Jilani K, Bibi I, Mushataq Z, Bari Khan MA, Fatima M. Stimulation of erythrocyte membrane blebbing by bifenthrin induced oxidative stress. *Dose Response*. 2022 Mar 3;20(1): 15593258221076710. [CrossRef PubMed](#)
  20. Ilyas S, Jilani K, Sikandar M, et al. Stimulation of erythrocyte membrane blebbing by naproxen sodium. *Dose Response*. 2020;18(1):1559325819899259. [CrossRef PubMed](#)
  21. Burger D, Turner M, Xiao F, et al. High glucose increases the formation and pro-oxidative activity of endothelial microparticles. *Diabetologia*. 2017;60:1791-1800. [CrossRef](#)
  22. Shabir K, Jilani K, Zbidah M, et al. Triggering of erythrocyte membrane blebbing by ciprofloxacin. *Acta Pol Pharm*. 2019;76(5):901-906. [CrossRef](#)
  23. Mischitelli M, Jemaà M, Almasry M, Faggio C, Lang F. Triggering of erythrocyte cell membrane scrambling by emodin. *Cell Physiol Biochem*. 2016;40(1-2):91-103. [CrossRef PubMed](#)
  24. Lupescu A, Bissinger R, Jilani K, Lang F. Triggering of suicidal erythrocyte death by celecoxib. *Toxins*. 2013;5(9):1543-1554. [CrossRef](#)
  25. Fish DN, Chow AT. The clinical pharmacokinetics of levofloxacin. *Clin Pharmacokinet*. 1997;32(2):101-119. [CrossRef PubMed](#)
  26. Vaziri ND, Dicus M, Ho ND, Boroujerdi-Rad L, Sindhu RK. Oxidative stress and dysregulation of superoxide dismutase and NADPH oxidase in renal insufficiency. *Kidney Int*. 2003;63(1):179-185. [CrossRef PubMed](#)
  27. Khan AM, Rampal S, Sood NK. Effect of repeated oral administration of levofloxacin, enrofloxacin, and meloxicam on antioxidant parameters and lipid peroxidation in rabbits. *Hum Exp Toxicol*. 2017;36(1):42-50. [CrossRef PubMed](#)
  28. Olayinka ET, Ore A, Ola OS. Influence of different doses of levofloxacin on antioxidant defense systems and markers of renal and hepatic dysfunctions in rats. *Adv Toxicol*. 2015. [CrossRef](#)
  29. Waggiallah H, Alzohairy M. The effect of oxidative stress on human red cells glutathione peroxidase, glutathione reductase level, and prevalence of anemia among diabetics. *N Am J Med Sci*. 2011;3(7):344-347. [CrossRef](#)
  30. Calderón-Salinas JV, Muñoz-Reyes EG, Guerrero-Romero JF, et al. Eryptosis and oxidative damage in type 2 diabetic mellitus patients with chronic kidney disease. *Mol Cell Biochem*. 2011;357(1-2):171-179. [CrossRef PubMed](#)
  31. Farid AS, Hegazy AM. Ameliorative effects of *Moringa oleifera* leaf extract on levofloxacin-induced hepatic toxicity in rats. *Drug Chem Toxicol*. 2020;43(6):616-622. [CrossRef PubMed](#)
  32. Lang KS, Duranton C, Poehlmann H, et al. Cation channels trigger apoptotic death of erythrocytes. *Cell Death Differ*. 2003;10(2):249-256. [CrossRef PubMed](#)
  33. Charras GT, Coughlin M, Mitchison TJ, Mahadevan L. Life and times of a cellular bleb. *Biophys J*. 2008 Mar 1;94(5):1836-1853. [CrossRef PubMed](#)
  34. Harrison HE, Bunting H, Ordway NK, Albrink WS. The pathogenesis of the renal injury produced in the dog by hemoglobin or methemoglobin. *J Exp Med*. 1947;86(4):339-356. [CrossRef PubMed](#)
  35. Rapido F. The potential adverse effects of haemolysis. *Blood Transfus*. 2017 May;15(3):218-221. [CrossRef PubMed](#)



# Cytotoxic activity, selectivity, and clonogenicity of fruits and resins of Saudi medicinal plants against human liver adenocarcinoma

Ali Hendi Alghamdi<sup>1</sup>, Aimun A.E. Ahmed<sup>2,3</sup>, Mahadi Bashir<sup>1</sup>, Haidar Abdalgadir<sup>4</sup>, Asaad Khalid<sup>5</sup>, Mohamed E. Abdallah<sup>6</sup>, Riyad Almaimani<sup>6</sup>, Bassem Refaat<sup>7</sup>, Ashraf N. Abdalla<sup>8,9</sup>

<sup>1</sup>Surgery Department, Faculty of Medicine, Al-Baha University, Al Baha - Saudi Arabia

<sup>2</sup>Pharmacology Department, Faculty of Medicine, Al-Baha University, Al Baha - Saudi Arabia

<sup>3</sup>Pharmacology Department, Faculty of Pharmacy, Omdurman Islamic University, Khartoum - Sudan

<sup>4</sup>Biology Department, Faculty of Science, Al-Baha University, Al Baha - Saudi Arabia

<sup>5</sup>Substance Abuse and Toxicology Research Center, Jazan University, Jazan - Saudi Arabia

<sup>6</sup>Department of Biochemistry, Faculty of Medicine, Umm Al-Qura University, Makkah - Saudi Arabia

<sup>7</sup>Laboratory Medicine Department, Faculty of Applied Medical Sciences, Umm Al-Qura University, Makkah - Saudi Arabia

<sup>8</sup>Department of Pharmacology and Toxicology, College of Pharmacy, Umm Al-Qura University, Makkah - Saudi Arabia

<sup>9</sup>Department of Pharmacology and Toxicology, Medicinal and Aromatic Plants Research Institute, National Center for Research, Khartoum - Sudan

## ABSTRACT

**Background:** Edible fruits and resins provide various benefits to mankind including potential medicinal applications. This study aimed to determine the cytotoxicity, selectivity, and clonogenicity of fruits and exudates of certain Saudi medicinal plants (*Anethum graveolens* (BEP-09), *Opuntia ficus-indica* (L.) Miller (BEP-10), *Boswellia serrata* Roxb. ex Colebr. (BEP-11), and *Commiphora myrrha* (BEP-12)) against human liver adenocarcinoma (HepG2).

**Methods:** Initial cytotoxicity and cell line selectivity against different cell lines were screened using MTT assay. The most promising extract was subjected to gas chromatography-mass spectrometry (GC-MS) analysis to determine the main phytoconstituents. Clonogenicity was checked for the most active extract.

**Results:** The selected plants' fruits and resins possess a significant cytotoxic activity estimated as  $IC_{50}$ . The fruit of BEP-10 was found to be the most active extract against liver cancer cells ( $IC_{50} = 2.82$ ) comparable to both doxorubicin ( $IC_{50} = 1.40$ ) and camptothecin ( $IC_{50} = 1.11$ ). It showed a selectivity index of 4.47 compared to the normal human foetal lung fibroblast (MRC5) cells. BEP-10 showed a dose-dependent clonogenic effect against HepG2 cells comparable to the effect of doxorubicin. The GC-MS chromatogram of BEP-10 extract revealed the presence of eight small polar molecules, representing 73% of the total identified compounds and the rest three molecules (27%) were non-polar constituents. The furan derivatives represent the chief components in BEP-10 (16.3%), while the aldehyde 5-(hydroxymethyl)-2-furancarboxaldehyde was found to be the main molecule (13.2%).

**Conclusion:** The fruits of BEP-10 have a potential cytotoxic effect particularly against HepG2. The identified phytoconstituents in the tested plant extract might contribute to the investigated cytotoxic activity.

**Keywords:** Clonogenicity, Cytotoxicity, MTT assay, *Opuntia ficus-indica*, Saudi plants, Selectivity index

## Introduction

*Anethum graveolens* L. is a member of the Apiaceae family locally known as Shabat-sanout. This plant has a long history of use as a spice in our food, where its seeds and leaves

are used as flavouring agents. It is an erect, robust, and rather glabrous annual aromatic herb. The leaves are three to four pinnate, with the ultimate segments narrowly linear to filiform. The flowers are yellow, and appear in umbels, with an elliptic cremocarp. It has been recognized in different systems of traditional medicine for the treatment of different diseases and ailments of humans. The plant is used as an antispasmodic, carminative, and anti-inflammatory. It is also used as medicine for loss of appetite, cough and cold, menstrual cramps, liver problems, oral care, strengthening the immune system, protection against bone degradation, and urinary tract disorders (1). The antioxidant and anticancer activities of *A. graveolens* were investigated in human,

Received: June 16, 2024

Accepted: September 18, 2024

Published online: October 22, 2024

### Corresponding author:

Ali Hendi Alghamdi  
email: [drahendi2030@gmail.com](mailto:drahendi2030@gmail.com)



lung, breast, and cervical carcinoma cell lines (2-4). Nam et al (5) studied the anti-inflammatory and protective properties of *A. graveolens* (dill seeds) on oesophageal mucosal damage in rats induced by reflux esophagitis and revealed good physiological activity and the possibility of being used as a medicinal, food, and functional resource for the prevention and therapy of gastro-oesophageal disorders. A systematic review and meta-analysis of randomized controlled trials investigated the effects of *A. graveolens* (dill) supplementation on lipid profile and glycaemic control, showing that *A. graveolens* could provide favourable effects on insulin resistance and serum low-density lipoprotein (6). The anthelmintic action of *A. graveolens* essential oil was found to be a promising alternative in the control of sheep gastrointestinal nematodes (7). Khare (8) reported that it was used for eye problems.

*Opuntia ficus-indica* (L.) Miller is a member of the family of Cactaceae locally known as ElBarshoumy–El TeenElShawki. It is a shrub or arborescent. Leaves are subulate and deciduous. Fruits are ellipsoidal or obovoid, red, yellow to orange, fleshy, edible. The plant is widely distributed in the south and the southwest of Saudi Arabia. It is widely known for its beneficial properties (9). Historically it was used as food for humans and farm animals and in folk medicine due to its nutritional properties and beneficial activities (10). Traditional medicine has used many plant extracts for human and animal wellness, due to their beneficial properties in wound healing and skin. In this regard, the study of Trombetta et al (11) is most helpful. Traditionally it was used as a treatment for gastritis, hyperglycaemia, hypercholesterolaemia, arteriosclerosis, diabetes, and prostatic hypertrophy, and it also has hypolipidaemic action and immune regulation function in the gastrointestinal tract (12). The protective properties of various plant extracts on airway inflammation related to exposure to PM10 and diesel exhaust particles were evaluated in mice (13). The antioxidants of *O. ficus-indica* as important inhibitors of free radical formation were reported by Castañeda-Arriaga et al (14), as well as antioxidants and inhibition of the sugar digestive enzyme activities of polyphenols by in vitro experiments (15). The powder of peel and seed of the plant efficiently removes the aqueous manganese cations (16). The gums were used to improve the quality of breads and cakes (17). The phenolic phytoconstituents, antioxidant and antiacetylcholinesterase activities of *O. ficus-indica* peel and flower teas were evaluated after in vitro gastrointestinal digestion (18). It modulates the intestinal microbiome in obese women and improves host metabolism (19). Polysaccharides from *O. ficus-indica* showed a regulating effect on intestinal flora of cyclophosphamide-induced immunosuppressed mice by effectively increasing the white blood cell count index and improving their thymus and spleen, while effectively promoting the secretion of interleukin (IL)-4, IL-1beta, tumour necrosis factor (TNF)-alpha and interferon (IFN)-gamma (20). Indicaxanthin isolated from fruits enhances glucose dysmetabolism and reduces insulin resistance in mice fed the high-fat diet (21).

*Boswellia serrata* Roxb. ex Colebr. belongs to the Burseraceae family locally known as luban-Kundur. These are moderate to large deciduous trees. They have papery flakes of bark and “yellowish green resin” inside. Leaves are

compound and alternate. Flowers are white and are distributed in southern Saudi Arabia.

The extract of *B. serrata* exhibited a potential effect in protecting the intestinal epithelium compared to lipopolysaccharide (LPS)-stimulated cells (22,23). The diuretic activity of gum extract in albino rats was investigated (24,25) and significant diuretic, kaliuretic, and natriuretic effects were observed. Synergistic antimicrobial activity of essential oil from *B. serrata* was studied with various azoles against azole-resistant strains of *Candida albicans* pathogens (26). The plant was used as a culture medium for micropropagation and as a natural source of nonsteroidal anti-inflammatory and antiarthritic agents (27). The antianaphylactic and mast cell stabilizing effects of boswellic acid have been assessed on passive paw anaphylaxis and revealed potential immunomodulatory activity (28). Recently, *Boswellia* spp. and its isolated bioactive phytoconstituents were traditionally used to treat chronic disease, inflammation, oral health, and microbial infection (29). Gum is traditionally used for the treatment of various inflammations that affect the skin, gums, eye, gastrointestinal tract (GIT) in addition to respiratory inflammation disorders such as bronchitis, asthma, laryngitis, etc. (30).

*Commiphora myrrha* (Nees) Engl. belongs to the Burseraceae family, locally known as El Murr Elihejazi. These are spiny, deciduous, almost shrub or small tree, with short thorns, producing a hard translucent yellowish gum resin. Leaves are green to greyish or glaucous, variable in shape, and minute in size. Native to Saudi Arabia, the plant is traditionally used as an anti-inflammatory and in the treatment of infectious diseases, making it a very popular and valuable alternative and traditional medicine (31,32). It was found to heal wounds, ulcers, and various diseases of the pulmonary, GIT, and urinary system (33).

Furanodienone and curzerene are bioactive components detected in the oil of the resinous exudate of *C. myrrha* that were tested and found to influence the spread of viruses by intervening at different stages of the virus life cycle (34). The antiosteoporotic effects of *C. myrrha* and its polysaccharide were inhibited through osteoclastogenesis (35). Sesquiterpenoids and its phytoconstituents isolated from the resinous exudate of *C. myrrha* were found to inhibit the migration of human hepatocellular liver carcinoma cells (HepG2) according to a dose-dependent pattern (36). A pilot study revealed that *C. myrrha* has significant analgesic properties (37). A combination of herbs (*Commiphora mukul*, *C. myrrha*, and *Terminalia chebula*) functions as an antioxidant, hypolipidemic, and antidiabetic substance; it could be recommended as a helpful herbal remedy for those with diabetes (38). The ethanolic extract of the resin of *C. myrrha* showed anti-obesity potential (39). It showed a hepatoprotective effect against D-GalN/LPS-induced liver injury in a rat model through multiple pathways (40). Murr (*C. myrrha*) is beneficial in treating eye diseases, as kahl forms in ulcers of the eye with other drugs. In Unani medicine, Murr is applied as a mixture with aabe mooli (radish juice) to eyes for cataracts, where the eyes are cleaned after dissolving murr in milk and in infraorbital haemorrhage (41-44).

Tumour-related destructive autoimmune responses can affect the eye, where autoantibody-mediated destruction

of retinal cells is induced by ectopic expression of peripheral tumour-related ocular antigens (45). Neuroendocrine tumours can metastasize to the orbits of the eyes of the midgut carcinoid (46). In the Philippines, the majority of conjunctival, eyelid, and orbit tumours were benign, and retinoblastoma was the most prevalent type of intraocular tumour, while the majority of them were malignant (47). An update is needed to reorient the way to predict the prognosis of paediatric cancers, such as rhabdomyosarcoma and retinoblastoma, and also adult cancers, such as uveal melanoma and lymphomas, and the benefit of targeted therapies, immunotherapy, or even chemotherapy (48).

Fruits and resins are usually used as nutritional supplements and are rarely used for medical purposes. Attempts are being made to look for the constituents of the plant that can prevent and reverse cancer. In this study, *in vitro* anti-cancer activity and cell line selectivity of two fruits and two resins were studied in three different cell lines, while clonogenicity was investigated against HepG2. Furthermore, the most promising extract was subjected to gas chromatography-mass spectrometry (GC-MS) analysis to determine the main active phytoconstituent(s).

## Materials and methods

### Phytochemical studies

#### Identification of plant materials

Four plants – *A. graveolens* (fruit, coded as BEP-09), *O. ficus-indica* (fruit, BEP-10), *B. serrata* (resin, BEP-11), and *C. myrrha* (resin, BEP-12) (Fig. 1) – were identified and taxonomically classified by an expert taxonomist (Dr. Mohamed, HAA, Department of Biology, Faculty of Sciences, Al-Baha University) and were compared to herbarium materials and different volumes of the flora of Saudi Arabia (49-51). Voucher herbarium specimen numbers (BUH-76,77,78, and 79) were deposited at the Department of Biology of the Faculty of Science of Al-Baha University.



**FIGURE 1** - *Opuntia ficus-indica* (L.) Miller (BEP-10) grows in the Al-Baha area, KSA.

### Collection and extraction of plant materials

Plant specimens were collected from different sites in Baljurashi province (Wadi El khaitan), Al-Baha area, in April 2021. Fruits (1 kg) and resins (1 kg) were shade-dried and then powdered using a mechanical grinder. The dried materials were macerated in 80% ethanol v/v for 1 week at room temperature. The resulting residues were filtered, pooled, and evaporated to dryness to provide viscous green to brownish syrups. The crude extracts, so obtained, were transferred to a Petri plate, allowed to dry, and finally weighed.

The percentage of yield was calculated using the formula:  $\text{yield\%} = (\text{Afforded extract weight}) / (\text{Air-dried weight}) \times 100$ .

The plants yielded extracts weighing 1.53, 1.73, 1.62, and 2.17 g, respectively.

### GC-MS analysis

The dried fruits of *O. ficus-indica* (L.) Miller (BEP-10) were dissolved in methanol to reach a concentration of 1 mg/mL and diluted 1:10 v/v in methanol (100 µg/mL). The diluted sample was analysed using a GC-MS instrument (Thermo Scientific, USA) attached to a trace ultra-GC and ISQ detector and an AS 3000 autosampler. The separation of components was carried out using a TR-5MS column (Thermo Scientific, USA) with a length of 30 cm, a diameter of 0.25 mm, and a film thickness of 0.25 mm. Helium was used as a carrier gas at 1.2 mL/min with constant flow. The injection port was set at 32°C for 5 minutes, followed by a ramp to 205°C at a rate of 5°C/min and a hold time of 5 minutes. This was followed by a ramp to 280°C at a rate of 5°C/min and hold time of 5 minutes and at the end to 300°C at a rate of 5°C/min and a hold time of 5 minutes. The maximum oven temperature was set at 320°C. A volume of 2 µL diluted extract was injected into the system in split mode with the mass spectrometer run in electron ionization mode with 0.6 scan periods throughout the mass range of 60-900 amu (minutes). Both the temperature of the MS ion source and the transfer line were adjusted to 320°C and 350°C, respectively, using a 1 kV electron multiplier voltage.

### Identification of phytoconstituents

Xcalibur software was used for mass spectral data analysis and the fragmentation patterns of each constituent were matched with MS data in the instrument database and built-in libraries including MAINLIB, NIST, and REPLIB. The phytochemicals present in the extract were identified by comparing them with the structures available in the computer library, and the percent abundance of each component was determined using the peak area as reference. The reported biological properties of the detected compounds are based on data from Duke's Phytochemical and Ethnobotanical Database (52).

### Cancer cell studies

#### Cancer cell culture

In this study, three cancer cell lines, MCF7 (human breast adenocarcinoma), HT29 (human colorectal adenocarcinoma),

and HepG2 (human liver adenocarcinoma), were used, in addition to MRC5 (normal human foetal lung fibroblast), all were from American Type Culture Collection (ATCC), USA. Three cancer cells were subcultured in RPMI-1640 medium (10% foetal bovine serum (FBS)), while MRC5 was preserved in Eagle's Minimum Essential Medium (EMEM, 10% FBS) – all at 37°C, 5% CO<sub>2</sub>, and 100% relative humidity, for a maximum of 5-10 passages.

#### Cytotoxicity and selectivity studies

The cytotoxic effect of four extracts, in addition to doxorubicin and camptothecin, was evaluated by the MTT assay, as reported by Alsanosy et al (53) and Abdalla et al (54). Each cell line was cultured separately in 96 wells (3 × 10<sup>3</sup>/well) and incubated with each of the extracts or doxorubicin at a final concentration of 0-100 µg/mL, for 3 days at 37°C overnight (dimethyl sulfoxide (DMSO) 0.1%; n = 3 of three independent experiments). After 3 days of incubation, the cytotoxicity of each extract was evaluated using an MTT assay. MTT was added to each well in culture medium at a concentration of 0.5 mg/mL and incubated for 3 hours at 37°C. The MTT solution was removed and the formazan granules were dissolved by DMSO. The absorbance was read on a multiplate reader (BIORAD, PR 4100, Hercules, CA, USA). The optical density of the purple formazan A<sub>550</sub> is proportional to the number of viable cells. The extract concentration causing 50% inhibition (IC<sub>50</sub>), compared to the control group, 100% cell growth, was estimated using GraphPad Prism. The selectivity index (SI) for the five extracts was calculated by dividing its IC<sub>50</sub> for MRC5 cells by the IC<sub>50</sub> for MCF7, HT29, or HepG2 cells.

#### Clonogenic assay

The clonogenic assay measures tumour cell survival and subsequent proliferative ability after drug exposure (55). The extract (BEP-10) was selected for a further clonogenic test, as it showed the highest selectivity to the normal cell line MRC5. Exponentially growing HepG2 cells in DMEM (supplemented with 10% FBS and 1% penicillin/streptomycin) were seeded in duplicates at a density of 200 cells/well in a 6-well plate and allowed to attach overnight and then exposed to an increasing concentration of BEP-10 (0, 0.75, 1.5, 2.25 µg/mL) for 72 hours. The wells containing the extract were then replaced with fresh media without the extract. The cells were left to grow at 37°C, 5% CO<sub>2</sub>, and 100% humidity. Daily wells were checked and the cells that form colonies were roughly counted. After 14 days, plates were rinsed in phosphate-buffered saline and fixed with pre-chilled methanol at room temperature for 20 minutes, then stained with 0.5 methylene blue in 1:1 methanol/H<sub>2</sub>O (v/v) for 10 minutes, washed thoroughly in dH<sub>2</sub>O, and air dried. Cell colonies were counted and recorded macroscopically.

#### Ethics approval of the study

According to the standards of Al-Baha University, all funded project proposals have undergone a critical review followed by approval by relevant scientific research committees before acceptance.

## Results

### Phytochemical studies

The four plant extracts produced the following yields: BEP-09 (15.3%), BEP-10 (17.3%), BEP-11 (16.2%), and BEP-13 (21.7) from fruits and resins (Fig. 2).

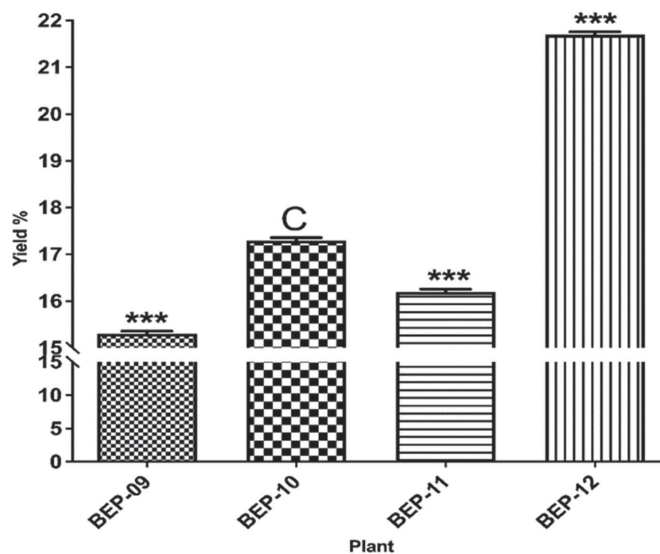


**FIGURE 2** - Yield % of dry extracts obtained after ethanolic extraction and evaporation of four different selected plants. C; control, \*\*\*, p < 0.001.

### Identification of phytoconstituents using GC-MS

Investigation of the GC-MS chromatogram (see the supplementary file) of the fruits of the Miller plant *O. ficus-indica* (L.) (BEP-10 extract) indicated the presence, mainly, of eight small polar molecules (18) (Tab. 1 and Fig. 3).

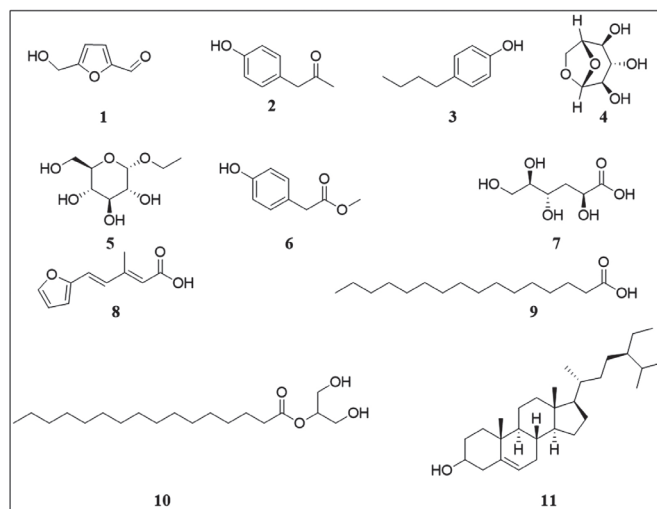


**FIGURE 3** - Structures of chemical constituents identified by gas chromatography-mass spectrometry for the fruits of *Opuntia ficus-indica* (L.) Miller (BEP-10 extract).

**TABLE 1** - Phytoconstituents identified by GC-MS analysis of the extract of *Opuntia ficus-indica* (L.) Miller (BEP-10)

Compound	Formula	Molecular weight	Peak area (%)	Retention time (minutes)	Biological activity
(1) 5-(hydroxymethyl)-2-furancarboxaldehyde	C <sub>6</sub> H <sub>6</sub> O <sub>3</sub>	126.11	13.2	5.875	Known to be associated with antimicrobial properties (56) used as an antifungal (57)
(2) 1-(4'-Hydroxyphenyl)-2-propanone	C <sub>9</sub> H <sub>10</sub> O <sub>2</sub>	150.17	2.52	7.752	Exhibits a myriad of pharmacological actions, such as antimicrobial, antitussive, antispasmodic, and anticancer properties (58)
(3) 4-Butyl-phenol	C <sub>10</sub> H <sub>14</sub> O	150.22	2.93	8.011	No significant report
(4) 1,6-Anhydro-beta-D-glucopyranose	C <sub>6</sub> H <sub>10</sub> O <sub>5</sub>	162.14	5.31	8.328	No significant report
(5) Ethylalpha-d-glucopyranoside	C <sub>8</sub> H <sub>16</sub> O <sub>6</sub>	208.09	4.60	9.245	Maintenance and improvement of skin homeostasis and moisturizing functions (59)
(6) Benzeneacetic acid, 4-hydroxy-, methyl ester	C <sub>9</sub> H <sub>10</sub> O <sub>3</sub>	166.06	4.66	9.438	-
(7) 3-Deoxy-d-mannonic acid	C <sub>6</sub> H <sub>12</sub> O <sub>6</sub>	180.16	6.43	9.651	-
(8) 5-(2-Furyl)-3-methyl-penta-2,4-dienoic acid	C <sub>10</sub> H <sub>10</sub> O <sub>3</sub>	178.18	3.1	9.843	-
(9) n-Hydroxydecanoic acid	C <sub>16</sub> H <sub>32</sub> O <sub>2</sub>	256.42	1.89	11.347	As anti-inflammatory (60), cytotoxic activity (61)
(10) Hexadecanoic acid, 2-hydroxy-1-(hydroxymethyl)ethyl ester	C <sub>19</sub> H <sub>38</sub> O <sub>4</sub>	330.50	3.01	14.656	-
(11) Stigmast-5-en-3-ol	C <sub>29</sub> H <sub>50</sub> O	414.71	1.54	23.313	Apoptotic and antiproliferative effects (62)

GC-MS = gas chromatography-mass spectrometry.

These molecules represent 73% of the total identified compounds. The rest (27%) were the non-polar constituents represented by compounds **9–11**. Therefore, polar molecules constitute >40% of the peak area % relative to the total peak area % of the components that existed in BEP-10 extract. In contrast, non-polar residues represented only 8% of the total peak area % of the components that existed in BEP-10 extract. 5-(Hydroxymethyl)-2-furancarboxaldehyde (**1**) was found to be the main molecule in BEP-10 extract (13.2%). The other furan derivative (**8**) was found to have a peak area % of 3.1. Thus, furan derivatives represent the main component of BEP-10 extract (Fig. 4) while phenolic

derivatives represented by compounds **2, 3, and 6** came at the second level (peak area % = 10.05) with carbohydrates **4** and **5** (peak area % = 9.91).

#### Cytotoxicity and cell line selectivity studies

The four extracts showed a variable IC<sub>50</sub> ranging from 0.75 to 19.32 µg/mL. The most active extract was BEP-10 against HepG2 cells, and showed ~4.5-fold selectivity compared to normal MRC5 cells. The selectivity of the extract BEP-10 was greater than that of doxorubicin and camptothecin (Tabs. 2 and 3).

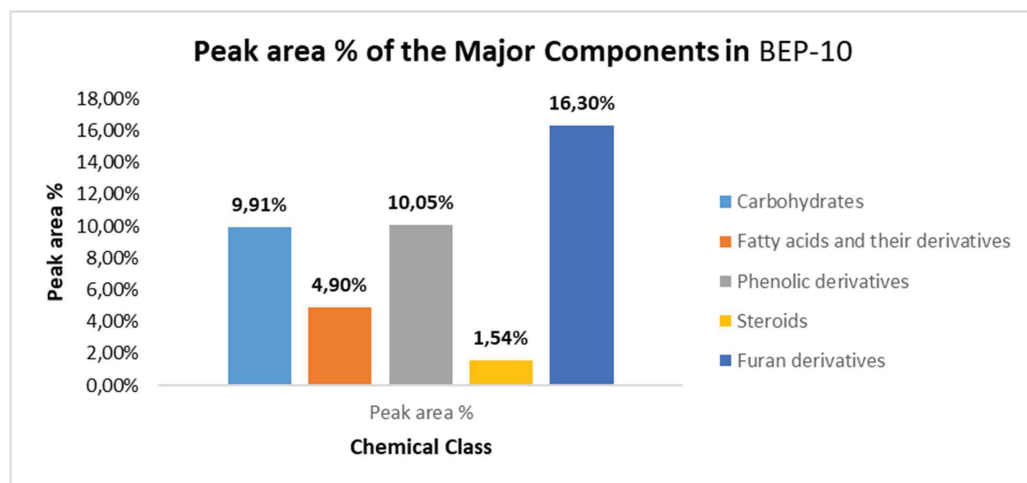


**FIGURE 4** - Peak areas (%) for the major components of *Opuntia ficus-indica* (L.) Miller (BEP-10 extract).

**TABLE 2** - Cytotoxic activity of the four extracts, doxorubicin and camptothecin, against three cell lines, and normal fibroblast (MTT 72 hours, IC<sub>50</sub>, µg/mL ±SD, n = 3)

Extract	MCF7	HT29	HepG2	Average* IC <sub>50</sub>	MRC5
BEP-09	6.00±1.61	8.20±0.57	5.20±0.58	6.47	2.94±0.71
BEP-10	1.85±0.73	5.85±0.23	<b>0.75±0.11**</b>	<b>2.82**</b>	3.34±0.41
BEP-11	16.93±0.66	16.07±0.11	14.07±1.04	15.69	10.77±0.54
BEP-12	16.53±0.43	19.32±0.64	9.60±0.82	15.15	8.72±1.56
Doxorubicin	0.07±0.01	1.98±0.10	2.15±0.15	1.40	5.86±0.35
Camptothecin	0.08±0.01	2.50±0.26	0.76±0.07	1.11	1.18±0.10

\*Average cytotoxicity (IC<sub>50</sub>) of each extract against the three cancer cells. \*\*p ≤ 0.01.

**TABLE 3** - Selectivity index of the five extracts, doxorubicin, and camptothecin, against normal MRC5 cells

Extract	MRC5	HT29	HepG2
BEP-09	0.49	0.36	0.57
BEP-10	1.80	0.57	4.47
BEP-11	0.64	0.67	0.77
BEP-12	0.53	0.45	0.91
Doxorubicin	78.57	2.96	2.73
Camptothecin	13.80	0.47	1.55

#### Clonogenic effect of the extract BEP-10 against HepG2 cells

The extract BEP-10 was tested for its possible clonogenic effect against HepG2 liver cancer cells. The extract revealed a dose-dependent clonogenic activity against a dose-dependent effect against HepG2 cells that was comparable to the effect of doxorubicin on the same cancer cells (Fig. 5).

#### Discussion

Fruits and resins have interesting medicinal uses. In vitro anticancer activity, cell line selectivity, and clonogenicity were considered as a useful trend to scavenge for a useful natural therapeutic agent(s) with putative anticancer property.

The extract of *O. ficus-indica* (fruits; BEP-10) yielded 17.3%. This indicates the high amounts of constituents that are expected to be available in these fruits.

The MTT assay of the four extracts showed a variable IC<sub>50</sub> ranging from 0.75 to 19.32 µg/mL comparable to both standards: doxorubicin (IC<sub>50</sub> = 1.40) and camptothecin (IC<sub>50</sub> = 1.11), respectively. Fruits appear to be more effective than resins, because they showed lower IC<sub>50</sub> values than those produced by standard drugs. These results were consistent with those of Castañeda-Arriaga et al (14) who studied the antioxidant effect of this plant and found that its chelating compounds can reduce the harmful effects caused by the most reactive free radical existing immediately.

The resulting selectivity (~4.5 fold) of the most active extract BEP-10 against HepG2 cells compared to normal MRC5 cells was found to be higher than that of doxorubicin and camptothecin. The extract BEP-10 was considered for

more cytotoxic and mechanistic studies. Selectivity indicates the ability of the extract to have a maximum effect on cancerous cells and a lesser effect on normal cells. This indicates both its safety and efficacy, and thus it can serve as a promising and useful drug candidate (63).

Due to its high selectivity for HepG2 liver cancer cells, the extract BEP-10 was chosen to test its possible clonogenic effect and showed a dose-dependent clonogenic effect comparable to the effect of doxorubicin in the same cells. The macroscopically counted cell colonies indicate the suppression ability of the active extract, which can be taken as evidence to support the preliminary cytotoxicity and selectivity effects. A study by Terzo et al (21) revealed that the *O. ficus-indica* fruit extract exerted significant antioxidant and anti-inflammatory effects.

Correlating the cytotoxic activity of the most promising BEP-10 extract with its phytochemical constituents, GC-MS was performed and different classes of phytoconstituents were detected, including polar molecules (73%) and lipophilic constituents (27%). These have been reviewed as anti-inflammatory (64), antioxidant (65), and anticancer agents (66).

Our results showed that in compound **1**, aldehyde 5-(hydroxymethyl)-2-furancarboxaldehyde, the furan derivative was the main compound of the BEP-10 extract. The literature revealed that the medicinal properties of furan include anticancer, antidepressant, antianxiolytic, analgesic, anti-inflammatory, muscle relaxant, antihypertensive, anti-arrhythmic, antimicrobial like antibacterial, antifungal, or antiviral (67), anti-ageing agents, anti-ulcer, antihistaminic, anticholinergic, antiparkinsonian, antidiuretic, and inhibition of sickle cell formation (68).

However, the GC-MS chromatogram showed three phenolic derivatives (compounds **2**, **3**, and **6**) that were classified as second contents in the BEP-10 extract. These findings were consistent with various studies such as the anticancer (69), anti-trypanosomal activity (70), antileishmanial, anti-inflammatory and antimicrobial activities (71), and anti-neuroinflammatory and neuroprotective activities (72).

#### Conclusion

The study concludes that the *O. ficus-indica* fruit (BEP-10) is widely distributed in the Al-Baha area and is locally considered a popular fruit. Its extract showed a significant cytotoxic



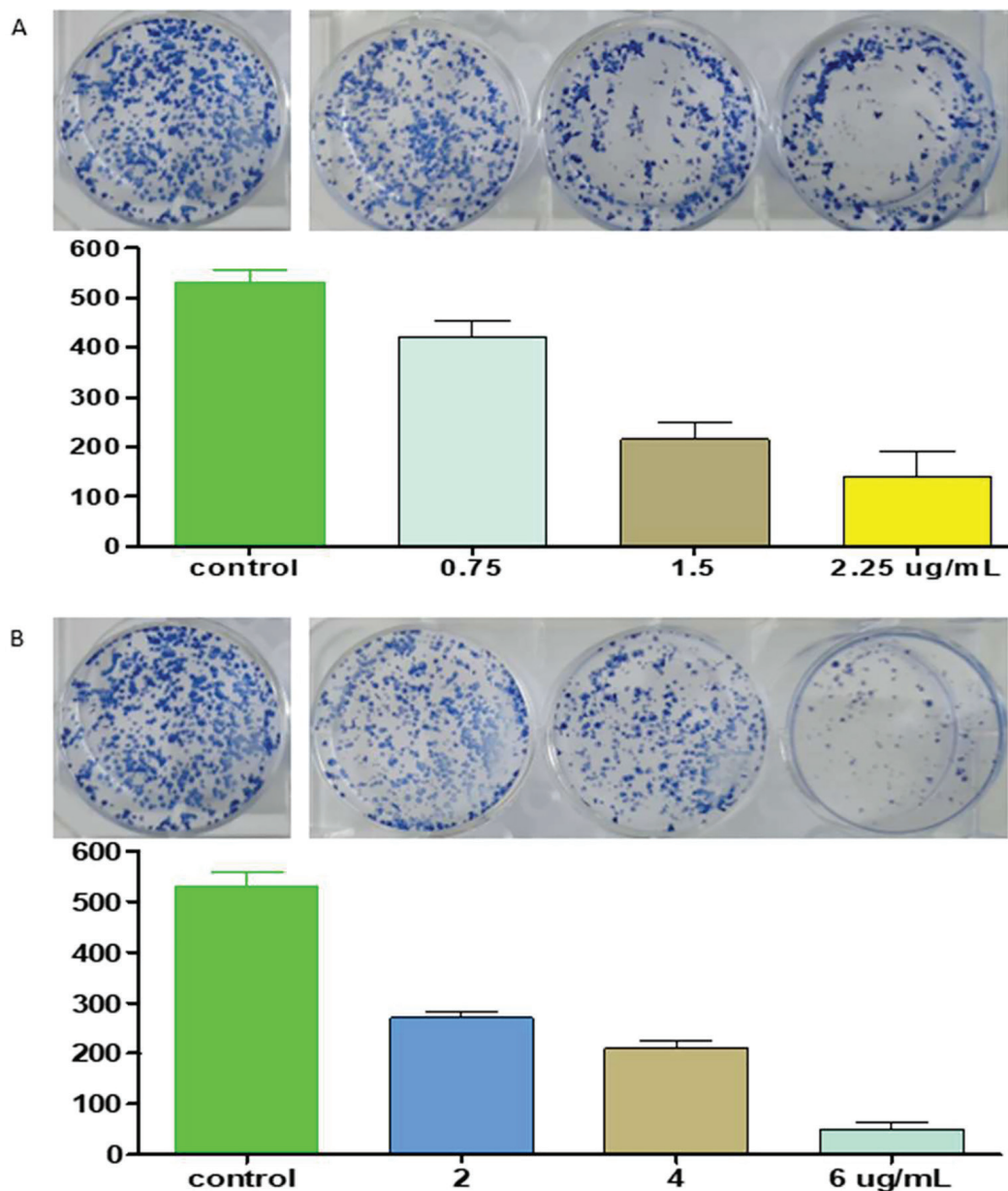


**FIGURE 5** - Colonies of HepG2 cells treated with A) extract BEP-10 (0, 0.75, 1.5, 2.25 µg/mL; n = 2), and B) doxorubicin (0, 2, 4, and 6 µg/mL; n = 2) for 72 hours in 6-well plates followed by a 14-day period of incubation without extract. Bar graph showing x-axis: extract concentrations (BEP-10) or doxorubicin concentrations; and y-axis: colony number. Results are expressed as cell number ± standard deviation of two independent experiments.

effect, particularly against HepG2 liver cancer cells with high cell selectivity.

Polar and lipophilic phytoconstituents were identified in the plant extract and could contribute to the investigated cytotoxic activity. The furan derivatives that are present as the main compound may play a vital role in the activity studied. Further research is required to obtain the profile of the drug candidate.

### Acknowledgements

This article is a part of the funded project: Investigation of Medicinal Plants with Putative Ocular Effects from Al-Baha Area, Southwestern, Saudi Arabia, Grant number (MOE-BU-4-2020); thus, the funder body is highly acknowledged for their financial support.

### Disclosures

**Data Availability Statement:** All data generated or analysed during this study are available with Dr. Ali as the correspondence author and can be provided upon request.

**Conflict of interest:** The authors declare that they have no competing interests.

**Funding:** The author(s) disclosed receiving the following financial support for the research, authorship, and/or publication of this article. This work was supported by the Department of Research and Innovation of the Ministry of Education of Saudi Arabia (grant number: MOE-BU-4-2020). Sponsors did not play a role in the design of the study, the collection and analysis of data, or the preparation of the manuscript.

**Authors' contribution:** Ali conceived the original idea. Mahadi, Hiadar, and Aimun designed the study. Ashraf, Mohamed EA, Riyadh A, and Bassem R conducted the experimental work and collected

the data. Aimun analysed the data and drafted the manuscript. Ali and Asaad, revised it. All approved the final version that was submitted. All authors equally contributed to the whole work preparation. All authors approved the version to be published and agreed to be accountable for all aspects of the work.

## References

- Meena SS, Lal G, Dubey PN, Meena MD. Medicinal and therapeutic uses of Dill (*Anethum graveolens* L.) – a review. *International J Seed Spices*. 2019;9(1):14-20. [Online](#)
- Al-Oqail MM, Farshori NN. Antioxidant and anticancer efficacies of *Anethum graveolens* against human breast carcinoma cells through oxidative stress and caspase dependency. *BioMed Res Int*. 2021;2021:5535570. [CrossRef PubMed](#)
- Kaur N, Chahal KK, Kumar A, Singh R, Bhardwaj U. Antioxidant activity of *Anethum graveolens* L. essential oil constituents and their chemical analogues. *J Food Biochem*. 2019;43(4):e12782. [CrossRef PubMed](#)
- Al-Sheddi ES, Al-Zaid NA, Al-Oqail MM, Al-Massarani SM, El-Gamal AA, Farshori NN. Evaluation of cytotoxicity, cell cycle arrest and apoptosis induced by *Anethum graveolens* L. essential oil in human hepatocellular carcinoma cell line. *Saudi Pharm J*. 2019;27(7):1053-1060. [CrossRef PubMed](#)
- Nam HH, Nan L, Choo BK. Anti-inflammation and protective effects of *Anethum graveolens* L. (Dill seeds) on esophageal mucosa damages in reflux esophagitis-induced rats. *Foods*. 2021;10(10):2500. [CrossRef PubMed](#)
- Mousavi SM, Beatriz Pizarro A, Akhgarjand C, et al. The effects of *Anethum graveolens* (dill) supplementation on lipid profile and glycemic control: a systematic review and meta-analysis of randomized controlled trials. *Crit Rev Food Sci Nutr*. 2022;62(21):5705-5716 [CrossRef PubMed](#)
- Castro LM, Pinto NB, Moura MQ, et al. Anthelmintic action of the *Anethum graveolens* essential oil on *Haemonchus contortus* eggs and larvae. *Braz J Biol*. 2021;81(1):183-188. [CrossRef PubMed](#)
- Khare CP. *Indian herbal remedies: rational Western therapy, ayurvedic and other traditional uses, botany*. Springer 2004.
- Aragona M, Lauriano ER, Pergolizzi S, Faggio C. *Opuntia ficus-indica* (L.) Miller as a source of bioactivity compounds for health and nutrition. *Nat Prod Res*. 2018;32(17):2037-2049. [CrossRef PubMed](#)
- Alimi H, Hfaiedh N, Bouoni Z, et al. Antioxidant and antiulcerogenic activities of *Opuntia ficus indica* f. inermis root extract in rats. *Phytomedicine*. 2010 Dec 1;17(14):1120-6 [CrossRef PubMed](#)
- Trombetta D, Puglia C, Perri D, et al. Effect of polysaccharides from *Opuntia ficus-indica* (L.) cladodes on the healing of dermal wounds in the rat. *Phytomedicine*. 2006;13(5):352-358. [CrossRef PubMed](#)
- El-Mostafa K, El Kharrassi Y, Badreddine A, et al. Nopal cactus (*Opuntia ficus-indica*) as a source of bioactive compounds for nutrition, health and disease. *Molecules*. 2014;19(9):14879-14901. [CrossRef PubMed](#)
- Lee YS, Yang WK, Park YR, et al. *Opuntia ficus-indica* alleviates particulate matter 10 plus diesel exhaust particles (PM10D)-induced airway inflammation by suppressing the expression of inflammatory cytokines and chemokines. *Plants*. 2022;11(4):520. [CrossRef PubMed](#)
- Castañeda-Arriaga R, Perez-Gonzalez A, Marino T, Russo N, Galano A. Antioxidants into nopal (*Opuntia ficus-indica*), important inhibitors of free radicals' formation. *Antioxidants*. 2021;10(12):2006. [CrossRef PubMed](#)
- Zhou M, Wen C, Ming Y, Zhang L, Lyu X. [Distribution and bio-activity of polyphenols in *Opuntia ficus-indica* (L.) Mill]. *Wei Sheng Yan Jiu*. 2022;51(3):463-469. [PubMed](#)
- Djobbi B, Miled GLB, Raddadi H, Hassen RB. Efficient removal of aqueous manganese (II) cations by activated *Opuntia ficus indica* powder: adsorption performance and mechanism. *Acta Chim Slov*. 2021;68(3):548-561. [CrossRef PubMed](#)
- Hussain S, Alamri MS, Mohamed AA, et al. Exploring the role of acacia (*Acacia seyal*) and cactus (*Opuntia ficus-indica*) gums on the dough performance and quality attributes of breads and cakes. *Foods*. 2022;11(9):1208. [CrossRef PubMed](#)
- Amrane-Abider M, Nerin C, Tamendjari A, Serralheiro MLM. Phenolic composition, antioxidant and antiacetylcholinesterase activities of *Opuntia ficus-indica* peel and flower teas after in vitro gastrointestinal digestion. *J Sci Food Agric*. 2022;102(11):4401-4409. [CrossRef PubMed](#)
- Corona-Cervantes K, Parra-Carriedo A, Hernández-Quiroz F, et al. Physical and dietary intervention with *Opuntia ficus-indica* (nopal) in women with obesity improves health condition through gut microbiota adjustment. *Nutrients*. 2022;14(5):1008. [CrossRef PubMed](#)
- Liu Z, Zhang J, Zhao Q, Wen A, Li L, Zhang Y. The regulating effect of Tibet *Opuntia ficus-indica* (Linn.) Mill. polysaccharides on the intestinal flora of cyclophosphamide-induced immunocompromised mice. *Int J Biol Macromol*. 2022;207:570-579. [CrossRef PubMed](#)
- Terzo S, Attanzio A, Calvi P, et al. Indicaxanthin from *Opuntia ficus-indica* fruit ameliorates glucose dysmetabolism and counteracts insulin resistance in high-fat-diet-fed mice. *Antioxidants*. 2021;11(1):80. [CrossRef PubMed](#)
- Governa P, Marchi M, Cocetta V, et al. Effects of *Boswellia serrata* Roxb. and *Curcuma longa* L. in an in vitro intestinal inflammation model using immune cells and CaCo-2. *Pharmaceuticals (Basel)*. 2018;11(4):126. [CrossRef PubMed](#)
- Catanzaro D, Rancan S, Orso G, et al. *Boswellia serrata* preserves intestinal epithelial barrier from oxidative and inflammatory damage. *PLoS One*. 2015;10(5):e0125375. [CrossRef PubMed](#)
- Asif M, Jabeen Q, Abdul-Majid AM, Atif M. Diuretic activity of *Boswellia serrata* Roxb. oleo gum extract in albino rats. *Pak J Pharm Sci*. 2014;27(6):1811-1817. [PubMed](#)
- Wahab, S.M.; Aboutabl, E.A.; El-Zalabani, S.M.; Fouad, H.A.; De Pooter, H.L.; El-Fallaha, B. The essential oil of olibanum. *Planta Med*. 1987, 53, 382–384. [CrossRef PubMed](#)
- Sadhasivam S, Palanivel S, Ghosh S. Synergistic antimicrobial activity of *Boswellia serrata* Roxb. ex Colebr. (Bursaceae) essential oil with various azoles against pathogens associated with skin, scalp and nail infections. *Lett Appl Microbiol*. 2016;63(6):495-501. [CrossRef PubMed](#)
- Nikam TD, Ghorpade RP, Nitnaware KM, Ahire ML, Lokhande VH, Chopra A. Micropropagation and non-steroidal anti-inflammatory and anti-arthritic agent boswellic acid production in callus cultures of *Boswellia serrata* Roxb. *Physiol Mol Biol Plants*. 2013;19(1):105-116. [CrossRef PubMed](#)
- Pungle P, Banavalikar M, Suthar A, Biyani M, Mengi S. Immunomodulatory activity of boswellic acids of *Boswellia serrata* Roxb. *Indian J Exp Biol*. 2003;41(12):1460-1462. [PubMed](#)
- Almeida-da-Silva CLC, Sivakumar N, Asadi H, et al. Effects of frankincense compounds on infection, inflammation, and oral health. *Molecules*. 2022;27(13):4174. [CrossRef PubMed](#)
- Siddiqui MZ. *Boswellia serrata*, a potential antiinflammatory agent: an overview. *Indian J Pharm Sci*. 2011;73(3):255-261. [PubMed](#)



31. Shen T, Li GH, Wang XN, Lou HX. The genus *Commiphora*: a review of its traditional uses, phytochemistry and pharmacology. *J Ethnopharmacol.* 2012;142(2):319-330. [CrossRef PubMed](#)
32. Al-Robai SA, Ahmed AA, Mohamed HA, Ahmed AA, Zabin SA, Alghamdi AA. Qualitative and quantitative ethnobotanical survey in Al Baha province, southwestern Saudi Arabia. *Diversity.* 2022 Oct 13;14(10):867. [CrossRef](#)
33. Galehdari H, Negahdari S, Kesmati M, Rezaie A, Shariati G. Effect of the herbal mixture composed of Aloe Vera, Henna, *Adiantum capillus-veneris*, and Myrrha on wound healing in streptozotocin-induced diabetic rats. *BMC Complement Altern Med.* 2016;16(1):386. [CrossRef PubMed](#)
34. Madia VN, De Angelis M, De Vita D, et al. Oil and its main components for antiviral activity. Investigation of *Commiphora myrrha* (Nees) Engl. *Pharmaceuticals (Basel).* 2021;14(3):243. [CrossRef PubMed](#)
35. Hwang YH, Lee A, Kim T, Jang SA, Ha H. Anti-osteoporotic effects of *Commiphora myrrha* and its poly-saccharide via osteoclastogenesis inhibition. *Plants.* 2021;10(5):945. [CrossRef PubMed](#)
36. Ge CY, Zhang JL. Bioactive sesquiterpenoids and steroids from the resinous exudates of *Commiphora myrrha*. *Nat Prod Res.* 2019;33(3):309-315. [CrossRef PubMed](#)
37. Germano A, Occhipinti A, Barbero F, Maffei ME. A pilot study on bioactive constituents and analgesic effects of MyrLiq®, a *Commiphora myrrha* extract with a high furanodiene content. *BioMed Res Int.* 2017;2017:3804356. [CrossRef PubMed](#)
38. Sotoudeh R, Hadjzadeh MA, Gholamnezhad Z, Aghaei A. The anti-diabetic and antioxidant effects of a combination of *Commiphora mukul*, *Commiphora myrrha* and *Terminalia chebula* in diabetic rats. *Avicenna J Phytomed.* 2019;9(5):454-464. [PubMed](#)
39. Orabi SH, Al-Sabbagh ES, Khalifa HK, et al. *Commiphora myrrha* resin alcoholic extract ameliorates high fat diet induced obesity via regulation of UCP1 and adiponectin proteins expression in rats. *Nutrients.* 2020;12(3):803. [CrossRef PubMed](#)
40. Ahmad A, Raish M, Ganaie MA, et al. Hepatoprotective effect of *Commiphora myrrha* against d-GalN/LPS-induced hepatic injury in a rat model through attenuation of pro inflammatory cytokines and related genes. *Pharm Biol.* 2015;53(12):1759-1767. [CrossRef PubMed](#)
41. Anonymous. Standardisation of single drugs of Unani medicine. 1st ed. Part II. New Delhi: CCRUM; 1992. [Online](#)
42. Usmani MI. Tanqeeh ul Mufradat. 1st ed. New Delhi: Famous Offset Press; 2007:229-230. [Online](#)
43. Ibn-e-Rushd AWM. *Kitab ul Kulliyat.* 2nd ed. CCRUM; 1987:79-81.
44. Ahmad Al-Undulisi ZA. *Al-Jami ul Mufaradat ul Advia Wa Al-Aghziya IB.* Vol IV. 2nd ed. New Delhi: CCRUM; 2003:316-320. [Online](#)
45. Wildner G. Tumors, tumor therapies, autoimmunity and the eye. *Autoimmun Rev.* 2021;20(9):102892. [CrossRef PubMed](#)
46. Das S, Pineda G, Goff L, Sobel R, Berlin J, Fisher G. The eye of the beholder: orbital metastases from midgut neuroendocrine tumors, a two institution experience. *Cancer Imaging.* 2018;18(1):47. [CrossRef PubMed](#)
47. Domingo RE, Manganip LE, Castro RM. Tumors of the eye and ocular adnexa at the Philippine Eye Research Institute: a 10-year review. *Clin Ophthalmol.* 2015;9:1239-1247. [CrossRef PubMed](#)
48. Nahon-Esteve S, Martel A, Maschi C, et al. The molecular pathology of eye tumors: A 2019 update main interests for routine clinical practice. *Curr Mol Med.* 2019;19(9):632-664. [CrossRef PubMed](#)
49. Collenette S. The ceropegias of Saudi Arabia. *Brit Cact Succ J.* 1999;17(4):181-187.
50. Chaudhary A, Mossa JS. Contribution to the flora of Saudi Arabia. *Pak J Bot.* 1991;23(2):257-82. [Online](#)
51. Gillett J. The genus *Trifolium* in southern Arabia and in Africa south of the Sahara. *Kew Bull.* 1952;7(3):367-404. [CrossRef](#)
52. U.S. Department of Agriculture. Dr. Duke's phytochemical and ethnobotanical databases. [Online](#). Accessed June 2024.
53. Alsanosy R, Alhazmi HA, Sultana S, et al. Phytochemical screening and cytotoxic properties of ethanolic extract of young and mature khat leaves. *J Chem.* 2020;1-9. [CrossRef](#)
54. Abdalla AN, Malki WH, Qattan A, Shahid I, Hossain MA, Ahmed M. Chemosensitization of HT29 and HT29-5FU cell lines by a combination of a multi-tyrosine kinase inhibitor and 5FU down-regulates ABCC1 and inhibits PIK3CA in light of their importance in Saudi colorectal cancer. *Molecules.* 2021;26(2):334. [CrossRef PubMed](#)
55. Abdalla AN, Qattan A, Malki WH, Shahid I, Hossain MA, Ahmed M. Significance of targeting VEGFR-2 and cyclin D1 in luminal-A breast cancer. *Molecules.* 2020;25(20):4606. [CrossRef PubMed](#)
56. Chu LI, Berahim Z, Mohamad S, Shahidan WNS, Yhaya MF, Zainuddin SLA. Phytochemical compounds of raw versus methanol-extracted Kelulut, Tualang, and Manuka honeys. *Cureus.* 2023;15(4):e38297. [CrossRef PubMed](#)
57. Subramenium GA, Swetha TK, Iyer PM, Balamurugan K, Pandian SK. 5-Hydroxymethyl-2-furaldehyde from marine bacterium *Bacillus subtilis* inhibits biofilm and virulence of *Candida albicans*. *Microbiol Res.* 2018;207:19-32. [CrossRef PubMed](#)
58. Patil MD, Grogan G, Yun H. Biocatalyzed C-C bond formation for the production of alkaloids. *ChemCatChem.* 2018;10(21):4783-4804. [CrossRef](#)
59. Bogaki T, Mitani K, Oura Y, Ozeki K. Effects of ethyl- $\alpha$ -D-glucoside on human dermal fibroblasts. *Biosci Biotechnol Biochem.* 2017;81(9):1706-1711. [CrossRef PubMed](#)
60. Aparna V, Dileep KV, Mandal PK, Karthe P, Sadasivan C, Haridas M. Anti-inflammatory property of n-hexadecanoic acid: structural evidence and kinetic assessment. *Chem Biol Drug Des.* 2012;80(3):434-439. [CrossRef PubMed](#)
61. Ravi L, Krishnan K. Research article cytotoxic potential of N-hexadecanoic acid extracted from *Kigelia pinnata* leaves. *Asian J Cell Biol.* 2017;12(1):20-27. [CrossRef](#)
62. Fernando IPS, Sanjeewa KKA, Ann Y-S, et al. Apoptotic and anti-proliferative effects of Stigmast-5-en-3-ol from *Dendronephthya gigantea* on human leukemia HL-60 and human breast cancer MCF-7 cells. *Toxicol In Vitro.* 2018;52:297-305. [CrossRef PubMed](#)
63. Kakuta S, Usutani S, Sirai M, Nagase M. [Selectivity index]. *Jpn J Clin Med.* 1997;55(suppl 2):610-613. [PubMed](#)
64. Pongprayoon U, Soontornsaratune P, Jarikasem S, Sematong T, Wasuwat S, Claeson P. Topical antiinflammatory activity of the major lipophilic constituents of the rhizome of *Zingiber cassumunar*. Part I: the essential oil. *Phytomedicine.* 1997;3(4):319-322. [CrossRef PubMed](#)
65. Cavin A, Hostettmann K, Dyatmyko W, Potterat O. Antioxidant and lipophilic constituents of *Tinospora crispa*. *Planta Med.* 1998;64(5):393-396. [CrossRef PubMed](#)
66. Shin J, Song M-H, Yu J-W, et al. Anticancer potential of lipophilic constituents of eleven shellfish species commonly consumed in Korea. *Antioxidants.* 2021;10(10):1629. [CrossRef PubMed](#)
67. Lukevits E, Demicheva L. Biological activity of furan derivatives. *Chem Heterocycl Compd.* 1993;29(3):243-267. [CrossRef](#)
68. Shingalapur RV, Hosamani KM, Keri RS. Synthesis and evaluation of in vitro anti-microbial and anti-tubercular activity of 2-styryl benzimidazoles. *Eur J Med Chem.* 2009;44(10):4244-4248. [CrossRef PubMed](#)



69. Roleira FM, Varela CL, Costa SC, Tavares-da-Silva EJ. Phenolic derivatives from medicinal herbs and plant extracts: anti-cancer effects and synthetic approaches to modulate biological activity. *Studies Nat Prod Chem.* 2018;57:115-156. [CrossRef](#)
70. Grecco Sdos S, Félix MJ, Lago JH, et al. Anti-trypanosomal phenolic derivatives from *Baccharis uncinella*. *Nat Prod Commun.* 2014 Feb;9(2):171-3. [PubMed](#).
71. Tracanna MI, Fortuna AM, Cárdenas AV, et al. Anti-leishmanial, anti-inflammatory and antimicrobial activities of phenolic derivatives from *Tibouchina paratropica*. *Phytother Res.* 2015;29(3):393-397. [CrossRef PubMed](#)
72. Woo KW, Kwon OW, Kim SY, et al. Phenolic derivatives from the rhizomes of *Dioscorea nipponica* and their anti-neuroinflammatory and neuroprotective activities. *J Ethnopharmacol.* 2014;155(2):1164-1170. [CrossRef PubMed](#)



# Investigating the combinatory effect of *Sclerocarya birrea* with doxorubicin against selected colorectal cancer cell lines

Thembelihle H. Nxasana<sup>1</sup>, Innocensia M. Mangoato<sup>1</sup>, Patricia M. Masiu<sup>1</sup>, Abhay P. Mishra<sup>1,2</sup>, Motlalepula G. Matsabisa<sup>1</sup>

<sup>1</sup>Department of Pharmacology, University of the Free State, Faculty of Health Sciences, School of Medicine, Bloemfontein - South Africa

<sup>2</sup>Cosmetics and Natural Products Research Center (CosNat), Faculty of Pharmaceutical Sciences, Naresuan University, Phitsanulok - Thailand

## ABSTRACT

**Introduction:** Colorectal cancer incidences continue to increase annually, worldwide. Herbal plants with antiproliferative properties received research interest as agents that can be adjuvant therapies with chemotherapy drugs to enhance their efficacy and reverse drug resistance.

**Methods:** *Sclerocarya birrea* ethanolic (SBE) and aqueous (SBW) extracts combined with doxorubicin (DOX) against drug-sensitive and drug-resistant colorectal cancer cells were investigated for their potential adjuvant and drug resistance reversal. The extracts were assessed for their potential anticancer activities on HCT15 and HT29 cell lines as well as their doxorubicin potentiating and drug resistance reversal effects respectively. The extracts were assessed for their cytotoxicity on normal 3T3-L1 fibroblast cells.

**Results:** Both SBE and SBW extracts exhibited no toxicity against normal 3T3 cells and showed low activity on the HT29 cell line. Contrarily, resistant HCT15 cells showed moderate to low activity with significantly higher inhibitory concentration (IC<sub>50</sub>) values. The combination of SBE with DOX and SBW with DOX resulted in antagonistic interactions, causing an increase in IC<sub>50</sub> values for HT29 and HCT15 cells. In contrast, the combination of DOX and verapamil (VER) produced an additive effect, with no change in their IC<sub>50</sub> values.

**Conclusion:** Based on the findings from the combination treatment, the SBE and SBW extracts demonstrated higher efficacy and synergistic effects combined with DOX at IC<sub>75</sub> compared to the combination of DOX and VER, suggesting their potential as anticancer agents. However, further research on both the SBE and SBW extracts' mechanisms of action and in vivo effects is warranted.

**Keywords:** Colorectal cancer, Doxorubicin drug resistance, *Sclerocarya birrea*, Synergy, Verapamil

## Introduction

Colorectal cancer (CRC) is ranked third in cancer incidences and second in terms of cancer fatalities, worldwide (1). According to the South African statistics, CRC is mostly ranked second in men and fourth in women. It tends to occur most frequently in White people (52%-54%), subsequently followed by African people (26%-28%), coloured people (14%-15%), and Indian people (4%-7%) (2). Conventional chemotherapy drugs, like doxorubicin (DOX) used for treating CRC, require higher doses for increased efficacy, which often leads to severe side effects in patients, drug resistance, and decreased treatment effectiveness (3). First-generation

P-glycoprotein (P-gp) inhibitors, such as verapamil (VER), have been shown to increase intracellular DOX accumulation; however, their usage also at higher doses produces unfavourable side effects, limiting their ability to treat patients with cancer (4). As a result, medicinal plants acquired attention as agents that can be used to potentiate the effect of conventional drugs at lower doses, thus minimizing the occurrence of drug resistance (5). The use of natural products in managing and treating colon cancer is extensively reported across various scientific studies that looked into in vitro and in vivo models (6-8). However, there is insufficient data on the effects of natural products to reverse or mitigate drug resistance, particularly doxorubicin resistance in colon cancer (9).

*Sclerocarya birrea*, also known as the Marula tree, is an African indigenous, dioecious tree belonging to the Anacardiaceae family (10). The fruits of the tree are commonly used for making food and alcoholic beverages, the leaves are traditionally used to treat heartburns, and the bark decoction of the tree is used to treat diarrhoea and abdominal pains (11). A study by Masoko et al showed that the ethanol extracts of the plant possess antifungal properties when

Received: July 23, 2024

Accepted: September 19, 2024

Published online: December 11, 2024

This article includes supplementary material

Corresponding author:

Motlalepula G. Matsabisa  
email: [MatsabisaMG@ufs.ac.za](mailto:MatsabisaMG@ufs.ac.za)



used together with standard antifungals (12). Other studies revealed that the bark extracts of this plant had other pharmacological activities such as anticancer, antidiabetic, anti-inflammatory, anti-atherogenic as well as antioxidant activities (11,13). However, research on the combinatory effect of this plant with DOX is still lacking in CRC.

Therefore, the present study examined the possible anti-tumour effects of ethanolic (SBE) and water (SBW) extracts of *S. birrea* bark. The synergistic, additive, or antagonistic effects of DOX when combined with ethanolic and water extracts from *S. birrea* bark have been evaluated in relation to selected human CRC cell lines. The effects have also been evaluated for reversing drug resistance against chemoresistant CRC cell lines.

## Methods

### Plant material collection and identification

The plant was collected by Rangers of Zuka in the Northern KwaZulu-Natal Private Conservancy, KwaZulu-Natal, South Africa. The South African National Biodiversity Institute documented the plant's identification, which was indicated by its national tree number of 360. Following the harvest, the plant was washed to remove debris, dried at room temperature, and grounded into fine powder using an electric hammermill (Roff, Kroonstad, South Africa).

### Preparation of *S. birrea* extract

The extraction process was performed according to Mohammed et al (14) and Nyoni et al (15) with slight modifications. Accurately weighed 40 g of the dried plant material was extracted (24 hours × 3) in ethanol and distilled water, respectively, at a ratio of 1:5 w/v, at room temperature using a horizontal shaker (ABC Hansen Africa, South Africa). The extract was filtered using a Whatman filter paper and the filtrate was stored at 4°C. Thereafter, SBE extract was concentrated using a rotary evaporator (Buchi, South Africa) and SBW extract was dried using freeze-dryer (Buchi, South Africa). Both dried extracts were stored away from direct sunlight and moisture for further use.

The percentage yield of both plant extracts was calculated using the below equation:

$$\text{Percentage yield} = \frac{\text{mass of the dry extract}}{\text{mass of the sample}} \times 100$$

### Analysis of *S. birrea* extracts using thin layer chromatography

To determine the chemical fingerprint of the extracts, thin layer chromatography (TLC) analysis was conducted according to methods adopted from Masoko et al (12) and Abdulhamid et al (16). For each crude extract, 1 mg/mL stock solution was prepared by reconstituting each extract with the solvent of extraction. The following mobile phases were used for the analysis:

- A. Benzene:methanol:ammonium hydroxide (90:10:1, v/v/v)
- B. Dichloromethane:ethyl acetate:hexane (5:2:1 v/v/v)

## TLC analysis

TLC was performed on aluminium TLC plates precoated with silica gel 60 PF<sub>254</sub> (Thermo Fisher Scientific, South Africa). The plates were spotted with 20 µL of *S. birrea* extracts approximately 1 cm from the bottom edge of the plates. Both plates were kept into presaturated Shandon chromatographic tanks containing mobile phases at room temperature. All the samples were left to run for 30 minutes. Ultraviolet light was used to visualize the spots on TLC plates at 254 and 366 nm. The sample and solvent fronts of the separated spots were marked and measured, and a retention factor (Rf) was calculated using the equation below:

$$Rf = \frac{\text{Distance travelled by spot}}{\text{Distance travelled by solvent front}}$$

### High-performance liquid chromatography analysis

The analysis was performed on an Agilent 1100 high-performance liquid chromatography (HPLC) system equipped with a diode array detector. In brief, 1 mg/mL stock solution was prepared by reconstituting each extract with the solvent of extraction. The stock solution was then filtered through a 0.45 µm filter. The liquid chromatography (Agilent 1100 HPLC with a diode detector) analysis was performed on a Phenomenex Luna 5u C<sub>18</sub> (2) column of 100 Å (150 × 4.6 mm, 5 µm) with gradient elution and peaks measured at wavelength of 280 nm. The column oven temperature was set to 30°C, and the flow rate was 1.0 mL/min. The injection volume was 10 µL, and the dwell volume of the HPLC system was 1.8 mL. Distilled water served as the mobile phase A and acetonitrile served as mobile phase B. The absolute run time was 40 minutes using the following multistep linear gradient: 0 minute, 95% A and 5% B; 7 minutes, 65% A and 35% B; 12 minutes, 55% A and 45% B; 17 minutes, 50% A and 50% B; 27 minutes, final conditioning cycle of 95% A and 5% B for 5 minutes was included before the next analysis. An OpenLab CDS ChemStation Edition Software was used for the result analysis.

### Bioanalysis of *S. birrea* bark extracts, DOX, and VER

*S. birrea* extracts, DOX, and VER were evaluated against a normal human embryonic fibroblast cell line, drug-sensitive human colorectal adenocarcinoma cell line (HT29) and drug-resistant human colorectal adenocarcinoma cell line (HCT15), to determine their cytotoxicity, anticancer, and resistant reversal effects.

## Cell culture

The cell lines 3T3-L1, HT-29, and HCT-15 were purchased from the American Type Cell Culture (ATCC, Manassas, Virginia). All the cells were cultured in Dulbecco's Modified Eagle Medium (DMEM) supplemented with 10% foetal bovine serum (FBS) and incubated in a humidified incubator at 37°C with 5% CO<sub>2</sub> and 95% atmosphere until 70%-80% confluency was reached. Details of cell lines used during the study are tabulated in Supplementary Table 1.



### Sample preparation

DOX and VER (positive controls) were prepared as stock solutions in dimethyl sulfoxide (DMSO) at concentrations of 5 and 2 mg/mL, respectively. DOX working stock solutions were prepared at 5.0, 4.0, 3.0, 2.0, 1.0, 0.5, 0.25, 0.13, 0.06, and 0.03 µg/mL while VER working concentration range was 200, 150, 100, 50, 25, 12.5, 6.25, 3.13, 1.56, and 0.78 µg/mL.

Ethanol (60 mg/ml) and water (50 mg/ml) extracts stock solutions were prepared in DMSO and DMSO:H<sub>2</sub>O at a ratio of 1:1 (v/v), respectively. A range of working concentrations were prepared for ethanol extract at 400, 300, 200, 100, 50, 25, 12.5, 6.25, 3.13, and 1.56 µg/mL while 500, 450, 400, 300, 200, 100, 50, 25, 12.5, and 6.25 µg/mL were prepared for the H<sub>2</sub>O extract. All samples and positive controls were prepared in culture medium.

### Cytotoxicity assay and anticancer activity of the extracts

The cytotoxicity of *S. birrea* extracts, DOX, and VER was studied to determine their inhibitory and anticancer activity on HT29 and HCT15 cells, as well as their influence on embryonic 3T3 cell growth (normal cells) by MTT assay. The cells were treated with single treatment of SBE and SBW extracts and/or DOX and VER at various concentrations and incubated for a period of 72 hours.

### MTT assay

MTT assay was performed to examine the cell viability. After 72 hours incubation period, 100 µL of MTT solution contained in 200 µL of fresh medium was added into each well and incubated for 3 hours at 37°C. After the incubation period was complete, purple formazan salts appeared in the bottom of the wells. Thereafter, a microplate reader (Multiskan GO, Thermo Fisher Scientific, South Africa) was used to read the absorbances of each plate at 570 nm, which were used to calculate growth inhibition values and further determine the inhibitory concentration (IC)<sub>50</sub> values of the test samples.

### Selectivity index

The selectivity index (SI) is an estimate of the ratio of the toxic concentrations in the test sample relative to its optimal bioactive concentration. Establishing the SI value is important for determining whether further work can be continued. It is given by the equation below and an SI value ≥3 indicates that the test sample can be further investigated (17):

$$SI (\text{cancer cells}) = \frac{IC_{50} (\text{normal cells})}{IC_{50} (\text{cancer cells})}$$

### Combination treatment of the selected cell lines with *S. birrea* extracts and the control drugs

#### Combination treatment in HT29 cells

The HT29 cells were seeded in a 96-well microplate (1.5 × 10<sup>4</sup> cells/well), and exposed, in duplicates, to each agent alone (100 µL) and both (50 µL/agent) in combination. The cells were subjected to a total of five concentrations of half-fold serial dilutions, with two concentration points above and below the IC<sub>50</sub> values of each *S. birrea* extract, DOX, and VER.

The treated plates were then incubated for 72 hours followed by MTT assay for cell growth inhibition determination. The IC<sub>50</sub> of combination treatment was then determined to calculate the combination index (CI).

#### Resistance reversal assay on HCT15 cells

A resistance reversal assay was performed on the drug-resistant cell line HCT15 to determine cell growth inhibition after exposure to a combination of SBE extract + DOX, SBW extract + DOX, as well as the combination of VER + DOX. HCT15 cells were seeded in a 96-well microplate (1.5 × 10<sup>4</sup> cells/well) and treated with 100 µL of DOX or VER and/or *S. birrea* extracts alone and also exposed to 50 µL of DOX combined with 50 µL of VER. The cells were also treated with 50 µL of DOX combined with 50 µL SBE as well as 50 µL of DOX combined with 50 µL SBW followed by 72 hours incubation.

### Analysis of combination cell treatment

#### Calculation of CI

One of the most used ways to evaluate whether the combined effect of *S. birrea* extracts and DOX is effective is to determine a CI that is calculated from Chou-Talalay's method on CompuSyn software ([Online](#)) using absorbance values from MTT assay (18). The computer software CompuSyn and the equation is used to calculate the CI.

$$CI = \frac{IC_{50} \text{ of doxorubicin in combination}}{IC_{50} \text{ of doxorubicin alone}} + \frac{IC_{50} \text{ of } S. \text{ birrea extract in combination}}{IC_{50} \text{ of } S. \text{ birrea extract alone}}$$

#### Calculation of dose reduction index

Dose reduction index (DRI), also known as the reversal ratio or the cytotoxicity enhancement ratio, is a measure of how many times the dose may be reduced when compared to the doses of each drug when used separately (18), which is calculated as follows:

$$DRI = \frac{IC_{50} \text{ of cytotoxic drug alone}}{IC_{50} \text{ of cytotoxic drug in combination with combination partner}}$$

#### Calculation of cell growth inhibition percentage

The following equation was used to calculate the cell growth inhibition (19) percentage:

$$\text{Percentage cell growth inhibition} = 1 - \left( \frac{At - Ab}{Ac - Ab} \right) \times 100$$

where *Ab* = absorbance value of the blank, *At* = absorbance value of the test compound, and *Ac* = absorbance value of the control.

#### Drug combination evaluation using Bliss independence model

To determine whether the anticancer effect of combining two drugs targeting different biological pathways shows



a synergistic effect of drug combinations, a bliss independent model was used, which employs average response measurements at each combination dosage. The bliss independence model was accessed using [Online](#).

### Statistical analysis

The data was expressed as means  $\pm$  standard error of the mean (SEM) of three independent experiments. Results were analysed using Microsoft Excel for anticancer and resistance reversal activity and graphs for anticancer were generated from GraphPad Prism version 8, 2008 software (GraphPad Software, Inc., La Jolla, CA, USA). For CI interactions and the dose-response index, the computer software CompuSyn was used. Synergy finder was used to determine the synergy dose points at 95% confidence interval and the level of significance was determined at  $p$  values  $\leq 0.05$ .

## Results and discussion

### Plant extraction

*S. birrea* bark was extracted using cold ethanol and distilled water. The SBE extract yield was found to be 12.75% and resulted in a sticky, dark brown, dry extract, while the

SBW extract resulted in a brown, spongy powder with a percentage yield of 11.43%.

### TLC analysis

TLC analysis was performed to obtain a chemical fingerprint of different compounds that separated in the *S. birrea* extracts using different mobile phases. Supplementary Figure 1 shows TLC bands obtained from the SBE extract using two mobile phases. The mobile phase as depicted in Supplementary Figure 1A resulted in yielding a total of four bands with  $R_f$  values ranging from 0.4 to 0.9, while the mobile phase as shown in Supplementary Figure 1B resulted in yielding five bands with  $R_f$  values ranging from 0.2 to 0.9 (Supplementary Tab. 3). SBW extract couldn't give good separation on TLC plates in aforementioned mobile phase.

### High-performance liquid chromatography

HPLC was performed to obtain the chemical fingerprint of the separated compounds from *S. birrea* bark extracts. Figure 1 shows the chromatogram of the SBE extract superimposed with the standard chromatogram of gallic acid at 220 nm, while Figure 2 shows the chromatogram peaks of

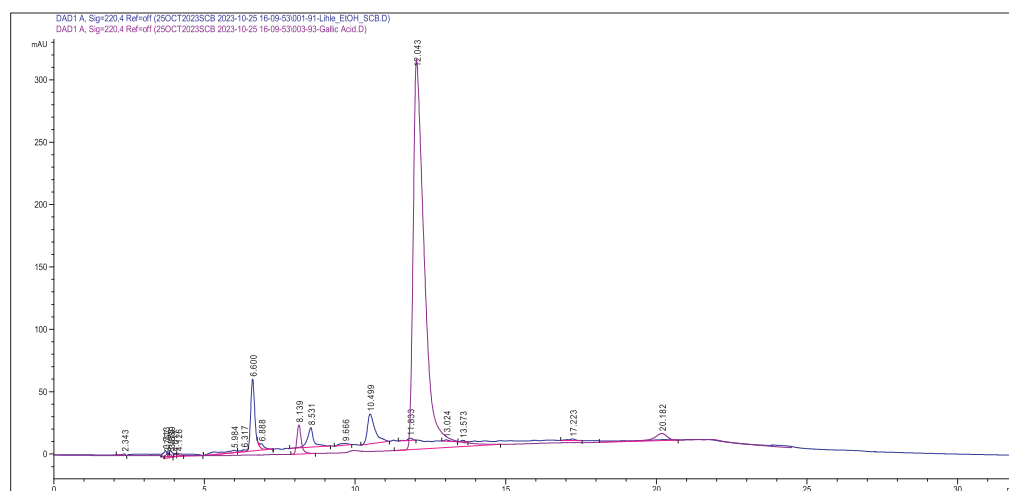


**FIGURE 1** - Chromatogram peaks of the SBE extract superimposed with the chromatogram of gallic acid. The HPLC conditions were as follows: The column oven temperature was set to 30°C; flow rate was 1.0 mL/min; injection volume was 10  $\mu$ L; and the dwell volume of the HPLC system was 1.8 mL. HPLC = high-performance liquid chromatography; SBE = *Sclerocarya birrea* ethanol.

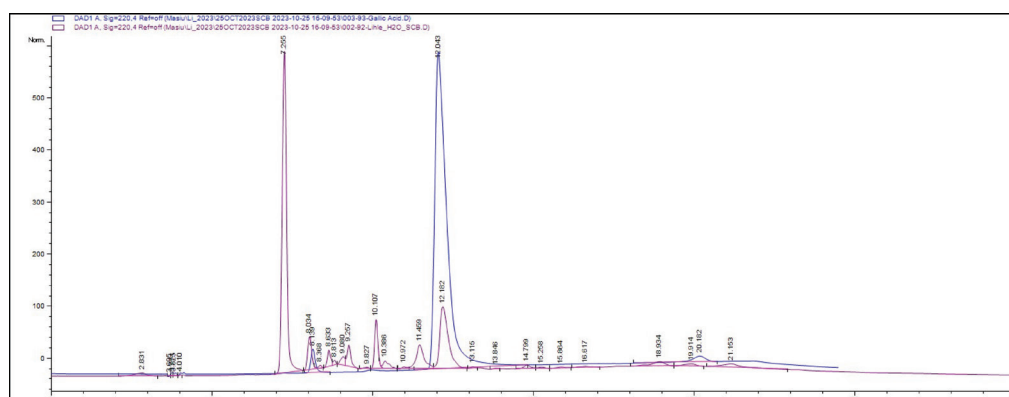


**FIGURE 2** - Chromatogram peaks of the SBW extract superimposed with the chromatogram of gallic acid. The HPLC conditions were as follows: The column oven temperature was set to 30°C; flow rate was 1.0 mL/min; injection volume was 10  $\mu$ L; and the dwell volume of the HPLC system was 1.8 mL. HPLC = high-performance liquid chromatography; SBW = *Sclerocarya birrea* water.

the SBW extract superimposed with the chromatogram of gallic acid at 220 nm. Therefore, chromatograms indicate the possible presence of gallic acid in both plant extracts.

### Anticancer effect of VER, DOX, and S. birrea bark extracts

*S. birrea* extracts, VER, and DOX were tested for their cytotoxicity against drug-sensitive HT29 and drug-resistant HCT15 cell lines to determine their anticancer activity by MTT assay.

The SBE extract induced an anticancer effect on both HT29 and HCT15 cells in a dose-dependent manner with the higher inhibition of ~70% and ~80% at 400 µg/mL and lowest percentage inhibition of ~1% and ~15% at 1.56 µg/mL (Figs. 3A and 4A) with an  $IC_{50}$  value of  $157.46 \pm 0.23$  and  $50.67 \pm 1.61$  µg/mL, respectively (Tab. 1). In addition, the

SBW extract also induced growth inhibitory effects in HT29 and HCT15 cell lines in a dose-dependent manner with the highest percentage inhibition of ~80% and ~60% at 500 µg/mL and lowest percentage inhibition of ~5% and ~10% recorded at concentrations of 6.25 µg/mL (Figs. 3B and 4B). The  $IC_{50}$  value of the SBW extract was  $181.80 \pm 0.41$  µg/mL in HT29 cells and  $438.42 \pm 0.12$  µg/mL in HCT15 cells as shown in Table 1.

DOX demonstrated anticancer effect on both HT29 and HCT15 cells with the higher percentage inhibition of 80% on both cell lines at 5 µg/mL and lowest percentage inhibition of 19% (on HT29) and 17% (on HCT15) at 0.03 µg/mL (Figs. 3C and 4C) with an  $IC_{50}$  value of  $0.45 \pm 0.10$  and  $1.34 \pm 0.1$  µg/mL, respectively (Tab. 1). In addition, VER also exhibited an anticancer effect on both the aforementioned cell lines (Figs. 3D

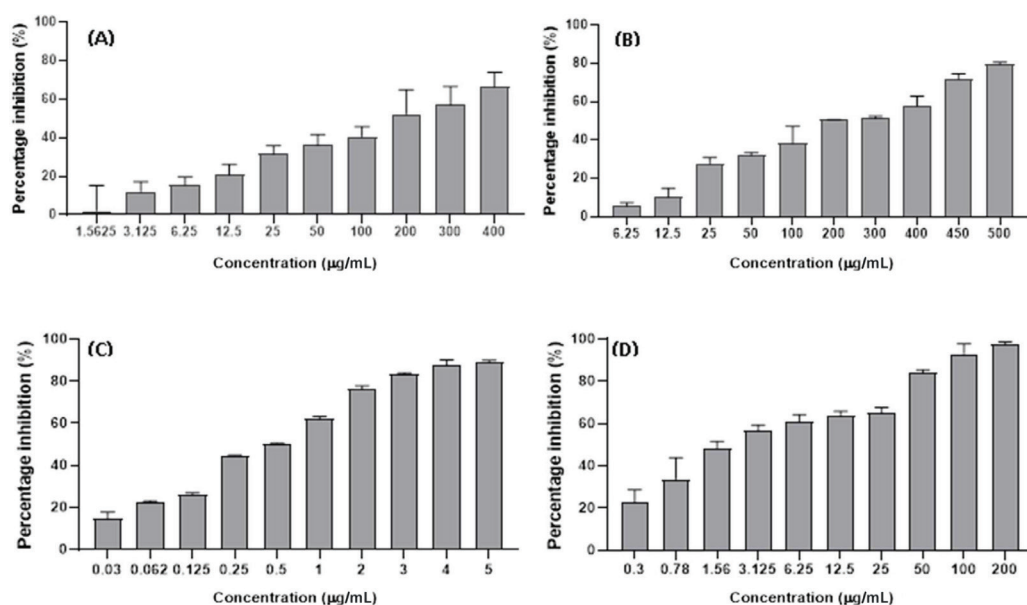


**FIGURE 3** - Anticancer effect of SBE (A), SBW (B), DOX (C), VER (D) on HT29 cell line. DOX = doxorubicin; SBE = *Sclerocarya birrea* ethanol; SBW = *Sclerocarya birrea* water; VER = verapamil.

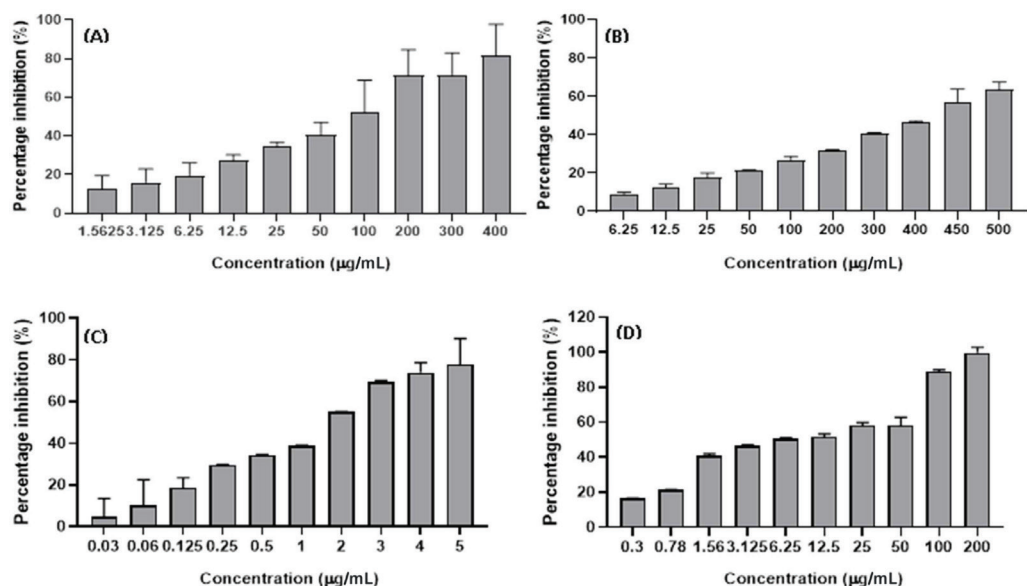


**FIGURE 4** - Anticancer effect of SBE (A), SBW (B), DOX(C), VER (D) on HCT15 cell line. DOX = doxorubicin; SBE = *Sclerocarya birrea* ethanol; SBW = *Sclerocarya birrea* water; VER = verapamil.

and 4D) with the highest percentage of ~99% inhibition at a concentration of 200 µg/mL whereas the lowest percentage inhibition was ~20% at a concentration of 0.3 µg/mL for HT29 and HCT15, respectively. Furthermore, the IC<sub>50</sub> of VER on HT29 cells obtained was 2.78 ± 0.46 µg/mL while VER on HCT15 cells was 8.75 ± 2.03 µg/mL (Tab. 1).

**TABLE 1** - The IC<sub>50</sub> values of the drugs and *Sclerocarya birrea* extracts

Cell type	DOX (µg/mL)	VER (µM)	SBE extract (µg/mL)	SBW extract (µg/mL)
HT29	0.45 ± 0.10	2.78 ± 0.46	157.46 ± 0.23	181.80 ± 0.41
HCT15	1.34 ± 0.1	8.75 ± 2.03	50.67 ± 1.61	438.42 ± 0.12

DOX = doxorubicin; IC = inhibitory concentration; SBE = *Sclerocarya birrea* ethanol; SBW = *Sclerocarya birrea* water; VER = verapamil.

### Combination treatment of the *S. birrea* extracts with DOX and DOX with VER on HT29 cell line

SBE and SBW extracts were also subjected to combination treatment with DOX and DOX with VER (control) to examine their interaction against HT29 cells. The nature of interaction was evaluated using CI values from CompuSyn, which gives a quantitative definition of an additive interaction, that is, when the CI value is 1.00; a synergistic interaction when the CI value is <1; and an antagonistic interaction when the CI value is >1.15 at IC<sub>50</sub>, IC<sub>75</sub>, IC<sub>90</sub>, and IC<sub>95</sub>. The combination treatment was also performed to determine the DRI of the test samples at IC<sub>50</sub>, IC<sub>75</sub>, IC<sub>90</sub>, and IC<sub>95</sub> in order to determine how much the doses of each test samples in combination were reduced to achieve effect levels that were comparable with those achieved with single test samples. The IC and CI values of the combined treatment of VER and DOX, *S. birrea* extracts, and DOX against HT29 cells are shown in Supplementary Table 4. The combined treatment was also evaluated using synergy finder to determine synergistic dose points and their synergy scores from their percentage inhibition.

As seen in Supplementary Table 4, the combined treatment of VER and DOX resulted in an additive effect with CI value of 1.0, while the IC<sub>50</sub> values decreased from 3.04 to 1.31 µg/mL for VER and 0.45 to 0.26 µg/mL for DOX. The decreased IC<sub>50</sub> values were achieved by DRI with a magnitude 2.3-fold and 1.7-fold for VER and DOX, respectively. However, IC<sub>75</sub>, IC<sub>90</sub>, and IC<sub>95</sub> demonstrated normal to strong synergistic effects coupled with a significant decrease in the concentrations of VER and DOX with greater DRI ratios, which indicated that there was reduced toxicity.

Three synergistic dose points were obtained with their synergy scores as well as their inhibition scores in the combination treatment of DOX and VER against HT29 cells. The highest synergy score recorded was 6.84 yielded by the combination of 0.11 µg/mL of DOX and 4.76 µg/mL of VER with a cell growth inhibition percentage of 57.85% as shown in Figure 5. The second synergistic dose points were 1.19 µg/mL of VER and 1.8 µg/mL of DOX with a synergy score of 2.56 and an inhibition percentage of 82.07%. The third synergistic dose points were found from the combination of 0.6 µg/mL of VER and 1.18 µg/mL of DOX with a synergy score of 0.99 and an inhibition percentage of 73.2%.

Other dosage points resulted in antagonistic scores and one additive score of 0.43.

SBE extract and DOX combinations exhibited normal to strong antagonistic effects from IC<sub>50</sub> to IC<sub>95</sub> as depicted in Supplementary Table 5. The DRI values of both the drug and the ethanol extract decreased drastically while synergy finder analysis showed no synergistic scores obtained from the combination of the ethanol extract and DOX as shown in Figure 5.

Combinations of the SBW extract and DOX yielded antagonistic interactions (CI of 2.5) while both IC<sub>50</sub> values were increased by a magnitude of 0.3-fold and 0.4-fold for SBW extract and DOX, respectively (Supplementary Table 6). Contrarily, IC<sub>75</sub>, IC<sub>90</sub>, and IC<sub>95</sub> resulted in normal synergistic to strong synergistic interactions with CI values of 0.97, 0.37, and 0.19, further attributed by a significant decrease in the concentrations of both the drug and the extract. Synergy finder analysis showed that this combination yielded no synergistic scores as shown in the bliss heatmap diagram in Figure 5.

### Combination treatment of the *S. birrea* extracts with DOX and DOX with VER on HCT15

SBE and SBW extract of *S. birrea* were also subjected to combination treatment with DOX and DOX with VER (control) to examine their interaction against HCT15 cells. The nature of interaction was evaluated using CI values (as mentioned above) from CompuSyn. The combination treatment was also performed to determine the DRI of the test samples at IC<sub>50</sub>, IC<sub>75</sub>, IC<sub>90</sub>, and IC<sub>95</sub> in order to determine how much the doses of each test samples in combination were reduced to achieve effect levels that were comparable with those achieved with single test samples. The IC and CI values of the combined treatment of VER and DOX, *S. birrea* extracts, and DOX against HCT15 cells are shown in Supplementary Table 7 and Supplementary Table 8, respectively. The combined treatment was also evaluated using synergy finder to determine synergistic dose points and their synergy scores from their percentage inhibition.

The combined treatment of VER and DOX resulted in an antagonistic effect with CI value of 1.33 coupled with decreased IC<sub>50</sub> values of VER (6.6 to 0.38 µg/mL) and DOX (2.99 to 0.33 µg/mL) by DRI magnitudes of 2.64-fold and 0.46-fold as shown in Supplementary Table 7. At IC<sub>75</sub>, IC<sub>90</sub>, and IC<sub>95</sub>, a strong synergistic interaction was observed when the two drugs were used against HCT15 cells (CI = between 0.3 and 0.09), which indicates that resistance reversal activity was observed from the combination treatment of these control drugs. According to the bliss heatmap model, there were ten synergy scores obtained from different concentrations of the combination treatment of DOX and VER as shown in Figure 6.

Combination of the SBE extract and DOX yielded an antagonistic effect (CI of 3.75) with increased IC<sub>50</sub> value of SBE extract (49.35 to 89.86 µg/mL) and DOX (0.68 to 1.32 µg/mL) by DRI ratios of 0.54-fold and 0.51-fold, respectively, as depicted in Supplementary Table 8. Moreover, strong synergistic interactions were demonstrated from IC<sub>75</sub> to IC<sub>95</sub>, with CI values ranging from 0.001 to 0.26, which suggests that drug resistance was reversed. Additionally, two synergistic dose

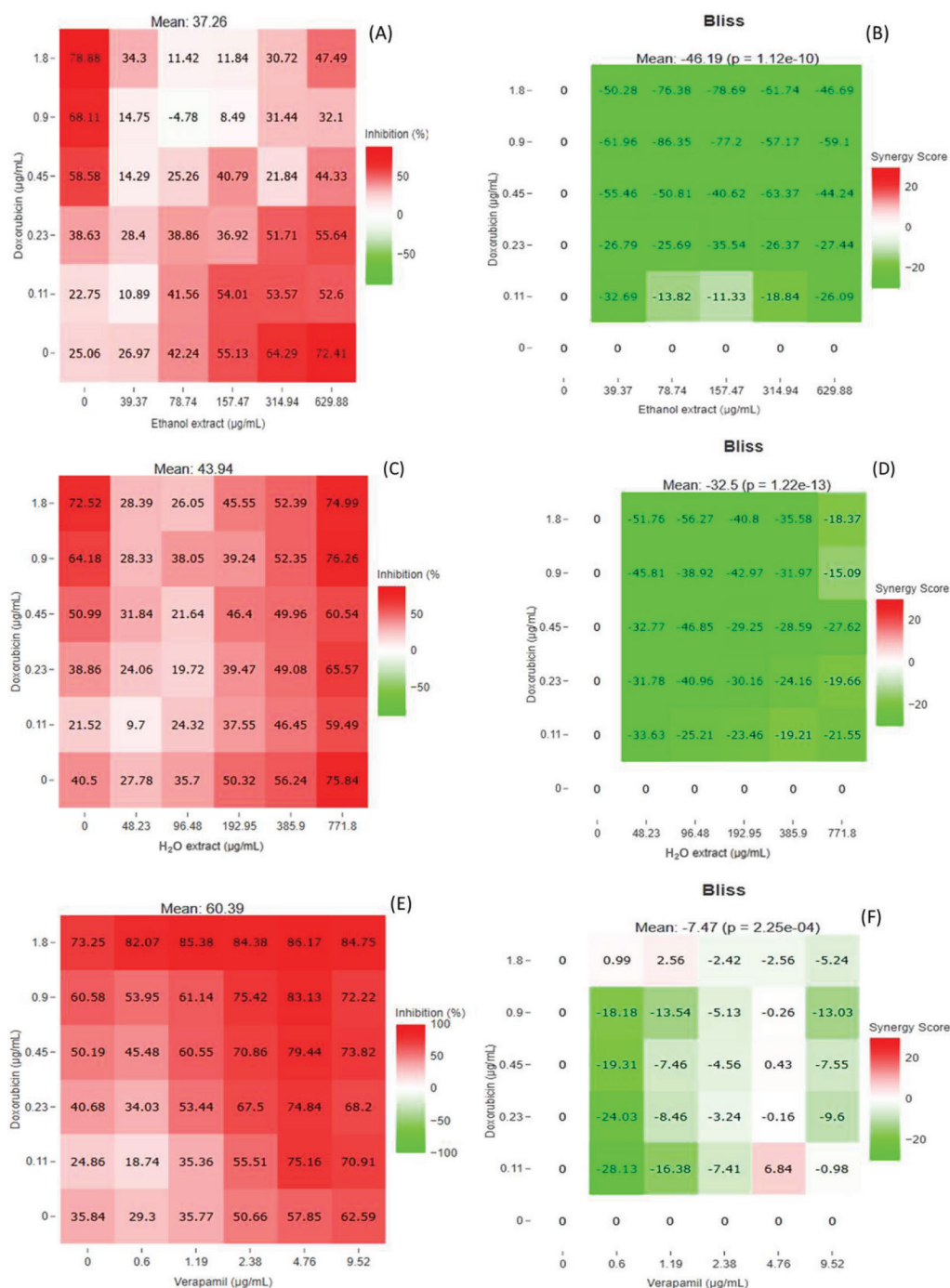


**FIGURE 5** - Heatmap diagrams generated using synergy finder. Heatmap diagram illustrating the inhibition percentages of the combination of the SBE extract and DOX (A), SBW extract and DOX (C), and VER and DOX (E) on HT29 cell line, while the bliss heatmap diagram shows synergistic, antagonistic, and additive scores between the dose points of the combination of SBE extract and DOX (B), combination of SBW extract and DOX (D), and combination of VER and DOX (F) on HT29 cell line. DOX = doxorubicin; SBE = *Sclerocarya birrea* ethanol; SBW = *Sclerocarya birrea* water; VER = verapamil.

points were obtained from this combination (Fig. 6), one from 40.84 µg/mL of the extract and 0.312 µg/mL of DOX with a synergy score of 4.7 and a highest synergy score of 6.63 was yielded by the combination of 40.84 µg/mL of the extract and 0.612 µg/mL of DOX with an inhibitory percentage of 73.57%.

The combinatory effect of the SBW extract and DOX yielded strong antagonistic interactions from IC<sub>50</sub> to IC<sub>95</sub>. The DRI ratios were decreased drastically while no synergistic dose points were recorded using synergy finder analysis as shown in Supplementary Table 9 and Figure 6.

The dose-response curve illustrates the combined effect of the drugs and *S. birrea* extracts in the supplementary data sheet depicted as the bliss independence model synergy map for each combination treatment.

#### Cytotoxic effects of test samples against 3T3 cell line

To comprehend the cytotoxic effects of the experimental samples, 3T3 cells were subjected to escalating doses of DOX, VER, SBE, and SBW extract. The assessment of cytotoxicity for the test samples was conducted through the MTT assay

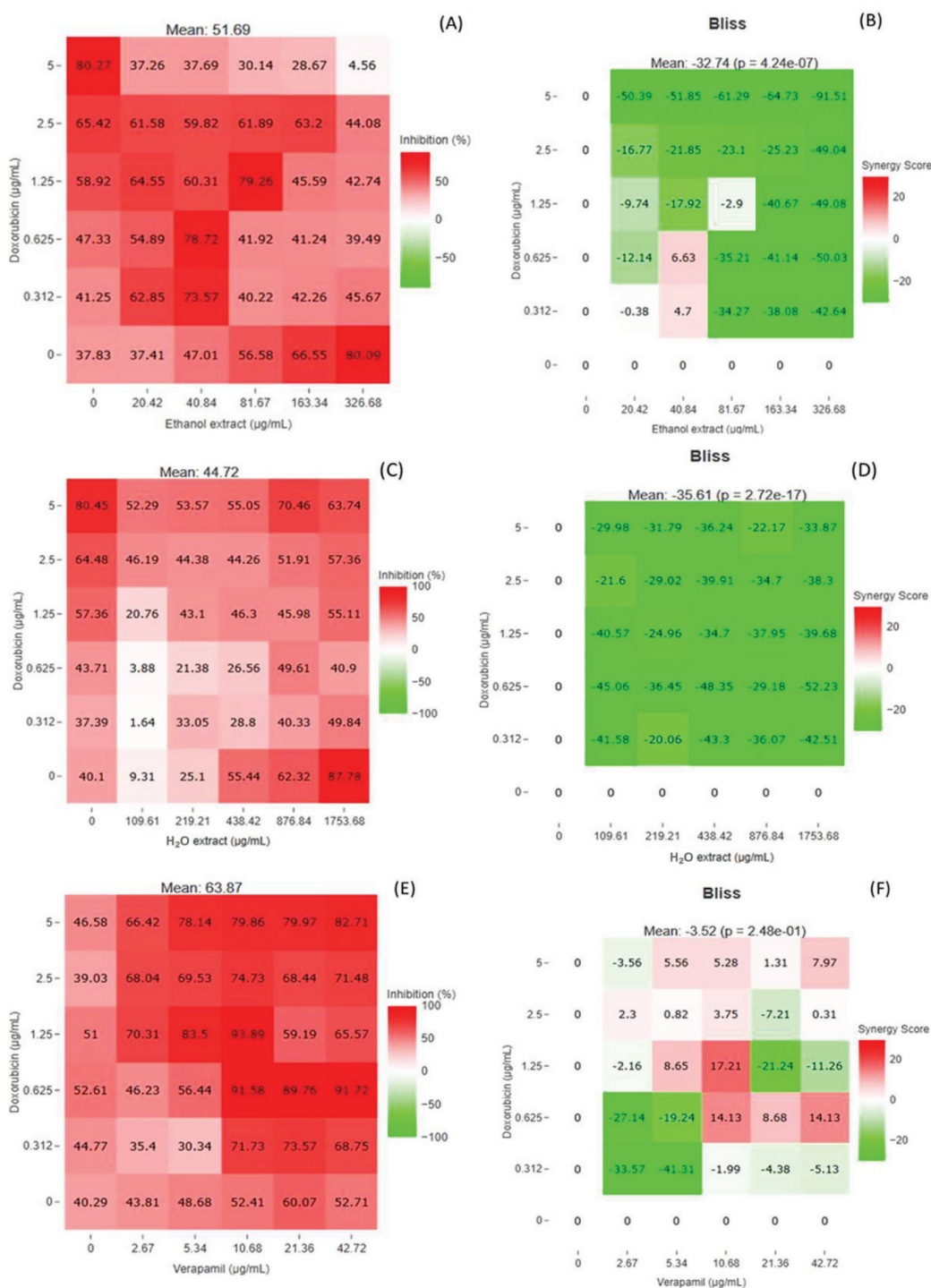


**FIGURE 6** - Heatmap diagrams generated using synergy finder. Heatmap diagram illustrating the inhibition percentages of the combination of the SBE extract and DOX (A), SBW extract and DOX (C), and VER and DOX (E) on HCT15 cells, while the bliss heatmap diagram shows synergistic, antagonistic, and additive scores and between the dose points of the combination of SBE extract and DOX (B), combination of SBW extract and DOX (D), and combination of VER and DOX (F) on HCT15 cells. DOX = doxorubicin; SBE = *Sclerocarya birrea* ethanol; SBW = *Sclerocarya birrea* water; VER = verapamil.

during a 72-hour incubation period. In general, the results indicated that the SBE and SBW extracts exhibited a greater impact on normal cell susceptibility compared to DOX and VER. Notably, cell viability demonstrated a dose-dependent decrease across all the test samples. DOX decreased the cell viability of normal cells when treated with a concentration range of 1-5 µg/mL and showed significant toxic effects on 3T3 cells with an IC<sub>50</sub> value of <1 (Tab. 2). Similarly, 3T3 cells

treated with VER (at concentration range of 25-100 µg/mL) also showed toxic effects with an IC<sub>50</sub> of 0.14 µg/mL (Tab. 2). SBE did not show toxic effects on the normal cell lines as it had an IC<sub>50</sub> of 80.38 ± 4.09 µg/mL (Tab. 2). Moreover, the SBW extract showed less toxicity (IC<sub>50</sub> in 290.62 ± 48.37 µg/mL) on the normal cells compared to the SBE extract (Tab. 2).

From the combinations analysis, cytotoxicity was only evaluated on the 3T3 cells using the strongest synergistic



dose points. Only combinations of VER and DOX as well as SBE extract and DOX yielded synergistic dose points. Therefore, the control inhibited the cell growth of 3T3 cells with  $IC_{50}$  value of  $58.18 \pm 0.98 \mu\text{g/mL}$  while SBE and DOX combinations yielded  $IC_{50}$  values of  $55.54 \pm 0.11 \mu\text{g/mL}$ . Compound selectivity is an essential criterion for chemotherapeutic evaluation.

**TABLE 2** -  $IC_{50}$  values and selectivity index of VER, DOX, and the extracts on 3T3 cells

Extract	DOX ( $\mu\text{g/mL}$ )	VER ( $\mu\text{g/mL}$ )	SBW ( $\mu\text{g/mL}$ )	SBE ( $\mu\text{g/mL}$ )
$IC_{50}$	<1	$0.14 \pm 0.04$	$290.62 \pm 48.37$	$80.38 \pm 4.09$

DOX = doxorubicin; IC = inhibitory concentration; SBE = *Sclerocarya birrea* ethanol; SBW = *Sclerocarya birrea* water; VER = verapamil.

## Discussion

The herbal plant extracts acquired increased attention as potential agents that can be used to potentiate the efficacy of conventional chemotherapy drugs when used in combination for the management of cancer (20). *S. birrea* possesses antitumour effects (21), which was investigated for its combined effect with DOX against HT29 and HCT15 cell lines in this study.

According to the National Cancer Institute, an extract is considered strongly active when the  $IC_{50}$  value is  $<20 \mu\text{g/mL}$ , moderately active when it is between 20 and  $100 \mu\text{g/mL}$ , and inactive when the  $IC_{50}$  is greater than  $100 \mu\text{g/mL}$  based on their cytotoxicity criteria (22). Based on the NCI criterion, findings from this study showed that the SBE and SBW extract showed no activity against HT29 cells while growth inhibition was demonstrated in a dose-dependent manner. Moreover, the SBE extract showed moderate inhibition of HCT15 cells while the SBW extract demonstrated no activity. Both SBE and SBW extracts of *S. birrea* have been reported in the literature to contain high levels of bioactive compounds (e.g., polyphenols) with potential medicinal properties (11). The polyphenols are known to exhibit antioxidant activity, which is considered crucial in preventing cancer development (23,24). The scavenging of free radicals by polyphenols may help prevent DNA damage, cell membrane damage, and oxidative stress, all of which can contribute to cancer development. Hence the presence of these compounds might be responsible for the remarkable anticancer activity observed for these extracts against the investigated CRC cells (25).

In addition, the extracts' cytotoxic activity was assessed in normal 3T3 cells. It was observed that DOX and VER were toxic while the extracts displayed no toxicity towards the normal cells, particularly the SBW extract ( $IC_{50}$  value of  $290.62 \pm 48.37 \mu\text{g/mL}$ ). According to a study by Russo et al (25), *S. birrea* extracts exhibited toxic effects at high concentrations, potentially due to the concentrated compounds found in the extracts, which results in cellular morphological changes considered as the key evidence of cytotoxicity to natural compounds or plant extracts, along with metabolic dysfunctions, differentiation processes, and apoptosis.

We also investigated the combination of the intercalating agent DOX with VER and plant extracts in drug-sensitive and drug-resistant colon cancer cells. The study focused on the CI method (based on the multiple drug effects equation), the DRI, and the synergistic dose scores to evaluate the combinatory effects in the cells. It is noteworthy to understand that one of the major objectives of synergistic drug combination is to reduce the dose of the cytotoxic drug, thereby reducing the toxicity while maintaining efficacy. The CI provides a quantitative definition of an additive effect or interaction, for example, a CI value of 1,  $<1$ , and  $>1$  indicates additivity, synergism, and antagonism, respectively. The DRI is a measure of how many folds a combination treatment reduces cytotoxicity dose (26).

The co-treatment of VER combined with DOX (control) moderately inhibited HT29 cells' growth and decreased the  $IC_{50}$  of VER and DOX from 3.04 and  $0.45 \mu\text{g/mL}$  to 1.31 and  $0.26 \mu\text{g/mL}$ , respectively, thus indicating decreased sensitivity of DOX. Interestingly,  $IC_{75}$  to  $IC_{95}$  resulted in a synergistic effect ascribed by an increase in the DRI, which was also observed in both drugs indicating that sensitivity at higher concentrations is required to exhibit good combinatory effect. Moreover, the combination of VER and DOX also showed three synergistic scores of 0.99, 2.56, and 6.84, whereby the strongest synergy score of 6.84 was achieved with a significantly higher concentration of VER ( $4.76 \mu\text{g/mL}$ ) and lower concentration of DOX ( $0.11 \mu\text{g/mL}$ ).

In HCT15, this combination showed moderate inhibition of the cells and decreased the  $IC_{50}$  of VER and DOX from 6.63 and  $0.38 \mu\text{g/mL}$  to 2.99 and  $0.33 \mu\text{g/mL}$ , respectively. Similarly, synergistic interactions were also depicted at  $IC_{75}$  and  $IC_{95}$  ascribed by ten synergistic dose points ranging from 1.3 to 17.21.

In HT29 cells, combinations of DOX with the SBE extract resulted in an antagonistic effect at  $IC_{50}$  with an increase in  $IC_{50}$  values from 0.35 and  $140.09 \mu\text{g/mL}$  to 1.70 and  $669.89 \mu\text{g/mL}$ , respectively. However, only the SBW extract combinations seemed to have depicted synergistic interactions from  $IC_{75}$  to  $IC_{95}$  in comparison to the SBE extract combinations that demonstrated antagonistic interactions. These results suggest the potentiation effects of each extract at  $IC_{50}$  when used in combination with DOX compared to the control as they were coupled with significantly lower DRI ratios.

A similar behavioural pattern was demonstrated by combinations involving DOX and the SBE extract where strong synergism was observed from  $IC_{75}$  to  $IC_{90}$ . This suggests that the SBE extract might potentially yield similar adverse effects to VER and thus cannot be considered as a resistant reversal agent seeing that extremely higher concentrations are required to yield strong synergistic interactions.

The SBW extract did not show any resistance reversal activity based on its antagonistic effects recorded at all the IC ranges compared to combinations that include ethanol and VER. It was also observed that the DRI of the SBE extract and DOX increased when they were used in combination but the DRI of the SBW extract decreased drastically. According to the bliss heatmap diagram, two synergistic dose points were found from the combination of the SBE extract ( $40.84 \mu\text{g/mL}$ ) and DOX ( $0.625 \mu\text{g/mL}$ ) with a synergy score of 6.63, while



the combination of the SBE extract (40.84 µg/mL) and DOX (0.312 µg/mL) synergy score was found to be 4.7. The dosage for DOX was decreased twice in these synergistic dose points and according to Poofery et al a reduction in the dosage of the drug in combination treatment potentially lessens toxicity and adverse side effects and subsequently reverses drug resistance (27).

## Conclusion

In this study, the combined effects of *S. birrea* extracts and DOX were examined on CRC cell lines, with a particular focus on sensitive and resistant cell types. Various compounds were identified within the plant extracts, with gallic acid being the most abundant and known for its anticancer properties. It was found that both SBE and SBW extracts were non-toxic to normal 3T3 cells at the concentrations tested. The efficacy of SBW and SBE extracts against sensitive HT29 and resistant HCT15 cells revealed that the SBE extract exhibited a more substantial anticancer effect compared to SBW. Furthermore, a synergistic effect was observed when combining SBE or SBW extract and DOX at higher concentrations of each extract, implying that concomitant use of *S. birrea* and DOX should be closely monitored, and DOX dosage adjusted as needed to achieve maximum therapeutic benefits while minimizing potential side effects. These findings indicate the need for further research on the SBE extract to investigate its potential as an anticancer agent *in vivo*, as well as to elucidate its underlying mechanisms of action. While some combinations of *S. birrea* extracts with doxorubicin showed synergistic or additive effects, other combinations exhibited an antagonistic effect, meaning that the extracts actually decreased the efficacy of the standard anticancer drug. The antagonistic effect could be due to various factors, such as interactions between the components of the extracts and doxorubicin, which could alter the pharmacokinetics or pharmacodynamics of the drug.

## Acknowledgements

The African Medicines Innovation and Technology Development Centre (AMITD), Department of Pharmacology, Faculty of Health Sciences, University of the Free State, AvaCare Health Honours Bursary, and Centre for Scientific and Industrial Research (CSIR) Inter-bursary are hereby acknowledged for their support and assistance, and Ms. Recardia Schoeman for her assistance with the culturing of the cells.

## Disclosures

**Financial support:** This research was supported by Technology Innovation Agency (TIA), South Africa, by seed funding Grant no. 1047L0521.

**Conflict of interest:** The authors declare no conflict of interest.

**Author's contribution:** Conceptualization: MGM; Data Curation: THN, IMM, PMM, APM; Formal Analysis: THN, IMM, APM; Investigation: THN, IMM; Methodology: IMM, PMM; Project Administration: IMM, MGM; Supervision: IMM, MGM; Writing Original Draft: THN; Writing – Review & Editing: APM, IMM, MGM.

## References

1. Sawicki T, Ruszkowska M, Danielewicz A, Niedźwiedzka E, Arłukowicz T, Przybyłowicz KE. A review of colorectal cancer in terms of epidemiology, risk factors, development, symptoms and diagnosis. *Cancers (Basel)*. 2021;13(9):2025. [CrossRef PubMed](#)
2. McCabe M, Perner Y, Magobo R, Mirza S, Penny C. Descriptive epidemiological study of South African colorectal cancer patients at a Johannesburg Hospital Academic institution. *JGH Open*. 2019;4(3):360-367. [CrossRef PubMed](#)
3. Yun UJ, Lee JH, Shim J, et al. Anti-cancer effect of doxorubicin is mediated by downregulation of HMG-Co A reductase via inhibition of EGFR/Src pathway. *Lab Invest*. 2019;99(8):1157-1172. [CrossRef PubMed](#)
4. Pilotto Heming C, Muriithi W, Wanjiku Macharia L, Niemeyer Filho P, Moura-Neto V, Aran V. P-glycoprotein and cancer: what do we currently know? *Heliyon*. 2022;8(10):e11171. [CrossRef PubMed](#)
5. Zhang T, Ma K, Huang J, et al. CDKN2B is critical for verapamil-mediated reversal of doxorubicin resistance in hepatocellular carcinoma. *Oncotarget*. 2017;8(66):110052-110063. [CrossRef PubMed](#)
6. Aiello P, Sharghi M, Mansourkhani SM, et al. Medicinal plants in the prevention and treatment of colon cancer. *Oxid Med Cell Longev*. 2019;2019:2075614. [CrossRef PubMed](#)
7. Esmeeta A, Adhikary S, Dharshnaa V, et al. Plant-derived bioactive compounds in colon cancer treatment: an updated review. *Biomed Pharmacother*. 2022;153:113384. [CrossRef PubMed](#)
8. Huang XM, Yang ZJ, Xie Q, Zhang ZK, Zhang H, Ma JY. Natural products for treating colorectal cancer: a mechanistic review. *Biomed Pharmacother*. 2019;117:109142. [CrossRef PubMed](#)
9. Yang C, Mai Z, Liu C, Yin S, Cai Y, Xia C. Natural products in preventing tumor drug resistance and related signaling pathways. *Molecules*. 2022;27(11):3513. [CrossRef PubMed](#)
10. Kamanula M, Munthali CY, Kamanula JF. Nutritional and phytochemical variation of Marula (*Sclerocarya birrea*) (Subspecies caffra and birrea) fruit among nine international provenances tested in Malawi. *Int J Food Sci*. 2022;2022:4686368. [CrossRef PubMed](#)
11. Cádiz-Gurrea ML, Lozano-Sánchez J, Fernández-Ochoa Á, Segura-Carretero A. Enhancing the yield of bioactive compounds from *Sclerocarya birrea* bark by green extraction approaches. *Molecules*. 2019;24(5):966. [CrossRef PubMed](#)
12. Masoko P, Mmushi TJ, Mogashoa MM, Mokgotho MP, Mampuru LJ, Howard RL. In vitro evaluation of the antifungal activity of *Sclerocarya birrea* extracts against pathogenic yeasts. *Afr J Biotechnol*. 2008;7(20):3521-3526.
13. Daniel JA, Mathiyazhagan J, Anbazhagan M, Jayaraj R, Gothandam KM. Phytochemistry and pharmacology of *Sclerocarya birrea* (A. Rich.) Hochst.: a review. In: Pullaiah T, ed. *Bioactives and pharmacology of medicinal plants*. Apple Academic Press; 2022:139-147. [CrossRef](#)
14. Mohammed M, Adamu H, Magashi L, Sarkinnoma A, Daniel S, Zakiyya R, Aisha S. Purification and characterization of extracts from the stem bark of *Sclerocarya birrea* (Marula). *International Journal of Modelling and Applied Science Research*. 2023;28(9):141-152. [Online](#) (Accessed July 2024)
15. Nyoni S, Muzenda E, Mukaratirwa-Muchanyereyi N. Characterization and evaluation of antibacterial activity of silver nanoparticles prepared from *Sclerocarva birrea* stem bark and leaf extracts. *Nano Biomed Eng*. 2019;11(1):28-34. [CrossRef](#)
16. Abdulhamid A, Sani I, Fakai IM, Kankiya IH, Shinkafi TS. Antibacterial potentials of compounds isolated from the stem



- bark extract of *Sclerocarya birrea* (A. Rich, Hochst). J Appl Sci. 2019;19(3):210-216. [CrossRef](#)
17. Indrayanto G, Putra GS, Suhud F. Validation of in-vitro bioassay methods: application in herbal drug research. In: Al-Majed AA. Profiles of drug substances, excipients and related methodology. Vol 46. Academic Press; 2021:273-307. [CrossRef](#)
  18. Chou TC. Drug combination studies and their synergy quantification using the Chou-Talalay method. Cancer Res. 2010; 70(2):440-6. [CrossRef](#). [PubMed](#).
  19. Aftab A, Yousaf Z, Rashid M, et al. Vegetative part of *Nigella sativa* L. potential antineoplastic sources against Hep2 and MCF7 human cancer cell lines. J Taibah Univ Sci. 2023;17(1): 2161294. [CrossRef](#)
  20. Lin SR, Chang CH, Hsu CF, et al. Natural compounds as potential adjuvants to cancer therapy: preclinical evidence. Br J Pharmacol. 2020;177(6):1409-1423. [CrossRef](#) [PubMed](#)
  21. Tanih NF, Ndip RN. The acetone extract of *Sclerocarya birrea* (Anacardiaceae) possesses antiproliferative and apoptotic potential against human breast cancer cell lines (MCF-7). Sci World J. 2013;2013(1):956206. [CrossRef](#) [PubMed](#)
  22. Al-Rajhi AMH, Yahya R, Abdelghany TM, et al. Anticancer, anticoagulant, antioxidant and antimicrobial activities of *Thevetia peruviana* Latex with molecular docking of antimicrobial and anticancer activities. Molecules. 2022;27(10):3165. [CrossRef](#) [PubMed](#)
  23. Luo M, Zhou L, Huang Z, et al. Antioxidant therapy in cancer: rationale and progress. Antioxidants. 2022;11(6):1128. [CrossRef](#) [PubMed](#)
  24. Piskounova E, Agathocleous M, Murphy MM, et al. Oxidative stress inhibits distant metastasis by human melanoma cells. Nature. 2015;527(7577):186-191. [CrossRef](#) [PubMed](#)
  25. Russo EB, Burnett A, Hall B, Parker KK. Agonistic properties of cannabidiol at 5-HT1a receptors. Neurochem Res. 2005;30(8):1037-1043. [CrossRef](#) [PubMed](#)
  26. Eid SY, Althubiti MA, Abdallah ME, Wink M, El-Readi MZ. The carotenoid fucoxanthin can sensitize multidrug resistant cancer cells to doxorubicin via induction of apoptosis, inhibition of multidrug resistance proteins and metabolic enzymes. Phytomedicine. 2020;77:153280. [CrossRef](#) [PubMed](#)
  27. Poofery J, Khaw-On P, Subhawa S, et al. Potential of Thai herbal extracts on lung cancer treatment by inducing apoptosis and synergizing chemotherapy. Molecules. 2020;25(1):231. [CrossRef](#) [PubMed](#)

# Faricimab versus the standard of care for neovascular age-related macular degeneration in Italy: an indirect treatment comparison

Carlotta Galeone<sup>1,2</sup>, Federica Turati<sup>3</sup>, Massimo Nicolò<sup>4</sup>, Mariacristina Parravano<sup>5</sup>, Stela Vujosevic<sup>6,7</sup>, Laura Bianchino<sup>8</sup>, Emilia Sicari<sup>8</sup>, Paolo Lanzetta<sup>9,10</sup>

<sup>1</sup>Bicocca Applied Statistics Center (BASC), Università degli Studi di Milano-Bicocca, Milan - Italy

<sup>2</sup>Biostatistics & Outcome Research, Statinfo, Milan - Italy

<sup>3</sup>Department of Clinical Sciences and Community Health, University of Milan, Milan - Italy

<sup>4</sup>Clinica Oculistica—DiNOGMi, IRCCS Ospedale Policlinico San Martino, Genoa - Italy

<sup>5</sup>IRCCS-Fondazione Bietti, Rome - Italy

<sup>6</sup>Department of Biomedical, Surgical, and Dental Sciences, University of Milan, Milan - Italy

<sup>7</sup>Eye Clinic, IRCCS MultiMedica, Milan - Italy

<sup>8</sup>Roche S.p.A., Monza - Italy

<sup>9</sup>Department of Medicine-Ophthalmology, University of Udine, Udine - Italy

<sup>10</sup>IEMO, Istituto Europeo di Microchirurgia Oculare, Udine - Italy

## ABSTRACT

**Objectives:** To assess through an indirect treatment comparison (ITC) the potential benefit of faricimab over the anti-vascular endothelial growth factor (VEGF) real-life scenario, hereby defined standard of care (SoC), in Italy, that is, aflibercept, bevacizumab, and ranibizumab, in patients with neovascular age-related macular degeneration (nAMD) naïve to any anti-VEGF treatment.

**Methods:** Individual patient-level data from the phase III clinical trials TENAYA and LUCERNE (faricimab cohort) and the real-world study RADIANCE (RADIANCE cohort) were used. Efficacy was evaluated with changes in best corrected visual acuity (BCVA) and central subfield thickness (CST) from baseline to 1 year (week 52 in the RADIANCE and week 48 in the faricimab cohorts, respectively). Propensity score-based inverse probability of treatment weighting was utilized to balance cohorts and mitigate bias due to potential confounding. Sensitivity analyses were performed to evaluate treatment differences adjusted for the number of injections.

**Results:** The ITC included 513 patients treated with faricimab and 263 patients treated with SoC. At 1 year, faricimab showed a greater mean BCVA gain (treatment difference +5.4 letters,  $p < 0.001$ ) and CST reduction (treatment difference  $-71.8 \mu\text{m}$ ,  $p < 0.001$ ) compared to SoC. Sensitivity analyses confirmed the robustness of results, showing a BCVA improvement of +4.0 letters and a CST reduction of  $-71.5 \mu\text{m}$  in favor of faricimab.

**Conclusions:** Despite the limitations due to the use of ITC and the comparison between clinical trials and real-world cohorts, the present analysis suggests potential benefits in terms of vision gain and CST reduction in naïve nAMD patients treated with faricimab compared with SoC in a real-world setting.

**Keywords:** Faricimab, Indirect treatment comparison, nAMD, Vascular endothelial growth factor A

## Introduction

Age-related macular degeneration (AMD) is the leading cause of blindness and visual impairment in elderly subjects (1-3). It is a chronic, multifactorial degenerative pathology affecting the macula, typically occurring after age 55 (1).

Neovascular AMD (nAMD) is an advanced form of AMD characterized by the development of subretinal new vessels that may lead to leakage, accumulation of fluid intra- and subretinally, macular edema, hemorrhage, and serous detachments of the retinal pigment epithelium. Angiogenesis and increased vascular permeability are mainly caused by an abnormally high expression of vascular endothelial growth factor (VEGF) (4-8). Over the last couple of decades, the treatment of nAMD has evolved, gradually shifting from laser therapy to the use of anti-VEGF intravitreal injections. Anti-VEGF agents have proven to be effective for the management of patients with nAMD, removing exudative fluid from the retina, suppressing the formation of leaking new blood vessels, and improving or maintaining visual acuity (VA) over

Received: July 18, 2024

Accepted: November 13, 2024

Published online: December 12, 2024

### Corresponding author:

Carlotta Galeone

email: [carlotta.galeone@unimib.it](mailto:carlotta.galeone@unimib.it)



time (9-17). In Italy, the prevalence of nAMD in individuals aged  $\geq 55$  was estimated at 4.6 per 1,000 inhabitants (18).

Currently, there is no single approach for anti-VEGF administration. The most common approaches are the reactive *pro-re-nata* (PRN), the proactive treat-and-extend (T&E), and the fixed bimonthly regimen. In the reactive PRN approach, three-monthly loading doses are followed by adaptable dosing based on monthly monitoring of VA and/or macular morphology. In clinical practice, this approach has been associated with suboptimal outcomes and risk of undertreatment (19). The proactive fixed bimonthly dosing consists of bimonthly injections for at least 1 year (13,15) and has been shown to improve outcomes compared to PRN (20), although it is associated with a considerable treatment burden (21).

In the proactive T&E regimen, anti-VEGF is administered at every visit. Following the loading phase, the treatment interval can be gradually extended or reduced based on anatomic and VA status. This approach allows the extension of treatment intervals, reducing the overall number of visits and improving VA outcomes (20-26).

In 2023, faricimab, a novel bispecific antibody that simultaneously binds and neutralizes Ang-2 and VEGF-A, received approval by the European Medicines Agency (EMA) and reimbursement by Italian Medicines Agency (*Agenzia Italiana del Farmaco*—AIFA) for the treatment of adult patients with nAMD (27). In Italy, the currently available anti-VEGFs include aflibercept, ranibizumab, bevacizumab, and brolucizumab (28). Aflibercept, ranibizumab, and brolucizumab have received marketing authorization from EMA for the treatment of nAMD, while bevacizumab can be administered on an off-label regimen according to the Law 648/96 (Law 648/96 provides for the reimbursement of the medicinal product by the National Health Service when there is no valid therapeutic alternative for innovative medicines authorized in other states but not in Italy, for medicines not yet authorized but undergoing clinical trials, and for medicines already authorized in Italy, for indications other than authorized one) (29).

Efficacy and safety of faricimab were evaluated in the randomized, double-masked, phase III, non-inferiority trials TENAYA and LUCERNE (30) that randomized patients to receive faricimab 6.0 mg up to every 16 weeks (TENAYA  $n = 334$ , LUCERNE  $n = 331$ ) or aflibercept 2.0 mg every 8 weeks (TENAYA  $n = 337$ , LUCERNE  $n = 327$ ). In both studies, faricimab was non-inferior to aflibercept in terms of change in best corrected VA (BCVA) from baseline averaged over weeks 40, 44, and 48, with mean changes of 5.8 letters (95% confidence interval, CI: 4.6 to 7.1) and 6.6 letters (95% CI: 5.23 to 7.8) in TENAYA and LUCERNE, respectively. The treatment difference was equal to 0.7 letters (95% CI: -1.1 to 2.5) in TENAYA and 0.0 letters (95% CI: -1.7 to 1.8) in LUCERNE.

RADIANCE is an Italian, retrospective, observational, multicenter cohort study (31) that aimed to describe the real-world treatment patterns of available intravitreal anti-VEGF in Italy and the associated effectiveness. The study enrolled all consecutive anti-VEGF treatment-naïve subjects with a diagnosis of nAMD who initiated therapy with one of the available agents (i.e., aflibercept, bevacizumab, and ranibizumab) between January 2017 and November 2018. The primary objective of the study was to evaluate the change in

VA 52 weeks after starting treatment with any of the three agents. All VA measurements were converted to the approximate ETDRS letter score. Overall, after 52 weeks of treatment, the patients showed a median change in VA of 1.0 letter (25th-75th percentile: -5; +1.9). By stratifying VA changes by the number of injections per year, patients treated with >6 injections in the first year of treatment showed a median VA improvement of 3 letters (25th-75th percentile: -1; 11), while no improvement was observed in patients treated with <2 (median 0 letters, 25th-75th percentile: -2; 0) and 3-5 injections (median 0 letters; 25th-75th percentile: -5.0; +9.0).

In this study an indirect treatment comparison using individual patient-level data (IPD) was performed to evaluate the potential benefit of faricimab vs. the real-life scenario of intravitreal anti-VEGF monotherapies available at the time of analysis (namely aflibercept 2 mg, bevacizumab, and ranibizumab, hereby defined standard of care—SoC) for nAMD patients in Italy.

## Methods

An indirect comparison of the efficacy at 1 year of faricimab in two phase III clinical trials and the corresponding effectiveness of anti-VEGF in a real-world study was performed on patients with nAMD matched through propensity score (PS) weighting. Efficacy was assessed in terms of change from baseline to 1 year (week 52 in the RADIANCE and week 48 in the faricimab cohorts) in BCVA, as assessed by ETDRS letter score, and central subfield thickness (CST), as determined by Spectral Domain-Optical Coherence Tomography.

## Data sources

IPD for the faricimab cohort was taken from the pivotal trials TENAYA (ClinicalTrials.gov identifier NCT03823287) and LUCERNE (ClinicalTrials.gov identifier NCT03823300) (30).

IPD for the RADIANCE cohort was taken from the Italian, real-world study RADIANCE (31).

In the TENAYA and LUCERNE studies bilateral treatment was not allowed and for patients with bilateral nAMD, the eye with the worst BCVA at diagnosis was included (study eye). In the RADIANCE study, in case of bilateral treatment during the index period, the eye with the worst condition at treatment start was selected as the study eye.

## Population

This analysis included all the patients enrolled in the RADIANCE study (31) with at least two VA measurements after the one at baseline, of which at least one was at week  $52 \pm 10$  (RADIANCE cohort). A cohort of patients treated with faricimab was created by combining data from the active arms in the LUCERNE and TENAYA trials (faricimab cohort). Since the pivotal trials (30) included patients worldwide and the RADIANCE study included Italian patients only, to ensure consistency across the cohorts, only Caucasian patients from LUCERNE and TENAYA were considered; in addition, patients with no VA and CST data at week 48 or with polypoidal choroidal vasculopathy (PCV) lesions were excluded from the faricimab cohort. We excluded PCV lesions from the faricimab



cohort because there were no patients with PCV in the RADIANCE cohort.

### Statistical analyses

PS-based inverse probability of treatment weighting (IPTW) was utilized to balance the two cohorts and mitigate bias due to potential confounding. In IPTW, weights are calculated for each individual as  $1/PS$  for the treated group and  $1/(1 - PS)$  for the control group, where the PS is defined as the inverse probability of receiving the treatment based on the baseline characteristics. This creates pseudo-populations to achieve a balanced distribution of baseline covariates between groups (32). In this analysis, the PS was estimated by logistic regression including the following baseline covariates, selected according to both expert opinion and evaluation of covariates' imbalance between cohorts:

- VA or CST at baseline, respectively, when analyzing BCVA and CST change;
- Age;
- Sex;
- Type of lesion (type 1, 2, and 3);
- Presence of intraretinal fluid (IRF) at baseline;
- Presence of subretinal fluid (SRF) at baseline.

Missing values in type of lesion, and baseline IRF and SRF were handled by inclusion of categories for missing values in the PS models.

Standardized mean differences (SMDs) and appropriate statistical tests (i.e., chi-square tests for categorical variables, and t-tests or non-parametric Mann-Whitney tests, respectively, for normally and not normally distributed continuous variables) were used to compare the distribution of baseline covariates between the RADIANCE and faricimab cohorts before and after IPTW.

A weighted one-way analysis of variance (ANOVA) was applied to compare mean changes in BCVA and CST between the two cohorts.

The frequency of injections may differ in randomized controlled trial (RCT) and clinical practice and, as already reported in the RADIANCE study, patients with a higher number of injections showed more favorable clinical outcomes (31). To account for the difference in treatment regime and protocol between the pivotal and real-world studies,

in a sensitivity analysis an analysis of covariance (ANCOVA) model incorporating the number of injections as covariate and weighting for IPTW was used to obtain adjusted mean treatment differences.

All tests were two-sided, and a p value  $<0.05$  was considered statistically significant.

Statistical analyses were performed with SAS Version 9.4 (SAS Institute, Cary, NC).

## Results

### Patients and baseline characteristics

The RADIANCE study enrolled 405 patients. Of those, 17 were excluded because they did not satisfy the inclusion criteria (i.e., patients with diagnosis of nAMD, naïve to any intraocular anti-VEGF treatment, with age  $\geq 50$  years on the date of the first anti-VEGF injection), 1 because of the lack of hospital charts/clinical records at anti-VEGF treatment start, 43 because of the lack of at least two VA measurements after the baseline, and 81 because of the lack of a VA measurement at week  $52 \pm 10$ . The TENAYA and LUCERNE studies included a total of 665 patients treated with faricimab; of those, 152 patients were not eligible for this analysis (85 were non-Caucasian, 65 had missing BCVA and CST data at week 48, and, among the remaining, 2 were diagnosed as having PCV at baseline by the centralized reading center). Thus, finally, a total of 513 patients treated with faricimab from TENAYA and LUCERNE trials and 263 patients treated with aflibercept ( $n = 101$ ), bevacizumab ( $n = 53$ ), or ranibizumab ( $n = 109$ ) from the RADIANCE study were included for comparison. All patients from both the faricimab and the RADIANCE cohorts had BCVA data at 1 year (i.e., week 48 and 52, respectively) and were therefore included in the analysis of BCVA change from baseline. CST data at week 48-52 were missing in 97 patients from the RADIANCE cohort and 4 patients from the faricimab cohort; therefore, the analysis of CST changes from baseline at 1 year was based on 509 patients treated with faricimab and 166 patients treated with the anti-VEGF SoC.

Before IPTW, significant differences in baseline patients' characteristics between the two groups were observed. Specifically, in the RADIANCE cohort, compared to the faricimab cohort, patients were older, had lower BCVA and higher CST, and there was a higher proportion of patients with IRF. After IPTW, the cohorts were well-balanced (Tabs. 1 and 2).

**TABLE 1** - Baseline demographic and clinical characteristics in the faricimab and RADIANCE cohorts before and after the IPTW in the analysis of the VA change

	Before IPTW				After IPTW			
	TENAYA+LUCERNE (faricimab)	RADIANCE (SoC)	SMD	p value for comparison*	TENAYA+LUCERNE (faricimab)	RADIANCE (SoC)	SMD	p value for comparison*
<b>N</b>	513	263			772.4	297.2		
<b>Age, median (IQR)</b>	76 (70-81)	78 (73-82)	-0.254	0.0007	77 (71-82)	76 (71-81)	0.040	0.601
<b>Sex, n (%)</b>								
Men	187 (36.5)	115 (43.7)	-0.149	0.049	315.2 (40.8)	319.7 (40.1)	0.014	0.778
Women	326 (63.6)	148 (56.3)			457.2 (59.2)	477.6 (59.9)		

(Continued)



TABLE 1 - (Continued)

	Before IPTW				After IPTW			
	TENAYA+LUCERNE (faricimab)	RADIANCE (SoC)	SMD	p value for comparison*	TENAYA+LUCERNE (faricimab)	RADIANCE (SoC)	SMD	p value for comparison*
<b>Lesion type, n (%)</b>								
Occult (type 1)	275 (54.6)	103 (40.9)	0.292	<0.001	395.7 (52.3)	406.4 (52.1)	0.005	0.951
Classic (type 2) <sup>†</sup>	210 (41.7)	121 (48.0)	-0.102		316.6 (41.8)	323.6 (41.5)	0.008	
Type 3	19 (3.8)	28 (11.1)	-0.271		45.1 (6.0)	49.4 (6.3)	-0.014	
Missing	9	11			14.9	17.8		
<b>IRF at baseline, n (%)</b>								
No	276 (54.9)	84 (42.6)	0.026	0.004	359.2 (51.5)	371.8 (51.5)	-0.003	0.998
Yes	227 (45.1)	113 (57.4)			337.9 (48.5)	349.9 (48.5)		
Missing	10	66			75.3	75.4		
<b>SRF at baseline, n (%)</b>								
No	172 (34.0)	58 (29.2)	0.236	0.217	233.4 (33.3)	264.5 (36.4)	0.055	0.211
Yes	334 (66.0)	141 (70.8)			468.2 (66.7)	461.7 (63.6)		
Missing	7	64			70.8	71.0		
<b>VA (ETDRS Letter) at baseline, mean ± SD</b>	60.5 ± 13.1	57.1 ± 21.1	0.219	0.004	59.6 ± 16.5	61.1 ± 34.3	-0.088	0.244

\*p values were nominal.

<sup>†</sup>Including “minimally” and “predominantly” classic lesions.

IPTW = inverse probability of treatment weighting; IQR = interquartile range; IRF = intraretinal fluid; SD = standard deviation; SMD = standardized mean difference; SoC = standard of care (aflibercept, ranibizumab, and bevacizumab); SRF = subretinal fluid; VA = visual acuity.

TABLE 2 - Baseline demographic and clinical characteristics in the faricimab and RADIANCE cohorts before and after the IPTW in the analysis of the CST change

	Before IPTW				After IPTW			
	TENAYA+LUCERNE (Faricimab)	RADIANCE (SoC)	SMD	p value for comparison*	TENAYA+LUCERNE (faricimab)	RADIANCE (SoC)	SMD	p value for comparison*
<b>N</b>	509	166			673.3	683.3		
<b>Age, median (IQR)</b>	76 (70-81)	77 (72-82)	-0.155	0.077	76 (70-81)	76 (70-80)	0.030	0.739
<b>Sex, n (%)</b>								
Men	184 (36.2)	80 (48.2)	-0.246	0.006	365.4 (39.4)	275.7 (40.4)	-0.019	0.727
Women	325 (63.8)	86 (51.8)			407.8 (60.6)	407.6 (59.7)		
<b>Lesion type, n (%)</b>								
Occult (type 1)	274 (54.8)	76 (47.2)	0.161	<0.001	350.5 (53.1)	363.1 (54.2)	-0.022	0.916
Classic (type 2) <sup>†</sup>	207 (41.4)	63 (39.1)	0.056		268.4 (40.7)	265.4 (39.6)	0.022	
Type 3	19 (3.8)	22 (13.7)	-0.346		40.8 (6.2)	41.9 (6.5)	-0.002	
Missing	9	5			13.3	12.8		
<b>IRF at baseline, n (%)</b>								
No	276 (55.2)	68 (43.9)	-0.168	0.004	343.4 (52.4)	342.6 (51.6)	-0.016	0.755
Yes	224 (44.8)	87 (56.1)			311.8 (47.6)	321.8 (48.4)		
Missing	9	11			18.0	18.8		
<b>SRF at baseline, n (%)</b>								
No	170 (33.9)	46 (29.5)	-0.022	0.309	219.3 (33.3)	242.6 (36.4)	0.065	0.244
Yes	332 (66.1)	110 (70.5)			438.8 (66.7)	424.4 (63.6)		
Missing	7	10			15.1	16.2		
<b>CST (µm) at baseline, mean ± SD</b>	359.8 ± 121.3	392.0 ± 163.6	-0.223	0.021	366.3 ± 144.3	362.0 ± 287.6	0.030	0.725

\*P values were nominal.

<sup>†</sup>Including “minimally” and “predominantly” classic lesions.

CST = central subfield thickness; IPTW = inverse probability of treatment weighting; IQR = interquartile range; IRF = intraretinal fluid; SD = standard deviation; SMD = standardized mean difference; SoC = standard of care (aflibercept, ranibizumab, and bevacizumab); SRF = subretinal fluid.



### Change from baseline in BCVA

After IPTW, mean vision gains in BCVA after 1 year of treatment were 6.4 letters (95% CI: 5.0 to 7.9) in the faricimab cohort and 1.0 letter (95% CI: -0.4 to 2.5) in the RADIANCE cohort, with a corresponding treatment difference of 5.4 letters (95% CI: 3.4 to 7.5,  $p < 0.001$ ) in favor of faricimab (Fig. 1).

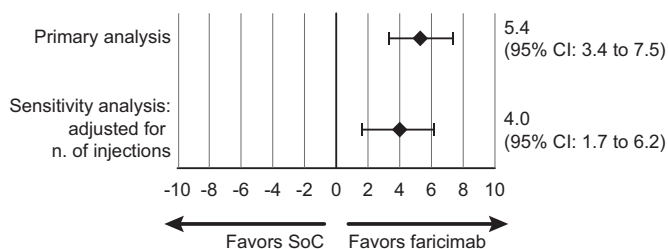


**FIGURE 1** - Difference in BCVA mean change (95% CI) from baseline to 1 year after IPTW. BCVA = best corrected visual acuity; CI = confidential interval; IPTW = inverse probability of treatment weighting; SoC = standard of care (aflibercept, ranibizumab, and bevacizumab).

### Change from baseline in CST

After IPTW, the mean CST change from baseline was  $-143.2 \mu\text{m}$  (95% CI:  $-156.2$  to  $-130.1$ ) in the faricimab cohort and  $-71.4 \mu\text{m}$  (95% CI:  $-84.3$  to  $-58.4$ ) in the RADIANCE cohort, with a corresponding treatment difference of  $-71.8 \mu\text{m}$  (95% CI:  $-90.2$  to  $-53.4$ ,  $p < 0.001$ ) in favor of faricimab (Fig. 2).

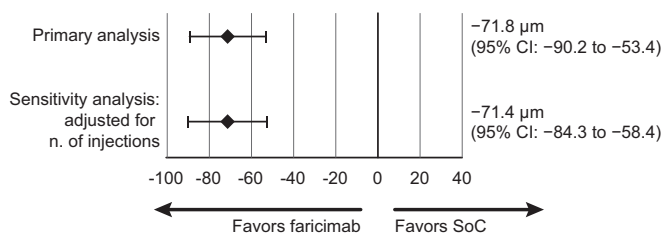


**FIGURE 2** - Difference in CST mean change (95% CI) from baseline to 1 year after IPTW. CI = confidential interval; CST = central subfield thickness; IPTW = inverse probability of treatment weighting; SoC = standard of care (aflibercept, ranibizumab, and bevacizumab).

### Sensitivity analysis

After adjusting for the number of injections, results were consistent with the main scenarios. There was a slight reduction in the weighted BCVA change from baseline in the faricimab cohort (+5.9 letters [95% CI: 4.4 to 7.4]) and a slight increase in the RADIANCE cohort (+1.9 letters [95% CI: 0.4 to 3.5]). The weighted treatment difference remained statistically significant and was consistent with that observed in the main scenario (+4.0 letters in favor of faricimab [95% CI: 1.7 to 6.2;  $p = 0.0005$ ]). Similarly, after adjusting for the number of injections, the estimated treatment difference in CST change from baseline remained in favor of faricimab ( $-71.5 \mu\text{m}$  [95% CI:  $-91$  to  $-52$ ;  $p < 0.001$ ]) (Figs. 1 and 2).

### Discussion

This indirect treatment comparison was conducted to evaluate the effectiveness of the novel anti-VEGF/Ang2 inhibitor faricimab compared to commonly used anti-VEGF agents in Italy. The analysis was performed using IPD from the real-world study RADIANCE (31) and a subset of faricimab-treated patients from the randomized clinical trials TENAYA and LUCERNE (30).

Despite the initial significant differences of baseline characteristics between the two cohorts, the IPTW allowed to balance the cohorts and mitigate the effect of potential confounding variables (i.e., age, sex, type of lesion, IRF, SRF, and baseline VA).

The base case analyses showed a favorable effect for faricimab with a treatment difference compared with SoC equal to a BCVA gain of 5.4 letters (95% CI: 3.4 to 7.5,  $p < 0.001$ ) and a CST reduction of  $-71.8 \mu\text{m}$  (95% CI:  $-90.2$  to  $-53.4$ ,  $p < 0.001$ ). The weighted BCVA change from baseline in the faricimab cohort (+6.5 letters [95% CI: 5.0 to 7.9]) was in line with the results of the TENAYA and LUCERNE trials (+6.2 letters, average of weeks 40-48) (30), and the weighted BCVA change from baseline in the RADIANCE cohort (+1.0 letter [95% CI:  $-0.4$  to 2.5]) was in line with that observed in the RADIANCE study (+1.0 letter [SD 19.3]) (31).

Similarly, the weighted CST changes observed in this analysis ( $-143 \mu\text{m}$  [95% CI:  $-156$  to  $-130$ ] for faricimab and  $-71 \mu\text{m}$  [95% CI:  $-84$  to 58]) for SoC) were comparable to those observed in the TENAYA and LUCERNE trials ( $-137 \mu\text{m}$ , average of weeks 40-48) and in the RADIANCE study ( $-58 \mu\text{m}$  [95% CI:  $-161$  to 15]), respectively.

In the RADIANCE study, after stratification by the number of anti-VEGF injections per year, the median VA improvement was better in patients treated with  $>6$  injections, whereas no improvement was observed in patients treated with fewer injections (31). The association observed in the RADIANCE study between the higher number of anti-VEGF injections and better outcomes was in line with what has been reported by other real-world studies (11,14,16,33). Since the injection frequency in the controlled setting of a clinical trial is often different to that observed in the real world (9,10,13,15,17,34,35), a sensitivity analysis was undertaken to adjust for the number of injections between the RADIANCE and faricimab cohorts. The BCVA gains and CST reductions observed in this sensitivity analysis were consistent with the main scenarios, with the weighted treatment difference in BCVA and CST equal to +4.0 letters and  $-71.5 \mu\text{m}$ , respectively, in favor of faricimab. Despite the adjustment for the number of injections, residual confounding by the different regime and protocol between the pivotal and real-world studies cannot be excluded, which may limit the interpretation and generalizability of the results.

To the best of our knowledge, this is the first study that compared faricimab with SoC for patients with nAMD in Italy. First-line treatment with faricimab was associated with greater visual gain and CST reduction, compared to current intravitreal anti-VEGF SoC, showing potential to redefine the treatment landscape for nAMD. Clinicians may consider faricimab as an effective option, particularly given its favorable outcomes in comparison to employed anti-VEGF agents.

The limitations of the study include the size of the real-world cohort, in particular for the analysis on CST, which was too small to allow subgroup analysis by anti-VEGF agent, along with all limitations associated with the comparison of clinical trial and real-world cohorts. In particular, the treatment regimens in the clinical trial setting are more controlled than in routine clinical practice. Although we used PS weighting to balance potential confounding factors, residual confounding as well as an impact of unmeasured confounders cannot be ruled out. In addition, in the RADIANCE cohort we included patients with at least two post-baseline endpoint measurements, including one around 52 weeks, and this could have introduced some selection bias if these patients were different from those with only one post-baseline measurement.

## Conclusions

Despite limitations of indirect treatment comparisons, which call for specific post-marketing real-world studies, and the possibility that the difference may be due to frequency and time of treatment rather than to type of agents used, the present analysis supports potential benefits in terms of VA and CST reduction in naïve nAMD patients treated with faricimab compared with intravitreal anti-VEGF SoC (aflibercept, ranibizumab, and bevacizumab). Additional evidence from the real-world setting is required to confirm our finding.

## Acknowledgments

The authors acknowledge Ombretta Bandi from SEEd Medical Publishers who provided writing assistance and journal styling services.

## Disclosures

**Financial support:** This study was sponsored and financially supported by Roche S.p.A.

The study was presented as a poster at ISPOR Europe 2023 (Copenhagen, November 12-15, 2023).

**Conflict of interest:** The authors declare the following financial interests/personal relationships which may be considered as potential competing interests:

CG Roche; FT None; MP Abbvie, Novartis, Bayer, Roche, Zeiss; FV Bayer, Novartis, Abbvie, Roche; MN Roche; SV Abbvie, Alimera, Apellis, Bayer, B&I, Novartis, Roche, Zeiss; LB is an employee at Roche; ES is an employee at Roche; GV is an employee at Roche; PL Aerie, Allergan, Annexon, Apellis, Bausch & Lomb, Bayer, Biogen, Boehringer Ingelheim, Eyepoint Pharmaceuticals, I-Care, Genentech, Novartis, Ocular Therapeutix, Outlook Therapeutics, and Roche

**Authors' contributions:** All authors contributed to conceptualization, writing—review and editing.

CG and FT performed data management and statistical analysis.

LB, ES, and GV contributed to funding acquisition, project administration, resources, and supervision.

All authors have read and agreed to the published version of the manuscript.

## References

- Colijn JM, Buitendijk GHS, Prokofyeva E, et al; EYE-RISK consortium; European Eye Epidemiology (E3) consortium. Prevalence of age-related macular degeneration in Europe: the past and the future. *Ophthalmology*. 2017;124(12):1753-1763. [CrossRef PubMed](#)
- Flaxman SR, Bourne RRA, Resnikoff S, et al; Vision Loss Expert Group of the Global Burden of Disease Study. Global causes of blindness and distance vision impairment 1990-2020: a systematic review and meta-analysis. *Lancet Glob Health*. 2017;5(12):e1221-e1234. [CrossRef PubMed](#)
- Steinmetz JD, Bourne RRA, Briant PS, et al; GBD 2019 Blindness and Vision Impairment Collaborators; Vision Loss Expert Group of the Global Burden of Disease Study. Causes of blindness and vision impairment in 2020 and trends over 30 years, and prevalence of avoidable blindness in relation to VISION 2020: the Right to Sight: an analysis for the Global Burden of Disease Study. *Lancet Glob Health*. 2021;9(2):e144-e160. [CrossRef PubMed](#)
- Ambati J, Fowler BJ. Mechanisms of age-related macular degeneration. *Neuron*. 2012;75(1):26-39. [CrossRef PubMed](#)
- Cheung LK, Eaton A. Age-related macular degeneration. *Pharmacotherapy*. 2013;33(8):838-855. [CrossRef PubMed](#)
- Ferris FL III, Wilkinson CP, Bird A, et al; Beckman Initiative for Macular Research Classification Committee. Clinical classification of age-related macular degeneration. *Ophthalmology*. 2013;120(4):844-851. [CrossRef PubMed](#)
- Gheorghe A, Mahdi L, Musat O. Age-related macular degeneration. *Rom J Ophthalmol*. 2015;59(2):74-77. [PubMed](#)
- Patel P, Sheth V. New and innovative treatments for neovascular age-related macular degeneration (nAMD). *J Clin Med*. 2021;10(11):2436. [CrossRef PubMed](#)
- Brown DM, Kaiser PK, Michels M, et al; ANCHOR Study Group. Ranibizumab versus verteporfin for neovascular age-related macular degeneration. *N Engl J Med*. 2006;355(14):1432-1444. [CrossRef PubMed](#)
- Busbee BG, Ho AC, Brown DM, et al; HARBOR Study Group. Twelve-month efficacy and safety of 0.5 mg or 2.0 mg ranibizumab in patients with subfoveal neovascular age-related macular degeneration. *Ophthalmology*. 2013;120(5):1046-1056. [CrossRef PubMed](#)
- Cohen SY, Mimoun G, Oubraham H, et al; LUMIERE Study Group. Changes in visual acuity in patients with wet age-related macular degeneration treated with intravitreal ranibizumab in daily clinical practice: the LUMIERE study. *Retina*. 2013;33(3):474-481. [CrossRef PubMed](#)
- Dugel PU, Koh A, Ogura Y, et al; HAWK and HARRIER Study Investigators. HAWK and HARRIER: phase 3, multicenter, randomized, double-masked trials of brolucizumab for neovascular age-related macular degeneration. *Ophthalmology*. 2020;127(1):72-84. [CrossRef PubMed](#)
- Heier JS, Brown DM, Chong V, et al; VIEW 1 and VIEW 2 Study Groups. Intravitreal aflibercept (VEGF trap-eye) in wet age-related macular degeneration. *Ophthalmology*. 2012;119(12):2537-2548. [CrossRef PubMed](#)
- Holz FG, Tadayoni R, Beatty S, et al. Multi-country real-life experience of anti-vascular endothelial growth factor therapy for wet age-related macular degeneration. *Br J Ophthalmol*. 2015;99(2):220-226. [CrossRef PubMed](#)
- Rosenfeld PJ, Brown DM, Heier JS, et al; MARINA Study Group. Ranibizumab for neovascular age-related macular degeneration. *N Engl J Med*. 2006;355(14):1419-1431. [CrossRef PubMed](#)



16. Staurenghi G, Bandello F, Viola F, et al. Effectiveness of anti-vascular endothelial growth factors in neovascular age-related macular degeneration and variables associated with visual acuity outcomes: results from the EAGLE study. Khetan V, ed. *PLoS One*. 2021;16(9):e0256461. [CrossRef PubMed](#)
17. Martin DF, Maguire MG, Ying GS, Grunwald JE, Fine SL, Jaffe GJ; CATT Research Group. Ranibizumab and bevacizumab for neovascular age-related macular degeneration. *N Engl J Med*. 2011;364(20):1897-1908. [CrossRef PubMed](#)
18. Calabria S, Ronconi G, Dondi L, et al. La popolazione con degenerazione maculare neovascolare correlata all'età trattata con anti-Vegf attraverso i dati amministrativi sanitari. *Recenti Prog Med*. 2023;114(7):447-461. [PubMed](#)
19. Kodjikian L, Mehanna CJ, Cohen SY, et al. The role of future treatments in the management of neovascular age-related macular degeneration in Europe. *Eur J Ophthalmol*. 2021;31(5):2179-2188. [CrossRef PubMed](#)
20. Lanzetta P. Anti-VEGF therapies for age-related macular degeneration: a powerful tactical gear or a blunt weapon? The choice is ours. *Graefes Arch Clin Exp Ophthalmol*. 2021;259(12):3561-3567. [CrossRef PubMed](#)
21. Daien V, Finger RP, Talks JS, et al. Evolution of treatment paradigms in neovascular age-related macular degeneration: a review of real-world evidence. *Br J Ophthalmol*. 2021;105(11):1475-1479. [CrossRef PubMed](#)
22. Kertes PJ, Galic IJ, Greve M, et al. Efficacy of a treat-and-extend regimen with ranibizumab in patients with neovascular age-related macular disease: a randomized clinical trial. *JAMA Ophthalmol*. 2020;138(3):244-250. [CrossRef PubMed](#)
23. Kim LN, Mehta H, Barthelmes D, Nguyen V, Gillies MC. Meta-analysis of real-world outcomes of intravitreal ranibizumab for the treatment of neovascular age-related macular degeneration. *Retina*. 2016;36(8):1418-1431. [CrossRef PubMed](#)
24. Okada M, Kandasamy R, Chong EW, McGuinness M, Guymer RH. The treat-and-extend injection regimen versus alternate dosing strategies in age-related macular degeneration: a systematic review and meta-analysis. *Am J Ophthalmol*. 2018;192:184-197. [CrossRef PubMed](#)
25. Silva R, Berta A, Larsen M, Macfadden W, Feller C, Monés J; TREND Study Group. Treat-and-extend versus monthly regimen in neovascular age-related macular degeneration: results with ranibizumab from the TREND study. *Ophthalmology*. 2018;125(1):57-65. [CrossRef PubMed](#)
26. Wykoff CC, Clark WL, Nielsen JS, Brill JV, Greene LS, Heggen CL. Optimizing anti-VEGF treatment outcomes for patients with neovascular age-related macular degeneration. *JMCP*. 2018;24(2-a Suppl):S3-S15. [CrossRef PubMed](#)
27. AIFA. Determina 2 Ottobre 2023 Riclassificazione Del Medicinale per Uso Umano «Vabysmo», Ai Sensi Dell'articolo 8, Comma 10, Della Legge 24 Dicembre 1993, n. 537. (Determina n. 602/2023). (23A05528) (GU n.235 Del 7-10-2023). 2023. [Online](#). (Accessed July 2024)
28. AIFA. Determina 28 Dicembre 2020 Istituzione Della Nota AIFA 98 Relativa Alla Prescrizione e Alla Somministrazione Intravitreale Di Anti-VEGF Nella AMD e DME. (Determina n. DG/1379/2020). (20A07338) (GU n.323 Del 31-12-2020). 2020. [Online](#). (Accessed July 2024)
29. AIFA. Determina 30 Gennaio 2015 Inserimento Di Una Indicazione Terapeutica Del Medicinale per Uso Umano «Bevacizumab – Avastin» Nell'elenco Ex Lege n. 648/1996 – Parziale Modifica Alla Determina n. 622 DG/2014 Del 23 Giugno 2014 e Sostituzione Della Stessa. (Determina n. 79/2015). (15A01013) (GU n.38 Del 16-2-2015). 2015. [Online](#). (Accessed July 2024)
30. Heier JS, Khanani AM, Quezada Ruiz C, et al; TENAYA and LUCERNE Investigators. Efficacy, durability, and safety of intravitreal faricimab up to every 16 weeks for neovascular age-related macular degeneration (TENAYA and LUCERNE): two randomised, double-masked, phase 3, non-inferiority trials. *Lancet*. 2022;399(10326):729-740. [CrossRef PubMed](#)
31. Parravano MC, Viola F, Nicolo M, et al. Real-world evidence of anti-VEGF therapies in neovascular age-related macular degeneration in Italy: the RADIANCE study. *Eur J Ophthalmol*. (In Press)
32. Chesnaye NC, Stel VS, Tripepi G, et al. An introduction to inverse probability of treatment weighting in observational research. *Clin Kidney J*. 2021;15(1):14-20. [CrossRef PubMed](#)
33. Holz FG, Tadayoni R, Beatty S, et al. Determinants of visual acuity outcomes in eyes with neovascular AMD treated with anti-VEGF agents: an instrumental variable analysis of the AURA study. *Eye (Lond)*. 2016;30(8):1063-1071. [CrossRef PubMed](#)
34. Li JQ, Welchowski T, Schmid M, Mauschitz MM, Holz FG, Finger RP. Prevalence and incidence of age-related macular degeneration in Europe: a systematic review and meta-analysis. *Br J Ophthalmol*. 2020;104(8):1077-1084. [CrossRef PubMed](#)
35. Pina Marín B, Gajate Paniagua NM, Gómez-Baldó L, Gallego-Pinazo R. Burden of disease assessment in patients with neovascular age-related macular degeneration in Spain: results of the AMD-MANAGE study. *Eur J Ophthalmol*. 2022;32(1):385-394. [CrossRef PubMed](#)



# Drug Target Insights

[www.aboutscience.eu](http://www.aboutscience.eu)

ISSN 1177-3928

**ABOUTSCIENCE**